SECURITY CLASSIFICATION OF THIS PAGE

PAGE MARKINGS DTIC FILE COPY

AD-A203 022

1a. REPORT SECURITY CLASSIFICATION

2a. SECURITY CLASSIFICATION AUTHORITY

2b. DECLASSIFICATION / DOWNGRADING SCHEDULE

AVAILABILITY OF REPORT
Approved for public release; distribution unlimited.

(2)

4. PERFORMING ORGANIZATION REPORT NUMBER(S)

5. MONITORING ORGANIZATION REPORT NUMBER(S)
AFOSR-TR- 88-1272

6a. NAME OF PERFORMING ORGANIZATION	6b. OFFICE SYMBOL (If applicable)	7a. NAME OF MONITORING ORGANIZATION
Optical Society of America		AFOSR/NE

6c. ADDRESS (City, State, and ZIP Code)	7b. ADDRESS (City, State, and ZIP Code)
1816 Jefferson Place NW Washington DC 20036	Bldg 410 Bolling AFB DC 20332-6448

8a. NAME OF FUNDING / SPONSORING ORGANIZATION	8b. OFFICE SYMBOL (If applicable)	9. PROCUREMENT INSTRUMENT IDENTIFICATION NUMBER
AFOSR/NE		AFOSR-88-0251

8c. ADDRESS (City, State, and ZIP Code)	10. SOURCE OF FUNDING NUMBERS			
	PROGRAM ELEMENT NO.	PROJECT NO.	TASK NO.	WORK UNIT ACCESSION NO.
Bldg 410 Bolling AFB DC 20332-6448	61102F	2305	B4	

11. TITLE (Include Security Classification)
ORGANIZATION OF THE TOPICAL MEETING ON OPTICAL COMPUTING, TOULON, France

12. PERSONAL AUTHOR(S)
Dr Quinn

13a. TYPE OF REPORT	13b. TIME COVERED	14. DATE OF REPORT (Year, Month, Day)	15. PAGE COUNT
Final	FROM 29Aug-2SEp 88		

16. SUPPLEMENTARY NOTATION

17. COSATI CODES			18. SUBJECT TERMS (Continue on reverse if necessary and identify by block number)
FIELD	GROUP	SUB-GROUP	

19. ABSTRACT (Continue on reverse if necessary and identify by block number)

Considerable attention is being focused in recent years on the development of high speed optoelectronic devices not only due to their internet speed and parallelism but also due to the ease with which these devices can be interfaced with the current Optical Distributed Arithmetic Unit (ODAU) which is capable of performing high speed binary arithmetic.

Keywords: liquid crystal devices, compound semiconductors (KR)

20. DISTRIBUTION / AVAILABILITY OF ABSTRACT	21. ABSTRACT SECURITY CLASSIFICATION
☐ UNCLASSIFIED/UNLIMITED ☐ SAME AS RPT. ☐ DTIC USERS	UNCLASSIFIED

22a. NAME OF RESPONSIBLE INDIVIDUAL	22b. TELEPHONE (Include Area Code)	22c. OFFICE SYMBOL
GILES	(202) 767-4931	NE

DD FORM 1473, 84 MAR 83 APR edition may be used until exhausted. All other editions are obsolete.

SECURITY CLASSIFICATION OF THIS PAGE

PROGRAM UPDATE

AND ERRATUM

P. 14 Poster P1.02 see new title and summary enclosed

P. 18 Paper C2 was omitted from the final program

C2 **Hybrid electronic/non coherent optical processor for large scale phased arrays**, J. Riehl, J. Appel, A.Thiriot, J. Dorey, Office National d'Etudes et de Recherches Aérospatiales, Châtillon (France)

P. 19 Paper C3, new title :

"Bit serial optical computing design"

P. 22 Paper B7 has been withdrawn and will be replaced bu an oral post-deadline paper

P. 23 Paper A6, new abstract :

"Different types of memories on the base of fiber optic round circuits of the data recirculation for the fast signal processing and optical computing are presented"

P. 26 Poster P2.10 see new title and summary enclosed

P. 28 Paper D4 : see summary enclosed

P. 33 Poster P3.02 has been withdrawn

POST DEADLINE PAPERS

(abstracts and summaries enclosed)

Postdeadline 1 : **Optical crossbar interconnection using vertical to surface transmission electo-photonic devices (VSTEP)** K. Kubota, Y Tashiro, K. Kasahara, S. Kawai.

Postdeadline 2 : **Multiple Quantum well nonlinear optical directional coupler as a logic/computing element** M. Cada, B.P. Keyworth, J.M. Geinski, AJ. Spring Thorpe, P. Mandaville.

Postdeadline 3 : **Experimental results from an optical implementation of a simple neural network** H.J. White.

Postdeadline 4 : **Dual resonator optical logic gate** D.A. Holm, B.A. Capron.

Postdeadline 5 : **Intrinsic spatial filtering properties in B S 0 crystals** L.M. Zerbino, N. Bolognini.

Postdeadline 6 : **Critical coupling strength for enhanced four-wave mixing by use of moving interference gratings in diffusion dominated photorefractive crystals** C. Denz, J. Goltz, T. Tschudi.

P1 02

Stochastic Modeling of the Optical Distributed Arithmetic Unit

C. D. Knittle and S. S. Udpa
NSF ERC for Optoelectronic Computing Systems
Department of Electrical Engineering
Colorado State University
Fort Collins, CO 80523, U. S. A.

Summary

Considerable attention is being focused in recent years on the development of high speed optoelectronic devices not only due to their inherent speed and parallelism but also due to the ease with which these devices can be interfaced with the current electronic world. This paper presents a new device called the Optical Distributed Arithmetic Unit (ODAU) which is capable of performing high speed binary arithmetic.

The Optical Distributed Arithmetic is conceptually somewhat similar to the time integrating correlator proposed by Kingston [1]. There are, however, substantial differences in the manner in which the data is processed. The ODAU consists of a spatial light modulator (SLM) optically coupled to a photo detector array (PDA) on a cell-by-cell basis. This doubled layered structure is placed in front of an injection laser and lens arrangement as shown in Figure 1. The SLM and PDA are charge coupled structures built on multiple quantum wells of InP/GaAs. Quantum wells are regions containing excitons, which are loosely bound pairs of electrons and holes. The excitons absorb light at wavelengths which are a function of the electric field and hence the amount of charge in the cell. As the laser is pulsed the light incident on the surface of the SLM is modulated according to the amount of charge present in the cell. The transmitted light then generates a charge in each PDA cell proportional to the intensity of the light incident on it integrated over the exposure period. The charge generation is cumulative in that the generated charge will be superimposed on any charge existing in a PDA cell. The ODAU includes a simple carry unit for each column to restore data in binary form as well as serve as a regeneration unit.

Addition is accomplished by clocking the two binary operand streams into the columns of the SLM and PDA and flashing the laser. The contents of the SLM are linearly superimposed on the contents of the PDA resulting in addition. In order to obtain the sum in a binary form, the contents of the PDA are clocked through the carry units. In the case of vector/scalar multiplication, the binary operand streams representing the elements of the vector are clocked into the SLM. The scalar operand stream is applied sequentially to the laser. Execution of an appropriate sequence of shifts and adds results in multiplication. Addition and multiplication operations can be performed simultaneously with no additional overhead for addition by clocking in the operands to be added into the PDA prior to the initiation of multiplication.

In addition to a detailed description of the device the paper presents a mathematical model incorporating several sources of noise and characterizing the device. Statistical expressions for the expected value and covariance of the charge in any cell of the SLM and PDA are presented. It is shown that the variance associated with the charge in a cell converges very rapidly within two or three shifts. The device was also simulated on the computer using the model to estimate bit error rates as a function of the signal-to-noise ratios (SNR) associated with the various noise sources. Simulation exercises were also carried out to estimate optimum threshold levels for the carry unit. These tests were repeated for devices where the result was allowed to accumulate in the PDA over more than one cycle before a carry operation was initiated. The simulation exercises have shown that the device is indeed viable if the SNR associated with the transfer efficiency can be held above a minimum value. The analysis has also revealed other limits of the device.

The paper concludes with a brief discussion on the applications of the device. It is shown that the device lends itself very well to implementations of signal processing algorithms.

References

[1] Kingston, R. H.,"Signal Correlation Using a One Dimensional Electroabsorptive CCD Spatial Light Modulator," Proc. of the IEEE, Vol. 72, No. 7, July 1984, pp. 954-961.

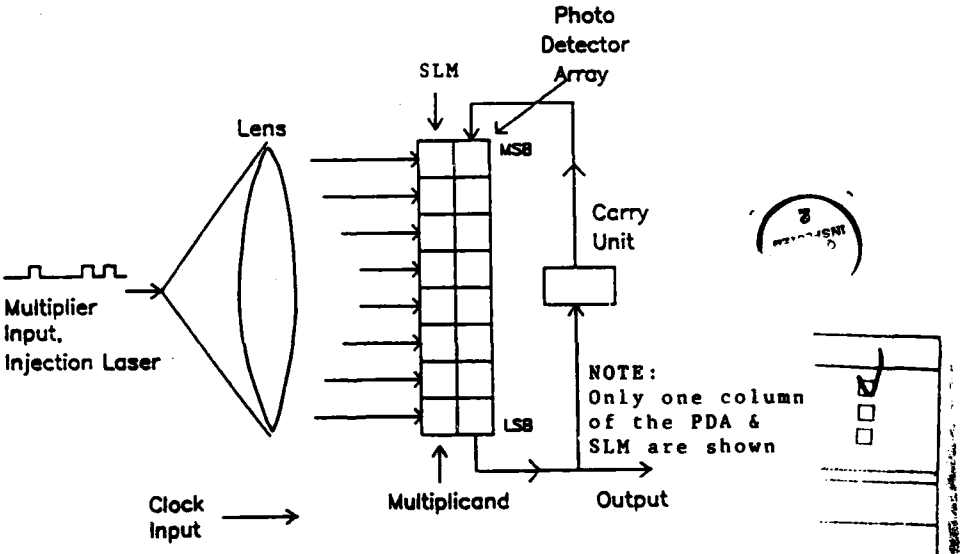

Fig. 1 Optical Distributed Arithmetic Unit

A6

FIBER OPTIC DYNAMIC MEMORY FOR THE FAST SIGNAL PROCESSING AND OPTICAL COMPUTING

M.I.Belovolov, B.M.Dianov, V.I.Karpov, V.N.Protopopov, V.N.Serkin

General Physics Institute, Academy of Sciences of the USSR,
38 Vavilov Street, Moscow 117942, USSR

ABSTRACT

Different types of memories on the base of fiber optic round circuits of the data recirculation for the fast signal processing and optical computing are presented.

P210

CONOSCOPIC TELEVISION SYSTEM

Didier CHARLOT

LE CONOSCOPE S.A.

and

Gabriel Y. SIRAT and Eric Y. DUFRESNE

Ecole Nationale Supérieure des Télécommunications Département Images,

46 rue Barrault,75634 Paris Cedex 13, France

Demetri PSALTIS

California institute of Technology

PASADENA CA 91125

A holographic camera and a three-dimensional workstation, based on the principle of conoscopic holography, are currently under development and will be presented. The development is pursued at "LE CONOSCOPE " in collaboration with E.N.S.T. for industrial three-dimensional imaging purposes.

Conoscopic holography is a holographic technique based on light propagation in uniaxial cristals. In this process the diffraction pattern is obtained by illuminating the object by an incoherent monochromatic light and by imaging it through a birefringent crystal located between two circular polarizers. A simple presentation of conoscopic holography is to consider the ordinary and the extraordinary waves, that are separated naturally by the uniaxial crystal, as equivalent to the object and reference beams in a coherent hologram.

The scale of the effect, characterized by an equivalent wavelength, is tunable and depends on the opto- geometrical parameters of the system. It can vary from 3 to 100 times the recording light wavelength. This scale factor allows digitization in real time of the holograms on a CCD camera. More over, there is no problem of stability between the ordinary and the extraordinary waves unlike between the object and reference waves in coherent holography. One of the main advantages of conoscopic holography is the simplicity of the system, built only with crystals, wave-plates and polarizers.

The camera is built on a *standard* CCD sensor, a *standard* optical system and the addition of the conoscopic pre-objective - the **conoscope** - mounted between the optics and the camera. The heart of the conoscope is a uniaxial birefrigent crystal. In the first prototype we used a cylindrical calcite crystal with a diameter of 20 mm and a length of 35 mm. The optical axis was parallel to the cylinder axis. The conoscope also contains two circular polarizers or a circular polarizer, a quarter wave-plate and a linear polarizer. The illuminating source was an **incoherent monochromatic** sodium lamp.

This system will record a *complex* conoscopic hologram containing the complete three-dimensional information of the viewed object.

The three-dimensional workstation is built from a *standard* frame grabber and a microcomputer. The video signal from the camera is digitized and processed by the station to yield either the complete three-dimensional object or differential information.

The numerical processing is based on the properties of the Fresnel Transform which is readily computed from the Fourier Transform, and so the bulk of the computational task can be parallelized and dedicated hardware can be used.

Utilising additional computer power such as an array processor or a FFT dedicated hardware (numerical or optical) a 128 x 128 x 128 resolution and a quasi real time (1s) are targeted for the prototype.

In this paper we will present parameters, theoretical and experimental results of the system, and possible applications.

D4

FREQUENCY MULTIPLEXED RASTER AND NEURAL NETWORKS

Raymond C. CHEVALLIER, Gabriel Y. SIRAT ,and Kevin HEGGARTY
Ecole Nationale Supérieure des Télécommunications,Département Images,
Groupe Optique, 46 rue Barrault, 75634 PARIS cedex 13 FRANCE

In the first part of this paper we will present Frequency Multiplexed Raster (FMR) optical implementation of neural networks. A hidden difficulty for hardware (optical and electronic) implementation is the dimensionality of the synaptic matrix which is twice the dimension of the input and output matrices or vectors.

For two-dimensional images, which is, we believe, one of the greatest potentialities of neural networks, the synaptic matrix is *4D* and cannot be directly implemented in optics.

We propose Frequency Multiplexed Raster (FMR) as a method to fold this matrix in a two-dimensional format. The FMR coding permits to map a four dimensional array on a two-dimensional array in such a way that the operations needed to implement a neural network can be performed by a *simple optical system.*

Let us start by discussing the simpler 2D $\rightarrow$ 1D mapping. For simplicity, we present the mapping of a two-dimensional image into a one-dimensional **time** signal. A standard way of coding a 2D object into a 1D time signal is the well known television raster : Time Multiplexed Raster; the image is scanned, one pixel after the other, line after line. As early as 1925, Fournier d'Albe proposed an alternative coding scheme, Frequency Multiplexed Raster, where each pixel is associated to one different temporal frequency. The spatial information of the original image is thus mapped onto the frequency domain of an electrical signal. A one to one relation exists between the spatial frequency domain and the time domain as well as between the spatial domain and the temporal frequency domain. This mapping allows spatial frequency manipulations through sequential processing of an electric signal.

The same formalism permitting to code a two-dimensional image on a one-dimensional time signal was extended to permit the coding of a four-dimensional matrix on a two-dimensional **spatial** matrix by performing FMR coding on x and y axis separetly. The 2D inputs, whether probes or memories, are also coded into N^2*N^2 arrays, for compatibility purposes.

In the second part of this paper we will describe the system built in our laboratory showing the feasability of FMR optical neural networks. The system is built from an optical input module, a fixed synaptic matrix coded on a transparency, a CCD camera and a micro-computer which perform the thresholding and feedback operations. In a later stage the fixed matrix will be replaced by a programmable matrix. Such a system is composed of three subsystems :

- a coding processor in which the binary original memories are coded into a synaptic matrix ;

- a mass storage element, to store the synaptic matrix ;

- a retrieval processor such that a probe introduced in this processor converges to the memory closest to it, provided the probe is within the "attracting basin" of that specific memory.

Each one of these subsystems can be implemented by an optical system, by an analog electronic system or by a digital system. The choice between the implementations has to be guided by technological and practical considerations, and evolves with availability of new technologies and devices.

We make the initial choice of a hybrid digital/optical system in which only the procedures in which N^4 operations are needed - (N^2 being the number of pixels) are implemented optically : all other operations are implemented digitally ; moreover, we keep a digital option for the coding processor, since a fast response time is not needed in that case. Although these choices may seem timid compared to proposed all-optics schemes, we observe that in the present state of the art, these conservative choices lead to systems available in an acceptable range of time. Of course, these systems may evolve, with the technologies, towards all optics systems.

OPTICAL CROSSBAR INTERCONNECTION USING VERTICAL-TO-SURFACE TRANSMISSION ELECTRO-PHOTONIC DEVICES (VSTEP)

K.Kubota, Y.Tashiro, K.Kasahara, S.Kawai

Opto-Electronics Research Laboratories, NEC corporation

1-1, Miyazaki 4-chome, Miyamae-ku, Kawasaki, Japan

Abstract

A new optical interconnection using 1-D electro-photonic semiconductor arrays (VSTEP), is presented. It realizes variable interconnection, signal summation and thresholding functions for optical neural networks.

postdeadline 1-1

OPTICAL CROSSBAR INTERCONNECTION USING VERTICAL-TO-SURFACE TRANSMISSION ELECTRO-PHOTONIC DEVICES (VSTEP)

K.Kubota, Y.Tashiro, K.Kasahara, S.Kawai
Opto-Electronics Research Laboratories, NEC corporation
1-1, Miyazaki 4-chome, Miyamae-ku, Kawasaki, Japan

Optical interconnection is a promising technology for neural networks and parallel processing, because of its ability to provide global interconnections without bandwidth deterioration according to the connection capacitance. Recently, various optical interconnections were proposed for this purpose.[1~3] However, optical implementations were complicated and their module sizes were difficult to be reduced. This paper presents a new category of optical crossbar interconnection, realizing variable interconnection, signal summation and thresholding in a simple configuration, using a Vertical-to-Surface Transmission Electro-Photonic device (VSTEP)[4] as a light source, detector and thresholding device.

Figure 1 shows a schematic drawing of the optical crossbar interconnection. It is composed of a couple of one dimensional(1-D) VSTEP arrays and a spatial light modulator(SLM). Those 1-D VSTEPs have a stripe shape, where the stripe directions are orthogonal with regard to each other. Input signal I_i(i=1~n) individually drives the strip $VSTEP_1$. Light emitted by the $VSTEP_1$ passes through the SLM, where the optical transmission of the matrix element (j,i) is W_{ji} and is detected by the 1-D $VSTEP_2$ in the stripe direction. This means that input signal I_i can be obtained from any output O_j, according to the SLM's pattern. The VSTEP also has a thresholding function as well as a light source and detector. Therefore, the output signal O_j(j=1~m) from the 1-D $VSTEP_2$ is obtained by multiplexing w_{ji} to I_i and thresholding, as follows.

$$O_j = f\left(\sum_{i}^{n} W_{ji} * I_i - I_b\right) \qquad (1)$$

where f is a thresholding function and I_b is a bias. Therefore, the presented crossbar interconnection works the same as neural networks.

Figure 2 shows a photomicrograph of 1-D VSTEP arrays (8 arrays), where each VSTEP has 8 windows in a stripe direction. The incident light is detected through these windows. A cross sectional view of the VSTEP is shown in Fig.3. The present VSTEP has pnpn structure,[5] grown on a semi-insulating GaAs substrate with molecular beam epitaxy. An n-GaAs gate layer acts as a light absorption and light emitting layer. When positive bias voltage V_b, which is lower than the switching voltage V_s, is applied to the VSTEP and light is fed to the device, VSTEP turns on, and radiates spontaneous light. The light power for switching the VSTEP depends on the bias voltage V_b. Therefore, the light signal summation and thresholding functions can be carried out.

The experimental set up for the optical crossbar interconnection, shown in Fig. 1, was built up using a couple of 1-D VSTEPs, a photomask in place of the SLM and a lens imaging the 1-D $VSTEP_1$ onto the 1-D $VSTEP_2$. Individual interconnections between the input and output channels were carried out, and the fundamental function of the neural networks, where the summation of the input signal multiplied by weighting factor is thresholded, was confirmed. Figure 4 shows the the switching voltage decrease ΔV of the $VSTEP_2$ with the $VSTEP_1$ light incident on the VSTEP2. The thresholding level could be determined by the bias voltage V_b. The clock rate for the operation was up to 8 Mbps, limited by the connection loss of the imaging lens. Other experiments indicate 400 Mbps operation with sufficient light power on the VSTEP.

postdeadline12

The presented optical interconnection, using VSTEP, has a simple configuration and has excellent potential for realizing a very large scale network at high speed, because of its functions regarding variable interconnection, signal summation and thresholding. Furthermore, the VSTEPs are used at the input and output in the presented configuration. Therefore, it is possible to connect them in cascade for constructing optical multilayer networks, such as back propagation machines or pipe-line optical processors.

The authors would like to thank Drs. M.Sakaguchi, N.Nishida, R.Lang and K.Yanase for their suggestions and encouragement.

References

1. D.Z.Anderson and D.M.Lininger;Appl.Opt.26,5031(1987).
2. K.Wagner and D.Psaltis;Appl.Opt.26,5061(1987).
3. M.E.Prise,S.J.Walker and M.M.Downs;IQEC'88,p318(1988).
4. K.Kasahara et al.;Appl.Phys.Lett.52,679(1988).
5. G.W.Taylor et al.;J.Appl.Phys.,59,596(1986).

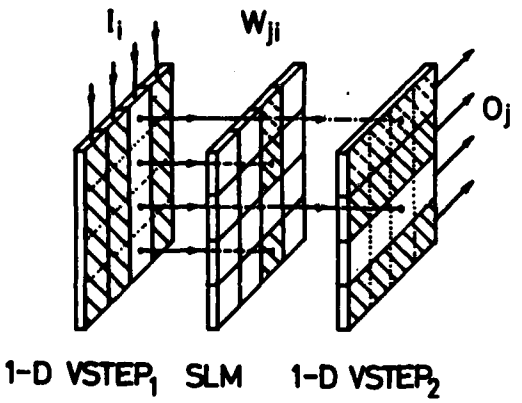

Fig.1 Schematic drawing of the optical crossbar interconnection

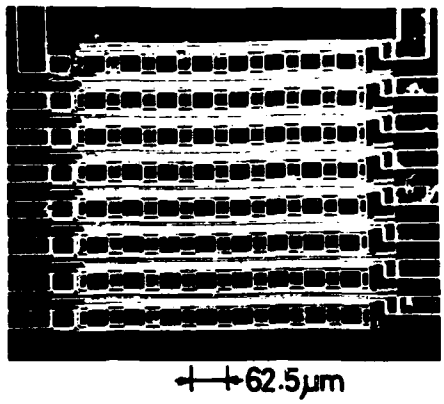

Fig.2 Photomicrograph of 1-D 8 VSTEP arrays. Each VSTEP has 8 windows for light absorption and emission

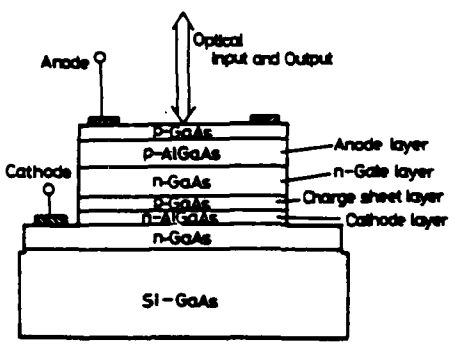

Fig.3 Cross sectional view of the VSTEP

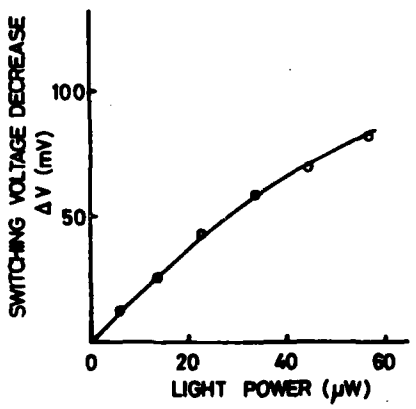

Fig.4 Switching voltage decrease with light incident on the VSTEP

post deadline 13

MULTIPLE QUANTUM WELL NONLINEAR OPTICAL DIRECTIONAL COUPLER AS A LOGIC/COMPUTING ELEMENT

M. Cada, B. P. Keyworth, J. M. Glinski*, A. J. SpringThorpe*, P. Mandaville*

Technical University of Nova Scotia, P. O. Box 1000, Halifax, N. S. B3J 2X4, Canada

TEL: (902) 429-8300, FAX: (902) 429-2176

*Bell-Northern Research Ltd., Ottawa, Ontario K1Y 4H7, Canada

TEL: (613) 763-5961

Abstract

We analyzed, designed and fabricated (using the molecular beam epitaxy technique) a planar GaAs-based multiple quantum well (MQW) directional coupler. Due to a large Kerr-type nonlinearity of the MQW coupling medium near the exciton resonance wavelength an efficient all-optical control of the transfer of energy between the two waveguides is achieved. An application to implementing optical computing devices is straight-forward and promising.

postdeadline 2-1

Summary

With the progress in optical communication technology, optical fibers have become the medium of choice for high data rate transmission. Currently, the processing of signals relies on conventional electronically controlled devices. These hybrid systems are often inefficient and limited in their information-carrying capacity.

Also in computing technology, high-performance systems of the future would suffer from interconnecting problems associated with electronic devices as well as from inherent limitations of purely electronic chips.

A better alternative seems to be to employ all-optical information processing or a combination of advantages of electronics and optics generally, using novel optical and optoelectronic devices which are now being studied and developed. One such device, the nonlinear coherent coupling element, is discussed in this contribution.

The directional coupler employs the coherent interaction of two optical waveguides placed in close proximity. The nonlinear version of the coupler utilizes a nonlinear medium to control this interaction.

Our group analyzed, designed and fabricated (using the molecular beam epitaxy technique) a planar GaAs-based multiple quantum well directional coupler. In this structure, two linear and lossless optical waveguides made of AlGaAs of a proper composition are coupled through a multiple quantum well material that exhibits a large Kerr-type nonlinearity at or near the exciton resonance wavelength.

Changes in the refractive index related to exciton resonances lead to variations of the interaction length of the coupler which in turn determines the distribution of optical power at the output. A strong nonlinear switching occurs near the so-called critical power.

In our experiments, the optical intensity-controlled transfer of energy between the two waveguides of the coupler was shown to be very efficient at low input optical powers (milliwatts) and for short lengths of the sample (hundreds of micrometers).

The element could be used, for example, for switching of optical signals using the intensity of the light itself as the controlling source. It also holds a promise for the development of future all-optical integrated logic or computing devices.

postdeadline 2-3

Experimental results from an optical implementation of a simple neural network

H.J. White

Sowerby Research Centre, FPC 267, British Aerospace plc
PO Box 5, Filton, Bristol, BS12 7QW, UK

1 Introduction

Much recent work in the field of optical computing has concentrated upon the parallel associative memory/neural network algorithms. Here we present results from an implementation of a simple neural network. An optically addressed spatial light modulator (SLM) is used to perform thresholding and thin amplitude computer generated holograms perform the weighted interconnections. Two 6-bit vectors and their complements were stored as the memories and the network was found to always converge to the memory closest in terms of Hamming distance to the input vector. This performance is better than that of an electronic simulation of the model and this difference has been found to result from the temporal characteristics of the SLM (a Hughes Liquid Crystal Light Valve (LCLV)). The temporal response acts to give greater stability to the memories and as such allows a larger number of memories to be stored on a given size of network. It is believed that this temporal response can be used to advantage in future fast switching SLMs.

2 The Neural Network Model

The model implemented was the Hopfield model [1] with bipolar vectors and with all the vector elements being updated simultaneously. As reported previously [2] this can be described by the equations:

$$T_{ii} = 0 \quad \text{and} \quad T_{ij} = \sum_{m=1}^{M} s_i^{(m)} s_j^{(m)} \tag{1}$$

$$T = T^+ - T^-, \quad s = s^+ - s^-, \quad s_j^+ + s_j^- = 1 \tag{2}$$

$$\left.\begin{aligned} s_i^{(out)+} &= 1 \\ s_i^{(out)-} &= 0 \end{aligned}\right\} \quad \text{if} \quad \sum_j^N (T_{ij}^+ s_j^{(in)+} + T_{ij}^- s_j^{(in)-}) \geq \tfrac{1}{2} \sum_j^N (T_{ij}^+ + T_{ij}^-)$$

$$\left.\begin{aligned} s_i^{(out)+} &= 0 \\ s_i^{(out)-} &= 1 \end{aligned}\right\} \quad \text{if} \quad \sum_j^N (T_{ij}^+ s_j^{(in)+} + T_{ij}^- s_j^{(in)-}) < \tfrac{1}{2} \sum_j^N (T_{ij}^+ + T_{ij}^-) \tag{3}$$

Where M=number of memories; T=matrix of interconnections; $s^{(in)}$=input vector; $s^{(out)}$=output vector (becoming the input vector for the next iteration); $s^{(m)}$=memory vector.

3 Optical Implementation

The optical system set up to implement the Hopfield neural net is shown in figure 1. The input vector $s^{(in)}$ is recorded on a photographic plate and entered into the system with a collimated laser beam. The LCLV is used as the thresholding device and it is biased in such a way to produce two binary vectors being the complement of each other from this input. In this arrangement if the input beam consists of the vector $s^{(in)}$ the outputs will

post-deadline 3-1

be the vectors $s^{+(in)}$ and $s^{-(in)}$. Typical output versus input curves for the LCLV are shown in figure 2.

Holographic interconnections are used to perform the vector–matrix multiplications in equation (3). The sub-products required for this are:

$$T_{ij}^{-} s_j^{-} \quad \text{and} \quad T_{ij}^{+} s_j^{+} \quad \text{for } j = 1 \rightarrow N$$

where s_j is a given element of the input vector. Holograms have been created which store all the elements of T_{ij}^{+} for a particular value of j. The operation of such a hologram is such that when addressed by a light intensity s_j^{+}, N spatially separated outputs are produced which have intensities equal to the products $T_{ij}^{+} s_j^{+}$. N holograms, one for each value of j, are used such that the output from the holograms overlap and incoherently add to produce N spots. This incoherent addition is performed by means of a diffusor on the write side of the LCLV. The intensity of the spots give the the resultant vector s'^{+} where:

$$s_i'^{+} = \sum_{j}^{N} T_{ij}^{+} s_j^{+} \tag{4}$$

The holograms are Lee type computer generated holograms which were calculated and plotted with a laser printer, before being photoreduced onto holographic plate.

Two 6-bit memories were stored on the system, these were folded to form 2×3 pixellated images. As is usual with the Hopfield model the complement vectors also become memory states. The memories stored were a 'T' (+1,+1,+1,-1,+1,-1) figure 3(a) and an 'L' (+1,-1,-1,+1,+1,-1) figure 3(b) and their complements (-1,-1,-1,+1,-1,+1) and (-1,+1,+1,-1,-1,+1) figures 3(c and d). The holograms storing the positive and negative weightings for these memories are shown in figure 4. The positive hologram only consists of four elements because there are no positive weightings from elements 4 and 6.

4 Results

Figures 5 to 8 show the output of the system in response to different inputs. This shows that the system is capable of retriving a stored vector from an input which is a noisy representation of that vector. All the 64 possible input vectors were entered into the system and in each case the output vector was the stored vector nearest in terms of Hamming distance to the input.

In a simulation of the system, sychronous updating of the thresholding elements was assumed. The results of this simulation showed that the 'T' stored vector was much more stable than the other stored vectors due to the greater number of positive ones it contains. This did not manifest itself in the optical system because the LCLV responds faster to an input which greatly exceeds the threshold level compared to an input which only just exceeds the threshold level. For certain inputs, the output from a quickly responding element is fedback through the holographic interconnections in time to prevent slowly responding elements from switching on at all. It is this effect which makes the stored vectors equally stable in this optical system. Although the LCLV is inadequate for any serious optical computing system it is believed that this temporal response can be used to advantage in future fast switching SLMs.

4 References

1. J.J.Hopfield *"Neural networks and physical systems with emergent collective computational abilities"* Proc. Natl. Acad. Sci. U.S.A. Vol. 79 2554–2558 (1982).

2. H.J.White, W.A.Wright *"Holographic implementation of a Discrete Hopfield Neural Network Model"* Proc. SPIE 882 (1988).

postdeadline 3-2

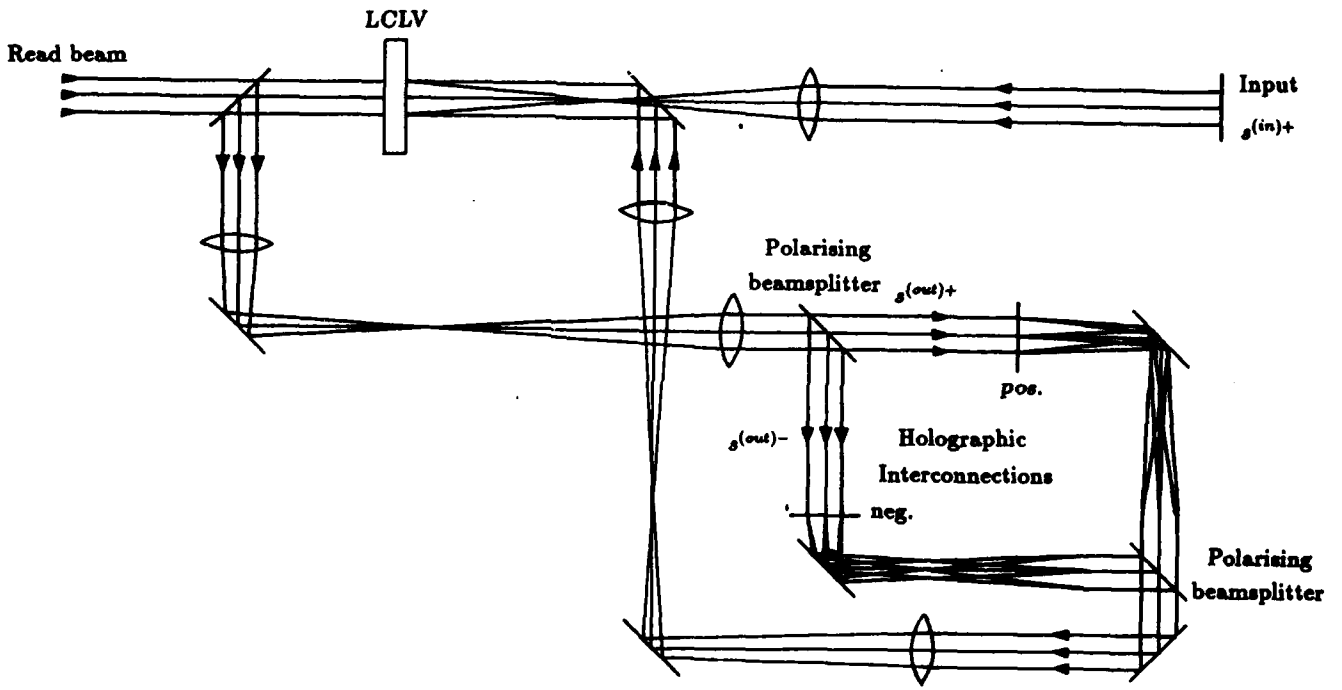

Figure 1: Optical system implementing a neural network

post deadline 3-3

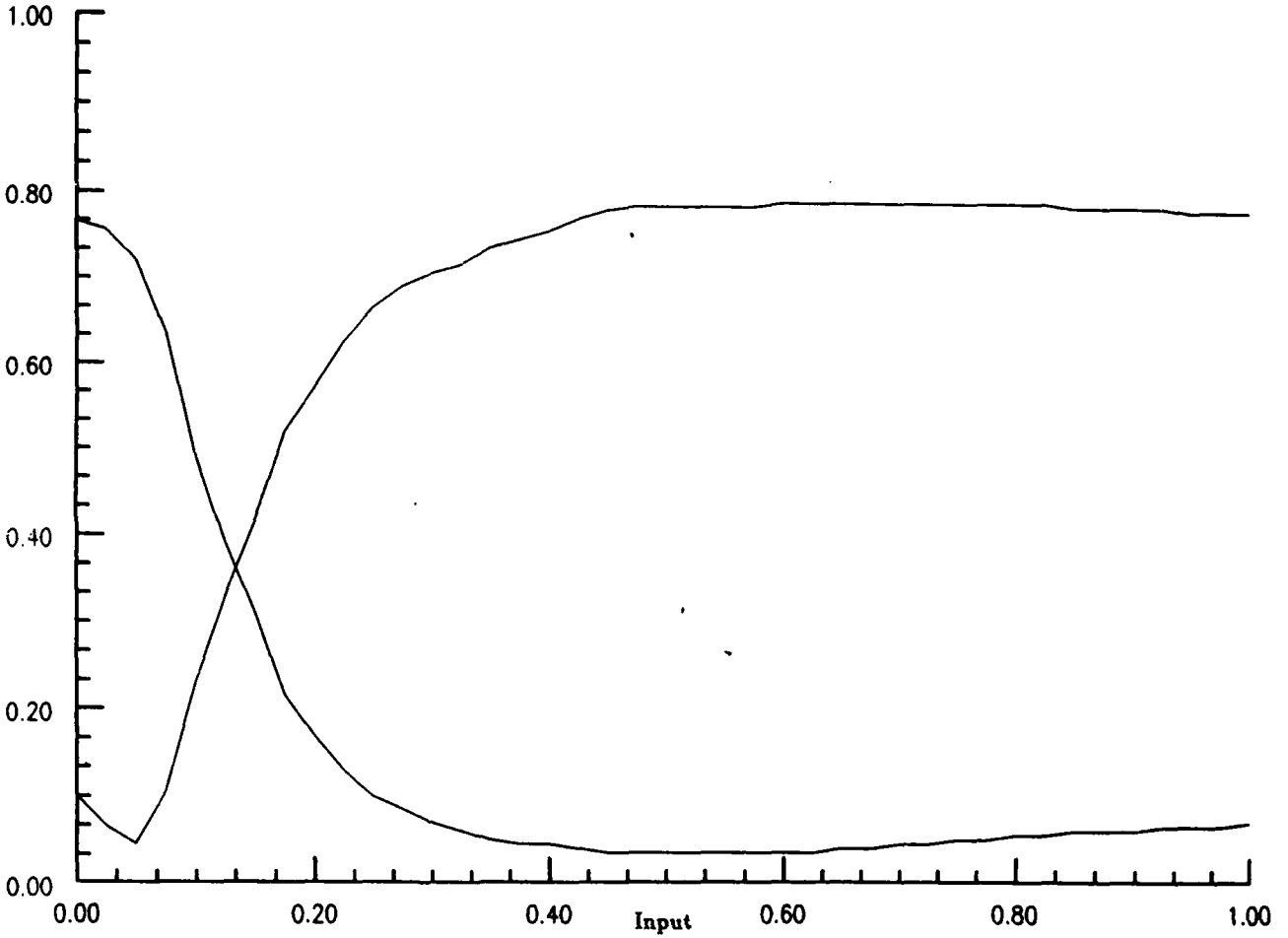

Figure 2: LCLV characteristics showing two complementary outputs simultaneously produced

Figure 3(a)

Figure 3(b)

Figure 3(c)

Figure 3(d)

Figure 3: Stored memories

(a) (+1,+1,+1,-1,+1,-1) (b) (+1,-1,-1,+1,+1,-1)
(c) (-1,-1,-1,+1,-1,+1) (d) (-1,+1,+1,-1,-1,+1)

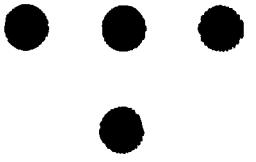

Figure 4(a)

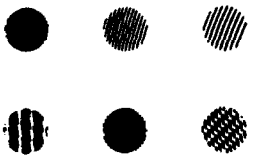

Figure 4(b)

Figure 4: Holograms storing the weightings
(a) positive (b) negative

postdeadline 3-5

Figure 5(a): Input
(+1,+1,+1,+1,+1,+1)

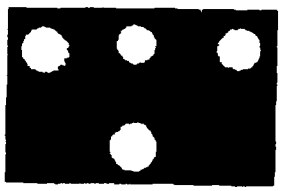

Figure 5(b): Output
(+1,+1,+1,-1,+1,-1)

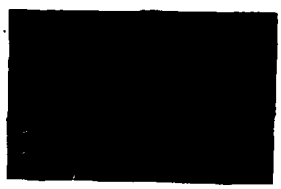

Figure 6(a): Input
(+1,-1,-1,+1,+1,+1)

Figure 6(b): Output
(+1,-1,-1,+1,+1,-1)

Figure 7(a): Input
(-1,+1,+1,+1,-1,+1)

Figure 7(b): Output
(-1,+1,+1,-1,-1,+1)

Figure 8(a): Input
(-1,-1,-1,-1,+1,+1)

Figure 8(b): Output
(-1,-1,-1,+1,-1,+1)

postdeadline 3-6

Dual Resonator Optical Logic Gate

David A. Holm and Barbara A. Capron
Boeing Electronics High Technology Center
P.O. Box 24969
M/S 7J-27
Seattle, Washington 98124-6269

ABSTRACT

We analyze the performance of a novel optical logic gate configured with two intersecting nonlinear Fabry-Perot resonators, illustrating the results for three different nonlinear media.

postdeadline 4-1

SUMMARY

We analyze the performance of a novel optical logic gate which is able to exhibit genuine three terminal behavior. Two Fabry-Perot resonators are configured such that the optical input beams intersect through a nonlinear material. One beam is the bias input and signal output, while the other beam acts as a control. The much weaker control beam may tune or detune the resonator containing the signal beam. Previous discussions of this configuration have been only qualitative.[1] In this work we present quantitative results based on analytical calculations for a medium possessing a linear background absorption and a Kerr nonlinearity. We model the device following the steady-state fields in a single Fabry-Perot cavity work of Miller.[2] The resulting coupled, transcendental equations are solved numerically to give the signal output power. By an appropriate optimization of the design parameters, the crossed resonator geometry can yield differential gains of roughly four, and perform as an optical transistor. Results for this device are compared for three sample media often discussed as potential material candidates for optical computing: bulk GaAs at 0.8 μm, the intraband transition in a GaAs-AlGaAs multiple quantum well at 10 μm, and organic polymers at around 1-2 μm. An important figure of merit relating to the absorption loss (α) and cavity length (L) for crossed

post-deadline 4-2

resonators is desired. Our calculations indicate that optical differential gain can be achieved when $\alpha \cdot L < 0.02$. More detailed calculations will be presented at the conference.

1. L.C. West,. Computer, 34, Dec. 1987.

2. D.A.B. Miller, IEEE J. Quant. Electron., 17, p. 306 (1981).

post deadline 4-3

INTRINSIC SPATIAL FILTERING PROPERTIES IN BSO CRYSTALS

L.M.ZERBINO and N.BOLOGNINI
Centro de Investigaciones Opticas (CIOp). CIC. Argentina

ABSTRACT:

The anisotropic spatial resolution of the photorefractive BSO crystal in the transversal configuration is analysed and showed. Such behavior provides a spatially variant filtering operation.

SUMMARY:

Image processing with photorefractive materials is a very active field. Particulary, BSO crystals are widely used. In this contribution results related with anisotropic resolution in BSO crystals are presented.

In the transversal configuration here employed, the face of light incidence was parallel to the (110) plane and an external field E_{xo} parallel to the $[110]$ direction was applied. With this configuration the induced birefringence $\Delta n(r)$ is evaluated as:

$$\Delta n(r) = \frac{r_{41}}{2} n_o^3 \left(E_{ysc}^2(r) + 4E_x^2(r)\right)^{\frac{1}{2}}$$

where r_{41} is the appropriate photorefractive coefficient of the electrooptical tensor; n_0 is the refractive index without external field; E_{ysc} represents the y-component of the induced space charge field; $E_x(r) = E_{xo} + E_{xsc}(r)$ represents the external applied field plus the x-component of the induced field; the attached coordinate system is x // $[110]$, y // $[001]$, z // $[1\bar{1}0]$; r = (x,y,z).

In order to analyse the mentioned behaviour a Mach-Zehnder interferometer was used. A system of interference fringes (λ = 514 nm) of fixed spatial frequency was projected on the (110) face. The crystal of dimensions $L_x = L_y = 10$ mm, $L_z = 3$ mm, was operated in the Drift dominant mode ($E_{xo} = 7$ kV/cm). The angle between $\vec{E}_{xo}$ and $\vec{K}$ was varied through in plane-rotation of the interference fringes system. The $\vec{K}$ vector is defined perpendicular to the projected fringes and always remains parallel to the (110) plane.

Postdeadline 5.1

Simultaneous read-out ($\lambda = 633$ nm) under different conditions of polarization showed that the measured diffraction efficiency decreases as the angle θ increases. Similar results with different spatial frequencies were obtained (10 to 100 ln/mm). These results could be interpreted considering that the distribution of Δn throughout the crystal tends to be uniform (the same in dark and bright regions) as θ increases for a fixed spatial frequency.

Also, when incoherent illumination was employed, the read-out images (Ronchi rulings) showed a increasingly faded resolution as the stripes rotate from the [001] direction.

This behaviour suggests the implementation of a spatially variant filtering operation with arbitrary selection of the direction to be filtered. Some examples are shown.

Postdeadline 5.2

Critical coupling strength for enhanced four-wave mixing by use of moving interference gratings in diffusion dominated photorefractive crystals

C. Denz, J. Gerst, T. Tschudi
Institut für angewandte Physik, Technische Hochschule Darmstadt
Hochschulstr. 2, 6100 Darmstadt, Western Germany

Abstract

With that technique an increased reflectivity is obtained for a coupling strength above a critical value. Our purely analytical study discusses the important dependence on the pump beam intensity ratio and the (temporal) grating frequency.

Postdeadline C.1

Critical coupling strength for enhanced four-wave mixing by use of moving interference gratings in diffusion dominated photorefractive crystals

C. Denz, J. Goltz, T. Tschudi (Inst. f. angew. Physik, TH Darmstadt)

In four-wave mixing processes (geometry see fig. 1) two writing beams - signal s_1 and pump beam p_1 - form an interference pattern which leads to a corresponding index grating via the photorefractive effect. Diffraction of the readout pump beam p_2 at this volume hologram leads to the phase conjugate signal s_2. In diffusion dominated photorefractive crystals (real coupling coefficient γ) that phase conjugate reflectivity is reduced by destructive interference:
For crystal orientation with $\gamma>0$ the interference grating $s_2p_2^*$ is phaseshifted about π relative to the interference grating $s_1p_1^*$ of the writing beams[1]. Thus the resulting interference grating and correspondingly the index grating is weak. In order to increase the index grating, this negative feedback must be broken. One possibility is deviation from the Bragg-condition[2,3], the other one is the application of a running interference grating which leads to a complex effective coupling coefficient[4]. Thus the light diffracted from the readout pump is modulated by a phase depending on the z-coordinate of the crystal which destroys the phaseshift of π. The final result of both possibilities to destroy negative feedback is an enhanced efficiency of four-wave mixing[3,4].
Numerical evaluations[4] showed that in a diffusion dominated crystal ($BaTiO_3$) an enhancement of reflectivity is possible only if the coupling strength is above a critical value: $\gamma_0 l > 2$, but its dependence on important four-wave-mixing parameters was not examined further. In our purely analytical treatment - assuming diffusion dominated crystals and weak input signals (undepleted pump approximation, guarantees large phase conjugate reflectivities) - we can show that the critical coupling strength depends on the pump beam intensity ratio and can be significantly above 2. We also examine the reflectivity R as a function of the grating (temporal-) frequency Ω. The four-wave mixing reflectivity $R = |s_2(z=0)|^2/|s_1(z=0)|^2$ is for small input signals given by[2]:

$$R = \varrho \cdot \left| \frac{1 - \exp(\gamma)}{\varrho + \exp(\gamma)} \right|^2 \qquad (1)$$

where γ is the coupling coefficient, l is the crystal length and $\varrho = |p_1|^2/|p_2|^2$ for $\gamma_0 > 0$ (or $|p_2|^2/|p_1|^2$ for $\gamma_0 < 0$) is the pump beam intensity ratio. .
The dependence of the coupling coefficient γ on the (temporal) frequency Ω of the interference grating can be calculated by solving Kukhtarev's charge transport equations[5] for a moving interference grating. For weak illumination intensity (arbitrary intensity leads to two time constants) the solution is:

$$\gamma = \gamma_0/(1+i\Omega\tau) \qquad (2)$$

where γ_0 and τ are real valued for diffusion dominated crystals.
Eq. (1) is illustrated in figs. 2 and 3 for several coupling coefficients. Fig. 2 shows the dependence of the reflectivity R on the pump beam intensity ratio ϱ for zero frequency detuning and for optimum frequency detuning. The dependence of the phase conjugate reflectivity R on the frequency detuning $|\Omega\tau|$ itself - with the parameters coupling strength and pump beam intensity ratio - is presented in fig. 3.
From (1) we derive that for

$$|\gamma_0 l| > 2 \left| \frac{\exp(2|\gamma_0 l|) + (\varrho-1)\cdot\exp(|\gamma_0 l| - \varrho}{\exp(2|\gamma_0 l|) + \varrho} \right| \qquad (3)$$

maximum phase conjugate reflectivity R is obtained for $\Omega = 0$. Condition (3) cannot be fulfilled for weak coupling. For strong coupling - $\exp(|\gamma_0 l|) >> 1$) - eq. (3) simplifies to:

$$|\gamma_0 l| > 2 + 2\cdot\varrho\cdot\exp(-|\gamma_0 l|) \qquad (4)$$

and thus the critical coupling strength $c \approx 2 + 2\cdot\varrho\cdot\exp(-c)$ can be significantly above 2. The case $c = 2$ is included in our solution for $\varrho << \exp(c)$[4].
From (4) we see that the critical coupling strength increases with increasing pump beam intensity ratio. Thus we get an enhanced phase conjugate reflectivity especially for weak pump beam intensity ratios. Nevertheless, in the case of strong coupling a significantly enhanced phase conjugate reflectivity can be obtained even for large pump beam intensity ratios, see fig. 2C or 3D.
For strong coupling ($\exp(-|\gamma_0 l|/(1+i\Omega\tau)) << 1$) we get from (1):

$$R = \frac{\varrho}{1 + u^2 + 2uv} \quad \text{with } u = r\cdot\exp\left\{-\frac{|\gamma_0 l|}{1+(\Omega\tau)^2}\right\} \text{ and } v = \cos\left\{\frac{|\gamma_0 l \Omega\tau|}{1+(\Omega\tau)^2}\right\} \qquad (5)$$

Antrag 90... C2

The term uv has for realistic coupling ($|\gamma_0 l| < 2\pi$) an extremum (minimum) only for a single value of $|\Omega|$, while u^2 is a monotonously increasing function. These considerations lead to the conclusion that $R(\Omega)$ has two maxima at $\Omega = \mp \Omega_{opt}$ or one maximum at $\Omega = 0$. The calculation of Ω_{opt} leads to a transcendental equation which must generally be computed numerically. But for the case close to the critical coupling strength ($|\gamma_0 l| \approx c$) we can use the Taylor decomposition to discuss and analyse the R versus Ω curve. The maximum of R is then obtained for

$$\Omega_{opt} = \frac{(6(1-c^{-1}))^{1/2}}{\tau \cdot c} \cdot (|\gamma_0 l| - c)^{1/2} \qquad (6)$$

As (6) shows the R versus Ω curve exhibits two peaks for $|\gamma_0 l| > c$ or the r versus $|\Omega\tau|$ curve exhibits one peak at $|\Omega\tau| = 0$.

To support and extend previous examinations of enhanced four wave mixing reflectivity in diffusion dominated photorefractive crystals by use of moving interference gratings we have analyzed this reflectivity for the case that the coupling strength is near the critical value and the input singal is weak. The reflectivity versus grating (temporal) frequency exhibits two peaks for a coupling strength above a critical value. Furthermore we discussed the critical coupling strength as a function of the pump beam intensity ratio. These examinations ensure systematic adjustment of four-wave mixing efficiency in optical data storage and image processing.

This work is partially supported by Sonderforschungsbereich 185 "Nichtlineare Dynamik" of the Deutsche Forschungsgemeinschaft.

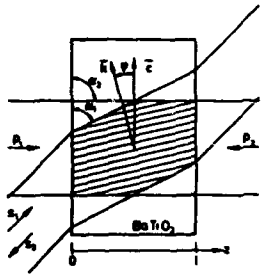

Fig. 1: Principle geometry of four-wave mixing

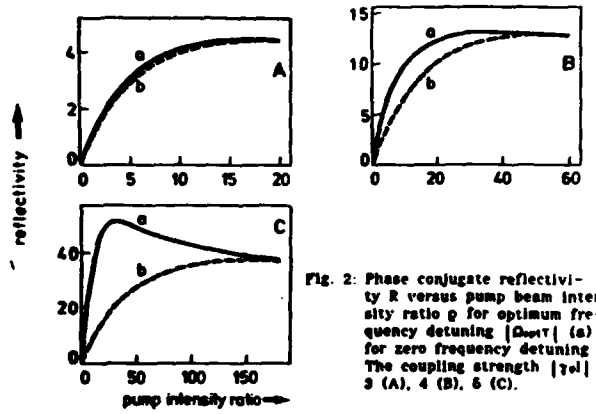

Fig. 2: Phase conjugate reflectivity R versus pump beam intensity ratio ϱ for optimum frequency detuning $|\Omega_{opt}\tau|$ (a) and for zero frequency detuning (b). The coupling strength $|\gamma_0 l|$ is 3 (A), 4 (B), 5 (C).

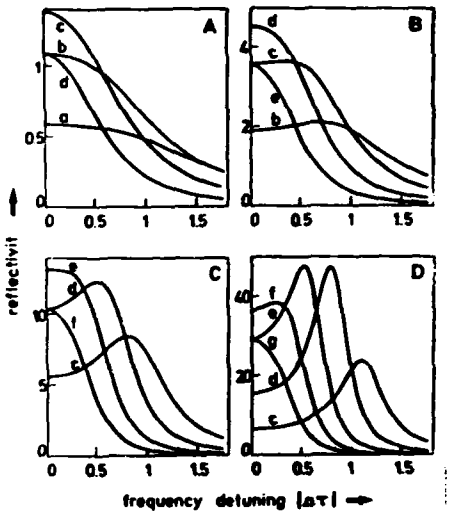

Fig. 3: Phase conjugate reflectivity R versus frequency detuning $|\Omega\tau|$. The parameters are coupling strength $|\gamma_0 l|$ and the pump beam intensity ratio ϱ. $|\gamma_0 l| = 2$ (A), 3 (B 4 (C), 5 (D). ϱ = 1 (a), 2.7 (b), 7.4 (c), 20 (d), 55 (e), 148 (f), 403 (g).

References

[1] B. Fischer, M. Cronin-Golomb, J.O. White, A. Yariv, Opt. Lett. 6, 519 (1981)
[2] J. Goltz, F. Laeri, T. Tschudi, Opt. Comm. 64, 63 (1987)
[3] C. Denz, J. Goltz, T. Tschudi, Opt. Lett., submitted
[4] K.R. MacDonald, J. Feinberg, Phys. Rev. Lett. 55, 821 (1985)
[5] N.V. Kukhtarev, V.B. Markov, S.G. Odulov, M.S. Soskin, V.L. Vinetskii, Ferroel. 22, 949 (1979).

Postdeadline C.3

Monsieur COLLINGS STC TECHNOLOGY LTD.

LONDON RD.

CM1 79NA HARLOW ENGLAND

Monsieur DAINTY IMPERIAL COLLEGE

BLACKETT LAB

SW7 2BZ LONDON ENGLAND

Monsieur FOOTE

BRITISH AEROSPACE PO BOX 5 FILTON

BRISTOL ENGLAND

Monsieur HUTLEY INSTITUT DE PHYS DE GDE BRETAGNE

NATIONAL PHYS. LAB. TEDDINGTON

TW 110 LW TEDDINGTON

Docteur MENDES IMPERIAL COLLEGE

BLACKETT LAB OPTICS

SW7 2BZ LONDON ENGLAND

Monsieur PAIGE OXFORD UNIVERSITY

DEPT OF ENGINEERING SCIENCE PARKS ROAD

OX1 3PJ OXFORD ENGLAND

Monsieur POULSON TAYLOR & FRANCIS LTD

4 JOHN STREET

WC1N 2ET LONDON ENGLAND

Monsieur SELYIAH UNIVERSITY COLLEGE LONDON

DEPT OF ELECTRONIC ENG. TORRINGTON

WCIE 7JE LONDON ENGLAND

Monsieur WHITE

BRITISH AEROSPACE PO BOX 5 FILTON

BS12 7QW BRISTOL ENGLAND

Monsieur XU BLACKETT LAB

IMPERIAL COLLEGE OPTICS SECTION

SW7 2BZ LONDRES ENGLAND

Madame ASTORG DRET

26 BOULEVARD VICTOR

75015 PARIS FRANCE

Monsieur BESSON SOCIETE ANONYME DES TELECOMMUNICATIONS

41 RUE CANTAGREL

75013 PARIS FRANCE

Monsieur BILLON ALCATEL ESPACE

26 AV. J.F. CHAMPOLLION

31037 TOULOUSE FRANCE

Monsieur BRUN INSTITUT D'OPTIQUE SFO

BAT 503 CENTRE UNIVERSITAIRE D'ORSAY

91406 ORSAY FRANCE

Monsieur CAMBON

ENST BRETAGNE ZI

KERNERRENT PLOUZANI FRANCE

Monsieur CHATAUX IOTA

CENTRE UNIVERSITAIRE ORSAY BP 43

91406 ORSAY CEDEX FRANCE

Monsieur CHAVEL INSTITUT D'OPTIQUE SFO

BP 43

91406 ORSAY CEDEX FRANCE

Monsieur CHENEVAS-PAULE

CEA LETI CENG/O.LETI 85X

38041 GRENOBLE CEDEX FRANCE

Monsieur CHRISTY DRET

26 BOULEVARD VICTOR

75015 PARIS FRANCE

Monsieur CLAIR UTC SEVENANS

BP 90010

90010 BELFORT FRANCE

Monsieur COUSSOT

THOMSON-CSF 122 BD GAL LECLERC

92105 BOULOGNE-BILLANCOURT

Monsieur DE BOUGRENET ENST DE BRETAGNE

BP 832

29263 BREST CEDEX FRANCE

Monsieur DUFRESNE

ENST 46 RUE BARRAULT

75013 PARIS FRANCE

Monsieur FERRIER LAB. D'OPTIQUE DES FLUIDES

BD LAVOISIER

49045 ANGERS CEDEX FRANCE

Monsieur FRACES ONERA CERT

2 AV. EDOUARD BELIN

31055 TOULOUSE CEDEX FRANCE

Monsieur FRANTZ CETIA

150 Rue Marcelin Berthelot Z.I TOULON EST

83088 TOULON FRANCE

Monsieur FRIEDRICH CEA

SERVICE CMM 85 X

38041 GRENOBLE CEDEX FRANCE

Monsieur GARDA I.E.F

BAT 220 UNIVERSITE DE PARIS SUD

91405 ORSAY CEDEX FRANCE

Madame GARNERO INSTITUT D'OPTIQUE SFO

BP 43

91406 ORSAY CEDEX FRANCE

Monsieur GARNIER OFFICE NATIONAL D'ETUDES ET DE RECHERCHES

29 AV. DE LA DIVISION LECLERC BP 72

92322 CHATILLON CEDEX FRANCE

Monsieur GORECKI LABORATOIRE D'OPTIQUE FAC SCIENCES

ROUTE DE GRAY

25030 BESANCON FRANCE

Monsieur GRAYEY CNET

ROUTE DE TREGASTEL BP 40

22301 LANNION FRANCE

Monsieur GRESSER

IRP BP 2438 34 RUE MARC SEGUIN

68067 MULHOUSE CEDEX FRANCE

Monsieur GRUN UNIVERSITE LOUIS PASTEUR

5 AV. DE L'UNIVERSITE

Monsieur HERRIAU THOMSON-CSF/LCR

BP 10

91401 ORSAY FRANCE

Monsieur HUIGNARD THOMSON-CSF/LCR

BP 10

91401 ORSAY FRANCE

Monsieur HYDE

ALP OPTICS 267 RUE DU CHATEAU DU ROI

38220 VIZILLE FRANCE

Monsieur IMBERT

INSTITUT D'OPTIQUE

91406 ORSAY FRANCE

Monsieur KOCHER SODERN

1 RUE DESCARTES

94451 LIMEIL BREVANNES

Monsieur LABRUNIE D. LETI-CEA/IROI

CENG- 85 X

38041 GRENOBLE CEDEX FRANCE

Monsieur LAUG ONERA/CERT

BP 4025

31055 TOULOUSE CEDEX FRANCE

Madame LAVAL

FRANCE

Monsieur LE GARREC CEA SACLAY DPC-STS

91191 GIF SUR YVETTE FRANCE

Monsieur LE PESANT THOMSON CSF LCR

DOMAINE DE CORBEILLE

91401 ORSAY FRANCE

Monsieur LEBRETON GESSY

639 BD DES ARMARIS

83100 TOULON FRANCE

Monsieur LEYWRAS

UNIV DE NICE PARC VALROSE

NICE FRANCE

Monsieur LOULERGUE INSTITUT D'OPTIQUE SFO

BAT 503 UNIVERSITE D'ORSAY BP 43

91406 ORSAY FRANCE

Monsieur LOWENTHAL INSTITUT D'OPTIQUE SFO

BP 43

91405 ORSAY CEDEX FRANCE

Monsieur MADANI Institut d'Electronique Fondamentale Univ. Paris Sud

University Paris-Sud Bat 220 I.E.F

91405 ORSAY FRANCE

Monsieur MAINGUET PTT ENST DE BRETAGNE

BP 832

29285 BREST CEDEX FRANCE

Madame MAISSIAT PTT ENST DE BRETAGNE

BP 832

29285 BREST CEDEX FRANCE

Monsieur MALLICK INSTITUT D'OPTIQUE SFO

BAT 503 BP 43

91406 ORSAY CEDEX FRANCE

Monsieur MASSON ANGENIEUX
43570 SAINT HEAND FRANCE

Monsieur NAUDIN IBM FRANCE CER

PLAN DU BOIS

06610 LA GAUDE FRANCE

Monsieur OUDAR CNET

196 AV. H. Ravera

92220 BAGNEUX FRANCE

Monsieur PELEGRIN CERT

BP 4025

31055 TOULOUSE-CEDEX FRANCE

Monsieur PELTIE CENG-DLETI

85 X

38041 GRENOBLE FRANCE

Monsieur PFEIFFER ECOLE NATIONALE SUPERIEURE DE PHYSIQUE

7 RUE DE L'UNIVERSITE

67000 STRASBOURG FRANCE

Monsieur PICOLI CNET

ROUTE DE TREGASTEL BP 40
22301 LANNION FRANCE

Monsieur PUGNET LAB DE PHYS SOL. ASS CNRS DEPT DE PHYSIQUE -

AVENUE DE RANGUEIL

31077 TOULOUSE FRANCE

Monsieur RAJBENBACH THOMSON-CSF/LCR

BP 10

91401 ORSAY FRANCE

Monsieur RIEHL

ONERA BP 72

92322 CHATILLON CEDEX FRANCE

Monsieur ROBLIN SFO INSTITUT D'OPTIQUE

BP 43

91406 ORSAY FRANCE

Madame ROBLIN GROUPE DE PHYSIQUE DES SOLIDES DE L'ENS

UNIVERSITE PARIS VII 2 PLACE JUSSIEU

75251 PARIS CEDEX 05 FRANCE

Madame ROUSSEAU FAC SCIENCES ROUEN

BP 134

76130 MT ST AIGNAU FRANCE

Monsieur SAGET INSTITUT D'OPTIQUE SFO

BP 43

91406 ORSAY CEDEX FRANCE

Monsieur SIRAT ECOLE NAT. SUP DES TELECOM

PARIS FRANCE

Monsieur TABOURY IOTA

BP 43

91406 ORSAY FRANCE

Monsieur TAULEMESSE CNRS

BP 3

91371 VERRIERES LE BUISSON

Monsieur UHRICH

ONERA BP 72

92322 CHATILLON CEDEX FRANCE

Monsieur WANG INSTITUT D'OPTIQUE SFO

BP 43 BAT 503

91406 ORSAY CEDEX FRANCE

Docteur BRENNER APPLIED OPTICS, UNIV. OF ERLANGEN

ERWIN ROMMEL STR.1

8520 ERLANGEN RFA

Docteur BURGGRAF KRUPP ATLAS ELEKTRONIK GmbH

SEBALDSBRUCKER HEERSTR. 235

2800 BREMEN RFA

Mademoiselle DENZ INSTITUT FUR ANGEWANDTE PHYSIK TECH.

HOCHSCHULSTRASSE 2

6100 DARMSTADT RFA

Monsieur DULTZ HEIDRUN SCHMITZER

UNIVERSITAT-PHYSIK

D-84 REGENSBURG RFA

Monsieur GIGLMAYR HEINRICH-HERTZ-INSTITUTE

EINSTEINUFER 37

D-1000 BERLIN 10 RFA

Docteur HARRIS FRIED. DRUPP GMBH

KRUPP FORSCHUNGSINSTITUT MUNCHENER

4300 ESSEN 1 RFA

Docteur HOHENHINNEBUSCH KERNFORSCHUNGSZENTRUM KARLSRUHE

POSTFACH 3640

D-7500 KARLSRUHE 1 RFA

Monsieur IYECHIKA MUNSTER UNIVERSITY

INSTITUT FUR ANGEWANDTE PHYSIK

D-4400 MUNSTER RFA

Docteur JAGER Universitat Munster Institut f. Angew. Physik

Corrensstr. 2/4

D-4400 MUNSTER RFA

Docteur KERSTEN STANDARD ELEKTRIK LORENZ AG

LORENZSTR. 10

7000 STUTTGART 40 RFA

Docteur KUHLOW HEINRICH-HERTZ-INSTITUT

EINSTEINUFER 37

1000 BERLIN RFA

Monsieur LANZL DFVLR

D-8031 OBERPFAFFENHOFEN RFA

Monsieur LOHMANN UNIVERSITAT, PHYSIK

ROMMEL STR. 1

8520 ERLANGEN RFA

Mademoiselle SCHMITZER UNIVERSITY OF REGENSBUR

84 REGENSBURG RFA

Monsieur MARTINI DFVLR

LINDER HOHE

5000 KOLN 90 RFA

Docteur STREIBL PHYSIKALISCHES INSTITUT

ERWIN-ROMMEL STR 1

D-8520 ERLANGEN RFA

Docteur MORGAN AMC

POSTFACH 170423

D-6000 FRANKFURT RFA

Docteur WOLF SIEMENS AG/ FKE 11

OTTO-HAHN-RING 6

D-8000 MUNCHEN RFA

Monsieur PAWLOWSKI HEINRICH-HERTZ-INSTITUT

EINSTEINUFER 37

1000 BERLIN RFA

Docteur ZENSEN SIEMENS AG

TTO-HAHN-RING 6

8000 MUNCHEN 83 RFA

Docteur RATHJEN KRUPP ATLAS ELEKTRONIK GmbH

SEBALKSBRUCKER HEERSTR. 235

2800 BREMEN RFA

Monsieur *REINER* SEL AG ZT/FZB

POSTF. 40 07 49

D-7000 STUTTGART 40 RFA

Monsieur HANEISHI TOKYO INSTITUTE OF TECHNOLOGY IMAGING SCIENCE &

4259 NAGATSUTA MIDORI-KU

227 YOKOHAMA Japon

Monsieur HAYASAKI UNIVERSITY OF TSUKUBA

INSTITUTE OF APPLIED PHYSICS

305 IBARAKI JAPON

Monsieur KUBOTA NEC CORPORATION

JAPON

Monsieur HAYASHI OPTOELECT. TECH. RES

5-5 TOHKODAI

300-26 TSOKOBA Japon

Monsieur KYUMA MITSUBISHI ELECTRIC CORPORATIC

1-1 TSUKAGUCHI-HONMACHI 8-CHOME

661 HYOGO Japon

Monsieur ICHIOKA OSAKA UNIVERSITY

FAC OF ENG. DEPT OF APPL PHYS.

OSAKA Japon

Monsieur MUKOHZAKA HAMAMATSU PHOTONICS K K

1126 1 ICHINO-CHO

435 HAMAMATSU Japon

Monsieur ISHIHARA OPTOELECTRONIC INDUSTRY AND TECHNOLOGY

20 th MORI BLDG, 2-7-4 NICHI SHIMBOSHI

105 MINATU-KU TOKYO Japon

Monsieur KITAYAMA NTT LABS

1-2356 TAKE

HOKOSUKA-SHI Japon

Monsieur OHYAMA TOKYO INSTITUTE OF TECHNOLOGY

4259 NAGATSUTA, MIDORI-KU

227 YOKOHAMA Japon

Monsieur PARK DEPT OF ELEC ENG TOHOKU UNIV.

AZA-AOBA ARAMAKI

980 SENDAI Japon

Monsieur SUZUKI HAMAMATSU PHOTONICS K.K.

1126-1 ICHINO-CHO

435 HAMAMATSU Japon

Monsieur KUROKAWA NTT OPTO-ELECTRONICS LABORATORY 3-

ATSUGI-SHI

24301 KANAGAWA Japon

Monsieur TANAKA MITSUBISHI ELECTRIC CORPORATION MANUFACTURING

1-1 TSUKAGUCHI HONMACHI 8 CHOME

661 HYOGO Japon

Monsieur TSUTOMU HAMAMATSU PHOTONICS K.K.

1126-1 ICHINO-CHO

435 HAMAMATSU Japon

Docteur NAKAGAWA SYSTEM SONGOU KAIHATSU CO., LT

1-28-23 HONGOU, BUNKYO-HU

113 TOKYO Japon

Monsieur UCHIDA DEPT OF ELEC. ENG. TOHOKU UNIV.

AZA-AOBA, ARAMAKI

980 SENDAI Japon

Monsieur YATAGAI UNIVERSITY OF TSUKUBA

TSUKUBA

305 IBARAKI Japon

Docteur ATHALE BDM CORP

7915 JONES BRANCH DR.

22102 MCLEAN ETATS UNIS

Monsieur FISHER NRL

CODE 6537 4555 OVERLOOH AVE SW

20375 WASHINGTON ETATS UNIS

Docteur BARRETT WJ SCHAFER ASSOCIATES INC

1901 NORTH FORT MYER DRIVE

22209 ARLINGTON ETATS UNIS

Monsieur GEORGE THE INSTITUTE OF OPTICS

UNIVERSITY OF ROCHESTER

14627 ROCHESTER ETATS UNIS

Monsieur BINAY SUGLA AT&T BEL LABORATORIES

CRAWFORDS CORNER RD

HOLWDEL ETATS UNIS

Monsieur GEORGIOU IBM T. J. WATSON RESEARCH CENTER

PO BOX 704

10598 YORKTOWN HTS

Monsieur BRADY CALIFORNIA INSTITUTE OF TECHNOLOGY

116-81

91125 PASADENA ETATS UNIS

Monsieur GOODMAN STANFORD UNIVERSITY

DURAND 127

94305 STANFORD ETATS UNIS

Monsieur BROCK LOS ALAMOS NATIONAL LABORATORY

BOX 503 MS B 231

87545 LOS ALAMOS ETATS UNIS

Monsieur GUILFOYLE OPTICOMP CORPORATION

ETATS UNIS

Monsieur BROWN DEPT OF DEFENSE

FT. MEADE

20755 ETATS UNIS

Monsieur HANEY BDM CORPORATION

7915 JONES BRANCH

22102 MCLEAN ETATS UNIS

Monsieur CASASENT CARNEGIE MELLON UNIVERSITY DEPT ECE

15213 PITTSBURGH ETATS UNIS

Monsieur CATHEY UNIV. OF COLORADO OPTOELECTRONIC COMPUTING SYST.

C.B.525

80309-0525 BOULDER

Docteur CAULFIELD THE UNIVERSITY OF ALABAMA IN HUNTSVILLE

Center for Applied Optics RI-E12

35899 HUNTSVILLE ETATS UNIS

Mademoiselle ESHAGHIAN

UNIV. OF SOUTHERN CALIFORNIA DEPT OF EE

90089-0781 SAL 377 LOS ANGELES

Monsieur FALK BOEING AEROSPACE

PO BOX 3999, MS 87-50

98124 SEATTLE ETATS UNIS

Docteur FIGUEROA BOEING ELECTRONICS HIGH TECH CENTER

PO BOX 24969 M/S 7J-05

98124-6269 SEATTLE

Docteur JOHNSON UNIVERSITY OF COLORADO

CAMPUS BOX 425

80309 BOULDER ETATS UNIS

Docteur HARTMANN MCC - ACA/STL

PO BOX 200195

78720-0195 AUSTIN ETATS UNIS

Monsieur KERNER

9519 WOODLEY AV.

20910 SILVER SPRING

Monsieur HENSHAW

SPARTA INC.

02173 WORTHEN ROAD

Monsieur LITYNSKI UNITED STATES MILITARY ACADEMY

DEPT OF ELECTRICAL ENGR, USMA WEST

10996-1787 WEST POINT

Monsieur HESSELINK

STANFORD UNIVERSITY

359 B DURAND ETATS UNIS

Monsieur MAIT university of Virginia

DEPARTMENT OF ELECTRICAL ENGIN.

22901 CHARLOTTESVILLE

Monsieur HEURING CENTER FOR OPTOELECTRONIC COMP. SY

UNIV. OF COLORADO

80309-0425 BOULDER

Monsieur MICELI

ONR

BOSTON ETATS UNIS

Monsieur JAHNS AT&T BELL LABORATORIES

CRAWFORDS CORNER RD RM 4G 510

07733 HOLMDEL ETATS UNIS

Monsieur MURDOCCA AT&T BELL LABS

00M 46-538

07733 HOLMDEL ETATS UNIS

Monsieur JENKINS USC

PHE 306

90089-0272 LOS ANGELES

Monsieur PETERSON MCC

3500 WEST BALCONES CENTER DRIVE

7875 AUSTIN ETATS UNIS

Monsieur PSALTIS CALTECH

MS 116-81

91125 PASADENA ETATS UNIS

Monsieur RALSTON MCC

3500 W. BALCONES CTR. DR.

AUSTIN ETATS UNIS

Monsieur REDFIELD MCC

PO BOX 200195

78720 0195 AUSTIN ETATS UNIS

Docteur REUDINK BOEING ELECTRONICS HIGH TECH CENTER

PO BOX 24969 M/S 7J-29

98124-6269 SEATTLE

Monsieur RHODES GEORGIA INST. OF TECHNOLOGY

SCHOOL OF ELECT. ENGRNG

30332 ATLANTA ETATS UNIS

Monsieur SATISH GUPA COLORADO STATE UNIVERSITY

DEPT OF ELECTRICAL ENG.

80523 FORT COLLINS ETATS UNIS

Monsieur SAWCHUK UNIVERSITY OF SOUTHERN CALIFORNIA

MC-0272

90089 LOS ANGELES ETATS UNIS

Monsieur SCHARF University of Colorado

Dept ECE BOX 425

80309-0425 BOULDER

Monsieur SOFFER HUGHES RESEARCH LABS

3011 MALIBU CANYON ROAD

90265 MALIBU ETATS UNIS

Monsieur STIRK CALTECH

DEPT OF ELECTRICAL ENGINEERING

91125 PASADENA ETATS UNIS

Docteur STUART A. COLLINS OHIO STATE UNIVERSITY

1320 KINNEAR RD

43085 COLUMBUS ETATS UNIS

Monsieur TICKNOR LOCKNEED MISSLES + SPACE CO B/202 O/9720

3251 HANOVER ST.

94304-1191 PALO AITO ETATS

Monsieur TRICOLES GENERAL DYNAMICS

PO BOX 85227

92138 SAN DIEGO ETATS UNIS

Monsieur TYLER CORPORATE TECHNOLOGY PARTNERS

12800 ALTA VERDE LN

LOS ALTOS HILLS ETATS UNIS

Monsieur YARMA IBM T.J. WATSON RESEARCH CENTER

PO BOX 704

10598 YORKTOWN HTS ETATS

Monsieur WAGNER OPTICAL SCIENCES UNIV. ARIZONA

85721 TUCSON ETATS UNIS

Monsieur WU HAMAMATSU CORPORATION

360 FOOTHILL RD

08807 BRIDGEWATER ETATS UNIS

Monsieur YAMAMURA CALTECH

CALTECH 116-81

91125 PASADENA ETATS UNIS

Monsieur YU ELECTRICAL ENGINEERING DEPT

PENN STATE UNIVERSITY

16802 UNIVERSITY PARK

Monsieur PANKOVE UNIVERSITY OF COLORADO

DEPT OF ELECTRICAL AND COMPUTER ENG.

80309-0425 BOULDER

Monsieur TIBOR FISLI

XEROX CORP. 3333 COYOTE HILL RD

94304 PALO ALTO ETATS UNIS

Monsieur DANDLIKER INSTITUT DE MICROTECHNIQUE DE L'UNIVERSITE

BREGUET 2

2000 NEUCHATEL Suisse

Madame CONSORTINI UNIVERSITY DEPT PHYSICS

VIA S. MARTA 3

50139 FIRENZE Italie

Monsieur KLUMB CIBA-GEIGY AG

R-1062 4 06

4002 BASEL Suisse

Monsieur VISIN CISE TECHNOLOGIE INNOVATIVE S.P.A.

LAB. D'HOLOGRAPHIE BP 12081

20134 MILANO Italie

Monsieur LUKOSZ ETH

PROFESSUR FUR OPTIK

8093 ZURICH Suisse

Madame RIZZI

SE LABS.SPA. PO BOX 12081

20134 MILANO ITALIE

Monsieur PIRANI INST. OF QUANTUM ELECTRONICS/ OPTICS

HPP J8

8093 ZURICH Suisse

Monsieur THALMANN INSTITUT DE MICROTECHNIQUE DE L'UNIVERSITE

BREGUET 2

2000 NEUCHATEL Suisse

Monsieur KEINONEN UNIVERSITY OF JOENSUU

DEPT OF PHYSICS PO BOX 111

SF-80101 JOENSUU Finlande

Monsieur BELOVOLOV ACADEMY OF SCIENCES USSR

MOSCOW URSS

Monsieur EVTIHIEV MOSC. PHYS. ENG. INST.

KASHIRSTOA ST.

115409 MOSCOU URSS

Monsieur MOROZOV P.N LEBEDEV INST. ACADEMY OF SCIENCE

LENINSKY PROSPECT 53

117924 MOSCOW RUSSIE

Monsieur PETROV ACADEMY OF SCI . OF THE USSR

LENINGRAD URSS

Monsieur SAARI INSTITUTE OF PHYSICS OF ESTONIAN ACAD. SCI.

RIIA 142 TARTU ESTONIAN

202400 URSS

Monsieur PERINA PALACKY UNIVERSITY

LENONAVA 26

77146 OLOMOUC Tchécoslovaquie

Docteur HARIHARAN CSIRO DIVISION OF APPLIED PHYSICS

BOX 218

2070 LINDFIELD Australie

Monsieur CHANG OPTICAL SCIENCES CENTER

NATIONAL CENTRAL UNIVERSITY CHUNG-LI

32054 CHUNG-LI Taiwan

Monsieur BAKKER FEL-TNO

PO 96864

2509 JG THE HAGUE PAYS-BAS

Monsieur BASTIAANS EINDHOVEN UNIVERSITY OF TECHNOLOGY

DEPT OF ELECTRICAL ENGINEERING PO BOX

5600 MB EINDHOVEN PAYS-BAS

Monsieur FRANKENA DELFT UNIVERSITY OF TECHNOLOGY

NOBELLAAN 13

2641XP PIJNACKER PAYS-BAS

Monsieur WHERRETT HERIOT-WATT UNIVERSITY

EH14 4AS EDINBURGH SCOTLAND

Monsieur EBBENI UNIVERSITE LIBRE DE BRUXELLES

194/5 50 Av F ROOSEVELT

1050 BRUXELLES Belgique

Monsieur THIENPONT VRIJE UNIV. BRUSSEL

PLEINLAAN 2

1050 BRUSSEL BELGIQUE

Monsieur CHALASINSKA-MACUKO INST. OF GEOPHISICS, WARSAW

PASTEURA 7

02-093 WARSAW Pologne

Monsieur SZOPLIK INST OF GEOPHYSICS, WARSAW UNIVERSITY

PASTEURA 7

02-093 WARSAW Pologne

Monsieur LAGERWALL

CHALMERS UNIV. OF TECHNOLOGY

SUEDE

Monsieur ARSENAULT LAVAL UNIVERSITY

2625 RUE PORT ROYAL

G1V-1A5 STE FOY Canada

Monsieur RAGNARSSON NAT'L SWED. BOARD FOR TECH DEV

BOX 43200

S-10072 STOCKHOLM Suede

Docteur SADA TECHNICAL UNIVERSITY OF N.S

PO BOX 1000, HALIFAX

B3J2X4 NOVA SCOTIA Canada

Monsieur SKARP PHYSICS DEPARTMENT

CHALMERS UNIVERSITY OF TECHNOLOGY

S-41296 GOTEBORG Suede

Monsieur TETU UNIVERSITE LAVAL

DEPT GENIE ELECTRIQUE

GEK 7P4 ST FOY QUEBEC Canada

Madame ZERBINO CIOp - FAC. ING. UNLP

CASILLA DE CORREO 124

1900 LA PLATA Argentine

Monsieur AITKEN DEPT ELECTRICAL ENG. QUEEN'S UNIVERSITY

K7L3N6 KINGSTON Canada

Monsieur RANSHAW EDINBURGH UNIVERSITY

MAYFIELD ROAD

EH9 3JZ EDINBURGH SCOTLAND

Monsieur SHABEER UNIVERSITY OF STRATHCLYDE ELECT. & ELECT. ENG

ROYAL COLLEGE BUILDING 204 GEORGE ST

G1 1XW GLASGOW Scotland

Monsieur SMITH HERIOT-WATT UNIVERSITY

PHYSICS DEPARTMENT RICCARTON

EH14 4AS EDINBURGH SCOTLAND

Monsieur SNOWDON HERIOT-WATT UNIVERSITY

PHYSICS DEPT. HERIOT-WATT UNIVERSITY

EH14 4AS EDINBURGH SCOTLAND

Docteur YASS EDINBURGH UNIVERSITY

PHYSICS DEPARTMENT MAYFIELD ROAD

EH9 3JZ EDINBURGH SCOTLAND

Docteur WALKER HERIOT-WATT UNIVERSITY

DEPT. PHYSICS RICCARTON

Monsieur CHEN HARBIN INSTITUTE OF TECH

DEPT OF APPLIED PHYSICS

HARBIN CHINE

Monsieur KEBIN XU HARBIN INSTITUTE OF TECH.

DEPT OF APPLIED PHYSICS

HARBIN CHINE

Monsieur PANTELIC

INST. OF PHYSICS BELGRADE ZEMUN

118 MAKSIMA GORKOG

Monsieur SOO-YOUNG KAIST

DEPT OF EE, PO BOX 150 CHONGRYANGNI

SEOUL Corée

Docteur MAROM TEL AVIV UNIVERSITY

FACULTY OF ENGINEERING RAMAT AVIV

TEL AVIV Israel

Docteur ANDRES Universidad de Valencia

Dpto. Optica

46100 BURJASOT Espagne

Monsieur MENDLOVIC TEL-AVIV UNIVERSITY

FACULTY OF ENGINEERING DEPT OF

69978 TEL-AVIV Israel

Monsieur CAMPOS UNIVERSIDAD DE BARCELONA

DIAGONAL 645

08028 BARCELONA ESPAGNE

Monsieur SAAD TEL AVIV UNIVERSITY RAMAT AVIV

FACULTY OF ENGINEERING EN DEVICES &

69978 TEL AVIV Israel

Madame GONZALO INSTITUTO DE OPTICA

SERRANO 121

28006 MADRID Espagne

Monsieur SHAMIR TECHNION

DEPT ELECTRICAL ENG. TECHNION

32000 HAIFA Israel

Monsieur SHECHTERMAN

EL-OP PO 1165

REHOVOT ISRAEL

OPTICAL COMPUTING 88

BOOK OF SUMMARIES

TOULON, FRANCE

august 29 - september 2, 1988

A topical meeting of the International Commission for Optics (ICO), organized by Société Française d'Optique (SFO), a member of EUROPTICA, with the sponsorship of Optical Society of America (OSA) and the International Society of Optical Engineering (SPIE) cooperating with Association Nationale de la Recherche Technique (ANRT).

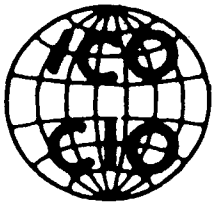

OPTICAL COMPUTING 88

BOOK OF SUMMARIES

TOULON, FRANCE

august 29 - september 2, 1988

A topical meeting of the International Commission for Optics (ICO), organized by Societé Française d'Optique (SFO), a member of EUROPTICA, with the sponsorship of Optical Society of America (OSA) and the International Society of Optical Engineering (SPIE) cooperating with Association Nationale de la Recherche Technique (ANRT).

OPTICAL COMPUTING 88

TOULON FRANCE
August 29-September 2, 1988

A TOPICAL MEETING
OF THE INTERNATIONAL COMMISSION FOR OPTICS,
ORGANIZED BY SOCIETE FRANÇAISE D'OPTIQUE
A MEMBER OF EUROPTICA

Cosponsoring organizations :

- Optical Society of America, O.S.A.
- The International Society of Optical Engineering, S.P.I.E., cooperating with Association Nationale de la Recherche Technique, A.N.R.T..

Collaborating organizations :

- Deutsche Gesellschaft für angewandte Optik, D.G.a.O.
- European Physical Society, E.P.S.
- I.E.E.E. Computer Society
- Institute of Physics, I. of P.
- Société des Electriciens et Electroniciens, S.E.E.
- Société Française de Physique, S.F.P.

With the help of :

- Centre National de la Recherche Scientifique
- Commissariat à l'Energie Atomique (division LETI)
- Conseil Général du Var
- Conseil Régional de Provence, Alpes et Cote d'Azur
- Direction de Recherches, Etudes et Techniques
- Université de Toulon et du Var
- Ville de la Garde
- Ville de Toulon

President of the Meeting	S. Lowenthal (France) I.C.O. president (1984-87)

TECHNICAL PROGRAMM COMMITTEE

- Chairman	J.W. Goodman (U.S.A.) I.C.O. president (1987-1990)
- Co-chairman	P. Chavel (France)
- Secretary	G. Roblin (France)
R. Athale (U.S.A.)	G. Lebreton (France)
J. Bardes (France)	A.W. Lohmann (F.R.G.)
A. Brun (France)	V. Morozov (U.S.S.R.)
D. Casasent (U.S.A.)	D. Psaltis (U.S.A.)
H.J. Caulfield (U.S.A.)	C. Puech (France)
J.P. Christy (France)	W.T. Rhodes (U.S.A.)
P. Gunter (Switzerland)	A.A. Sawchuk (U.S.A.)
S. Ishihara (Japon)	J. Shamir (Israel)
S. Laval (France)	S.D. Smith (U.K.)

ORGANIZING COMMITTEE

- Chairman	J.C. Loulergue
- Ex officio	J.C. Dainty I.C.O. secretary general
J.C. Saget	G. Lebreton Local Chairman
J. Taboury	D. Tessier ARAVI, Arrangements.

Foreword

This is the book of summaries for the International Topical Meeting "Optical Computing 88", to be held in Toulon (France), august 30-september 2, 1988 with organization by the French Optical Society on behalf of the International Commission for Optics. This meeting is one of a series of topical meetings devoted to Optical Computing, which also includes the meeting held at Lake Tahoe (U.S.A.) in march 1987 ; plans are being made to held forthcoming meetings in Salt Lake City (U.S.A.) in march 1989 and in Japan in april 1990.

The call for papers of the present meeting attracted considerable response from the community of Optical Computing, so that the Technical Program Committee was able to compose a multidisciplinary, very international program that seems to announce a very interesting conference.

Sessions are arranged to cover the major aspects of Optical Computing.
Active and nonlinear components are in a phase of fundamental progress and much is hoped from their emergence in an industrial context. They include liquid crystal devices, whose applications to computing have been renewed by the advent of fast ferroelectric liquid crystal light modulators, but also compound semi-conductors, that are used in a steadily increasing number of demonstration components.
To a large extent, developments in the domain of optical interconnects are independant of those of nonlinear components. Three-dimensional, and even two-dimensional optical connectors offer an attractive potential for their interconnect density and may be made compatible with silicon or gallium arsenide integrated circuits for a number of applications.
New components imply new systems : the architectural aspects of optical computing have attracted a large interest, that is visible in more than half of the communications in this meeting. Symbolic substitution processors have become the archetype of a series of new concepts in optical cellular processors. An alternative approach is that of neuromimetic computing, which lends itself well to optical implementations because of the many non local interconnections needed. Whether the above two aspects of optical computing architectures are compatible or opposed, they both rely on the central concept of parallelism as derived from high interconnect density.

The program includes 14 invited papers and 95 contributed papers (47 oral presentations, 48 posters) covering three and a half dense working days. Authors come from 19 countries and no one country represents more than about one third of the total, so that the international character of the meeting is obvious.

The Technical Program Committee wishes to thank the Organizing and Local Committees for their work in the preparation of the meeting and the associated social events and the Organizing, Cosponsoring and Cooperating Societies for their respective contributions. Financial support from governmental and from industrial bodies was of capital importance for the possibility to held the meeting and is gratefully acknowledged.

Tuesday august, 30, 8.45

SESSION 1 (Chairman S. LOWENTHAL)

ACTIVE COMPONENTS
COMPOSANTS ACTIFS

A1 - S.T. LAGERWALL : Ferroelectric Liquid Crystals, a new class of materials for optics and optical information processing.

A2 - A.C. WALKER, S.D. SMITH, J.G.H. MATHEW and R.J. CAMPBELL : A electron-beam addressable digital optical spatial light modulator.

A3 - S. REDFIELD and B. HESSELINK : Data storage in photorefractives revisited.

A4 - N. COLLINGS, W.A. CROSSLAND, R.C. CHITTICK and M.F. BONE : The novel application of the electroclinic electro-optic effect to light valve technology.

Ferroelectric Liquid Crystals

- a new class of materials for optics and optical information processing

S.T.Lagerwall
Physics Department
Chalmers University of Technology
S-412 96 Göteborg, Sweden

Liquid crystals have traditionally been slow (> ms) materials which has been a limiting factor in spite of their many other attractive features as electro-optic materials. With the advent of surface-stabilized ferroelectric liquid crystals (SSFLC) and soft-mode ferroelectric liquid crystals (SMFLC) their performance has been brought up to the μs regime and beyond. We give a review of their properties and outline their applications.

AN ELECTRON-BEAM ADDRESSABLE DIGITAL OPTICAL SPATIAL LIGHT MODULATOR

A.C. Walker, S.D. Smith, J.G.H. Mathew and R.J. Campbell

Department of Physics, Heriot-Watt University,

Riccarton, Edinburgh EH14 4AS, UK

Summary

There is a high probability that successful optical computing devices will consist of massively parallel arrays of logic elements, read/write memories, etc. One major obstacle to the adoption of such a technology will be that of providing a suitable interface to conventional electronic information processing.

We here present a new type of electron beam addressed spatial light modulator which can use the standard inputs to a conventional cathode ray tube and thus provide a route to creating this interface. The optical component is an array of optothermal bistable switching elements. Importantly, the power available in a CRT electron beam is such that sufficient energy can be dumped in sequentially addressed elements for an entire frame to be written in less than the relaxation time of the individual elements themselves. Operated in a bistable holding mode the entire frame can then be reset in the same time.

Optothermal optical nonlinear interference filters (NLIF) have been exploited as bistable switches and optical logic elements for some time. If the size scaling of such devices is exploited, by thermal pixellation, sub-milliwatt operating powers and microsecond switching and recovery speeds

are attainable. We have developed an electron beam tuned interference filter spatial light modulator using such nonlinear devices. It is based on a small CRT with a thin film multilayer target. This target is formed by thermal evaporation of a NLIF on the innermost surface of the tube face plate. Refractive index changes and consequent shifts in the peak transmission wavelength of the filter (which can also be locked to the shifted wavelength) can be introduced by any absorbable power input. Normally this is done using optical beams alone and is well documented. In the present device the electron beam can be used to switch the state of an optically bistable element, initially held (say) in its off position, by a pulse of electron beam energy. This provides electronic address. On the basis of minimum theoretical switch powers of $\sim$ 100 μW and switching energies of $\sim$ 10 pJ μm^{-2}, an e-beam of average power 10 W would be able to address 10^8 pixels in 10 μs. An overall frame time of 30 μs would appear to be practicable, in experimental terms, leading to an overall data processing rate of 3×10^9, a factor around 100 times higher than exists on light valve SLM's.

We present the experimental results obtained from early versions of this device operating in the above manner and also purely as spatial light modulators with low power laser beams. In this case the electron beam is not used as an 'extra switch power' but rather in the role of the hold beam which controls the wavelength at which the device is operating. Demonstration at both 514 nm and 633 nm is shown.

The device therefore provides a method of loading an input plane in a parallel optical processor, a potential interrogator of a parallel memory and in general a programmable logic array plane.

Data Storage in Photorefractives Revisited

Steve REDFIELD* and Bert HESSELINK†

(*) Microelectronics and Computer Technology Corporation and (†) Stanford University

The results of a fresh new look at holographic data storage in photorefractives is reported. Two innovations, a technique for a highly asymmetric write/read cycle and a method for building artificial crystals, are described.

Introduction

A serious new look has recently been made at the possibility of a mass storage subsystem based on holographic storage in photorefractive materials leveraging recent advances in electroptic technology and quality of photorefractives. The activity, called the Bobcat project, lead to a method for dramatically increasing write/read asymmetry and produced a novel idea for constructing a substitute for bulk material out of a composite of fibers or small photorefractive volumes.

Construction

The optical configuration built is fairly standard using input data in the form of a 2-d array of spots, called a page. A hologram of the Fourier transform of this array is stored. Data is placed in the photorefractive crystal as a 2-d array of stacks of the pages. Some refinements were made. Ganged acoustic optic (AO) deflectors with intervening lens is the x-y deflection system which achieves stack addressing by moving both reference and object beam in tandem (for the experiments a micrometer adjusted mirror mount was substituted). Holographic Optical Elements (HOE) were used in several places. A fly's eye HOE was used to illuminate different stack positions. The angular positioning was achieved by a HOE which was essentially the equivalent of a lens and a wedge. The reference beam was deflected laterally across this HOE by the page deflection system which is an AO deflector (the deflection in the experiment was done by a flat mounted on a stepper motor). Fig. 1 shows the optical configuration.

SBN was chosen as the photorefractive material. Cerium doped SBN:60 which is now becoming available has good sensitivity and also reasonably slow dark decay. SBN has the additional advantage in that it can be electrically fixed. Electrical fixing requires a procedure by which the hologram is first poled to align all polarization domains. A hologram is recorded and then fixed by applying an electric field of 1.2 Kv/cm for .5 seconds antiparallel to the original poling field. Polarization reversal occurs at those locations where the sum of the space charge field plus applied field is above the coercive field. The result is a replication of the original trapped charge pattern. This pattern masks the holographic space charge field and the efficiency of the reconstruction is initially quite small. Upon illumination with the reference beam the charges redistribute themselves revealing the domain pattern. The ultimate efficiency is quite high (often higher than the original efficiency before the switching field was applied), which is attributed to over cancellation of the space charge field by local polarization switching.

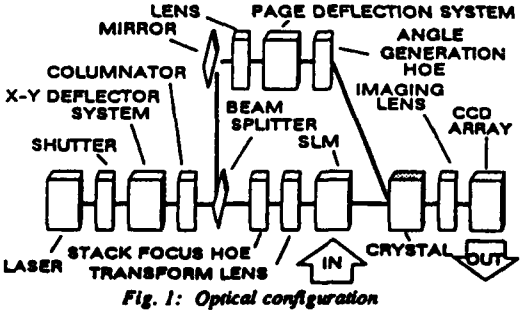

Fig. 1: Optical configuration

In place of a bulk photorefractive crystal an array of cubits (referred to as crystallytes) is used, each holding a single stack. This permits a large storage volume and allows selective control over applied electric field on a stack by stack basis.

Recently high bandwidth A-O deflectors have become available. An example is a GaP A-O modulator offered by Brimrose Corp. which has a 1 GHz bandwidth. This means a large deflection angle making throw length practical (1GHz gives a 6 degree max deflection). This device also has a deflection time around 200 ns for a 1 mm beam. Another advance is the improvement in size and quality of CCD arrays.

To deal with stability problems a non destructive readout technique is employed and electrical fixing. Stacks are electrically fixed as soon as all pages are written. A update strategy is chosen, common for database systems, which does not write in place but creates a new version. Old versions are eventually garbage collected.

Spatial Light Modulators (SLM) are still seen as a problem, however we acquired a 128 x 128 Semetek Corp SLM which can switch a row in around 100 ns which gives a frame rate of 1 3 us with the right supporting electronics and better than a 20:1 contrast ratio was measured. A 256 x 256 version is supposed to be available in the future.

Capabilities Measured

Measurement results are shown in Fig. 2. Also shown are the targets needed to be met for a competitive mass storage device and what was felt achievable on the other side of the experiments.

The capacity is going to be a close one to call, even though Bobcat did well in its demonstration of capacity, because the signal-to-noise-ratio, SNR, will be small at these high capacities. Speed is the advantage of this technology. Speed targets look easily obtainable, in fact should be exceeded for readout. Read speed limitation occurs in the CCD array which require a certain energy for a SNR. Write speed for the material depends on power and can meet SLM speeds. Stability targets should be achieved through electrical fixing and the non destructive readout technique. The quality measurements were the most difficult to make and the most subjective.

Within the limited capabilities of Bobcat they were found to be substantially acceptable with no obvious problems.

	target	achieved	projected
speed	1ms write 100us read	2ms write 100us read	1ms write 10us read
density	100Kb/pg 100pg/stk 1K stk 10^{10} bits	99Kb/pg 10pg/stk 1K stk 10^{9} bits	200Kb/pg 10pg/stk 2.5K stk 10^{10} bits
stability	10^{7}stk reads 24hr retention	$>10^{9}$ reads $1/_{64}$image @24hr	$>10^{9}$ reads >1wk retention
quality	$<10^{-6}$BER	140x140 & 280x280 res.	$<10^{-6}$BER edge fading

Fig. 2: Key measurement results

One has to temper the speed and capacity results with error rate considerations. The faster the read, the less energy on the detector and the lower the SNR and the higher the bit-error-rate (BER). BER translates into loss of useful capacity because a larger percentage of the raw capacity needed for redundancy.

Non Destructive Read Out

A major difficulty with data storage using holograms recorded in photorefractive media has been the destructive readout which limits the number of reads that can be made before the SNR becomes too low.

A non destructive readout technique was discovered which provides a new method to promote construction/reconstruction asymmetry. The technique can, under certain conditions, produce an enhanced reconstruction that is substantially nondestructive over a very large number of reconstruction cycles.

The key new ingredient is utilization of degrees of freedom in polarization of the reconstruction beam. The procedure, in its optimum form, involves first recording at a spatial frequency of around 200 l/mm for a particular length of time with a high applied electric field, around 6 Kv/cm, and ordinary polarized beams. The reconstruction is then done with the electric field reduced to around 1 Kv/cm and the polarization of the reconstruction beam rotated 90°. The reconstructed beam first drops in intensity, but subsequently grows above the starting value, approaching 100% efficiency in some cases. The reconstruction is almost nondestructive with erasure times exceeding 6 hours of continuous readout. This equates to over 1 billion 10 us readouts with SNR exceeding 20 db due to high efficiency. Recording exposures were approximately 0.3 mJ/cm^2.

Crystallytes

Previous work with photorefractive materials has been with bulk crystals on the order of one centimeter by one centimeter on the face and half a centimeter in depth. It is difficult to grow larger crystals of optical quality and, in fact, it is difficult to grow electro-optically superior crystals such as $BaTiO_3$ and SBN to half this size. As a consequence of this difficulty wide spread

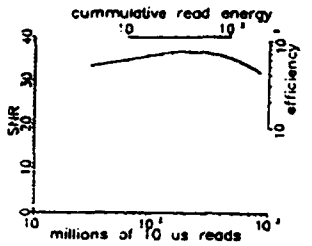

Fig. 3: Nondestructive reads

application of photorefractive technology has not occurred, despite an initial surge in the 1970's.

The crystallyte idea is to use a composite array of small, isolated photorefractive recording volumes which may be either cubits (small crystals) or fibers which are assembled in a matrix to synthesize a larger volume and used in place of a bulk crystal. Typically, the cross-section of each crystallyte is less than one millimeter and in the case of fibers can be very long, presently of the order of ten's of centimeters. The array geometry can be tailored to specific applications and may take different configurations. Isolation may be achieved by the refractive index differences, coatings on the sides, or the intervention of a substrate material.

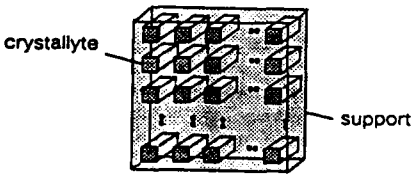

Fig. 4: Generic crystallytes

We have achieved, to our knowledge, the first photorefractive holographic recordings in a fiber. A plane wave reference and an image carrying object beam were used; the beams are incident on the fiber in a reflection geometry with the object beam propagating along the bore. The image recorded was an Air Force RES 1 test pattern. To date best resolution has been group 3 set 2 which gives 9 l/mm. The limitation seems to be fiber surfaces and improvement is expected. Angular sensitivity ranged from ±0.3° off Bragg for on axis recordings to ±0.15° for 20° off axis recordings.

These experiments were carried out for two relatively short 4 mm and 10 mm multimode 1 mm diameter fibers. The results suggest that an array of fibers might favorably replace bulk materials for certain computer and signal processing applications.

Conclusions

At this juncture holostore devices still appear to have the potential for orders of magnitude better latencies than magnetic or optical disk. With respect to density, however, because of difficulties in getting true volumetric or 3-d storage, it looks like these devices may only have the potential of matching the densities of magnetic or optical disk.

The Novel Application of the electroclinic electro-optic effect to light valve technology

N. Collings, W.A. Crossland, R.C. Chittick and M.F. Bone.
of: STC Technology Ltd
London Road
HARLOW
Essex CM17 9NA

The promise of optically addressed spatial light modulators for optical computing includes such applications as: arrays of threshold gates with isolation and amplification; programmable array beam deflectors; image relay devices; and intensity-to-phase convertors. In order to improve performance in these areas, the sensitivity, resolution and speed should be enhanced over existing light valves. Sensitivity and resolution can be increased together when a thin layer of amorphous silicon is used for the photoconductor. Values of 20 $\mu W/cm^2$ and 35 lp/mm were reported for nematic liquid crystal light valves using 5 μm thickness of amorphous silicon [1]. Speed is increased by employing a faster liquid crystal effect, and the use of a ferroelectric crystal gives submillisecond response times for both switch-on and switch-off [2]. The ferroelectric crystal has two stable in-plane orientations of the optic axis, and switching between these is accomplished by the reversal of the DC voltage across the cell. The result is a binary modulation capability which is important for thresholding applications. However, a number of applications would benefit from grey-scale. This can now be obtained, while maintaining the fast speed of response of the ferroelectric, by employing the electroclinic effect [3,4,5,6].

The electroclinic effect is exhibited by liquid crystals which have been heated from the ferroelectric smectic C phase into the non-ferroelectric smetic A phase. When a DC voltage is applied across the layer, the optic axis tilts in the plane proportionately to the applied voltage, up to a maximum angle. Our measurements on lactate electroclinic liquid crystal mixtures indicate that a maximum tilt angle (for the optic axis) of greater than 10 degrees can be achieved (Fig.1) Reversing the voltage will reverse the direction of tilt, so that the overall change in the orientation of the axis is greater than 20 degrees. The speed of response for the reorientation of the axis is less than 10 μsec at 35 V. As the temperature is increased, the maximum tilt angle and the response time decrease (Fig 2). Therefore, a device which is not thermostatted will only have a limited grey scale capability. However, we estimate that a thermostatted device will have a least 300 distinguishable grey levels.

Our experience with amorphous silicon/ferroelectric light valves [7], and, in particular, the relative ease with which they can be fabricated, leads us to believe that the present device will mark a new era in light valve technology. We will present results on prototype devices made with related electroclinic mixtures.

References

[1] Ashley, P.R. and Davis, J.H. 1987 "Amorphous silicon photoconductor in a liquid crystal spatial light modulator Appl. Opt. 26(2) 241
[2] Takahashi, N.S. et al. 1987 "High-speed light valve using amorphous silicon photosensor and ferroelectric liquid Crystals" Appl. Phys. Lett. 51(16) 1233.

[3] Garoff, S. and Meyer, R.B. 1977 "Electroclinic effect at the A-C phase change in a chiral smectic liquid Crystal" Phys. Rev. Lett 38(15) 848
[4] Andersson G. et al. 1987 "Submicrosecond electro-optic switching in the liquid-crystal smectic A phase: The soft-mode ferroelectric effect" Appl. Phys Lett 51(9) 640
[5] Nishiyama S. et al. 1987 "Giant electroclinic effect in chiral smectic A phase of ferroelectric liquid crystals" Jap J Appl Phys., 26(11) 1787
[6] Bone. M.F et al. 1988 "The electroclinic effect in some novel chiral smectic A mixtures" Paper submitted to the 12th International Liquid Crystal Conference in Freiburg, West Germany (12-19 August)
[7] Williams. D. et al 1988 "An amorphous silicon chiral smectic spatial light modulator" Paper presented at ECOOSA 88 in Birmingham, England (22-25 March).

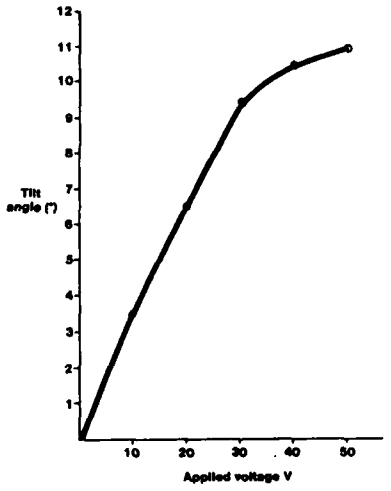

Fig.1 Tilt angle V applied voltage @ 60°C in 2μm thick device

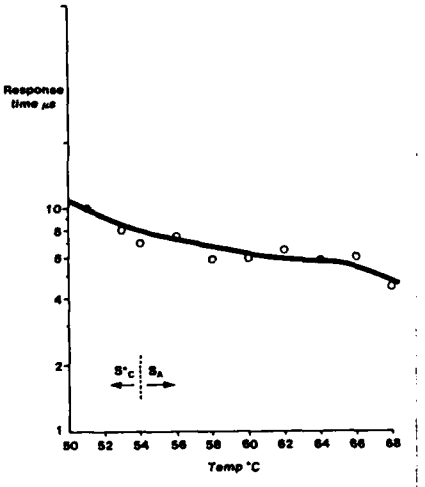

Fig.2 Temperature variation of response time at 35V drive voltage

Tuesday august, 30, 10.45

SESSION 2 (Chairman R.A. ATHALE)

OPTICAL NEURONAL PROCESSORS
PROCESSEURS OPTIQUES NEURONAUX

D1 - D. PSALTIS and X.G. GU : Fractal sampling grids for holographic optical interconnections.

D_1 - K. WAGNER and R. FEINLEIB : Adaptive optical neural networks.

D_2 - C. PETERSON and S. REDFIELD : Adaptive learning with hidden units using a single photorefractive crystal.

FRACTAL SAMPLING GRIDS FOR HOLOGRAPHIC OPTICAL INTERCONNECTIONS

Demetri Psaltis and Xiang-guang Gu

California Institute of Technology
Department of Electrical Engineering
Pasadena, California 91125

ABSTRACT

The complete family of fractal sampling grids for performing $N^{3/2} \mapsto N^{3/2}$ mappings will be derived. A new set of grids capable of performing any $N^d \mapsto N^{3-d}$, $1 \leq d \leq 2$, will be introduced.

SUMMARY

The fact that volume holograms store information in 3-D provides us with the capability to store the connecting weights at very high density in optical neural computers. Typically, a volume hologram is used to interconnect pixels ("neurons") arranged in 2-D surfaces. In order to fully interconnect a 2-D array of neurons to another 2-D array of neurons we need a 4-D tensor of weights. Since a volume hologram is a 3-D storage device, we cannot realize this interconnection with a hologram whose dimension is comparable to the dimension of the planes being interconnected.

We have previously derived a sampling grids of fractal dimension 3/2 that is capable of implementing a $N^{3/2} \mapsto N^{3/2}$ mapping where N is the number of pixels in 1-D at the planes that are being interconnected. In this presentation we will derive the set of necessary and sufficient conditions that a sampling grid must satisfy such that each holographic grating recorded in the volume hologram can independently interconnect a separate pair of pixels. Based on this we will derive the complete family of fractal grids of dimension 3/2, to implement $N^{3/2} \mapsto N^{3/2}$ mappings. We will then define a new set of sampling grids that is capable of interconnecting patterns $N^d \mapsto N^{3-d}$ for any d in the range $1 \leq d \leq 2$. We will derive the optimal relationships between the parameters of the optical system (focal length and aperture of the lenses) to optimally realize the capacity of the volume hologram for any rectangularly shaped crystal, and calculate the storage density (connection/cm^3) for this optimized geometry. Finally, we will show the results of an experimental demonstration that verifies the very high density ($> 10^9$ connection/cm^3) obtainable with volume holograms.

Adaptive Optical Neural Networks

Kelvin Wagner and Rick Feinleib
Optical Sciences Center
University of Arizona
Tucson Az 85721

Optical implementations of neural network models of learning using photorefractive holographic interconnections and optical neurons will be presented, and the capabilities and limitations of this approach will be explored. Previously, we have described optical implementations of the back propagation supervised learning procedure[1], and a competitive unsupervised learning architecture[2], and the salient features of all optical implementations of these algorithms will be summarized and compared with optoelectronic implementations of the neurons.

The back propagation network is a self aligning architecture that can utilize nonlinear etalons as the neurons, in a polarization multiplexed pump probe mode that can be implemented using the giant I_2 bound exciton in cryogenic anisotropic CdS platelets. The transmissions from an array of nonlinear etalons can also be used to implement a competitive network. This is based on the competitive dynamics realized from mutually interconnecting the reflections from the array of nonlinear etalons operating when they are aoperating in the regime of negative differential reflectance. The power requirements of the nonlinear etalons are quite high in both of these networks, so a hybrid optoelectonic nonlinear mechanism was designed for incorporation in a self-aligning competitive optical learning network.

This optoelectronic competitive mechanism can be realized using an integrated array of modulator-detector pairs connected to an electronic nonspecific global inhibition circuit. An electroabsorbtion modulator can be grown on top of a PIN photodiode with an integrated dielectric multilayer mirror structure underneath, and each such unit is connected to a transistor pair of the nonspecific inhibition circuit. The modulator and detector share a common central lead for biasing, but each has its own additional wire for separate modulation and detection signals, so this structure is similar to a symmetric SEED. An array of these devices is connected to the nonspecific global inhibition circuit, and the operation is as follows. Initially under no illumination or uniform illumination all of the modulators have a low voltage applied and are in the high absorption state, so very little photocurrent is generated in any of the photodiodes. When slightly more light is applied to one device than any of the others, then a little of the applied light leaks through the modulator to the photodiode, producing more current, so this device begins to win the electronic competition, and consequently an exponentially higher voltage is applied to its modulator. This increases the transmittance of the modulator so that even more current is generated by the photodiode so that the modulator voltage and transmittance continue to go up, etc., until it hits the voltage rails. At this point the modulator associated with the the slightly larger input is fully transmitting. Thus a large reflected intensity is produced from the integrated mirror structure, while all of the rest of the devices are fully absorbing and produce very little reflectance. This combination of electronic competition with optical inputs and outputs may be the most practical approach to implementing a competitive optical

network, and the power requirements could be quite low, allowing the practical implementation of an unsupervised optical learning systems.

This device can be used as the basis for the optoelectronic implementation of one of the simplest unsupervised learning schemes, the competitive learning network. Upon each pattern presentation this network strengthens the interconnections to the neuron with the largest presynaptic input, while slightly weakening all of the other interconnections. This adaptive network is able to discover topologically salient statistical invariants in stationary input environments without the aid of a teacher, and multilayer groupings of these networks can perform classifications that are not linearly separable. An attractive feature of this network is that all of the learned interconnections are excitatory, or positive, so that the optical implementation does not have to include phase encoding for interferometric bipolar holographic interconnections. In order to stabilize this type of learning procedure, an input pattern normalization and weight matrix decay are required. A Euclidean input pattern normalization is automatically accomplished when using photorefractive crystals for the adaptive interconnections because of their sensitivity to interferometric contrast, or modulation depth, which gives a space charge exposure perturbation that is proportional to the outer product of the input fields divided by the total incident intensity. At the same time the holograms are always forgetting some of the stored interconnections through incoherent erasure and thermal (or dark) erasure. These features can be incorporated into the self aligning hybrid optoelectronic competitive learning architecture shown schematically in the Figure.

Finally, preliminary experimental results of an optical learning network will be presented for a very simple unsupervised two class recognition problem. In this experiment an input image is diffracted by a volume hologram into one of two diffracted beams, which are detected and compared. The larger diffracted image inner product initiates an electromechanical competition that opens one of two apertures, thereby illuminating the crystal with the appropriate reference beam, and strengthening the corresponding image interconnections while slightly erasing the others, in order to complete a learning cycle.

1. K. Wagner and D. Psaltis, Multilayer Optical Learning Networks, Applied Optics, vol. 26(23), p. 5061 (1987).

2. K. Wagner and D. Psaltis, Nonlinear etalons in competitive optical learning networks, ICNN (1987).

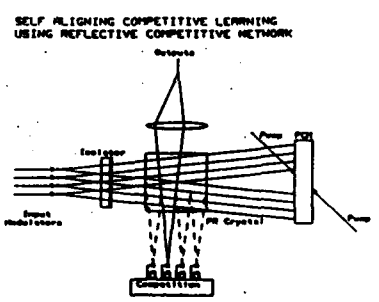

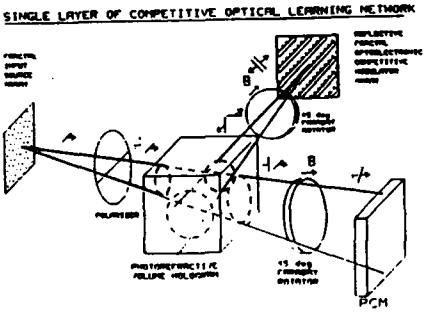

Adaptive Learning with Hidden Units Using a Single Photorefractive Crystal

Carsten Peterson and Steve Redfield
Microelectronics and Computer Technology Corporation

A novel optical neural network architecture based on photorefractive technology is presented. Learning with hidden units is handled with a mean field theory algorithm.

Generalities

Several proposals for optical neural networks that perform associative memory tasks have emerged the last 2 years. Synaptic strengths are implemented with Hebbian learning either through programmable SLM or photorefractive crystals. However, many feature recognition applications are characterized by higher order constraints and therefore require so called hidden units, which makes Hebbian learning intractable. Supervised learning algorithms like back-propagation, Boltzmann machine and mean field theory have shown great promise with this situation. We have found a slightly modified version of the mean field theory very suitable for optical implementation using recently discovered read/write phenomena in photorefractive crystals.

Mean Field Theory Learning Revisited

First list the main ingredients of this algorithm. Learning takes place by updating the synaptic weights according to:

$$\Delta T_{ij} = \beta(V_i V_j - V_i' V_j') \qquad [1]$$

where β is learning rate and V_i, V_i' result from:

$$V_i^{(\prime)} = 1/2\,[1-\tanh(\Sigma T_{ij} V_j^{(\prime)}/T)] \qquad [2]$$

where visible units are clamped, V_i, and partially clamped, V_i', respectively. In order to utilize this algorithm in an efficient way for a photorefractive crystal two minor, but important, modifications are needed.

- *Synchronous updating:* In the original formulation asynchronous updating was assumed in Eq. [2]. However, in optical implementations synchronous updating is natural. Using simulation we found that solving Eq. [2] with synchronous updating only requires a factor 2 more iterations.
- *Intermediate Updating:* Eq. [1] requires memorizing of $V_i V_j$ and a subtraction, neither of which are natural in an optical environment. There are no fundamental obstacles however for doing intermediate updating with the following sequence:

$$\Delta T_{ij} = \beta V_i V_j \qquad [3]$$

$$\Delta T_{ij} = -\beta V_i' V_j' \qquad [4]$$

We have checked the performance with this modification and again find very little degradation. In Fig. 1 we show the encouraging results from a 10×10 mirror symmetry learning experiment comparing original MFT results with the modified MFT

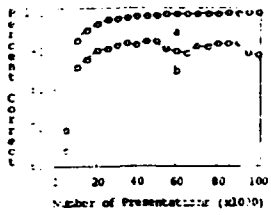

*Fig.1 Generalization of the 10*10 mirror symmetry problem using MFT (a) and the modified algorithm (b)*

Photorefractive Read-write Process; Decreasing Weights and Novel Phenomena

Photorefractive materials can be used as a dynamic storage media for interconnect state of a neural network. The method involves recording holograms or gratings via two wave mixing. An incident object beam, whose intensity can be made to correspond to a V_i, together with a reference beam, whose intensity can be made to correspond to a V_j, forms a grating in a record phase. The coupling efficiency or strength of this grating is then proportional to $V_i V_j$. In a read or production phase an impinging reference beam reconstructs the object beam from the grating.

The recording process in a photorefractive material is complex. When considering applications certain simplifying assumptions can usually be made. Under these assumptions during recording, for a given write energy density, efficiency, η, grows with write exposure time approaching asymptotically a saturation value, η_s, with time constant, T_s. This time constant is inversely proportional to write intensity or $T_s=(C_s I_w)^{-1}$. For short times, $t_1 \ll T_s$, and nearly balanced beam strengths, the following approximation is reasonable:

$$\sqrt{\eta} \equiv \sqrt{\eta_s}\,\frac{t}{T_s} = \sqrt{\eta_s}\; t_1 C_s I_w. \qquad [5]$$

The reconstruction or readout process, again making certain simplifying assumptions, is partially destructive. The start efficiency, η_0, decays exponentially, for a given read energy density, with exposure time with time constant T_d. This time constant is inversely proportional to read intensity, or $T_d=(C_d I_r)^{-1}$. Again for short times, $t_2 \ll T_d$, we use:

$$\sqrt{\eta} \equiv \sqrt{\eta_0}\,[1-t_2/T_d] = \sqrt{\eta_0}\,[1-t_2 C_d I_r]. \qquad [6]$$

The connection between a pair of neurons is represented by a small diffraction grating. The efficiency of this grating corresponds to the interconnect weight between the pair. The partial destructive nature of a readout can be taken advantage of to give negative weight modification as illustrated by Fig. 2 The change in coupling efficiency or weight strength, Δw_i, during the modification period is given by:

$$w_i \cong \sqrt{\eta} = \text{read decay} + \text{write construction}$$

$$\cong \sqrt{\eta_0}\,[1 - t_2 C_d I_r] + \sqrt{\eta_0}\, t_1 C_s I_w$$

$$\Delta w_i \cong \Delta\sqrt{\eta} \cong t_2 C_d I_r - t_1 C_s I_w . \qquad [7]$$

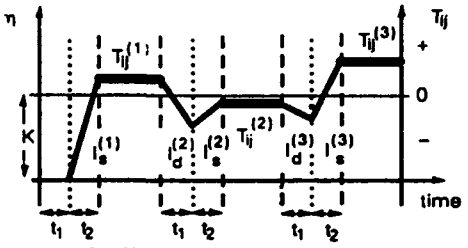

Fig. 2: Use of photorefractive destruction to accomplish negative reinforcement.

The "unlearning" phase of Eq. 4 is slightly more complicated since all gratings are by definition positive. However by manipulating V_i in the SLM's according to the following 4 steps the negative increment of Eq. 4 can be accomplished.

beam 1	beam 2	grating
$\sqrt{k}$	V_i'	$\sqrt{k}\,V_i'$
$\sqrt{k} - V_j'$	$\sqrt{k}$	$k - \sqrt{k}\,V_j'$
$\sqrt{k} + V_j'$	$\sqrt{k} - V_i'$	$k - \sqrt{k}\,V_i + \sqrt{k}\,V_j' - V_i'V_j'$
	$2k$	$-2k$

At the completion of the learning one now wants to freeze grating efficiencies. In the past this has been a problem because with use the neural network would gradually fade the recordings. We have discovered a technique for controlling destruction rate. It was successfully demonstrated that by varying the polarization directions of the object and reference beams with respect to the crystal axis the decay could be almost completely tuned.

Photorefractive Learning

The system configuration has two principal optical paths, reference path and object path. Each path has a spatial filter, beam splitter, SLM, and imaging lens system. The object path ends with a CCD array. The photorefractive crystal is SBN and an argon ion laser is used as a coherent light source (Fig. 3). For each pair of neurons, $n_i n_j$, a small grating is held in the crystal whose strength corresponds to their interconnect weight, T_{ij}. To fully utilize the capacity of the volume hologram incident patterns on the SLM will be arranged in a fractal fashion. Learning takes place iteratively with each cycle having two phases, a clamped phase which computes a set of V_i, and a partially clamped phase which computes a set of V_i'. A clamped phase proceeds as follows: (1) the input/output neuron are fixed or clamped to a predetermined set of values, (2) the SBN crystal, holding the current values of T_{ij}, acts as a matrix multiplier for Eq. [2] the V_j being imposed on the reference beam SLM, (3) after a large number of iterations a stable state for the V_i is reached. (4) the V_i are imposed on both SLM's so V_iV_j interfere in the crystal at the location of the grating corresponding to T_{ij} and the system is taken out of nondestructive mode so a grating enhancement occurs per Eq. 3 A partially clamped phase is identical to a clamped except not all the input/output neurons are fixed and the extra steps described in the above table. The method described in the previous section is used for accomplishing negative adjustments.

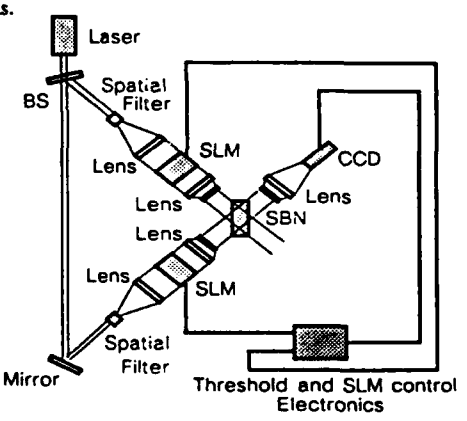

Fig. 3: The configuration of the Optical Neural Network Machine

When using the neural network for production (feature recognition, etc.) appropriate input neurons are clamped corresponding to an input and the corresponding V_i are imposed on the reference path SLM.

Summary

The architecture described is a clean simple way for implementing a neural network with hidden units optically. We are presently in the process of constructing such a machine at MCC and hope to have results at the time of the conference.

Tuesday august, 30, 13.30

SESSION POSTERS P1

ACTIVE COMPONENTS
COMPOSANTS ACTIFS

P_1 01 - A.V. KHOMENKO, S.V. MIRIDINOV and M.G. SHLYAGIN : information capacity of spatial lights modulators.

P_1 02 - C.D. KNITTLE and S.S. UDPA : Stochastic modeling of optoelectronic distributed arithmetic units.

P_1 03 - Y. KOCHER, G. LEBRETON and B. MOREAU : The TITUS light modulator in optical processing.

P_1 04 - M.J. RAMSHAW, D.G. VASS and R.M. SILLITTO : Phase or amplitude modulation by birefringence in a liquid-crystal spatial light modulator.

OPTICAL PROCESSING CONCEPTS
CONCEPTS DE TRAITEMENT OPTIQUE

P_1 05 - J. CAMPOS and H.H. ARSENAULT : Optimum sidelobe-reducing invariant filters for pattern recognition.

P_1 06 - A.K. DATTA, A. BASURAY and S. MUKHOPADHYAY : Addition of decimal number through fibre optic spatial maps.

P_1 07 - D. MENDLOVIC, E. MAROM and N. KONFORTI : Scale invariant pattern recognition.

P_1 08 - D.V. PANTELIC : Incoherent Abel inversion processor based on series expansion.

P_1 09 - E.L. ROPE, J. MILLES and G. TRICOLES : Spatially non-coherent processing with infrared or millimeter waves.

P_1 10 - F.T.S. YU, Q.W. SONG, Y. SUZUKI and M. WU : Application of a microchannel spatial light modulator to real-time joint transform correlation.

OPTICAL NEURONAL PROCESSORS
PROCESSEURS OPTIQUES NEURONAUX

P$_1$ 11 - P. DAS, C. DE CUSATIS and D.M. LITYNSKI : Integrated optical implementation of the Hopfield neural network model.

P$_1$ 12 - S.Y. LEE, J.S. JANG, J.S. PARK, S.Y. SHIN and C.S. SHIN : Modification of the Hopfield model and its optical implementation for correlated images.

PARALLEL PROCESSORS
PROCESSEURS PARALLELES

P$_1$ 13 - P. DEMALEPRADE, P. CHAVEL, K. HIBINO, H. YAJIMA and T. YATAGAI : Use of a micro-channel spatial light modulator in a sequential logic optical adder.

P$_1$ 14 - Y. HAYASAKI, M. IKEDA, T. YATAGAI, S. ISHIHARA and Y. MITSUHASHI : Space-variant logic operation using micro-channel plate spatial light modulator.

P$_1$ 15 - K. KITAYAMA, M. HASHIMOTO and N. MUKOHZAKA : Programmable optical parallel processor by polarization encoding : cascade operation.

Information Capacity of Spatial Light Modulators

A.V.Khomenko, S.V.Miridonov, M.G.Shlyagin

A.F.Ioffe Physical Technical Institute of the Academy of Sciences, Leningrad, 194021, USSR

Spatial light modulators (SLMs) are mainly used as input devices in optical information processing systems. Among the parameters which typically characterize a SLM, the information capacity is of special importance because it takes into account both the transfer function and dynamic range governed by the inherent noise level and maximum light modulation amplitude achievable for a SLM when a wideband signal is recorded.

In this report we suggest the experimental technique for estimating the information capacity of a SLM used in coherent optical systems. The technique involves recording a Fourier-hologram of a diffuse scatterer whose shape determines the spectrum of the wideband signal and measuring the signal-to-noise ratio as a function of spatial frequency in the Fourier plane of the optical system. The specific information capacity of the optical signal reconstructed from the SLM was calculated using our experimental data and the expression taken from /1/.

The technique is illustrated using the PRIZ SLM as an example /2-3/. It is shown that the maximum information capacity is reached for the optimum width of the recorded signal spectrum determined by the noise level of the system. The specific information capacity of the reconstructed signal for the optimum width of the spectrum of 15 mm^{-1} for the PRIZ was 10^5 bit/cm^2.

Since the information capacity gives an adequate estimate of the information processing capabilities of the optical systems utilizing SLMs, the technique can be used for comparison of different types of modulators and a proper choice of the SLM.

References

1. Shannon C. Communication in the presence of noise. PIRE, 37, 1, 10 (1949).
2. M.P.Petrov, A.V.Khomenko. Physical basis of operation of the PRIZ spatial light modulator. Optik, 67, 247-256 (1984).
3. M.G.Shlyagin, A.V.Khomenko. Studies of the PRIZ SLM noise. Zh.Tekh.Fiz., 57, 2101-2104 (1987).

Stochastic Modeling of Optoelectronic Distributed Arithmetic Units

C.D. Knittle and S.S. Udpa
NSF ERC for Optoelectronic Computing Systems
Department of Electrical Engineering
Colorado State University
Fort Collins, CO 80523, U.S.A.

Abstract

The Optical Distributed Arithmetic Unit (ODAU), in its simplest form, consists of an Optical Modulator Array (OMA) coupled to a photodetector array. The OMA uses a charge coupled device structure built on multiple quantum wells of InP/GaAs. The stack is placed in front of a lens and laser diode arrangement which ensures uniform distribution of the light generated by the diode over the OMA. The ODAU is capable of multiplying and adding two binary bit streams. Multiplication, for example, is performed by clocking the multiplicand into the OMA and applying the multiplier bit stream to the laser diode. Implementation of a controlled sequence of shifts, additions and carry operations results in the multiplication of the two numbers. Two dimensional versions of the device allow vector-scalar multiplication. After a detailed description of the device, the paper presents a model describing the operation of the device incorporating several sources of noise. Analytical expressions for the mean and variance of the cell voltages in the OMA and the photodetector are presented. Results characterizing the operation of an adder are also presented. These results have not only confirmed that the device is viable but has also enabled the optimum selection of device parameters. The paper concludes with a discussion on variations of the device which can greatly enhance the utility of the device.

SODERN

le 23 février 1988
CPV/GD/YK/fb - 520

THE TITUS LIGHT MODULATOR IN OPTICAL PROCESSING

Par :
Yves KOCHER (SODERN*), Guy LEBRETON (GESSY**), Bernard MOREAU (ONERA***)

SUMMARY :

The TITUS Spatial Light Modulator (SLM) has been developped for large screen videoprojection applications (TV projection, data display in command rooms, training simulators).

Its use in optical processing applications, especially with coherent light, is considered in this paper.

The TITUS SLM is based on the Pockels effect using a DKDP (KD_2PO_4) crystal. We will describe how this effect is used in the TITUS tube and the various operating modes :

. amplitude or phase modulation,
. voltage stabilization mode (providing simultaneous erasing and writing of the image),
. or charge accumulation mode (with sequential writing and erasing).

We describe the test equipment used to characterize electrically-addressed spatial light modulators, and give the descrip-tion of the tests with specific resulting data : impulse response, resolution, linearity and uniformity of response, writing/erasing speed,...

We examine several optical processing applications and analyze at functional and performance point of view which ones are promoting :

. SAR signal processing,
. sonar signal processing,
. adaptative optics.
. analog or digital optical matrix calculations (especially for high data, flux applications).

In conclusion, we address the potential evolution of TITUS. Some possible modifications of the tube are presented, together with the expected performance improvements.

ABSTRACT :

After a review of the principles of operation and the main characteristics of the TITUS SLM, we discuss its use in some optical processing applications and the expected results.

* SOCIETE ANONYME D'ETUDES ET DE REALISATIONS NUCLEAIRES
** GROUPE D'ETUDES DE SIGNAUX ET SYSTEMES (Université de Toulon et du Var)
*** OFFICE NATIONAL D'ETUDES ET DE RECHERCHES AEROSPATIALES

Phase or amplitude modulation by birefringence in a liquid-crystal spatial light modulator.

M.J. Ranshaw, D.G. Vass and R.M. Sillitto,
Department of Physics, University of Edinburgh,
Mayfield Road, Edinburgh. EH9 3JZ. U.K.

Introduction

We describe an electronically-addressed liquid-crystal SLM. The device consists of a parallel nematic LC above a VLSI backplane and uses the field-induced birefringence effect[1]). By suitable polariser / analyser combinations, the device can be configured as either an amplitude or phase modulator.

The SLM structure

The prototype array[2]) used to drive the device has 16 x 16 pixels spaced 200μm apart on a square array. Each pixel has a static memory element which determines the electronic state of a 100 x 100 μm^2 electrode / mirror. The 12μm liquid crystal layer (BDH E7) is contained between the drive chip and a counter-electrode of indium tin oxide coated glass. The LC is secured in the homogeneous configuration by obliquely evaporated magnesium fluoride layers on the chip and counter-electrode surfaces. Each pixel thus acts as a variably birefringent plate whose extraordinary refractive index depends on the applied peak to peak voltage.

A consequence of using nMOS circuitry is that the logic "1" value of the electrode voltage (- V_{DD}) is restricted to be above about 3.5 V. This requires using an off-set wave train on the counter-electrode to obtain the required a.c. voltages across the LC. The electronic circuitry, truth table and voltage drive signals are illustrated in fig.1.

Amplitude modulation

The SLM can be operated as an amplitude modulator by placing it between crossed polaroids at 45° to the optic axis of the LC layer. In this case a phase difference δ is introduced between the e- and o-components reflected from each pixel having a LC layer thickness d such that

$$\delta = \frac{4\pi\, d}{\lambda} \left(n_e(V) - n_o\right).$$

The transmitted intensity is given by $I = I_o \cos^2\left(\frac{\delta}{2}\right)$.

The pixel acts as a binary amplitude filter by arranging that $\delta = 2m\pi$ for a logic value 0 and $\delta = (2m+1)\pi$ for a logic value 1; m is a small integer. Preferably m = 0 to reduce the effect of cell thickness non-uniformities.

Figure 2(a) shows a SLM imaged in coherent light and programmed with a high pass filter pattern. We will present results of simple binary amplitude filtering operations by the device.

Phase modulation

The SLM can also be operated as a pure phase-modulator by arranging

that the incident light is polarised parallel to the extraordinary refractive index of the LC. Any change induced in this refractive index manifests itself as a phase change of the transmitted light.

Figure 2(b)shows the SLM programmed with phase differences of π radians between alternate columns of the array. Figure 2(c) shows the optical Fourier Transform of this phase grating, with the expected spatial frequency component associated with the columns twice that associated with the rows.

Binary phase correlator [3]

The device has been used successfully as a phase only filter in the Fourier plane of a coherent optical correlator. We will present results of this application.

References

1. Wu S-T, Efron U., Hess L.D., Applied Optics 23, 3911-3915, 1984.
2. Underwood I., Vass D.G., Sillitto R.M., IEE Proc. J. Optoelectronics 133, 77-82, 1986.
3. Horner J.L., Bartelt H.O., Applied Optics 24, 2889-2893, 1985.

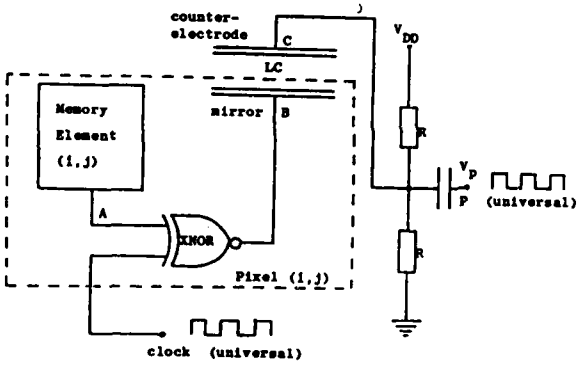

Fig. 1

	LOGIC TRUTH TABLE			NODE VOLTAGES			L.C. VOLTAGE
	A	clock	B	B	P	C	
'OFF'	0	0	1	V_{DD}	0	$\frac{1}{2}(V_{DD}-V_p)$	$\pm \frac{1}{2}(V_{DD}+V_p)$
	0	1	0	0	V_p	$\frac{1}{2}(V_{DD}+V_p)$	
'ON'	1	0	0	0	0	$\frac{1}{2}(V_{DD}-V_p)$	$\pm \frac{1}{2}(V_{DD}-V_p)$
	1	1	1	V_{DD}	V_p	$\frac{1}{2}(V_{DD}+V_p)$	

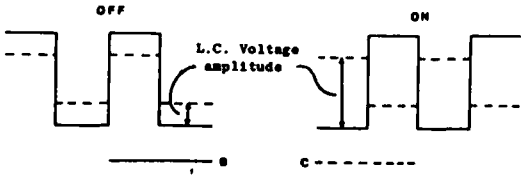

Fig.2a

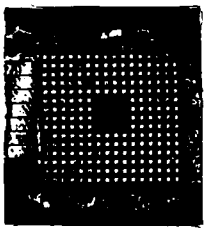

Fig.2b

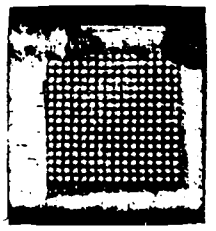

Fig.2c

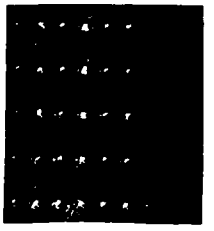

Optimum sidelobe-reducing invariant filters for pattern recognition

J. Campos
Departamento de fisica, Universidad de Barcelona, c/Diagonal, 647, 08028 Barcelona, Spain

H. H. Arsenault
Laboratoire de recherches en optique et laser, Université Laval, Québec, P. Q., Canada, G1K 7P4

SUMMARY

Matched filters based on Circular harmonic components allow objects to be recognized independently of their position or orientation. Linear combinations of such filters, or CHC composite filters, improve the recognition and classification performance of the method. Composite filters are however associated with high sidelobes that degrade the performance of the filter. New techniques to improve the peak to sidelobe ratio of the outputs from invariant filters will be reviewed. One of them is to choose the coefficients of a composite filter in such a way that the peak to sidelobe ratio is increased. We have found that an efficient way to accomplish this is to minimize the energy that goes into the sidelobes.

The filter h_m is a linear combination of the CH components

$$h_m = \sum_{i=1}^{n} a_i \, f_m^i \ ,$$

where the coefficients a_i of the linear combination are chosen to satisfy the following constraints

$$f^{jT} h_m^* = f_m^{jT} h_m^* = r_j \ , \quad j=1, 2, ..., n \ ,$$

where the superscript T denotes the transpose, * denotes complex conjugate, and ζ is a desired cross-correlation output value.

If the filter h_m is a m-th CH component with $m \neq 0$, the average filter amplitude is $< h_m > = 0$. In this case, the correlation amplitude variance is proportional to correlation energy, and the problem of minimizing the correlation amplitude variance is equivalent to minimizing the correlation energy. The energy of the i-th correlation plane is

$$E_i = H_m^+ \, Q_i \, H_m ,$$

where the superscript + denotes the conjugate transpose of a complex vector, and Q_i is a diagonal matrix of size dxd whose diagonal elements are the magnitude square of the associated elements of F_m^i, i.e,

$$D_i (u,u) = |F_m^i(u)|^2 .$$

Experimental results show that a considerable decrease of sidelobes may be achieved with this method. The performance of the method will be compared with that of other existing methods. The matched filters can be made as computer-generated holograms, and the method can be implemented either optically or by digital means.

ADDITION OF DECIMAL NUMBER THROUGH FIBRE OPTIC SPATIAL MAPS

A.K.Datta, A.Basuray, S.Mukhopadhyay

Educational Resources Centre on Optical Electronics
Department of Applied Physics, Calcutta University,
92, Acharyya Prafulla Chandra Road
Calcutta - 700009, INDIA.

To exploit the full advantages of parallelism in optics, for computing and processing, each digit must be independent to its preceeding digit, ie, there should not be any 'carry' or 'borrow'. Many coding, masking, decoding techniques have been proposed and many new systems are reported where carry less operations in 2-D are performed. In this context the importance of residue number system is well felt, which allows simultaneous operations of all digits without any interference between them. Second important advantage offered by the residue technique arises from the fact that the calculations can be decomposed into small sub-calculations with reduction in the complexity. Three steps are to be considered when our attempts to use residue technique for optical computations in parallel. They are (a) conversion of decimal number to residue (b) arithmetic operation in residue form and (c) conversion of the result from residue to decimal number.

In this paper we propose a scheme where the above mentioned three steps are performed with the help of light sources, fibre optic maps and electronic or optical logic gates. Basic building block and heart of the system is a fibre optic spatial map as proposed by Huang etal [App.Optics 18, 2, 1979]. It has been shown and established mathematically that only two types of map are necessary for converting any decimal number to its residue, provided certain rules are observed. Once the residue of a number is available, we may switch on the respective light sources in the 'adder' section which is again a fibre optics map. These maps have two channels instead of a single connection as proposed earlier. The addend decimal number is also converted to residue.

This residue number allows the switching of proper map from upper channel to lower channel. The result is obtained in the residue system and is represented by light coming out of the proper fibre. Electronic or optical logic grates can then be used to convert the residue number to decimal number. In this context the application of optical Fredkin gate is also explored.

The system is explained in the proposed paper. It must be appreciated that the system proposed intends to establish the possibility of arithmetic operation through residue system with the help of fibre optic spatial maps, modified according to the need of operations.

SCALE INVARIANT PATTERN RECOGNITION

D. Mendlovic, E. Marom and N. Konforti

Faculty of Engineering, Tel Aviv University, Tel Aviv, Israel, 69978

Optical pattern recognition has been long considered a very useful tool in machine vision, robotics, automation and image understanding. However, being based on pattern correlation, conventional matched filter schemes, also known as Vander Lugt correlators, suffer from the need to handle scenes that have the same size and orientation, thus allowing only for lateral shift invariances. For many applications it would be highly desirable to generate filters that provide not only lateral shift invariance, automatically provided by the matched filter, but rotation and scale invariances as well. In this work we present a novel approach for a scale and shift invariant filter. This approach is dual to the one used for the circular harmonics expansion[1]. It is based on decomposing the object into an orthogonal set of functions, called here Mellin Radial Harmonics, each harmonic exhibiting scale invariancy.

Borrowing from the Mellin transform definition, one can treat a pattern expressed in polar coordinates $f(r,\theta)$, by decomposing it into a set of functions $(\rho^{i2\pi M-1})$, each one of them being invariant to scale changes:

$$f(\rho,\theta) = \sum_{M=-\infty}^{\infty} f_M(\theta)\, \rho^{i2\pi M-1} \tag{1}$$

with

$$f_M(\theta) = \int_{\frac{r_0}{R}}^{1} f(\rho,\theta)\, \rho^{-i2\pi M-1}\, w\, d\rho \tag{2}$$

where w is a weighting constant, R is the finite size of the pattern (at its maximal scale) r_0 is the smallest radius used in defining the expansion and $\rho = r/R$ is a normalized radius. To get the orthogonality of this set the choice of r_0 will be such that $(\ln R - \ln r_0)$ is an integer L. The weighting constant was found to be $w=1/L$. This expansion provides shift and scale invariance in deriving the correlation of images, if a single radial harmonic is used.

The notation $f(r,\theta;\xi,\zeta)$ will be used to point out the polar coordinates (r,θ) as well as (ξ,ζ) the location of the origin (in Cartesian coordinates) of the polar expansion. The same notation in a Cartesian representation would be $f(x,y;\xi,\zeta)$. Due to the orthogonality and the completeness of the Mellin radial harmonics set, the correlation function between this matched filter and any input pattern $g(x,y)$ can be written as:

$$C_{fg}(x',y';\xi,\zeta) = \int_{-\infty}^{\infty}\int_{-\infty}^{\infty} g(x+x',y+y')\, f_F^*(x,y;\xi,\zeta)\, dx\, dy \tag{3}$$

where (x',y') identify the Cartesian coordinates in the correlation plane, (ξ,ζ) is the expansion center

used in making the filter and $f_F(x,y;\xi,\varsigma)$ is the filter function expressed in Cartesian coordinates. Using the same radial harmonics expansion for g, one can get the correlation function with an object $g(\beta\rho,\theta)$:

$$C_{fg}^{[\beta]}(x',y';\xi,\varsigma) = \frac{1}{\beta} e^{i2\pi M \ln\beta} C_{fg}^{[1]}(x',y';\xi,\varsigma) \qquad (4)$$

A scale change thus results in only an additional phase factor in the correlation function expression, the relative intensity distribution of the correlation pattern remaining unaffected. Therefore using a single radial harmonic, lateral shift and scale invariant correlations can be obtained. For a better signal to noise ratio use of multiple harmonics is preferred, but unfortunately, the use of two or more harmonics simultaneously is detrimental, since different phase terms are associated with each harmonic.

The concepts derived in this paper have been experimentally tested with images of various sizes consisting of binary alphabethic letters. We chose the letter E and the filter was calculated using the second harmonic M=2; R was 50 units and L was 3 (resulting in $r_0 \simeq 2.5$). The height of the original letter E was 25 units. The filter is a binary computed generated hologram calculated and plotted via Lohmann's detour phase method[2] with a resolution of 64x64 pixels. This filter pattern was photoreduced to a size of 10x10 mm on Agfa Gevaert Millimask plates. Using a conventional correlation set-up, we observe in Fig. 1 the cross-correlation of several letters E having different sizes.

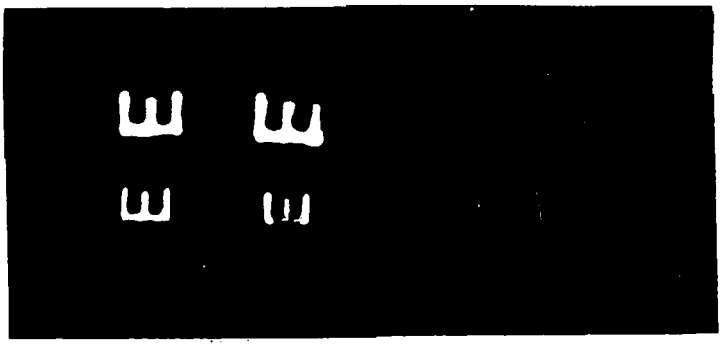

Fig. 1: Input objects (four letters E of different scales) are on the left and the corresponding four cross-correlation patterns are on the right.

We should note that the recognition is limited to input patterns that are within the dynamic range of $r_0<r<R$. In our experiments this area is $3<r<50$ units, the original size of the E being 25 units, with 5 units allowed to each branch of the letter. The system was able to recognize letters that where in the range of 50% - 200% only of the original size.

References

1. H. H. Arsenault and Y. N. Hsu, Appl. Opt. 22, 130 (1983).
2. A. W. Lohmann and D. P. Paris, Appl. Opt. 6, 1567 (1967).

INCOHERENT ABEL INVERSION PROCESSOR, BASED ON SERIES EXPANSION

Dejan V. Pantelic
Institute of Physics Belgrade

Abel inversion is an important technique in a various applications like: plasma physics, interferometry, aerodynamics. It is, also, numerically intense, requiring different regularisation techniques. Therefore, it is of great interest to perform Abel inversion optically, because of its inherent parallelism.

In this paper we are proposing an incoherent optical processor that can perform Abel inversion. The purpose of this kind of processor is the real time inversion in plasma physics. Classically, radial distribution of emissivity in cylindrical plasma was determined in the following way: emitted radiation was detected, results discretized and inversion was performed numerically. It is obvious that the real time operation is not possible, because Abel inversion is numerically intense.

Let's explain the principle of operation of our processor. We were not able to use classical inversion formula:

$$F(r) = -\frac{1}{\pi}\int_{r}^{\infty}\frac{f'(x)\,dx}{(x^2-r^2)^{1/2}} \qquad (1)$$

for the two reasons: kernel possesses a singularity and the first derivation of the function f(x) should be computed.

We avoided the problem using the series expansion technique. The function f(x), whose inversion had to be found, was expanded in a series of Tchebycheff orthogonal polynomials:

(2) $$f(x) = \sum_{n=0}^{N} C_{2n}\, T_{2n}(x)$$

where T_{2n} is 2n-th Tchebycheff polynomial. Expansion coefficients C_n were found as (this operation is easily performed optically):

(3) $$C_{2n} = \int_{-1}^{1} f(x) T_{2n}(x) (1-x^2)^{-1/2}\, dx$$

We have shown that the Abel inversion of Tchebycheff polynomial $T_{2n}(x)$ is Zernike polynomial $Z_{2n}(r)$. Therefore, the Abel inversion of the function f(x) is the function F(r), given as (this is, also, implemented optically):

(4) $$f(r) = \sum_{n=0}^{N} C_n\, Z_{2n}(r)$$

In an experimental setup we have represented orthogonal polynomials T_{2n} and Z_{2n} as computer generated transparencies (bias was added since T_{2n} and Z_{2n} are functions of variable sign). Light distribution, that had to be inverted, was a line source. Integration in equation (3) and summation in equation (4) were done by cylindrical optics.

Experiments showed good agreement with theoretical predictions. Also, we were able to chose a degree of smoothness of the reconstructed function, simply by increasing or decreasing the number of terms in a series expansion. Experimentally, it was done by masking appropriate part of the computer generated transparencies T_{2n} and Z_{2n}.

Similar technique can be used to perform some other integral transformations. However, systems of orthogonal polynomials should be chosen such that interval of orthogonality is finite and weighting function is without singularities.

Spatially Non-Coherent Processing With Infra-Red or Millimeter Waves

E. L. Rope, J. Nilles, and Dr. G. Tricoles

General Dynamics Electronics Div., P.O.Box 85227, San Diego, CA 92138 USA

In many cases microwave and radio wave holography suffer from time delays and image distortions. Delays occur in data acquisition, processing, and display; this paper treats processing and display, but it omits the acquisition delay which depends on sensor architecture. Image distortion occurs when formation and reconstruction wavelengths differ. Although digital reconstruction avoids this scaling problem, delays occur in sampling, digitizing, and processing.

To overcome delays we have made reconstructions with spatially non-coherent arrangements that compute Fourier transforms. In these experiments a hologram is doubled; that is a pair of axially symmetric holograms are produced. An axially symmetric pair of points in the holograms radiate coherently, but pairs are spatially non-coherent. Intensities from pairs add.

To reduce distortions that arise when formation and reconstruction wavelengths differ significantly we have utilized an infra-red setup and another millimeter wave setup for reconstruction from microwave holograms.

Two theoretical descriptions of the reconstruction are given. One starts with a hologram configuration and computes Fraunhofer region image intensity of doubled hologram, assuming point sources. The other also computes farfield intensity, but it includes hologram formation for a point object and reference source; this theory involves integration over continuous apertures rather than discrete point sources.

Both theories predict image locations that agree with measurement. The discrete theory predicts magnitudes that more closely agree with the experiment. The continuous theory provides physical interpretation for image properties.

Reconstruction experiments were done with previously formed holograms. The holograms were of a log periodic antenna radiating first in its sum mode and then in its difference mode. Wavelength was 3.30 cm.

Reconstructions were done with coherent infra-red radiation from a line array of four 0.85μm solid-state lasers, which replicated the hologram intensities. Holograms were doubled by directing the output of a laser to a pair of optical fibers. Reconstruction intensity was measured by an array of charge-coupled devices.

Reconstructions were also done with 8.57 mm waves. A pair of waveguides was connected to a signal generator. Both dielectric and hollow metallic waveguides were used. Interference fringe intensity was separetely measured for four spacings of the radiating ends of the waveguides by scanning the image region with a small receiving antenna. The intensity for each spacing was stored in a computer and intensities for the four spacings were summed to effect noncoherent superposition.

The 0.85μm reconstructions were described better by the discrete theory rather than the continuous; image locations were correct for both, but second-order image intensity was more accurate for the discrete theory. The continuous theory described the magnitudes of the millimeter wave reconstruction better than did the discrete theory. The apparent reason is in the width of hologram fringes compared to widths of radiation sources. That is, the element factor enters.

Application of a Microchannel Spatial Light Modulator to Real-time Joint Transform Correlation

F.T.S. Yu, Q.W. Song
Electrical Engineering Department
The Pennsylvania State University, University Park, PA 16802

Y. Suzuki, M. Wu
Hamamatsu Photonics KK. Hamamatsu city, Japan

I. Introduction

The fast developing, optically addressed, microchannel spatial light modulator (MSLM) [1] is a very promising interfacing device for optical information processing. The MSLM consists of a photocathode, a microchannel plate, an accelerating grid, and an electro-optical (E-O) crystal plate arranged sequentially in a vacuum device. In operation, the functions such as photo electron generation, multiplication, transfer, and read-out light modulation are performed with each functional component. It is rather easy to tailor the MSLM device for various optical operations. Recently, this MSLM has drawn some attention in various optical processing applications.

In this paper, we shall present a programmable real-time optical joint transform correlator [2] that uses the threshold hard-clipping property of a MSLM to generate sharper and higher autocorrelation peaks. Basic principle and a preliminary experimental result are given.

II. Basic principle

The schematic diagram of the microcomputer based JTC is shown in Fig.1.

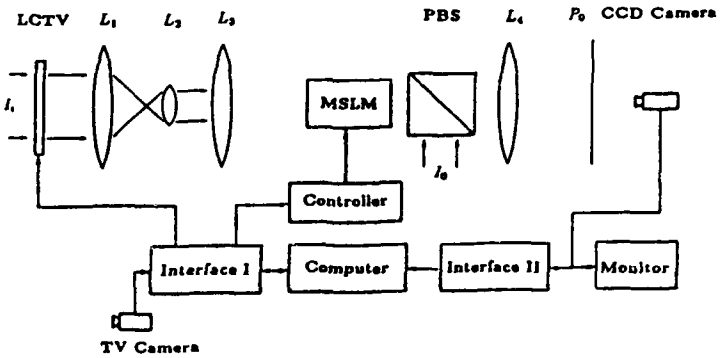

Fig.1 The schematic of a programmable optical joint transform correlator.

The liquid crystal plate of a LCTV is used to display a real-time target and a reference image, at the input plane of an optical processor. The working principle of the LCTV as an optical element is described elsewhere [3]. The major advantage of using LCTV must be that it can be addressed by a microcomputer, for the generation of various reference images. The output light field is detected by a CCD camera. This detected electrical signal can be sent to a TV monitor for observation. or fed back to the microcomputer for further instruction. Thus an adaptive hybrid electro-optic correlator may be constructed.

Let's assume that the target and reference image at the input plane are binary type with square apertures of width w. The main separation between them is l. The amplitude transmittance function of these input objects can be expressed as

$$f(x,y) = [rect(\frac{x-\frac{l}{2}}{w}) + rect(\frac{x+\frac{l}{2}}{w})]rect(\frac{y}{w}). \quad (1)$$

Thus the light intensity distribution at the input window of the MSLM would be

$$I(\nu,\mu) = I[\frac{sin(\pi w\nu)}{\pi\nu}\frac{sin(\pi w\mu)}{\pi\mu}cos(\pi l\nu)]^2, \quad (2)$$

where I is a constant, ν and μ are spatial frequency cordinates corresponding to the X and Y directions. Notice that, the grid structure of the LCTV, which is beyond the resolution limit of the MSLM, is omitted. To obtain a binarized power spectral distribution for joint transform correlation, the bias voltages of the MSLM are adjusted such that those values above the threshold level will be written into the device in a saturated manner, while those below the value will not be responded. This threshold hard-clipping operatioin of the MSLM converts the input irradiance $I(\nu,\mu)$ into a series of binary phase distribution, between the X and the Y components of the read-out light. Using the half power criterion, the output autocorrelation functions can shown as

$$E = \frac{A}{\pi}\{\frac{sin[\pi(x-l)/w]}{\pi(x-l)} + \frac{sin[\pi(x+l)/w]}{\pi(x+l)}\}\frac{sin(\pi y/w)}{\pi y}. \quad (3)$$

We see that the correlation peak intensity of the proposed system is A^2/π^2w^4, which is about 1.62 times higher than the conventional one. Moreover, if the bias voltages are controlled, such that the threshold hard-clipping takes place at a lower intensity level, the output would further improve to have higher and sharper peaks. We proved that ideal hard-clipping offers better correlation peak than the conventional JTC. Detailed numerical analysis and an experimental result will be presented at the meeting.

III. Concluding Remarks

We have presented a joint transform correlation system utilizing the threshold hard-clipping property of the MSLM. This JTC can produce sharper and higher correlation peaks than the convetional techniques. By combining the flexibility of the microcomputer and the high speed operation of the optical processor, the system would offer the advantages of real-time programmable processing capability, for which an adaptive smart correlator can be developed.

We acknowledge the support of the US Air Force, Rome Air Development Center, Hanscrom Air Force Base, Mass., under contract F19628-84-K-0031.

Reference

[1] C. Warde, A. Fisher, D. Cocco, and M. Butmswi, "Microchannel Spatial Light Modulator," Opt. Lett. 3, 196(1978).

[2] F.T.S. Yu, X.J. Lu."A real-time programmable joint transform correlator," Opt. Commun. **52**. 10(1984).

[3] H.K. Liu, J.A. Davis, and R. A. Lilly,"Optical Data Processing Properties of a Liquid Crystal Television Spatial Light Modulator," Opt. Lett. **10**,635(1985).

Integrated Optical Implementation of the Hopfield Neural Network Model

by: P. Das*, C.DeCusatis*, and D.M. Litynski**

*Electrical, Computer, and Systems Engineering Department
Rensselaer Polytechnic Institute
Troy, New York 12180-3590

**Department of Electrical Engineering
United States Military Academy
West Point, New York 10996-1787

Abstract

An integrated optics implementation of content addressable associative memory based on the Hopfield Neural Network Model is proposed. The device uses frequency multiplexed surface acoustic waves (FM-SAW) to input the information matrix, which may be stored as a volume hologram using photorefractive memory. Stored information may then be recovered in real time by applying a partial or distorted input to the system. This input is presented in the form of coherent optical pulses, which may be modulated by an external CCD camera. Phase conjugate mirrors are used to obtain the nonlinear thresholding inherent in the Hopfield model, and to provide feedback and gain.

Summary

The principle of information retrieval by association has been recognized as an important mechanism in parallel computing and machine vision systems(1). A model for neural networks capable of implementing this principle was recently proposed by Hopfield(2); information stored in an interconnection matrix may be recovered by applying a partial or distorted input to the system. This model has been implemented by Farhat and Psaltis et.al. using an optical matrix processor(3), and by Soffer and Dunning et.al using holographic memory(4). We present a conceptual implementation of

the Hopfield model using integrated optics techniques to produce a compact, rugged device.

The interconnection matrix is input as a series of acousto-optic SAW pulses, frequency multiplexed so that each pulse represents an entire column vector. This matrix is stored as a volume hologram using the photorefractive effect. Distorted or incomplete versions of the stored signals may then be applied as intensity modulated optical pulses; for example, the modulating signal may be obtained directly from a CCD camera. When the device is addressed in this manner, it converges to a reconstructed version of the input signal in real time; the output is in the form of a series of modulated optical pulses. A pair of phase conjugate mirrors is used to obtain the nonlinear thresholding inherent in the Hopfield model, and to provide feedback and gain for the optical signals. A theoretical design for such a device using currently available technology is presented.

References

1. R. P. Lippman, IEEE ASSP Magazine, p. 4, April 1987
2. J. J. Hopfield, Proc. Natl. Acad. Sci. USA 79, 2554 (1982)
3. N. H. Farhat, D. Psaltis et.al., App. Optics 24, no. 10, p. 1469 (1985)
4. B. H. Soffer, G. J. Dunning et.al., Optics Lett. 22, no. 2, p. 118 (1986)

Modification of the Hopfield model and its optical implementation for correlated images

Soo-Young Lee, Ju-Seog Jang, Jin-Soo Park, and Sang-Yung Shin
Korea Advanced Institute of Science and Technology
Department of Elecrical Engineering
P.O. Box 150, Cheongryang, Seoul, Korea
and
Chang-Sup Shim
Korea Electronic and Telecommunication Research Institute

Summary

Associative memory based on the Hopfield neural network model can be used directly to store and retrieve information with robustness and error-correction capability. Numerical simulation and optical implementation show that an associative memory based on this simple model can successfully retrieve data only when the number of stored data is much smaller than the number of neurons and when the stored vectors are (pseudo) orthogonal. For many practical systems such as number and/or alphabet recognition, the orthogonality is not satisfied. In Ref. 1, we had introduced a modification on the Hopfield model to incorporate relative significance of each bit, and how a priori knowledge on bit significance improves error-corrective association performance. Here we first introduce an inner product bound of stored vectors in the Hopfield model, and show that optimization of the bit significance for given stored vectors removes or at least relaxes the orthogonality condition and increases storage capacity.

In the Hopfield model a new estimate is obtained by thresholding

$$\hat{V}_i^t = (2V_i^t - 1)\, N(t,\, t) + \sum_{s \neq t}^{M} (2V_i^s - 1)[2N(s,\, t) - N(t,\, t)] \qquad (1)$$

where $N(s,\, t) = N(t,\, s)$ is the inner product of two vectors $\mathbf{V}^s$ and $\mathbf{V}^t$, and the input to the memory $\mathbf{V}^t$ is one of the complete vectors that are stored in $\mathbf{T}$. The ith bits of the M vectors $(V_i^1, V_i^2, \ldots, V_i^M)$ appearing in Eq. (1) can have total 2^M distinguishable cases. In all these cases, if the thresholded value of Eq. (1) is equal to the value of ith bit in $\mathbf{V}^t$, the stability of $\mathbf{V}^t$ can be guaranteed. We found that the number of mutually independent stability conditions of the vector $\mathbf{V}^t$ is 2^{M-1}, and that these inequality conditions define in geometrical sense the interior of a regular 2^{M-1}-faced polyhedron with the side length of $N(t,\, t)/\sqrt{2}$ centered at $\big(N(t,\, t)/2,\, N(t,\, t)/2, \ldots, N(t,\, t)/2\big)$ in the $(M-1)$-dimensional inner product space whose axes are $\big(N(1,\, t), N(2,\, t), \ldots, N(t-1,\, t), N(t+1,\, t), \ldots, N(M,\, t)\big)$. For

a large number of neurons, the polyhedron stable region may be approximated by $(M-1)$ dimensional sphere, and the stability condition becomes

$$\sum_{s \neq t}^{M} \left[N(s,\ t) - \frac{N(t,\ t)}{2} \right]^2 < \frac{N(t,\ t)^2}{4(M-1)} \tag{2}$$

which clearly shows the orthogonality requirement.

To overcome this drawback we start with a simple modification on the retrieving algorithm of the Hopfield model to obtain

$$\hat{V}_i^t = \sum_j T_{ij} \omega_j (2V_j^t - 1) \tag{3}$$

where ω_j is positive bit significance of the jth bit of image vectors. The interconnection matrix $\mathbf{T}$ and thresholding operation are same as the Hopfield model. If the input vector $\mathbf{V}^t$ is one of the stored images, one obtains

$$\hat{V}_i^t = (2V_i^t - 1) \sum_{j=1}^{N} \omega_j + \sum_{s \neq t} [(2V_i^s - 1) \sum_{j=1}^{N} \omega_j (2V_j^s - 1)(2V_j^t - 1)] \tag{4}$$

where unipolar binary images are assumed and the second term corresponds to noise. Because one has $(N-1)$ degrees of freedom to select relative significance ω_j, the correlation noise term can be minimized for given stored image vectors. The minimization is based on the least-square solution algorithm, and may be implemented by another optimization neural network as described in Ref. 2. A simple learning algorithm for adding a new image to existing optimized associative memory is also devised.

In numerical simulation ten highly correlated binary images, i.e. numbers "0" to "9", are successfully stored and retrieved in 6×8 node system. Conventional Hopfield model with same configuration could not retrieve even five images, numbers "0" to "4", mainly due to their high correlation terms. These results clearly demonstrate usefulness of the new bit-significance optimization model. A design for electro-optic implementation including the optimization network will also be introduced.

References

1. S.-Y. Lee, C.-S. Shim, J.-S. Jang, and S.-Y. Shin, "Optical implementation of associative memory with controlled bit-significance," J. Opt. Soc. Am. A4, (13), 131 (1987).
2. J.-S. Jang, S.-Y. Lee, and S.-Y. Shin, "An optimization network for matrix inversion," presented at the IEEE Conf. on Neural Information Processing Systems - Natural and Synthetic, Denver, Colorado (1987).

Use of a Micro-channel Spatial Light Modulator in a Sequential logic optical adder

Ph. Demaleprade, P. Chavel, K. Hibino, H. Yajima, T. Yatagai

One of the present challenges of optical computing is to demonstrate processors combining the digital accuracy usual in electronic computers with the parallelism and high interconnect density of optics. We therefore want to investigate the feasibility of an optical processor according to the general scheme of figure 1.

Such an architecture requires a 2-D nonlinear gate array. One possible candidate is the Micro Channel Plate Spatial Light Modulator (MSLM). which can be used as an OR or as a NOR gate (see figure 2). One problem for sequential logic or arithmetic is the quasi-permanent inherent memory of the device, which has to be reset externally. In this communication, even though we demonstrate cascadability of the device as a whole, we used each pixel only once. The whole MSLM was reset after the complete processing.

The example of the half adder implemented in parallel over a data plane by fully space-invariant connections is used here to demonstrate the following combination of the desirable features mentionned above :
- massive parallelism
- all-optical arithmetics
- use of a MSLM as a two-input NOR gate array
- cascadability of the device.

Figure 3-a shows a space invariant interconnect pattern. When applied to the two data bits A and B at locations 1a and 1b of figure 3-b, this interconnect pattern provides after three iterations through a NOR-ing MSLM the seven useful bits shown in 3-b and in particular the sum and carry bits S and C of the half-adder. Note that location 2c has to be masked out. Calculations can be performed in parallel :
- by leaving enough blank pixels around each computing site to avoid cross-talk
- or alternatively each site of figure 3-b may represent a whole 2-D array.

We choose the first option. The interconnect pattern was provided by a computer-generated hologram. Figure 3-c shows experimental results obtained after each of the three cycles from the four initial configurations (A and B = 0,0 ; 0,1 ; 1,0 and 1,1) as shown on the right-hand column.

Références :

P. Chavel, R. Forchheimer, B.K. Jenkins, A.A Sawchuk and T.C. Strand, Proceedings, Tenth International Optical Computing Conference IEEE, cat. 83CH1880-4, p 6, (1983).
B.K. Jenkins, A.A. Sawchuk, T.C. Strand, R. Forchheimer and B.H. Soffer, Applied Optics, vol 23, n°19, p 3455, (1984).
C. Warde, J. Thackara, Optical Engineering, vol 22 n°6, p695, (1983).
C. Warde & all, Applied Optics, vol 20, n°12, p 2069, (1981).

When this work was done , Ph. Demaleprade and T. Yatagai were with University of Tsukuba, Institue of Applied Physics, Ibaraki 305 (Japan)
P. Chavel with Institut d'Optique,BP 43, 91406 Orsay cedex, (France),
K. Hibino with Mechanical Engineering Laboratory, Optical Engineering Division, Tsukuba, Ibaraki 305, and H. Yajima with Electro-technical Laboratory, Opto Electronics Section, Tsukuba, Ibaraki 305. Ph. Demaleprade is now with Institut d'Optique, Orsay.

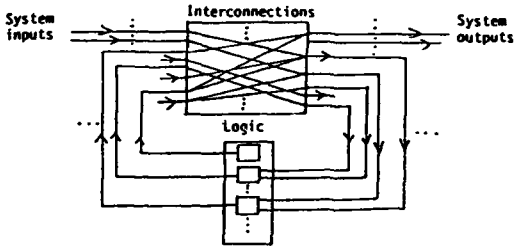

Fig 1 : Sequential logic Optical Processor, general architecture.

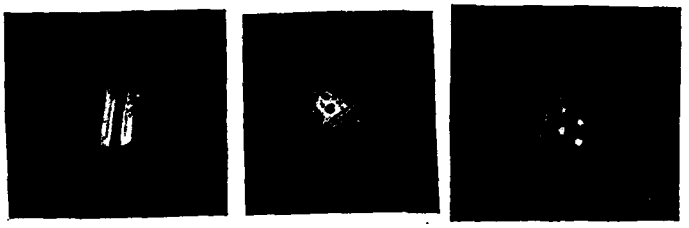

object A (B and C are rotated by 60 and 120 degrees)

OR(A,B,C)

NOR(A,B,C)

Fig 2 : NOR implementation of three variables using the MSLM.

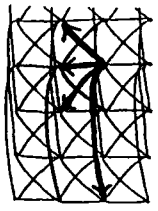

Fig 3-a : Space invariant interconnection net.

Carry = NOR(NOR(A) , NOR(B))

Sum = NOR(NOR(A,B) , Carry)

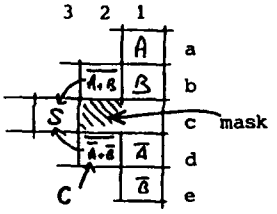

Fig 3-b : Logic implementation of a Half-adder using the interconnection net 3-a

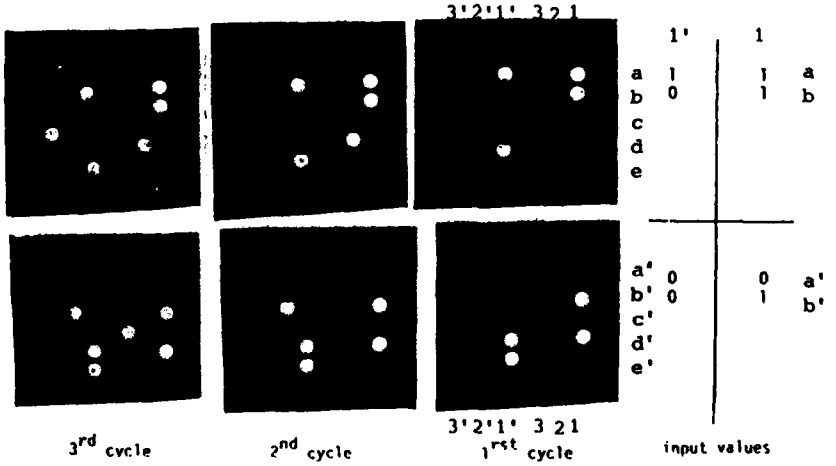

3rd cycle 2nd cycle 1rst cycle

Fig 3-c : Experimental results for Half-adding implementation.

Space-Variant Logic Operation Using Micro-Channel Plate Spatial Light Modulator

Yoshio Hayasaki, Makoto Ikeda and Toyohiko Yatagai
University of Tsukuba, Institute of Applied Physics
Tsukuba, Ibaraki 305, Japan

Satoshi Ishihara and Yoshinobu Mitsuhashi
Electrotechnical Laboratory, Opto-Electronics Section
Tsukuba, Ibaraki 305, Japan

Optical parallel processing techniques for performing binary logic operations are key elements of developing optical computers. Many efforts have been done to achieve increased throughput of binary digital logic by introducing optical parallelism. Ichioka and Tanida described a parallel optical logic array processor based on a shadow-casting system with LED light sources. All 16 logical functions for two binary variables realized in parallel by changing the illumination with LEDs. Bartelt and Lohmann proposed an optical logic processor by spatial filtering. We have described another type of an optical binary logic technique in which a variety of logical operations different in space can be performed in parallel.

As in the shadow-casting method and the spatial filtering method, a binary input pattern is spatially encoded. Consider input binary image data A and B are divided into NxN square cells. To represent states of logical "1" and "0", each square cell is divided into two sub-cells. The cells of one of the input binary images, called Aij, are coded in the horizontal direction, while the cells of the other input binary pattern, called Bij,in the vertical direction. We have proposed an interference pattern encoding technique for such spatial encoding.

In order to make a space-variant binary logic, we have proposed the use of a specific structured decoding mask of which cells are divided into four sub-cells. As shown in Fig. 1, a decoding mask is superimposed on the encoded input patterns. Decoding cells are arranged so that desired logic operations can be done in desired positions in the input patterns. The coded logic pattern is observed through the decoding mask.

In the present paper, we propose a simple encoding technique, based on XOR operation between an input pattern and a grating pattern. The encoding principle is shown in Fig. 2. For encoding the input A, we use a horizontal binary grating of which period is the size of the input pixel. For the input B, a vertical binary grating is used.

This XOR operation and superposition of the encoded input patterns can be performed by using a micro-channel plate spatial light modulator(MSLM). Figure 3 shows an optical arrangement of the MSLM space-variant parallel logic operation. The input area of the MSLM is divided into three parts, which are used for encoding input patterns A and B and for decoding operation. Superposition of the encoded input patterns are made by adjusting the feedback mirrors. Figure 4 shown experimental

results of encoding. The final result of space-variant logic is shown in Fig. 5

We described an optical logic operation technique based on spatial encoding and superposition of a decoding mask with the coded input patterns. Sixteen logical functions of two logical variables can be realized by using a single MSLM. This type of binary optical logic could be applied to general purpose optical computers, including cellular logic optical computers.

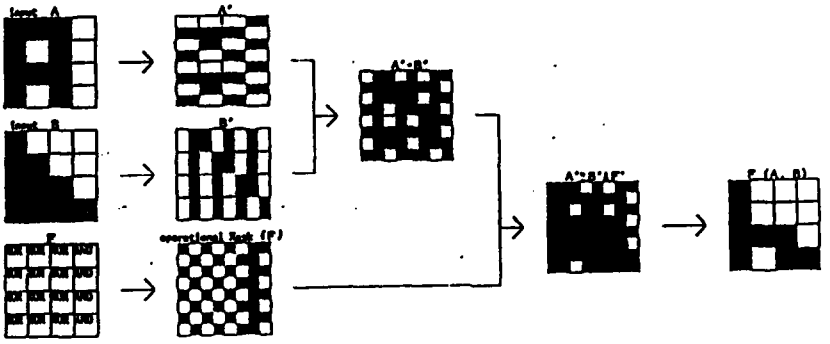

Fig. 1 Principle of space-variant parallel logic.

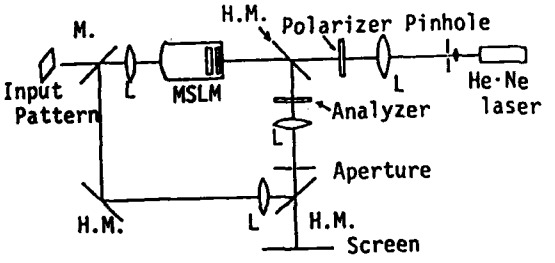

Fig. 2 MSLM implementation system.

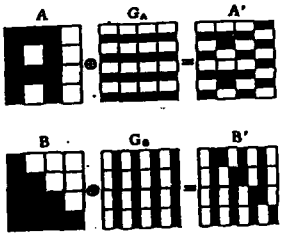

Fig. 3 Spatial coding based on XOR.

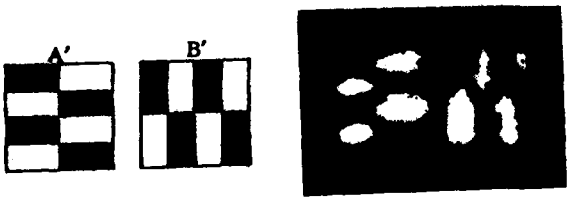

Fig. 4 Experimental result of coding.

Fig. 5 Output of space-variant gate.

Programmable optical parallel processor by polarization encoding: Cascade operation

By

Ken-ichi Kitayama, Masashi Hashimoto, and Naohisa Mukohzaka*

NTT Transmission Systems Laboratories,
1-2356 Take, Yokosuka-shi, Kanagawa 238-03, Japan
*Hamamatsu Photonics K.K.
1126-1 Ichino-cho, Hamamatsu 435, Japan

Cascade programmable logic operation in parallel is featured by optical processor using microchannel spatial light modulator(MSLM)[1] as well as spatial and pixel by pixel binary encoding by polarization state using birefringent plate.[2] In Fig.1 the schematic diagram for the experimental setup is illustrated. MSLM's are used to address optically input binary pattern. Readout He-Ne laser beam at λ=0.633 μm from MSLM is modulated in phase. Pixel mask is placed in front of MSLM1. Encoding is carried out by passing the beam through three birefringent plates(B.S.) consecutively and separating it spatially by polarization state according to binary logic of pixel. In Fig.2 the experimental encoded patterns are shown. After passing third B.S., eight positions in a pixel are allowed due to the logic combination of three inputs. Operation kernel serves to execute any logic operation according to the instruction addressed. It can be programmable by using spatial light modulator as 2D optical shutter based on polarization state.

In Fig.3 the example of experimental cascade three patterns' logic is shown. In this experiment, polarizers are temporarily used replacing the operation kernel. A variety of experimental logic operations will be presented in the conference. Finally, the implementation of the upgraded version of processor with feedback system shown in Fig.4 will also be presented. Latch and memory which could be implemented by MSLM to execute complex(or universal) pattern logics.

In conclusion, programmable optical processor performing cascade logic operation in parallel has been constructed. Experimental three patterns' logic in tandem has been shown.

References

1.C.Warde et al., Appl. Opt., 20, 2006(1981).
2.The present method is different from the one(A.W.Lohmann et al., Appl. Opt., 25, 131(1986)) in which a whole image is encoded together not by beam position but by beam direction.

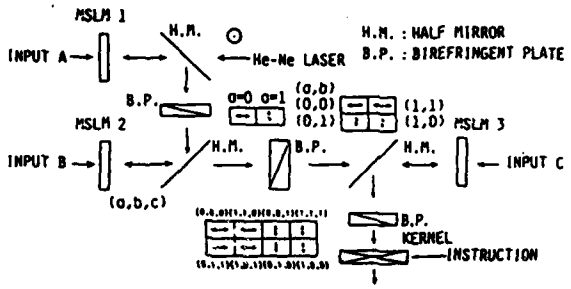

Fig.1 Experimental setup of optical processor

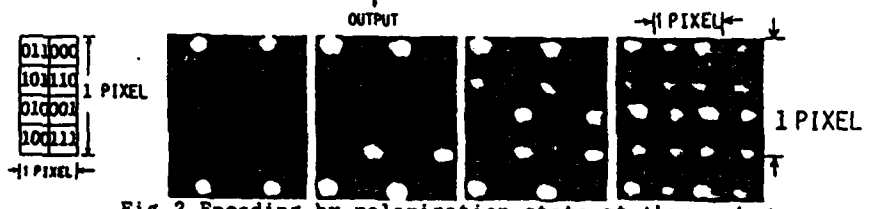

Fig.2 Encoding by polarization state at three stages

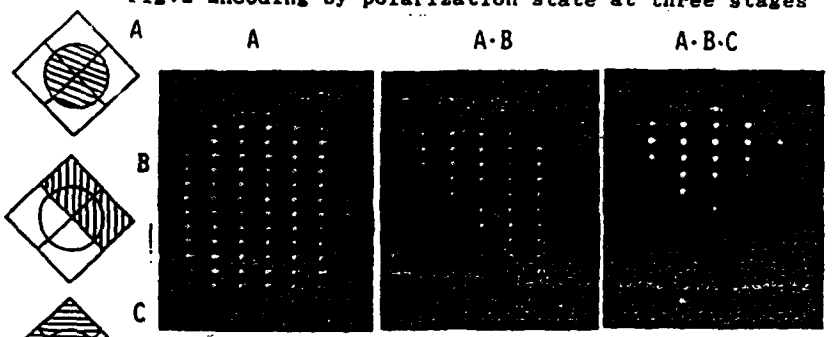

Fig.3 Experimental three patterns' logic; A, A·B, and A·B·C

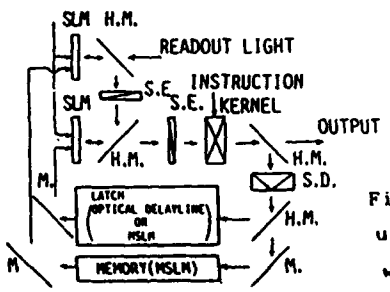

Fig.4 Schemtic diagram of upgraded optical processor with feedback system

Tuesday august, 30, 14.45

SESSION 3 (Chairman J.W. GOODMAN)

PARALLEL PROCESSORS
PROCESSEURS PARALLELES

E1 - K.H. BRENNER : Digital optical computing with symbolic substitution.

E2 - G.G. VOEVODKIN, E.N. DIANOV, A.A. KUZNETSOV and S.N. NEFJODOV : Polychromatism in optical digital processors.

E3 - T. UCHIDA and K. TADOKORO : Optical parallel logic device using liquid crystal.

E5 - P. CANDON, J.L. de BOUGRENET de la TOCHAYE : An optical processor for mathematical morphology.

E4 - R. THALMANN, G. PEDRINI, B. ACKLIN and R. DÄNDLIKER : Optical symbolic substitution using diffraction gratings.

Digital optical computing with symbolic substitution

Karl-Heinz Brenner
Physikalisches Institut der
Universität Erlangen
Fed. Rep. of Germany

Abstract:

Symbolic substitution is a spatial logic which is adapted well to optical processing. Unlike Boolean logic it also includes spatial information in the coding. It requires only regular interconnections and nonlinear devices with limited fan-out. Nevertheless the potential of this kind of logic ranges from parallel binary arithmetic to a programmable MIMD processor. Fundamentals of symbolic substitution and its applications are presented.

POLYCHROMATISM IN OPTICAL DIGITAL PROCESSORS

G.G.Voevodkin, E.M.Dianov, A.A.Kuznetsov, S.M.Nefjodov

General Physics Institute, Academy of Sciences of the USSR
38 Vavilov Street, Moscow 117942, USSR

Photons of different wavelengths in a single beam can interact with a binary logic gate independently and in different ways; this fact can increase the speed of the optical computers. A polychromatic flow with 10^3 spectrally distinct emissions may be transmitted independently and in parallel through a single channel (an optical fiber) [1]. We describe here the parallel realization of 16 logical functions with two binary matrix elements in the real time scale (two light flows with distinct wavelengths are used - bichromatic logic) and fast digital multiplication by analog convolution with a polychromatic light source.

For 16 logical functions realization with binary matrix elements two liquid crystal light valves (LCLV, S-effect) and the light sources with the wavelengths of λ_1 (green) and λ_2 (red) were used. The digital data were presented as spatial distribution of binary object transmission: transparent parts present logical 1 and opaque parts - 0. When the external data matrix is projected at LCLV photosensitive layer, it is possible to obtain at the LCLV output (after the analyzer) the positive image of the input matrix at the readout light wavelength λ_1 and inverted (negative) image at λ_2. Thus if A is the input image, at the output we have a green A and a red $\overline{A}$ [2].

For the optical realization of logical functions the scheme was used consisting of two LCLV (with two input matrix projections), of two light sources with different wavelengths, polarizers, optics and of a Wollaston prism as an output analyzer for spatial discrimination of the images with orthogonal polarizations (similar to direct and inverse outputs of the electronic digital schemes). 16 logical function realization is possible for the input matrices A and B, speed of operation for 6 functions being limited only by the sources operating time (less than 10^{-9} s for LD).

The features of the method are the following:

- all 16 logical functions are realized in parallel;
- combinatory logic operations are realized by a simple source switching (due to this fact the system can be easily programmed);

- application of LCLV with large functional possibilities (magnification, high sensitivity, coherent light readout, small power consumption) will provide an opportunity to create simple and flexible devices for optical computers.

One of the main operations in a digital computer is multiplication. Recently suggested digital convolution algorithm decreases essentially the multiplication time for large numbers [3,4]. We have optically realized this operation with a polychromatic light source (N laser diodes with equidistant emission wavelengths). The information launching is accomplished by the laser modulation (on/off). All the beams are united in a single one by a diffraction grating. The resulting polychromatic beam after the broadening illuminates the transparency with an external data matrix and then meets the second grating. The lens creates a transparency image in a photodiode matrix plane. At the corresponding grating dispersion the transparency images in each colour will be shifted in the PD plane by the step of the external data matrix. The light intensity distribution in each line of PD matrix will correspond to the convolution of the first input signal (LD combination) with each line of the external data matrix. LCLV with the twist effect can be used as the data launching device. After the convolution computing the mixed binary product is transformed into the binary one with the parallel A/D converter (for example, on the base of an electro-optical interferometer). The computing accuracy depends on the number of spectrally distinct sources and the number of independent elements in a photodiode matrix line.

Optical multiplication has been accomplished by the simultaneous realization of two logical functions and analog convolution operation

References

1. G.G.Voevodkin, E.M.Dianov, A.A.Kuznetsov, S.M.Nefjodov, Sov.J. Radiotekhnika, No.10, 91(1986)
2. G.G.Voevodkin, E.M.Dianov, A.A.Kuznetsov, S.M.Nefjodov, Sov.J. Pis'ma Zh.Tekh.Fiz., vol.12, 22, 1373(1986)
3. H.J.Whithouse, J.Speiser, Aspects of Signal Processing, vol.2, (1977)
4. D.Psaltis, D.Casasent, D.Neft, M.Carlotto, Proc.SPIE, 232(1980).

OPTICAL PARALLEL LOGIC DEVICE USING LIQUID CRYSTAL

TATSUO UCHIDA and KAZUHIKO TADOKORO
Department of Electronic Engineering, Tohoku University

The authors propose an optical parallel logic devices using twisted nematic liquid crystal cells (TN-cells) doped with dichroic dyes and dichroic filters such as shown in Fig.1. In addition, the general expression of the operated logical results is induced by using simple combination of transfer function of 2X2 matrix for the TN-cells and the dichroic filters.

The relation between input and output polarized lights of the single TN-cell doped with dichroic dye such as TN_1 shown in Fig. 1 is expressed as follows:

$$\begin{bmatrix} V_o \\ H_o \end{bmatrix} = \begin{bmatrix} A & \bar{A} \\ D\cdot\bar{A} & A \end{bmatrix} \begin{bmatrix} V_i \\ H_i \end{bmatrix} \qquad (1)$$

where V and H denote vertically and horizontally polarized lights, respectively, and their subscripts o and i output and input lights, respectively. A denotes input logic signal for a pixel of the TN-cell, and takes 1 or 0 according to on- or off-state of the TN-cell, and D is defined to be 0 or 1 corresponding to absorption- or non-absorption wavelength of the doped dichroic dye, respectively. The 2X2 matrix on the right hand side of eq.(1) is regarded as transfer function of the TN-cell. In the same way, the transfer function of the dichroic filter is expressed as $\begin{bmatrix} 1 & 0 \\ 0 & P \end{bmatrix}$ where P is

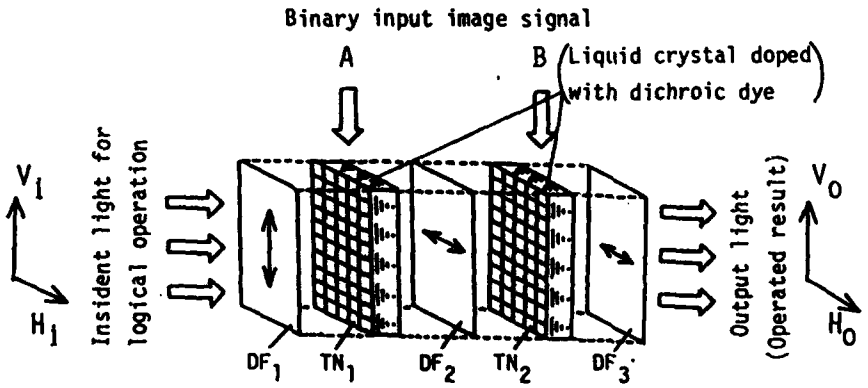

Fig.1 Configuration of parallel optical logic device

defined to be 0 or 1 according to absorption- or non-absorption-wavelength, respectively. By using these expressions, the result of logical operation of the whole logic device shown in Fig. 1 is expressed as follows:

$$\begin{bmatrix} V_o \\ H_o \end{bmatrix} = \begin{bmatrix} P_3 & 0 \\ 0 & 1 \end{bmatrix} \begin{bmatrix} B & \overline{B} \\ D_3 \cdot \overline{B} & B \end{bmatrix} \begin{bmatrix} P_2 & 0 \\ 0 & 1 \end{bmatrix} \begin{bmatrix} A & \overline{A} \\ D_1 \cdot \overline{A} & A \end{bmatrix} \begin{bmatrix} 1 & 0 \\ 0 & P_1 \end{bmatrix} \begin{bmatrix} V_i \\ H_i \end{bmatrix}$$

$$= \begin{bmatrix} P_3 \, (P_2 \, A \cdot B + D_1 \cdot \overline{A} \cdot \overline{B}) \, V_i + P_1 \cdot P_3 \, (A \cdot \overline{B} + P_2 \cdot \overline{A} \cdot B) \, H_i \\ (D_2 \cdot P_2 \cdot A \cdot \overline{B} + D_1 \cdot \overline{A} \cdot B) \, V_i + P_1 \, (A \cdot B + D_2 \cdot P_2 \cdot \overline{A} \cdot \overline{B}) \, H_i \end{bmatrix} \qquad (2)$$

where, subscripts 1-3 correspond to subscript numbers of the TN-cells and the dichroic filters shown in Fig.1. From this equation, it is seen that suitable combination of 1 or 0 for P_1, P_2, P_3, D_1 and D_2 as well as choice of V_i, H_i, V_o and H_o enables the following fifteen logical operations to be executed: 0, A, B, $\overline{A}$, $\overline{B}$, $A \cdot B$, $A \cdot \overline{B}$, $\overline{A} \cdot B$, $\overline{A} \cdot \overline{B}$, $A \oplus B$, $\overline{A \oplus B}$, $A+B$, $A+\overline{B}$, $\overline{A}+B$, 1, which covers almost all binary logical operations except $\overline{A}+\overline{B}$. Eq.(2) also implies that several logical operations are simultaneously executed by different wavelength and different polarized lights. In actual, it is experimentally confirmed that sum and carry of half-adder, for instance, between input signals A and B shown in Fig.1 can be simultaneously obtained by different wavelength.

For the next step, a higher function is introduced to this logic device by adding image sensor and feedback loop as shown in Fig.2 for iterative processing. As an example of possible logical operation by this system, template matching was tried to be executed and the validity of the results was confirmed.

Finally, it will be discussed that optical input system can be introduced to this device instead of the present electrical input system by combining photoconductor and thin-film-transistor array with the liquid crystal layer.

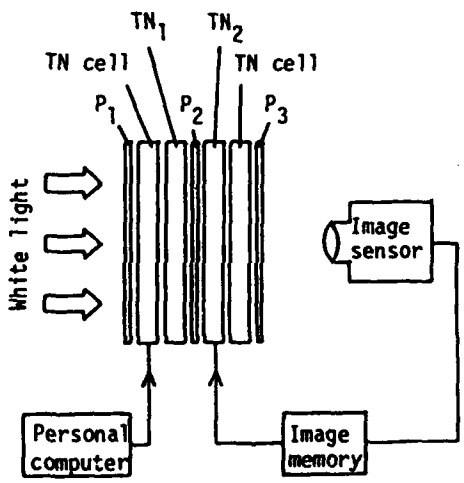

Fig.2 Configuration for iterative processing

" AN OPTICAL PROCESSOR FOR MATHEMATICAL MORPHOLOGY "

P. Cambon, J.L. de Bougrenet de la Tocnaye

Groupe Optique et Systèmes de communication

E.N.S.T. de Bretagne
BP 832
29285 BREST-CEDEX

Introduction:

The use of the mathematical morphology is of great interest in the field of robotic-vision and pattern recognition. The computational costing of a digital approach is related principally to the size of the pixel array to be processed and the spatial complexity of the chosen structuring element. By using a spatial light modulator as an optical logic array processor it is possible to overcome these difficulties to some extent.

Basic operator of mathematical morphology:

The mathematical morphology operators are linear for boolean inclusion, union and intersection . The two basic operations, called dilatation and erosion, are defined in binary pictures by Minkowski algebra :

$$X \oplus B = \bigcup_{x \in X} B_x = \bigcup_{b \in B} X_b \qquad (1)$$

Each point x of the object X spreads out to occupy the area of the structuring element B_x, then the union of these areas is processed. This processing is known as a dilatation: its inverse (i.e. using the intersection) is an erosion.

The various possible combinations between dilatations and erosions give rise to an infinite set of new mappings which can be concatenated with each other (opening, closing, skeleton etc...).

Optical version of a morphology operator :

The basic relation (1) can be rewritten as follows:

$$X \oplus B = X \cup X^1 \cup X^2 \cup \ldots \qquad (2)$$

where the X^i are translated versions of X according to the geometry of B.

This means that this sum can be obtained only with spatial logical operations and object translations.

The use of a liquid crystal matrix (LCD) is well suited for such an application. The two logical states can be coded through the two states of polarization obtained from a monochromatic light wave linearly polarized by using the electrical birefringence of the LCD . The AND and OR logical operations are achieved simply by sandwiching the two LCD with two crossed polarizors.

The object translation is achieved by register shift of the LCD matrix controler, and the result of the logical operation is observed on a CCD camera (or an optical RAM).

Experimental Set-up :

The timing of the processing is provided by a digital microcomputer and the scheme of the relation (2) is achieved as follows:

First step: The object is loaded into the first LCD matrix and its translated in the second one, the result is then observed on the CCD detector (the AND or OR is selected by simple binary complementation).

Second step: The result is transferred onto the first matrix in place of the initial object and the second translation loaded in the second LCD and so on.

Such a set-up is well suited to performing iterative processings as required in the case of the programming of mathematical morphology operators. In the case of using a simple structuring element, the optical iteration (2) can be replaced by a cascading series of LCD matrices .

The spatial resolution of the chosen LCD matrix is of 128 x128 pels, and the expected processing time for a basic operation like an erosion is only of a few hundred milliseconds.

Optical Symbolic Substitution using Diffraction Gratings

R. Thalmann, G. Pedrini, B. Acklin, and R. Dändliker
Institute of Microtechnology, University, CH-2000 Neuchâtel, Switzerland

Symbolic substitution is a concept to perform parallel and space-invariant logic operations on a binary input pattern [1]. It recognizes all occurrencies of a set of symbols (predefined spatial distribution of binary values) and substitutes them with other predefined symbols. For practical use, a universal optical implementation for symbolic substitution should feature: possibility to substitute symbols with many pixels; multiple channel substitution (different symbols in parallel); dual-rail (true/false) recognition; programmability of the symbols to be recognized; high spatial bandwidth; lack of sophisticated components. In the following, we describe an optical implementation based on the use of diffraction gratings, which meets the above requirements.

The optical arrangement for symbolic substitution is sketched in Fig.1. A grating splits the input pattern into different diffraction orders. The distance a between the grating and the input pattern is chosen so that the patterns of two adjacent diffraction orders are shifted by one pixel in the image plane. Spatial filtering in the Fourier plane allows to choose the search symbol by selecting only the appropriate diffraction orders. The optically nonlinear thresholding device (usually a NOR gate array, we use a liquid crystal light valve) restores the output pattern of the recognition unit to binary values. The substitution unit consists of an identical arrangement, where the substitution symbol is again defined by spatial filtering. The simple experimental patterns in Fig.1 illustrate the optical processing: a) input mask, as seen at the output; c) output pattern of the recognition unit after spatial filtering for the search symbol b); e) output pattern of the substitution unit after spatial filtering for the replace symbol d).

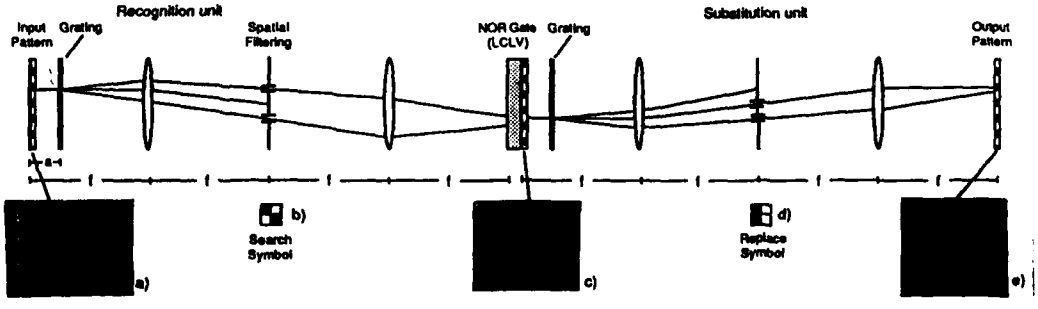

Fig.1. Optical arrangement for symbolic substitution and illustrative experimental results.

The diffraction gratings are used as fanout elements to produce multiple copies of the input image. Two crossed transmission (phase) gratings with several diffraction orders allow to realize any 2-dim. search or substitution symbol. Using the thresholding device in the NOR mode lowers the requirements on uniformity: the intensity of each diffraction order must be above the threshold of the light valve. To realize the phase gratings we used two different approaches, both based on bleached silver halide photographic plates. The ease of fabrication and the high obtainable space bandwidth product (SBWP) favor sinusoidal holographic gratings, if the fanout does not exceed three. For higher fanouts, binary Dammann gratings [2] were drawn on a Laser printer (SBWP > 2400) and photographically reduced. The experimental results of Fig.2 show intensity profiles through the diffraction orders of a holographic grating and a binary grating with 7 equal diffraction orders, respectively.

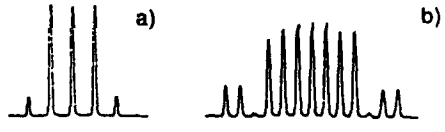

Fig.2. Measured intensity profiles through a) holographic and b) binary grating.

In the following, several more advanced arrangements for optical symbolic substitution using diffraction gratings shall be presented, some of them with experimental results and potential applications.

a) **Complex search symbols:** Using two crossed gratings with several diffraction orders, arbitrary complex search symbols can be recognized. The Figure 3 shows the recognition of a 3x3 symbol.

b) For **dual-rail substitution** (true/false recognition), two similar approaches can be applied. One possibility is the coding of each bit by a pair of two complementary pixels [1]. Instead of a 3x3 symbol, e.g., a 6x3 symbol must then be recognized. Another way of dual-rail coding is the representation of the positive and negative input mask, one beside the other, and then recombining the two masks on the NOR gate array. This recombination can be carried out either by a grating with only two diffraction orders or by a prism placed behind one of the two parts of the mask. Figure 4 shows the experimental result of a dual-rail recognition, performed by the latter of the above described methods.

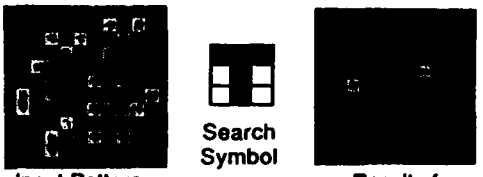

Fig.3. Recognition of a 3x3 symbol.

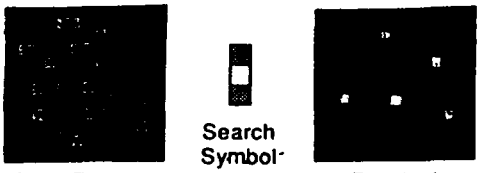

Fig.4. Dual-rail recognition of a 3x1 symbol.

c) **Multiple channel substitution** can be realized by introducing an additional grating in order to produce multiple spatially separated images on the thresholding device. The corresponding diffraction orders in the Fourier plane have to be sufficiently separated that for each channel another search symbol can be chosen by appropriate filtering of the diffraction orders. The different recognition symbols at the output of the NOR gate array are then again recombined through the substitution unit, either by prisms or by gratings, as explained above for dual-rail substitution. Multiple channel symbolic substitution could be applied to optical residue arithmetic computing [3].

d) **Polarization coded symbolic substitution** [4] can be easily implemented using the proposed arrangement based on diffraction gratings. Here, instead of blocking the appropriate diffraction orders in the Fourier plane, their polarization state is changed, using a half wave plate or an element with 90° optical activity. This can be accomplished, e.g., with the help of an electronically addressable liquid crystal display. Corresponding experimental results will be presented.

e) **Iterative symbolic substitution** is realized by using a second thresholding light valve in the input plane and feeding the substitution pattern back to the input. An interesting application of iterative symbolic substitution is the binary adder with carry propagation.

The described optical implementation of symbolic substitution using diffraction gratings offers interesting features, such as the possibility of substituting arbitrary complex symbols and multi-channel substitution. Holographic and binary gratings turn out to be very appropriate fanout elements which are cost-effective and relatively easy to produce. The gartings can be specially tailered and optimized for the desired application. If fully programmable symbols with many pixels are to be recognized and replaced, however, an important loss of optical power must be accepted, because many diffraction orders have to be blocked for the spatial filtering. This can be avoided by the use of special purpose binary gratings and polarization coded symbolic substitution.

References

1. see, e.g., K.-H. Brenner, A. Huang, and N. Streibl, Appl.Opt. 25, 3054 (1986).
2. H. Dammann and K. Görtler, Opt. Commun. 3, 312 (1971).
3. A. Huang, Y. Tsunoda, J.W. Goodman, and S. Ishihara, Appl. Opt. 18, 149 (1979).
4. K.-H. Brenner, Appl. Opt. 25, 3061 (1986).

Tuesday august, 30, 17.00

SESSION 4 (Chairman W. NICKLI)

ACTIVE COMPONENTS
COMPOSANTS ACTIFS

A2 - M. PAPUCHON : Integraded optics and computing.

OPTICAL PROCESSING CONCEPTS
CONCEPTS DE TRAITEMENT OPTIQUE

C_1 - M. SHABEER, I. ANDONOVIC and B. CULSHAW : Fibre-optic systolic array architectures.

C_2 - J. RIEHL, J. APPEL, A. THIRIOT and J. DOREY : Hybrid electronic/non coherent optical processor for large scale phased array.

C_3 - V.P. HEURING, H.F. JORDAN and J.P. PRATT : A bit serial architecture for optical computing.

C_4 - Y.A. BYKOVSKY, A.A. MARKILOV, M.F. SHAZHELIUK and S.M. STRARIKOV : Optical computing by double transformation of spatical coherence of light.

INTEGRATED OPTICS AND COMPUTING

M.PAPUCHON
THOMSON-CSF/LCR
Domaine de Corbeville - 91401 ORSAY (FRANCE)

ABSTRACT

Some integrated optic devices are now commercially available. The potential applications of this technology to the field of optical computing will be reviewed in that paper including state of the art results on active circuits.

FIBRE-OPTIC SYSTOLIC ARRAY ARCHITECTURES

M Shabeer, I Andonovic, B Culshaw

Department of Electronics & Electrical Engineering

University of Strathclyde

Royal College Building

204 George Street

Glasgow G1 1XW.

INTRODUCTION.

Fibre-optic signal processing has concentrated on tapped delay lines[1], lattice structures[2] and systolic arrays[3]. For guided-wave processors, one special area of interest has been the matrix-vector[4] and matrix-matrix[5] multiplication. Although the schemes are elegant and fast, the main disadvantages lies in limited accuracy, and failure to handle bipolar/complex quantities.

Here, a configuration based on systolic array architecture[4] is presented for improving the accuracy of, amongst other things, matrix multipliers. The technique is based on 2's complement number representation and digital multiplication by an analogue convolution algorithm[6]. The 2's complement number representation allows bipolar data handling capability, and thus eliminates the need for matrix partitioning when the matrices of interest are real. Following this scheme, the matrix elements are represented by the same number of bits (in 2's complement number representation) as that required to represent their (largest) product. The product of the binary numbers is then calculated by performing the normal multiplication. Any bits generated to the left of the most significant bit are truncated[6]. Furthermore, the output is allowed to assume mixed binary values[6], and no carries are generated. The mixed binary output can be converted to signed binary by passing it through a fast A/D converter.

The operation of one such systolic matrix multiplier is depicted in Fig.1. The input matrix elements to the (2x2) systolic matrix are represented by pulses from a pulsed source and the fixed matrix elements are represented by optical fibre couplers(Fig. 2.). Each block(BT) in Fig.1. is represented by N couplers for a N-bit number representation.Fig.3. shows the results of a simple multiplication for matrix elements ±1 with ±1. Fig.3(a). shows the result of +1 x +1, Fig.3(b). shows the result of +1 x -1, and Fig.3(c). shows the result of -1 x -1. The upper traces show the mixed binary output whilst the bottom traces show the corresponding signed binary outputs.

The presentation will further consider the criteria for efficient implementation of these configurations. Factors such as programmability, and cascadability will be addressed and several specific application areas will be described.

In summary optical systolic based architectures have been investigated and matrix multiplication of real and complex quantities has been realised. Increases in accuracy of what are otherwise analogue processors and the ability to handle bipolar/complex quantities are two main advantages that accrue with this approach.

ACKNOWLEDGEMENT

M Shabeer would like to thank Pilkington Guided Wave Optics (Barr & Stroud Ltd.) for their financial support and for provision of the integrated optical coupler.

.REFERENCES

1. K P Jackson, J E Bowers, S A Newton, and C C Cutler; Appl. Phys. Lett, 41, pp139(1982).

2. B Moslehi, J W Goodman, M Tur, and H J Shaw; Proc. IEEE, 72, pp930(1984).

3. M Shabeer, I Andonovic, and B Culshaw; Opt. Lett; 12, pp959(1987).

4. H T Kung; Computer, 15, pp37(1982).

5. R P Bocker, K Bromley, and S R Clayton; Proc. Soc. Photo-Opt. Instrum. Eng; 431, pp194(1983).

FIGURE CAPTIONS

Fig. 1. Systolic 2x2 matrix multiplier.

Fig. 2. N-bit number representation.

Fig. 3. Experimental results showing the mixed binary outputs(top traces) and the signed binary outputs(bottm traces) for (a) +1x+1, (b)+1x-1, (c)-1x-1 binary multiplication.

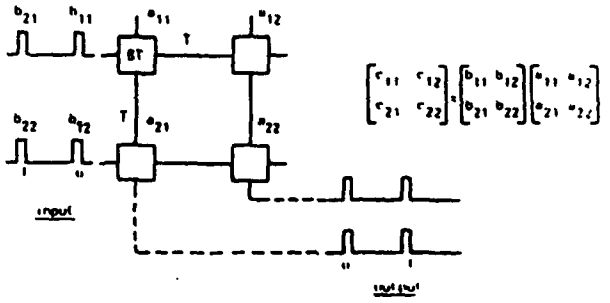

Fig. 1

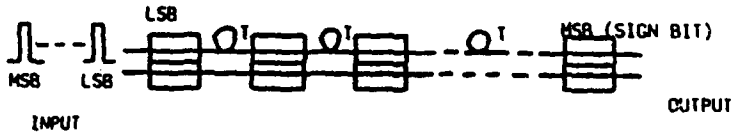

Fig. 2

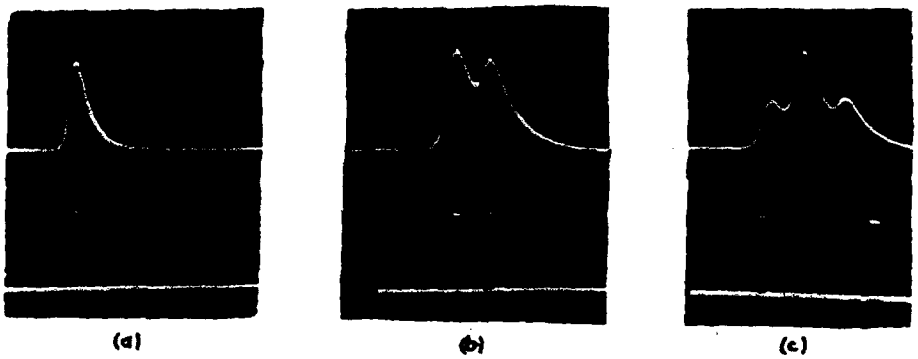

Fig. 3

HYBRID ELECTRONIC/NON COHERENT OPTICAL PROCESSOR FOR LARGE SCALE PHASED ARRAY

J.RIEHL , J.APPEL , A.THIRIOT , J.DOREY
ONERA
29 av. de la Division Leclerc - BP72 - F92322 Châtillon Cedex (France)

1. Introduction

The processing of large scale phased array radars requires advanced signal processing techniques and architectures with real-time and parallel processing capability . Non coherent analog optical signal processors appear to be quite appropriate for this problem , because of the inherent parallelism of optics and the availabilty of high speed incoherent light emitters .

In this paper we present an hybrid electronic/optical processor for the air coverage radar RIAS (Synthetic Aperture Pulse Radar) data processing ; the optical stage , based on a lensless shadow-casting architecture , is particularly detailed .

2. RIAS processing

The RIAS phased array is a cicular array of emitting and receiving antennas , with spatial coding of the emitting array through orthogonal frequencies . The signal received at the j-th antenna , with a target at range r , is :

$$s_j(t) = \sum_i e^{j\,(\,2\pi f_i (t - 2r/c) + \phi_{i,j,\theta,\varphi}\,)}$$

where $\phi_{i,j,\theta,\varphi}$ is a phase information .

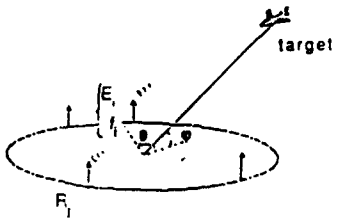

Fig 1 : radar geometry

RIAS processing steps are the following : (1) frequency filtering of each $s_j(t)$ (2) phase compensation of $\phi_{i,j,\theta,\varphi}$ and signals addition for each (θ,φ) direction . When phase compensations are correct , temporal pulse compression occurs which gives (θ,φ) and range information after thresholding .

The RIAS processor schematic diagram is the following :

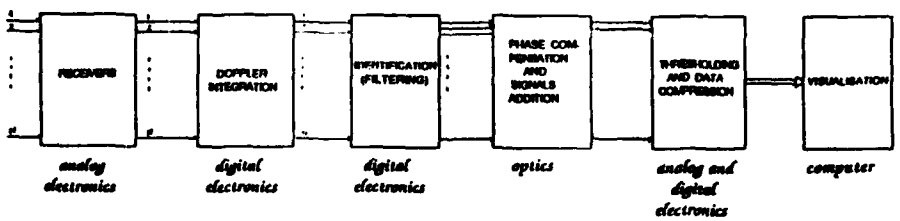

Fig 2 : processor schematic diagram

3. Optical processor

The real-time and parallel processing features of optical systems make them attractive candidates for simultaneous phase compensation and signal addition at numerous (θ,φ) directions , which is a critical computing step for high speed RIAS processing .

A lensless shadow-casting system with a light emitting diode (LED) array as input , a photographic mask and a photodetector (PD) array as output , has proved to be well suited to this problem :

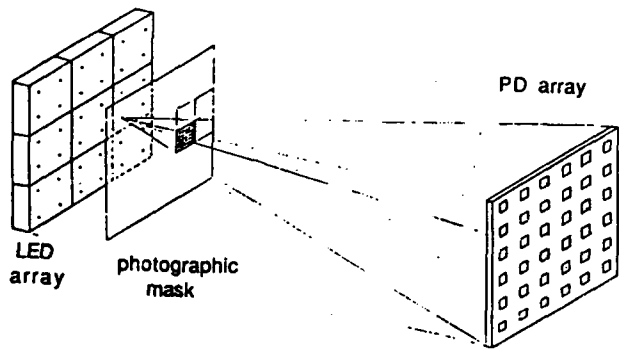

Fig 3 : shadow-casting architecture

Each PD receives a signal of the following form :

$$S(n,m) = \sum\sum E(i,j) \cdot M(i,j,n,m)$$

With $E(i,j) = s_{i,j}(t)$ and $M(i,j,n,m) = e^{-j\phi_{i,j}.\theta.\varphi}$, the RIAS ambiguity function can be easily computed . Because only real positive values can be handled with both incoherent light and photographic mask , we uses four LED and four elementary transparencies for each basic operation :

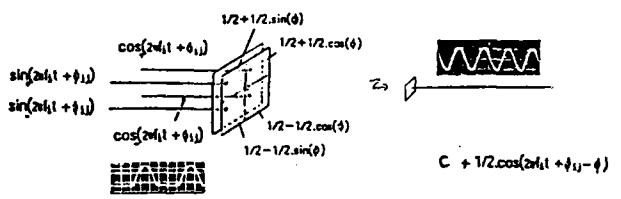

Fig 4 : elementary computing cell

Parallelism is extended at the output stage with simultaneous electronic thresholding on each receiving channel . Data compression then allows detected targets data storage through electronic computer .

4. Experimental results

An experimental prototype has been built , with 10×10 LED , 500×500 transparencies and 100 PD arrays , the geometrical implementation being already suited to 50×50 LED , 2500×2500 transparencies and 50×50 PD arrays . The design of this processor concentrated on minimisation of diffraction effects and correct positioning of the LED array and mask .

Dynamic range exceeds 1000:1 , with a computing rate of about 30 Gops . With faster Doppler processing , computing rate of about 1 Tops is soon expected .

A BIT SERIAL ARCHITECTURE FOR OPTICAL COMPUTING

Vincent P. Heuring Harry F. Jordan Jonathan P. Pratt

Center for Optoelectronic Computing Systems
Department of Electrical and Computer Engineering
University of Colorado
Boulder CO 80309-0425

ABSTRACT

The design of a bit-serial optical computer is described. The central components are $LiNbO_3$ directional couplers as logic elements, and fiber optic delay lines as memory elements. The key device characteristics are discussed, including the special properties and limitations that are important when designing with them. Following this the key design issues are addressed. These include computation in a realm where propagation delays are much greater than logic delays, and implementation of circuits without flip-flops. Design principles are exemplified by the design of a *n*-bit counter. Following this, the design for a simple bit-serial computer is described.

INTRODUCTION

This paper describes an architecture for a practical digital computer constructed from optical components, which use photons rather than electrons to convey information. There have been a number of proposals for optical computer architectures in the literature, but they are either architectures for special-purpose machines, or they rely on devices that are in the research category.

Our objective in this research was to design a machine that could be constructed from commercially available components. As such, we faced some of the same constraints as were faced by early architects of electronic computers: a severe limitation on the number and kinds of devices that could be used in a practical implementation. As our predecessors did, we chose a bit-serial architecture to minimise device count. Our studies have shown that the $LiNbO_3$ directional coupler will serve as the logic device, and a glass fiber loop as delay-line memory.

PHYSICAL COMPONENTS

The Lithium Niobate Directional Coupler as a Logic Element

The $LiNbO_3$ electrooptic switch is an optical guided wave device produced by diffusing precisely placed titanium waveguides into high-purity optical lithium niobate crystals. This paper will show how the $LiNbO_3$ serves as a "complete" logic element, having the functionality of a buffer, inverter, AND gate, multiplexer, and demultiplexer depending on its configuration in the logic circuit. The directional couplers, which usually contain 4 optical terminals and one electronic control terminal, are converted to 5-terminal optical devices by incorporating a detector and drive electronics at each device. The design also uses conventional 3dB optical splitters for signal fan-out, and optical combiners that serve as the optical equivalent of the "wired or"gate.

The Optical Delay-Line Memory and System Clock

The optical delay-line memory is simply a loop of optical fiber whose length is computed to hold a specified number of circulating bits, at a given clock frequency. Key to the use of optical fiber in this capacity is the use of the $LiNbO_3$ directional coupler for synchronisation and amplitude

restoration in the loop. This synchronization and amplitude restoration is important, since losses in the directional couplers can approach 7 dB, in addition to fiber losses. Thermal coefficients of expansion and refractive index impose limitations on the size of the loop, unless measures are taken to control this source of variation in the optical length of the delay line. The paper discusses measures to minimize or compensate for this effect. System clocking is provided by a 1300 nm laser modulated at the desired frequency. Clock duty cycle is less than 50%.

SYSTEM DESIGN

Design techniques employed here did not use any flip-flops or latches for synchronization. Rather, the design relies on temporal synchronization *during the design process*. Fiber lengths were calculated so pulses arrive at key locations in synchronization. The first design iteration was done assuming no delays anywhere except where they are desired. A second interation takes into account component delays and incorporates them when computing fiber interconnect lengths.

System Architecture

The system employs 49 directional couplers. The system is accumulator based, with a single accumulator, instruction register, and program counter, all 16 bits in length. The main memory is a fiber delay loop. The ALU is capable of simultaneous calculation of complement, sum, and, or, clear, and rotate right. Instruction execution has four phases, instruction search, instruction fetch, operand search, and instruction execution. The instruction set is fairly conventional, with eight instructions. These instructions each permit a computation, and conditional or unconditional branch capabilities, however, allowing some instructions to perform "double duty."

SUMMARY

We describe an optical computer based on fiber delay line storage, optoelectronic directional coupler logic and switching, and fiber interconnections. Such a system bears a distinct similarity to early electronic computers resulting in both cases from the technological problemsinvolved in building and reliably operating large numbers of active devices. The fact that signal propagation time is large relative to gate delay gives a major geometrical component to the architecture. The signal propagation time is even used as the basis for storage of information, so that each signal path in the machine must be considered as a storage element, or at least modifying the behavior of a storage element that is the source or destination of the signal. The use of optoelectronic directional couplers as the active elements of the machine leads to a unique solution to the signal amplitude and timing restoration problem. The architecture for a first optical, stored program computer has two goals: it is a short route to an operating optical computer, and it permits computer architects to become involved in optical computer design. This effort should result in technology which will permit high-speed all optical controllers for control of fiber optic communications systems.

OPTICAL COMPUTING BY DOUBLE TRANSFORMATION OF SPATIAL COHERENCE OF LIGHT

Yu.A.Bykovsky, A.A.Markilov, M.F.Smazheliuk, S.N.Starikov
Moscow Engineering-Physics Institute, U.S.S.R.

Summary

The possibility of spatial frequency filtering and correlation analysis of images by double transformation of spatial coherence of light is considered. Experimental setups and results on image processing with partially coherent light are described.

Abstract

Spatial coherence, as well as amplitude, phase and polarization of light passed through an optical system can be modulated by the information to be processed. The transformations of spatial coherence permit to perform computing operations on images formated by quasimonochromatic spatially incoherent light. The transformation of spatial coherence on free space path with following visualization by a wavefront rotating interferometer allows to compute Fourier-transform of the input image intensity distribution. The double transformation of spatial coherence with masking in spatial frequency plane makes available spatial frequency image filtering. The bipolar impulse response of the filter can be realized too. The intermediate holographic recording the visualized spatial coherence offers the possibility to carry out both linear and nonlinear computing operations. For instance, the autocorrelation function for the input image can be calculated when the hologram is illuminated by partially coherent light and Fourier-transform of the hologram intensity distribution is optically fulfiled. The experimental comparison of optical computing by the described method with coherent light computing demonstrates that inaccuracy due to phase aberrations and displacements of optical elements is considerably smaller in the first case. Thus, the use of the double transformation of spatial coherence of light in optical systems with spatial incoherent quasimonochromatic input illumination provides to implement linear and nonlinear computing operations.

Wednesday august, 31, 8.30

SESSION 5 (Chairman A.A. SAWCHUK)

INTERCONNECTIONS
INTERCONNEXIONS

B1 - D. CONTE : Massively parallel computing and optical interconnection architectures.

B_2 - H. HASKAL, P.D. HENSHAW, R.C. KNOWLTON and P.B. SCOTT : Applicability of laser beamsteering for rapid access to 2D, 3D and 4D optical memories.

B_3 - J. JAHNS : Optical crossover interconnections.

B_4 - A. HARTMANN and S. REDFIELD: "Ox", optical crossbar switch designs for parallel processing.

B_5 - P. CHEROUX, M. FRACES, M. LAUG, D. CONTE, P. SIRON and X. THIBAULT : A multiprocessor based on optical crossbar network (MILORD project).

MASSIVELY PARALLEL COMPUTING AND OPTICAL INTERCONNECTION ARCHITECTURES

D. COMTE, ONERA-CERT/DERI

Massively parallel architectures play a key role in the development of supercomputing. They must face the difficult problem of interconnecting thousands of electronic units (processors with private memory). Potentially, optics exhibits valuable properties which confer to the parallel architectures specific characteristics that will be analysed in this presentation.

Applicability of Laser Beamsteering for Rapid Access to 2D, 3D, and 4D Optical Memories

Haim Haskal, Philip D. Henshaw,
Robert C. Knowlton and Peter B. Scott

SPARTA, Inc.
21 Worthen Road
Lexington, MA 02173 USA
(617) 863–1060

SUMMARY

This paper will discuss recent progress and future possibilities in the area of rapid access to optical memories containing large amounts of data. The talk will be divided into three parts. First, laser beamsteering techniques will be reviewed, second, optical memory configurations will be discussed, and third, the possible combinations of these concepts which can lead to useful devices will be presented.

Laser beamsteering devices can be grouped into several methods according to their principle of operation; each of these methods has inherent limitations. The number of beam positions available using each method is a key parameter for optical memory access, and the limitations on this figure of merit will be presented. Recent progress in two areas, beamsteering using photorefractive materials,

and beamsteering using an agile frequency laser and dispersive structure will be presented. A wideband (50 nm), high speed (1 msec to 100 μsec), laser tuning mechanism capable to producing 500 to 5000 addressable beam positions using the frequency agile technique will be reported. Each of these methods has the potential for producing a much larger number of addressable beam positions than currently available techniques.

Second, optical memory configurations will be characterized and reviewed. This review will consider current techniques such as optical disk storage and projected future techniques using spatial and spectral storage. For example, bits can be stored on a plane or in a volume, and recent results indicate a spectral dimension is also conceivable, leading to 2D, 3D, and 4D memory configuration. Other characteristics include holographic versus bit-oriented storage, moving versus stationary media, and parallel versus serial readout. Simple relationships governing the projected capacity of each of these media will also be discussed. These relationships will motivate requirements for the beamsteering or spectral memory access techniques.

The available beamsteering techniques combined with the possible memory architectures produce a large number of possible memory device configurations; which of these configurations should be pursued? In the third part of this paper, we will discuss criteria by which to judge these devices, and then present several combinations which appear promising for either near-term or far-term projects. Specific research results in rapid access to optical disk media will be presented.

This work is being sponsored by DARPA and the Naval Ocean Systems Center under contract number N66001-86-OC-0095. The Technical Monitor for this work is Dr. John Neff of DARPA.

Optical Crossover Interconnections

Jürgen Jahns
AT&T Bell Laboratories
Crawfords Corner Road
Holmdel, NJ 07733

SUMMARY

Optical digital computers and switching systems offer the potential for massively parallel operation. Their performance, however, will depend strongly on the efficiency of interconnecting various layers of logic gates. Data networks such as the perfect shuffle and the banyan network have been considered recently for an optical implementation. These networks consist of $log(N)$ stages where N is the number of inputs. It has been shown that $log(N)$ type networks can be used efficiently in a parallel digital computer in terms of gate count and throughput [1].

In this paper, we present crossover networks as an alternative to the banyan and the perfect shuffle. Crossover networks offer the potential for a simple implementation using free-space optics. Specifically the use of crossover networks allows to exploit the full space-bandwidth product of an optical system [2].

The flow diagram for a crossover interconnect is shown in Fig. 1. For N = 8 inputs the network consists of log N = 3 stages. As we see, each stage of the network consists of straight-through connections and crossover connections. These crossover connections are applied to varying partitions of the input data. The partitions have the size N, N/2, N/4, ... as we proceed from one stage to the next.

An optical setup to implement the first stage of the network is shown in Figure 2. The input gets split into two different branches. One branch with a mirror in the image plane implements the straight-through connections. The other branch with a 90 degree prism accomplishes the flipping of the top position to the bottom, the second from the top to the second from the bottom, etc. The outputs of both branches are superimposed in the output plane. Using polarization optics, it is possible to implement the operation without loss of light. An experimental result is shown for the implementation of the first stage in Figure 3.

The crossover network is isomorphic to the perfect shuffle and the banyan network. From this isomorphism result applications to a variety of tasks in optical computing, signal processing, and photonic switching.

[1] M.J. Murdocca, A. Huang, J. Jahns, N. Streibl, "Optical Design of Programmable Logic Arrays", to be published in Appl. Optics.

[2] J. Jahns, M.J. Murdocca, "Crossover Interconnects and their Optical Implementation", submitted to Applied Optics.

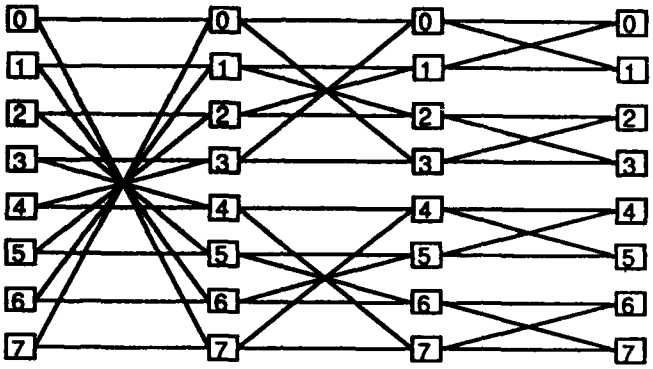

Fig. 1

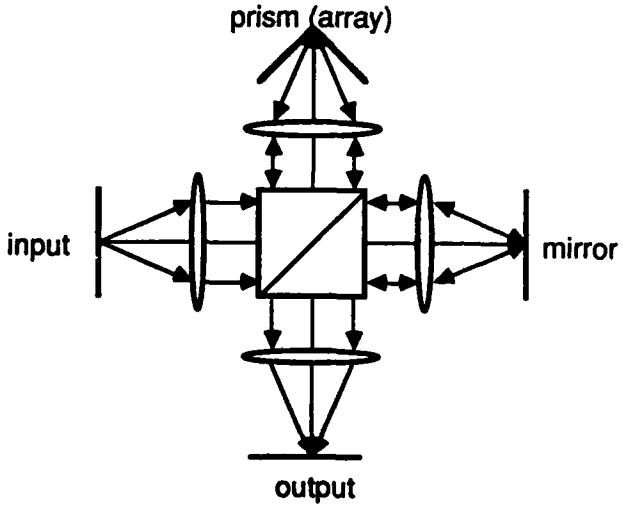

Fig. 2

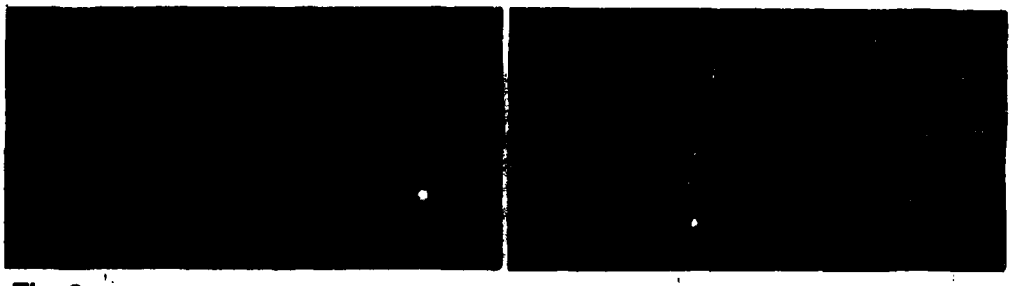

Fig. 3 input ouput

"Ox"—Optical crossbar switch designs for parallel processing

Alfred Hartmann and Steve Redfield
Microelectronics and Computer Technology Corporation (MCC)

As an alternative to electronic networks, large-scale (1000×1000) optical crossbar switching networks for use in parallel processing supercomputers may employ freespace optical transmission and known communications protocols in either a beam spreading/masking model or in a beam steering model, with either single- or double-sided nodal arrangements.

1. Problem statement

The problem is to design a crossbar switching network suitable for general-purpose, large-scale parallel processing applications in high performance computing systems. The network *must* interconnect at least 1000 independent computing nodes operating asynchronously with respect to each other and incorporate indigenous local control for complete nodal autonomy. The assumed network workload consists of short (~100-bit) messages corresponding to processor-to-memory and memory-to-processor read and write operations. Message delivery latencies through the switching network must be of the same order as typical computer memory access latencies (i.e., o(100ns)) in order for the entire computing system to appear to the programmer as tantamount to an *ideal parallel computer*. An ideal parallel computer is one with an arbitrarily large number of independent processors and an arbitrarily large memory space, with constant unit delay for any processor to independently access any memory location.

2. Design issues

Interconnection density: The first design issue is the crossbar size limitation imposed by constraints on interconnection density. We attack this in two ways—

- use bit-serial rather than parallel communications links; and
- use freespace communications links rather than fixed guideways.

Using bit-serial (optical) links rather than conventional parallel links in the network reduces the number of communications pathways, allowing more nodes for a given density limit. Using freespace communications links rather than fixed guideways provides three dimensions for pathways. It is easily shown that interconnecting n nodes so as to provide uniform $O(n)$ communications capacity among the nodes requires $O(n^2)$ space in two-dimensions vs. $O(n^{3/2})$ space in three dimensions, assuming links have a fixed minimum separation distance.

Message delivery latency: For these short messages, latency is dominated by connection establishment time, which is limited by the need to perform arbitration over possibly multiple processing nodes requesting connection to the same memory node. For maximum parallelism, each memory bus in the crossbar network must independently arbitrate over its own set of connection requests. We call this *local arbitration*, as opposed to *global arbitration* in which separate external logic receives all n connection requests, performs arbitration over them, and returns the crossbar switch settings to be used for the subsequent data transfers.

Power dissipation: Heat removal limitations or thermal effects on components could impose a new density limitation that would impact the performance and scalability of designs. Both crosspoint switching energies and bit signal energies must be accounted for.

Architecture: Given our choice of freespace transmission to avoid interconnection density constraints, two alternative switching strategies allow one-to-one interconnections of processor nodes with memory nodes:

1. Spread the transmitted beam across all receivers, but use a masking mechanism to mask off all but one receiver—*beam spreading/masking*.
2. Maintain a small beam diameter and alter the beam trajectory to directly target a single receiver site—*beam steering*.

3. Beam spreading/masking

A typical design in this category is shown in Fig. 1. This design interconnects n processors, to m memories. Processor node p_i broadcasts to all receivers by spreading its transmitted beam over the ith row of the masking device, a spatial light modulator (SLM). The SLM may be either transmissive or reflective, while the one shown in the figure happens to be transmissive. In a transmissive masking device, the (i,j)'th masking cell is "opened" (made transparent) to permit the ith processor node to communicate with the jth memory node, and the cell is "closed" (made opaque)

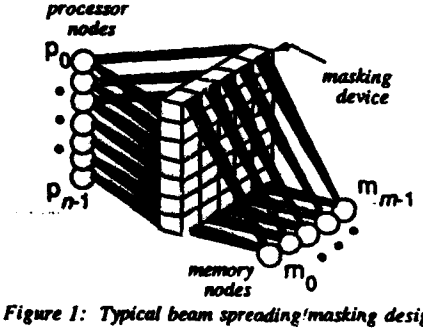

Figure 1: Typical beam spreading/masking design

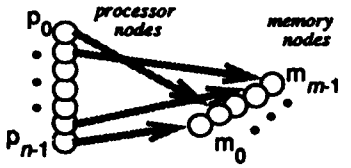

Figure 2: Typical beam steering design

to disallow communication between the two nodes. For one-to-one communication among nodes, at most one cell in each row and one cell in each column may be open, and all other cells must be closed.

We were repeatedly foiled in our attempts to design an $o(1000$ nodes) crossbar network with $o(100$ns) latency and $o(1$Gb/s) link bandwidth by the technological limitations of current SLM technology. The SLM *speed-contrast product*, the product of switching speed (in Hertz) times contrast ratio, is our major concern in the beam spreading/masking design. If typical values for this figure of merit are $o(1\text{KHz})\cdot o(10{:}1)=o(10^4)$, and if our design target is $o(100\text{MHz})\cdot o(1000{:}1)=o(10^{11})$, then we are not optimistic that SLM technology improvements will intercept our target in the near future.

4. Beam steering

A typical design in this category is shown in Fig. 2, connecting n processors to m memories without an intermediate masking device. Each transmitting node steers its beam directly to the intended receiving node using a beam deflection device integral to the node. Single-axis beam deflection or biaxial beam deflection is possible. Using single-axis beam deflection, n receivers can be addressed if the beam deflector can resolve n spots along its axis. Using biaxial beam deflection, n receivers can be addressed if the beam deflector can resolve $\sqrt{n}$ spots along each axis. This is an important issue for deflector resolution, physical optics design, system packaging, and connection establishment latency.

Beam deflection setup latency is important to achieving the goal for connection establishment latency. For example, if an acousto-optic uniaxial deflector with a 1GHz modulation bandwidth (say, 0.5–1.5GHz modulation range) is used, then at the 1GHz center frequency it would require $o(1\mu s)$ just to inject a thousand cycles of the modulation waveform into the deflector crystal so that it could conceivably resolve one part in a thousand. This is unacceptable deflector setup latency. On the other hand, resolving to one part in $\sqrt{n}$, or roughly one part in 32, using a biaxial deflector, would require only $o(10$ns). Gigahertz bandwidth acousto-optic beam deflectors are commercially available as are biaxial beam deflectors.

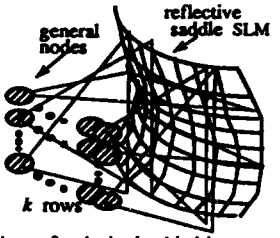

Figure 3: A single-sided beam spreading/masking design

5. Single-sided nodal arrangements

An abstract double-sided beam spreading/masking design was shown in Fig. 1. By fabricating a composite reflective SLM in a quasi-paraboloid saddle shape, a realistic single-sided layout can be achieved, as shown in Figure 3. The convex horizontal curvature provides the broadcast beam spreading, while the concave vertical curvature focuses down on the node array. The vertical curvature could also be convex, though, if the SLM height is less than the array height. Ray tracing analysis can be used to determine the proper curvatures.

An abstract double-sided beam steering design was shown in Fig. 2 without regard to concrete issues of system diameter or beam angles. A single-sided arrangement is easily possible using an appropriate mirror design, such as that shown in Fig. 4. The twisted mirror provides different horizontal deflection angles at each different vertical position on the mirror, allowing any target to be reached.

6. Protocols

Switch architecture affects the choice of communications protocol, affecting performance. Carrier-sense multiple access (CSMA) channel protocols can be used in beam spreading/masking architectures, but not in beam steering architectures, because of the lack of broadcast capability. Less efficient ALOHA-style protocols can be used for beam steering arrangements, but result in longer latencies due to increased message collision probabilities.

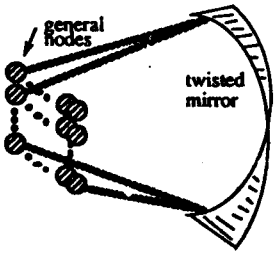

Figure 4: Single-sided beam steering arrangement

CERT

A multiprocessor based on optical crossbar network (MILORD project)

Autors : P.CHUROUX, M.FRACES, M.LAUG (Optics department)
D.COMTE, P.SIRON, X.THIBAULT (Computing department)

Summary

Apart from the traditional advantages of optics (high bandwidth, interference immunity), its high degree of parallelism will permit in a near future to connect a great number of processors communicating between themselves at high information rates. So it seems natural to consider the possible applications of optics to reconfigurable interconnection networks.

The MILORD project (Multiprocesseur Interconnecté par Liaisons Optiques Reconfigurables Dynamiquement) was born in 1985 from the collaboration of the CERT's Optics and Computing Departments

MILORD is a multiprocessor architecture organized around a 35x35 optical crossbar network, interconnecting 8 INMOS T414 microprocessors and a ninth T414 host transputer having three links on the network. The executing unit of the MILORD machine contains 8 INMOS T414 microprocessors each connected by four serial bidirectional links on the optical crossbar network. Each transputer is a 32 bits processor providing up to 10 Mips processing power (the MILORD machine information rate) and a 256 kbytes own memory.

The optical crossbar network is a N^2 parallel matrix-vector inner product processor. The optical switching matrix is achieved in the output window of a H4060 DIR HUGHES LCLV. The output links of the transputers modulate 35 laser diodes, each coupled by a pigtail to a linear 35 optical fibers array. This fiber array constitutes the 35 input links of the network. A cylindrical optics conjugates

this array on the LCLV output window and after reflection, on a linear photo diode array. 35 independent elements of the photodiode array deliver after amplification and numerical treatment the crossbar output signals on the input links of the transputers.

The network reconfiguration function is achieved by an optical way with a green CRT applied on the input window of the LCLV. The host T414 transputer allows to modify the entire switching matrix when all the transputers elementary works are finished. Apart from the reconfiguration phase, the processors may communicate with an asynchronous mode. The network reconfiguration time, which is about tens of milliseconds, depends on the LCLV rise and decay times. The LCLV rise and decay times are in direct ratio to the write light intensity and in inverse ratio to the LCLV modulation frequency.

The number of available links on the network (35 in our machine) cannot in any case overpass the contrast ratio of the LCLV which is about 100/1.

The intensive investigation which is carried out for several years about ferroelectric liquid crystals would permit to low the switching time per point to about tens of microseconds. So it would be possible in a next future to reduce the whole matrix reconfiguration time by a factor 1000 with a parallel command on the matrix lines for example (with the condition of a transfer line time negligible in front of the switching time per point).

Wednesday august, 31, 10.45

SESSION 6 (Chairman G. ROBLIN)

ACTIVE COMPONENTS
COMPOSANTS ACTIFS

A3 - I. HAYASHI : Opto-electronic integration will be the key for the optical computing.

A4 - J.H. COLLET and M. PUGNET : Picosecond NOR gates without Fabry-Perot cavity.

A5 - M.P. PETROV, V.I. BELOTITSKII, V.V. SPIRIN, E.A. KUZIN, M.A MAKSUTENKO : Storage and generation of optically encoded pulse sequence using a SRS-inverter with feedback.

OPTOELECTRONICS TECHNOLOGY
RESEARCH LABORATORY
(OTL)
5-5 TOHKODAI, TSUKUBA,
IBARAKI 300-26, JAPAN

PHONE 029747-4331
FAX 029747-4180

Title:

Opto-electronic Integration will be the key for the Optical Computing

Izuo Hayashi
Optoelectronic Technology Research Laboratory

Summary:

In many cases of optical computing system, use of electronic subsystem would be essential, provided (photon-electron) converting (or controlling) devices are available. In order to fabricate such devices, technology for integration of optoelectronic devices with electronic devices will be mandatory.

In this talk recent developments in OEIC technologies, such as precise dry etching, ultra-high vacuum fine pattern doping or highly mismatched hetero epitaxy (GaAs on Si) will be presented.

OPTOELECTRONICS TECHNOLOGY
RESEARCH LABORATORY
(OTL)
5-5 TOHKODAI, TSUKUBA.
IBARAKI 300-26, JAPAN
PHONE 029747-4331
FAX 029747-4180

The first motivation of such OEIC technology research is to provide (electron-photon) converting device for optical interconnection in electronic systems, such as communication or computing systems. However it is evident the same technology will be useful to provide (photon-electron) converting or controlling device in optical computing systems, such as two dimentional emitter arrays, space light modulators with electronic control.

Feasibility of such OEIC devices and their future prospect will be presented.

Izuo Hayashi

PICOSECOND NOR GATES WITHOUT FABRY-PEROT CAVITY

J.H. Collet and M Pugnet

Laboratoire de Physique des Solides associé au CNRS
Département de Physique.INSA
Avenue de Rangueil, 31077 TOULOUSE CEDEX, FRANCE

Several optical induced absorption phenomena appear in semiconductors in the presence of a dense electron-hole plasma which is most readily generated using picosecond laser pulses. These effects may be used to work out an all-optical picosecond inverter gate and more generally a many input NOR gate. It must be stressed that *no Fabry-Perot cavity is necessary*: These are bulk effects.

A first possible induced absorption effect appears for photons the energy of which is close to the material bandgap one. It is related to exciton screening and bandgap renormalization in case of *hot pumping* of the electron-hole plasma. The operation of such an all-optical modulator will be reported on a II-VI semiconductor material, namely CdSe at 77 K. The NOR gate operation conditions are discussed in relation with the possible development of optical cellular coprocessors (compatible with a parallel processing of data) and especially in relation with the critical

problem of associating and cascading optical NOR gates. We report a first step toward cascadable picosecond NOR gates by demonstrating the possible operation of an all-optical inverter gate which uses an intermediate frequency doubling of the output signal. This implies that a cascadable all-optical NOR gate operating in an one-wavelength mode is possible. Experiments were carried out at liquid Nitrogen temperature. The operation wavelength is around 673 nm in CdSe. The switching energy of the NOR gate was 30 mJ/cm^2/pulse at 337 nm.

A second possible induced absorption effect appears in semiconductors, due to transitions in picosecond regime of electrons from the split-off valence band to the heavy and ligth holes bands. The operation of such a NOR gate is demonstrated on 300 μm thick GaAs platelets at room temperature. The modulation wavelength is around 1.57 μm. Cascadability and switching energy are discussed.

Storage and Generation of Optically Encoded Pulse Sequence Using a SRS-Inverter with Feedback

M.P.Petrov, V.I.Belotitskii, V.V.Spirin, E.A.Kuzin, M.A.Maksutenko

A.F.Ioffe Physical Technical Institute of the Academy of Sciences, Leningrad, 194021, USSR

The report discusses the possible ways of utilization of a fiber-optic SRS-inverter (NOT gate) first reported in /1-3/ as an optical code generator in digital optical computers. The inverters of this type can be operated with a pulse repetition rate of up to 10^{11}-10^{12} Hz and require the pump pulses of sufficiently low energy of 10^{-10}-10^{-12} J. The energy of signal pulses can be even two orders of magnitude lower.

As the studies have shown, the inverter exhibits a fairly high differential gain coefficient, has a suitable input-output characteristic, and the signal from its output can serve as a driving signal for several other inverters. Therefore, the element is cascadable.

The use of even a single inverter allows however important problems related to optical information processing to be solved. For instance, if the signal from the inverter output is applied to its input, we can obtain the devices of the type of code generators, pulse repetition rate dividers, and dynamic memories.

The scheme of the fiber-optic inverter with feedback used for division of the repetition rate of optical pulses has been experimentally studied. In operation, the round-trip transit time of the pulse was set equal to the repetition period of the laser pump pulses. As a result, the pulse sequence with the repetition rate half as high as that of pump pulses was observed at the output of the inverter. Duration of the pump pulses used was of the order of 25 ps, the repetition rate was 10^8 Hz.

References.

1. M.P.Petrov, E.A.Kuzin. Preprint of Phys.-Tech.Institute, Leningrad, 1985, No.975.
2. E.A.Kuzin, M.P.Petrov. Avtometria, 1986, No.2, p.87-92.
3. E.A.Kuzin, M.P.Petrov, V.V.Spirin. Sov.Tech.Phys.Lett., v.12, No.4, 1986, p.165-166.

Thursday september, 1, 8.30

SESSION 7 (Chairman V. MOROZOV)

ACTIVE COMPONENTS
COMPOSANTS ACTIFS

A4 - J.L. OUDAR : All-epitaxial AlAs/GaAs bistable etalons for low power optical logic.

INTERCONNECTIONS
INTERCONNEXIONS

B6 - A.W. LOHMANN, W. LUKOSZ, J. SCHNIDER, N. STREIBL and J.A. THOMAS : Array illuminators for the optical computer.

B8 - P.C. GRIFFITH and S.A. COLLINS Jr : Efficient holographic optical interconnects using resonated holograms.

B7 - J.I. SOOS and R.G. ROSEMEIER : Global interconnection with single element 2.D acousto-optic laser beam deflector.

B9 - C.J. GEORGIOU and A. VARMA : A hybrid electro-optic switching system.

ALL-EPITAXIAL AlAs/GaAs BISTABLE ETALONS FOR LOW POWER OPTICAL LOGIC

J.L. Oudar

Centre National d'Etudes des Télécommunications

196, avenue Henri Ravera F-92220 Bagneux, France.

Intrinsic bistable devices represent a very promising approach for the fabrication of large two-dimensional arrays of optical logic elements, since the simplicity of their structure allows their miniaturization down to the micrometer scale, hence reducing the optical power requirements. The use of excitonic or band-gap resonant optical nonlinearities in III-V semiconductors, eventually as multiple quantum wells, have proven to be very effective for making such bistable devices, in the form of nonlinear Fabry-Pérot étalons operating at semiconductor wavelengths and power levels.

We report experimental results on such bistable devices, grown by metalorganic vapor phase epitaxy, which include GaAs as the active nonlinear material and AlAs/GaAs or AlAs/AlGaAs Bragg reflectors grown during the same epitaxial process [1]. This allows very compact structures, with a total thickness of 4 μm along the light propagation direction. Without any further technological processing, hysteresis cycles have been observed in the reflective mode with high reflectivity contrast, approximately 10 ns switching time, and 4 mW threshold power. With a holding beam at this power level, NOR gate operation can be achieved with submilliwatt logic inputs. The efficient heat-sinking realized by direct-contacting the étalon to the heat-sink results in a considerable reduction of the thermally-induced nonlinear effects that usually arise in such semiconductor bistable devices. Still better characteristics are expected when a lateral structure is

defined on the plane of the multilayer. Etching techniques have led to the fabrication of two-dimensional arrays of small-size étalons, potentially useful for parallel optical logic.

(1) R. Kuszelewicz, R. Azoulay, J.C. Michel, J. Brandon and J.L. Oudar, Proc. of the Int. Conf. on Optical Bistability IV, Aussois, March 1988.

ARRAY ILLUMINATORS FOR THE OPTICAL COMPUTER

A. W. Lohmann, W.Lukosz[1], J. Schwider, N. Streibl, J. A. Thomas
Physikalisches Institut der Universität Erlangen-Nürnberg
Erwin Rommel Str. 1, D-8520 Erlangen, FRG
[1]Optics Laboratory, Swiss Federal Institute of Technology
CH-8093 Zürich, Switzerland

Abstract:

An array illuminator splits one incoming light beam into many power supply beams for an array of optical logic devices. Several optical arrangements are investigated.

Summary:

Optical bistable devices need strong holding beams to maintain their stored information. Optical logic devices need optical power supply beams. A periodic structure of devices can be illuminated by an optical setup which transforms an incoming beam into a set of sub-beams of equal intensity separated by a dark surrounding. There are several possibilities to achieve this goal. For example lenslet arrays may be employed to generate arrays of spots. Also, the compression can be brought about by an array of telescopes of holographical /1/ or pure optical design. The light compression in this case is proportional to the square of the ratio of the focal lengths of the two lenses forming the telescope. Other illuminator arrays rely on Fraunhofer diffraction on binary phase gratings of Dammann design /2,3/. High accuracy of the grating structure is necessary, if many diffraction orders (say 17x17) of uniform brightness are required/3/. In the Fresnel region the Talbot-effect delivers self-images of a diffracting phase grating in space. These self-images show strong intensity modulation and at certain distances behind the grating the light energy is concentrated in a set of bright patches as

required /4/. Another array illuminator is based on the wellknown phase contrast method where phase variations of an object are transformed into intensity variations in an image /5/. The obtainable compression ratio is limited to about 4, i.e. the energy of a quadratic subaperture is concentrated in ¼-th of its area. As has been indicated by Lukosz /6/ an additional improvement of the phase contrast illuminator can be obtained if one uses a different phase shifter with a different shape in the Fourier plane. Yet another increase in compression can be obtained if the background does not have to be totally dark.

We compare the different approaches to the array illumination problem in terms of splitting ratio (number of spots), compression ratio (dark / bright area), homogeneity (intensity deviations between different spots), light efficiency and manufacturing problems.

References:

/1/ A. W. Lohmann, F. Sauer, 'Holographic Telescope-Arrays' Appl.Opt.,1988, in print

/2/ H. Damann, K. Goertler, 'High-efficiency in line multiple imaging by means of multiple phase holograms' Opt.Comm.3,(1971) 312-315

/3/ J. Jahns, M. Price, M. Downs, S. Walker, N. Streibl, 'Dammann gratings as array illuminators', OSA-Meeting Rochester Oct.1987

/4/ A. W. Lohmann, An Array Illuminator Based on the Talbot-Effect, Optik 1988 in print

/5/ A. W. Lohmann, J. Schwider, N. Streibl, J. Thomas 'An Array Illuminator Based on Phase Contrast' Appl.Opt.1988 in print

/6/ W. Lukosz, private communication 1987

EFFICIENT HOLOGRAPHIC OPTICAL INTERCONNECTS USING RESONATED HOLOGRAMS

Paul C. Griffith and Stuart A. Collins, Jr.

The Ohio State University
ElectroScience Laboratory
1320 Kinnear Road
Columbus, OH 43212
U.S.A.

Summary

Holograms show promise as optical interconnects both for electronic intra- and inter-chip applications and for numerical optical computing. We are concerned with aplications where it is desirable to store many interconnects in the same hologram while maintaining good diffraction efficiency. In such cases neither presently available film nor electrooptic crystals can give the desired combination of high diffraction efficiency and large numbers of exposures. Resonant mirrors eliminate the problem by bouncing the light many times back and forth through the hologram to achieve the desired efficiency. Up to one hundred percent efficiency is possible for lossless multiexposure holograms. Experimental data on low loss holograms is presented showing agreement with theory and indicating potential problems and their solutions.

The concept is shown schematically in the figure where we see a single thick hologram with four mirrors. The incident beam enters through mirror one, intersects the hologram at the Bragg angle, and the diffracted beam exits through mirror number four. Mirrors number two and three are fully reflecting and mirrors one and four are partially transmitting. Optimum performance is achieved by choosing the reflectivities of mirrors one and four to match the hologram characteristics and by adjusting hologram-to-mirror distances. This approach works equally well with only three mirrors and has shown reasonable performance with only two mirrors. It can be used with either transmision or reflection holograms.

We have built and demonstrated such structures using a hologram with some loss and intentionally chosen small diffraction efficiency and made measurements which agree with theoretical predictions. These will be presented. In addition, further theoretical analyses predicting efficiency and angular widths for two, three, and four mirrors, and configurations for extending this approach to holograms with many exposures will be presented.

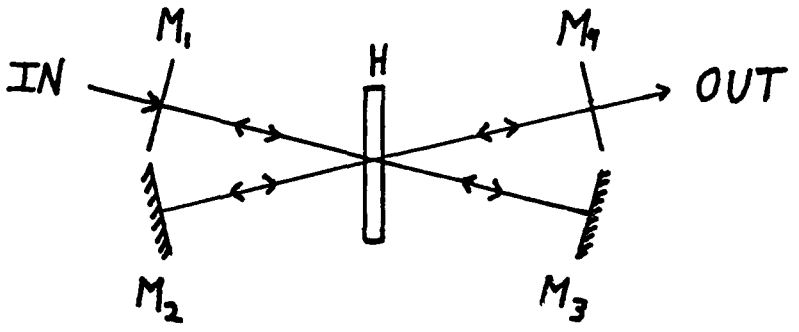

brimrose

GLOBAL INTERCONNECTION WITH SINGLE ELEMENT 2-D ACOUSTO-OPTIC LASER BEAM DEFLECTOR

J. I. Soos and R. G. Rosemeier

Brimrose Corporation of America
7720 Belair Road
Baltimore, MD 21236
(301)668-5800

ABSTRACT

A novel device for optical computing applications is a single element 2-D acousto-optic device. Recently, Brimrose Corporation of America designed and built such a device with two longitudinal acoustic waves propagating 90 deg to each other in the same substrate. This device can be used for vector multiplication as well as for global interconnection applications.

SUMMARY

The 2-D device operates at a center frequency of 475 MHz with a 100 MHz bandwidth. The laser wavelength range is from 570nm to 1.15μm. A single crystal of GaP was chosen as the optical substrate, because of its symmetry and high figure of merit. The figure of merit, M_2, is only material dependent and can be described by the following equation

$$(1) \quad M_2 = \frac{n^6 \cdot p^2}{\rho \cdot V^3}$$

where n is the index of refraction, p is the photo-elastic constant, ρ is the density and V is the velocity of sound.

Optical bandwidth is wavelength dependent and can be expressed as:

$$(2) \quad \Delta f = \frac{1.8\, n\, V^2}{L\, f_1\, \lambda}$$

where f_1 is the center frequency and λ is the laser wavelength.

This paper will describe the usefulness of this single element A-O device for global interconnection applications.

A Hybrid Electro-Optic Switching System

Christos J. Georgiou
Anujan Varma

Computer Science Department
***IBM* Thomas J. Watson Research Center**
P.O. Box 704
Yorktown Heights, New York 10598

The use of optical techniques has been widely recognized as a solution for overcoming some of the fundamental problems in data communication and switching. An important application of optical technology is in the coupling of high-performance computers to form powerful multiprocessors. A central switching network, connected to the computers through high-speed fiber-optic links is a suitable candidate for interconnection in such systems. These networks can provide high bandwidth and low latency, together with modular expansion. The number of processors in the system is relatively small, allowing the use of a central non-blocking switch.

An all-optical implementation of the switch would eliminate the problem of optoelectronic conversion of the signals. Optical switching techniques possess several desirable features such as high data bandwidth, large amount of inherent parallelism, small size and power requirements, and relative freedom from mutual interference of signals. However, in general, their reconfiguration time is much higher than electronic implementations, resulting in higher latency. In addition, they are difficult to control optically. Although optically-controlled switching has been demonstrated, it lacks the flexibility of electronic control. In addition to setting up the path for the desired connection, the controller is also required to resolve conflicts among requests for connection and administer the protocols to establish, maintain, and terminate connections through the switch. These functions are beyond the limits of current optical technology. Therefore, an optical switch with all-optical controller is difficult to implement.

In this paper we attempt to combine some of the merits of electronic and and optical switching technologies, namely the high bandwidth of optics with the fast reconfiguration of electronic switches. This is achieved by providing two independent switching subsystems, one a high-speed optical crossbar and the other a slower electronic crossbar. Both subsystems are controlled by a single electronic controller. The optical crossbar provides a high-bandwidth high-latency path while the electronic crossbar provides a path with lower bandwidth but low latency. The overall communication time for a message can be minimized by selective use of the electronic and optical crossbars.

Our switching system is a central switch connected to the processors through fiber-optic links. Each processor is connected to the switch by means of a pair of high-speed links and a pair of low-speed links, providing two full-duplex communication paths. The low-speed links are interfaced to the switch by full-duplex ports whereas the high-speed links are connected directly to the switch with no interface components. The switching system consists of two *switching planes*, an electronic plane and and an optical plane. This is illustrated in Figure 1. The optical plane is an optical crossbar network controlled electronically. The electronic plane is a conventional electronic crossbar network. The high-speed links associated with the switch ports are connected to the optical plane and the low-speed links are connected to the electronic plane. Optoelectronic conversion is performed only for the low-speed links. A single electronic controller controls both switching planes. While no assumption is made regarding the absolute bandwidths of the two sets of links, we expect the bandwidth of the high-speed links to be about ten times that of the low-speed links, while the reconfiguration time of the optical plane is about a hundred times that of the electronic plane. For example, it is practical to use 100 Mbps fibers for the low-speed links and 1 Gbps links for the high-speed links. Control information is sent through the low speed links whereas data can be sent through either of the links. Each low-speed port has hardware for serialization/deserialization of data. Additionally, buffers are provided on each low-speed port to allow queueing of messages at the switch. No such conversion or buffering is performed for the high-speed links.

The system can be used either as a circuit switch or a message switch. Message switching is done through the low-speed links. In this mode, the address of the destination node is encoded in the header of the message and is sent by the source node to the low-speed port of the switch. All incoming data is buffered at the low-speed ports. The port generates a request for the designated destination to the controller. If the desired destination is available, the controller then sets up the electronic switching plane and allows the data to be transmitted to the destination. The optical switching plane and the high-speed links do not participate in the data transfer and hence the available bandwidth is that of the low-speed link. Therefore, the message switching mode is suited to small blocks of data.

The second mode of operation, circuit switching, is useful for large blocks of data. Under this scheme, a node desirous of communicating with a destination sends a connect request as a control message through its low-speed link to the switch. The switch controller decodes this message and sets up the optical plane, thereby creating a physical path between the high-speed links associated with the source and destination ports. The controller simultaneously notifies the destination node through the low-speed link about the connect request, so that the interface adapter at the destination port can set itself up for the transfer of data. On receipt of a favorable response from the destination, and after the setup operation of the optical plane is complete, the controller sends a response message to the source node as acknowledgement. The source node, on receiving the acknowledgement, sends the data over its high-speed link to the destination. No additional handshaking is necessary till the transfer is complete. Thus, in the circuit switched mode, the low-speed links are used only for control. An overhead is paid in terms of the time required for the handshake and the setup time of the optical crossbar, but, for large blocks of data, this is offset by the higher bandwidth available in the circuit switched mode of operation. An analysis and comparison of the two modes of operation is provided in the full manuscript.

In summary, the novelty of the architecture is in combining the strong aspects of both electronic and optical technologies. This enables the switch to approximate the transfer time of an all-optical switch and the latency of an all-electronic switch. The electronic switching plane can be implemented using the relatively slower CMOS technology. All the optical and optoelectronic parts are available or can be built with current technology for speeds as high as 1 Gbps. This is an attractive alternative to building all electronic high-speed switching systems using an expensive technology like GaAs or ECL.

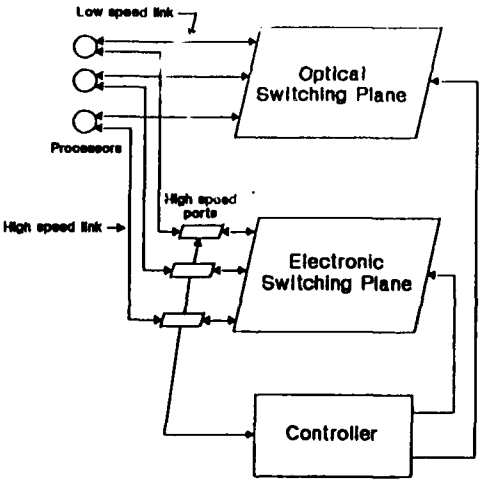

Figure 1: Architecture of the hybrid switching system.

Thursday september, 1, 10.45

SESSION 8 (Chairman G. LEBRETON)

ACTIVE COMPONENTS
COMPOSANTS ACTIFS

A5 - B.S. WHERRETT : Prospects for optical computing devices based on bistable and logic plates.

A6 - M.I BELOVOLOV, E.M. DIANOV, V.I. KARPOV, V.N. PROTOPOPOV and V.N. SERKIN : Fiber optic dynamic memory for the fast signal processing and optical computing.

A7 - V.Y. BAZHENOV, M.S. SOSKIN and V.B. TARANENKO : Optical bistability and autowaves in a nonlinear planar waveguide.

Prospects for Optical Computing Devices based on Bistable and Logic Plates

B.S. Wherrett

Department of Physics, Heriot-Watt University, Edinburgh EH14 4AS, U.K.

Optical cellular logic image processing is discussed, and existence-proof implementations of the basic components and circuit features are described.

FIBER OPTIC DYNAMIC MEMORY FOR THE FAST SIGNAL PROCESSING AND OPTICAL COMPUTING

M.I.Belovolov, E.M.Dianov, V.I.Karpov, V.N.Protopopov, V.N.Serkin

General Physics Institute, Academy of Sciences of the USSR
38 Vavilov Street, Moscow 117942, USSR

Progress in the measurement and computer engineering, in particular in the optical computing and optical computers, requires fast memory devices of sufficiently high capacity, capable of operating with fast parallel coded sequences of electrical and optical data (0.1-100 Gbit/s), which can be coupled with modern computation systems (fiber optic ones). The application of single-mode fibers as elements of great information capacity makes possible to create fast dynamic memory devices on the base of optoelectronical or optical ring circuits for the data circulation which provide the long-time storage of the data signals, keeping constant their shape and value (regeneration). The product of the bandwidth and the delay time in a single-mode fiber in a linear regime at one wavelengt of the optical carrier amounts to about 10^6 and determines the information capacity of a fiber. The information capacity of a fiber memory device can be practically increased by 10÷100 times using the spectral division multiplexing.

The main physical principles of construction and operation of fast fiber optic memory devices are presented. Some types of dynamic fiber memory devices are considered:

1. optoelectronic memory with a repeater in a circuit;
2. coherent optoelectronic memory;
3. fiber memory with an optical amplification (regeneration) in a circuit;

4. optical memory operating on solitons in fibers.

We have constructed the first system for the data processing on the base of microcomputers and digital dynamic memory of the first type with parallel spectral multiplexing of 6 different wavelengths operating on a single graded-index 5 km-long fiber at the wavelengths in the vicinity of 1.3 μm. The system includes the analog-to-digital and digital-to-analog converters, a fiber digital memory block, a controller and an interface for the connection with a computer. The scheme provides fast digital processing of analog signals of up to 25 μs in duration with the sampling time of 14 ns and the resolution of 64 levels or digital 6-channel data sequences.

The special feature of the processing system with a digital fiber memory is that it provides a long-time information storage (minutes and hours) while its sampling time is practically limited by the broadband of electronic components.

The fiber optic memory device using solitons as digital data carriers is very promising for the ultrafast data processing.

Here we have calculated the nonlinear dynamics of noise evolution in the fiber optic line with the Raman amplification of solitons. It was shown that solitons are cleared from noise in the process of Raman amplification - they throw down "the noise coat" -providing the possibility to store the solitons in a ring circuit for a long time.

The complete optical scheme of a memory device using a ring circuit of the soliton recirculation in a single-mode fiber with Raman amplification for the loss compensation is suggested here. The operation of soliton memory devices is based on the full soliton self-regeneration without noise accumulation ar frequent recirculations in the process of Raman amplification.

OPTICAL BISTABILITY AND AUTOWAVES IN A NONLINEAR PLANAR WAVEGUIDE

V.Yu.Bazhenov, M.S.Soskin, V.B.Taranenko

Institute of Physics, Acad.Sci.UkrSSR, Kiev, USSR

An important advantage of the optical bistable systems consists in their spatial distributivity giving rise to both transverse and longitudinal light field transformations. Such systems can be used for two- and three-dimensional optical information processing. One of the new bistable systems is based on the excitation of leaky waves in the nonlinear planar waveguide (NPW). Earlier in refs 1,2 the bistable NPW was studied theoretically in the plane wave approximation.

The present report is devoted to both theoretical and experimental investigations of spatial and temporal light field transformations in NPW with leaky wave excited by the spatially limited light beam. Gelatin NPW having thickness of 5 μm with slow thermal nonlinearity ($\tau \sim 1$ s) was used as an experimental model. Leaky wave excitation was provided by means of the glass prism coupler. Light field transformations in NPW were studied by measuring the intensity, phase and polarization distributions in the beam reflected from the guide layer. Different kinds of nonlinear effects (power stabilization, differential gain, optical bistability) were realized under excitation of the NPW with nonfocused beam of argon laser having intensity less then 1 W/cm^2. The switching wave in NPW is shown to possess significant spatial asymmetry as compared to one in the system of nonlinear cavity type (ref 3).

Theoretical description of the system has been provided by

means of the numerical solution of two-dimensional wave equation taking into account thermal conductivity of the waveguide layer. The results of calculations are in a good qualitative agreement with the experimental data.

Theoretical analysis has shown that the autowaves in NPW can be effectively controlled by varying the spatial and temporal parameters of the exciting light beam. The hysteresis of the switching wave profile during its tunneling through the nonilluminated region of the guide layer was realized experimentally. The optical multistability with comparatively small ($\lesssim \pi$) nonlinear phase variations can be realized. The steady states have different spatial configurations and the change of the mode number in this case is not required.

Another interesting autowave process in NPW is due to the significant asymmetry of the nonlinear perturbation transfer in the guide layer caused by the unidirectional propagation of a light in the layer. In this case forward and backward fronts of the switching wave can move in the same direction. The unidirectional movement of the switching wave without capture of the switched-on state was realized experimentally by the pulse perturbation of NPW with an additional light beam.

Thus the bistable NPW seems to be a good candidate as an element for the systems with parallel optical processing.

References

1. Vincent P., Paraire N., Neviere M. et al.-JOSA B,1985,v.2,p.1106
2. Montemayor V.J. and Deck R.T.-JOSA B,1985,v.2,p.1010
3. Firth W.J. and Gallbraith I.-IEEE J. Quantum Electr.,1985, v.QE-21, p.1399-1403.

Thursday september, 1, 13.30

SESSION POSTERS P2

ACTIVE COMPONENTS
COMPOSANTS ACTIFS

Ps 01 - Y. IYECHIKA, G. WINGEN, D. JÄGER, M. WEGENER, A. WITT and C. KLINGSHIRN : Optical bistability in evapored thin films of CdS.

Ps 02 - W. LUKOSZ, P. PIRANI and G. COMBE : Optical bistability in air-spaced Fabry-Perot etalons caused by thermal expansion.

Ps 03 - P. PIRANI and W. LUKOSZ : Optical bistability by photothermal displacement in prism coupler excitation of surface plasmons or waveguide modes.

Ps 04 - M.V. VASNETSOV and A.I. PETROPAVLOVSKII : Bistability of coupled cavities.

Ps 05 - T.R. WOLINSKI, M.A. KARPIERZ, A.W. DOMANSKI, K. CHALASINSKA-MACUKOW and T. SZOPLICK : Optical bistability in thin-film waveguides with liquid crystalline nonlinear prism coupler.

INTERCONNECTIONS
INTERCONNEXIONS

Ps 06 - E. FRIEDRICH and S. VALETTE : Optical interconnections for WSI.

Ps 07 - A.A. SAWCHUK and I. GLASER : Geometries for optical implementations of the perfect shuffle.

Ps 08 - J. SHAMIR, H.J. CAULFIELD and M.M. MIRSALEHI : Architectures for massive holographic interconnection network.

Ps 09 - S. XU, K. BAZARGAN, G. MENDES and J.C. DAINTY : Pinhole imaging holograms for optical interconnects.

OPTICAL PROCESSING CONCEPTS
CONCEPTS DE TRAITEMENT OPTIQUE

P$_2$ 10 - E.Y. DUFRESNE, J.P. LIKFORMAN, G.Y. SIRAT, D. CHARLOT and D. PSALTIS : Signal processing in conoscopic holography.

P$_2$ 11 - C. GORECKI : Moments computing using a coherent optical/digital processor.

P$_2$ 12 - D.M. SITTER and W.T. RHODES : Generalized falling-raster/folded-spectrum relationship.

P$_2$ 13 - M.H. WU : Optical realization of parity function and its application.

PARALLEL PROCESSORS
PROCESSEURS PARALLELES

P$_2$ 14 - P. ANDRES, J. OJEDA-CASTANEDA and J.C. BARREIRO : Lau effect and binary logic.

P$_2$ 15 - J.N. HAIT : Design of Dammann gratings for optical symbolic substitution.

P$_2$ 16 - W. XUE, L.X. CHEN, Q.S. HU abd C.F. LI : Symbolic substitution using shadow-casting.

Optical Bistability in Evaporated Thin Films of CdS

Y. Iyechika*, G. Wingen, D. Jäger,
M. Wegener+, A. Witt+ and C. Klingshirn+

Institut für Angewandte Physik der Universität,
Correnssstr. 2/4, D-4400 Münster, Fed. Rep. Germany
*Takatsuki Res. Lab., Sumitomo Chemical, Osaka, Japan
+Fachbereich Physik der Universität, Erwin Schrödinger Str.46,
D-6750 Kaiserslautern, Fed. Rep. Germany

Summary: Large areas of homogeneous active materials are needed to fabricate two-dimensional arrays of optical switching elements for parallel processing. Evaporation seems to be a superior technique for this purpose. Here, we discuss the optical bistability (OB) in evaporated thin films of CdS at 514 nm. Due to its high photosensitivity, this material also provides a great potential for super-integration of opto-electronic devices such as SEED elements /1/.

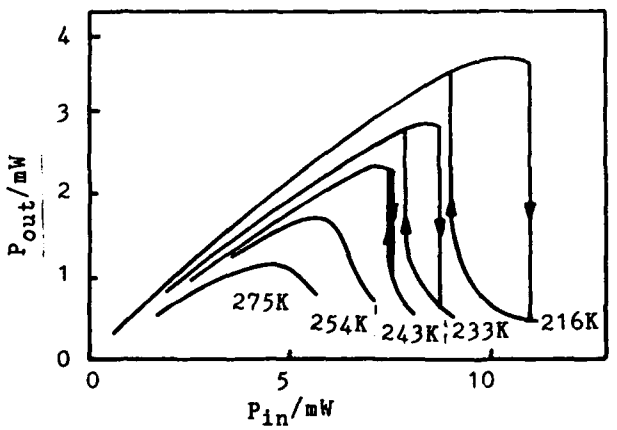

Fig. 1. Induced absorption OB in evaporated CdS thin film (thickness 0.8 µm) on glass substrate, experimental results for different substrate temperatures, T_0.

We have found a large room temperature optical non-linearity in thin evaporated CdS films due to thermal effects. For T_0 below 245 K, induced absorption bistability is clearly observed (Fig. 1). Moreover, the measurements have also pointed out, that a hybrid device on evaporated CdS material exhibits a pronounced influence of the applied electric field on the optical transmission (Fig. 2). The observed switching times of these thin film devices are small since the active layer is directly prepared on the heat sink.

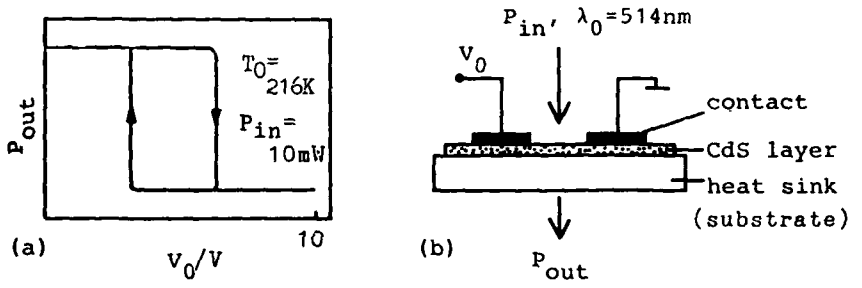

Fig. 2. Influence of electrical field on OB (a), and the sketch of the CdS SEED device (b).

It is noticed that the characteristics of the evaporated films are easily controlled by the thickness and the technology of the process, such as substrate and crucible temperatures and annealing conditions. By a suitable choice of the substrate, fast switching becomes possible.

/1/ M. Wegener, A. Witt, C. Klingshirn, D. Gnass and D. Jäger, Appl. Phys. Lett., 52, 342-344(1988).

Optical Bistability in Air-Spaced Fabry-Perot Etalons Caused by Thermal Expansion

W. Lukosz, P. Pirani, and G. Combe
Optics Laboratory, Swiss Federal Institute of Technology,
8093 Zürich, Switzerland

Optical bistability (OB) in Fabry-Perot resonators (FP's) of the interference filter type caused by the thermo-optic effect in the spacer material is well-known. We report on a new mechanism for OB in air-spaced FP's, viz. thermal expansion of the mirror substrates, which leads to a buckling of the mirror surfaces, and thus to a reduction of the mirror separation d (see Fig.1). We present a theoretical analysis of this OB mechanism and experimental results obtained with metal mirrors on glass or polymethylmethracrylate (PMMA) substrates, at He-Ne- and semiconductor-laser wavelengths. We also compare the performance limits of these bistable FP's with those based on the thermo-optic effect.

The mirrors M_1 and M_2 can be both absorbing metal coatings, or one absorbing, the other dielectric, or both dielectric, if an absorbing layer is located between mirror M_2 and its substrate. The theory starts from a calculation of the FP's transmission T(d), reflectance R(d), and absorbance A(d)=1-T(d)-R(d). In the steady state d is reduced from its initial value d_o linearly proportional to the absorbed power P_A=A(d)P, i.e,

$$d = d_o - \tan\theta\, A(d), \quad \text{with} \quad \tan\theta = g(\beta/\Lambda)P, \qquad (1)$$

where P is the incident power, β the thermal expansion coefficient, Λ the thermal conductivity, and g a dimension-free geometrical factor which depends on the laser spot size $2\rho_e$ and the thermal boundary conditions. From the graphical solution of Eq.1 shown in Fig.2, it follows that OB can occur. Figure 3 shows calculated hysteresis curves of transmitted power P_T=TP and reflected power P_R=RP versus P. In the calculations we used the value $\beta/\Lambda \approx 330$ nm/mW for PMMA and assumed g=0.5. We obtained for symmetric FP's with gold or silver coatings of thickness d_M on PMMA critical powers P_c as follows: 1) at λ=632.8 nm, P_c=85 and 130 μW for Au with d_M=50 and 40 nm, respectively (in good agreement with the experimental results shown in Fig. 4), and P_c=20 μW for Ag with d_M=60 nm; 2) at λ=780 nm, P_c=50 μW for Au with d_M=50 nm, and P_c=9 μW for Ag with d_M=60 nm. The critical powers on glass substrates, for which $\beta/\Lambda \approx 10$ nm/mW, are about 30 times higher.

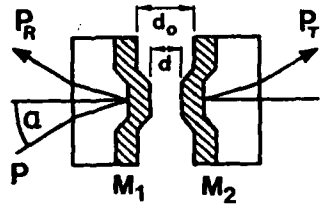

Fig.1. Fabry-Perot resonator. M_1, M_2, mirror coatings; P, incident power; α, angle of incidence; P_T, transmitted power; P_R, reflected power; d, mirror separation reduced from its initial value d_o by buckling of mirror surfaces.

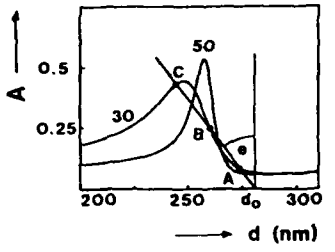

Fig.2. Calculated absorption A(d) versus mirror separation d of a symmetric FP with 30 and 50 nm thick Au coatings on PMMA substrates. λ=632.8 nm; α=0°. Intersections A and C of A(d) curve with straight line yield the stationary bistable states.

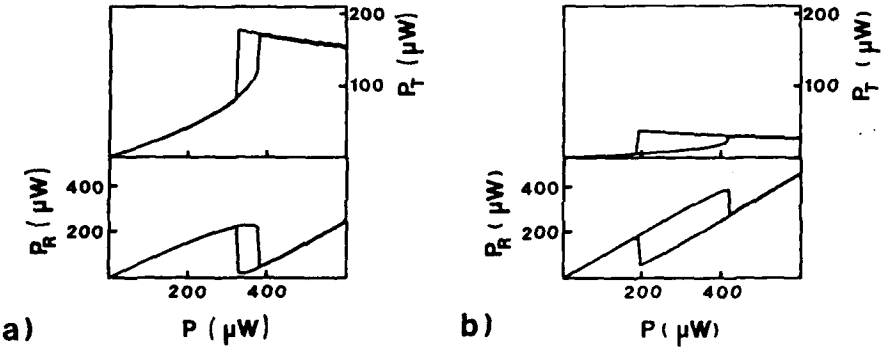

Fig.3. Reflected power P_R and transmitted power P_T versus input power P for FP described in Fig. 2 with a) 30 nm and b) 50 nm thick Au mirror coatings calculated with the constant B/Λ=330 nm/mW, and g=0.5. d_o=275 nm.

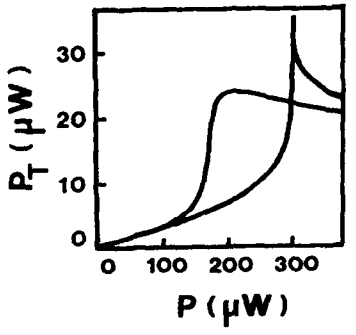

Fig.4. Experimental result. Transmitted power P_T versus input power P for symmetric FP with 40 nm Au coated 0.7 mm thick PMMA substrates. The incident He-Ne laser beam is focused with a f=30 mm lens. λ=632.8 nm. α=0°. Scan time was 100 s (↑↓).

Optical Bistability by Photothermal Displacement in Prism Coupler Excitation of Surface Plasmons or Waveguide Modes

P. Pirani and W. Lukosz
Optics Laboratory, Swiss Federal Institute of Technology
8093 Zürich, Switzerland

We demonstrated a new type of optical bistability (OB) by prism coupler excitation of surface plasmons (SP's) on metal films in the attenuated total reflection arrangements shown in Figs. 1a and c. The OB is caused not by a thermooptic nonlinearity, but by the photothermal displacement effect, which induces a reduction of the gap width d in the coupling region. The same mechanism is responsible for the OB in prism coupler excitation of guided modes in absorbing planar waveguides (see Figs. 1b and d) [1]. We shall present both a theoretical analysis and experimental results.

The SP's at the metal film M - air interface reach with their evanescent field through the air gap of width d into the prism or the glass plate S, respectively. Therefore, at constant angle of incidence α, the optimum SP excitation depends on d, and the absorbance A(d) versus d has the form of a resonance curve (see Fig. 2). An analogous resonance occurs when a guided mode is coupled into an absorbing waveguide. Heating of the metal film M or of the waveguide, respectively, by the absorbed part $P_a = A(d)P$ of the incident power P causes photothermal displacements of the surfaces, and thus a reduction in gap width d. In the steady state d is reduced from its initial value d_o linearly proportional to P_A, i.e., we have

$$d = d_o - \tan\theta\, A(d), \qquad \text{with} \quad \tan\theta = g(\beta/\Lambda)P, \tag{1}$$

where β is the thermal expansion coefficient, Λ the thermal conductivity and g is a dimension-free geometrical factor which increases with decreasing laser spot size. The graphical solution of Eq.(1) shows that OB occurs for suitably chosen initial gap widths d_o (see Fig. 2a).

In Fig. 3 we compare theoretical and experimental results for the excitation of SP's on a gold film. For SP's on a silver film deposited on a high index prism the resonances are much sharper (cf. Figs. 2b with 2a). In the latter case we calculated a critical input power $P_c \approx 0.4$ mW for glass with $\beta/\Lambda \approx 10$ nm/mW and assuming g= 0.5. Interesting effects occur for gap widths $d \leq 10$ nm, since strong attractive van der Waals forces between the glass and metal surfaces influence the behaviour of the bistable system.

[1] W. Lukosz, P. Pirani, and V. Briguet, Opt. Lett 12, 263-365 (1987), and in 'Photoacoustic and Photothermal Phenomena', Springer Series in Optical Sciences, Vol. 58, (Springer Verlag, Berlin) 1988, pp. 466-469.

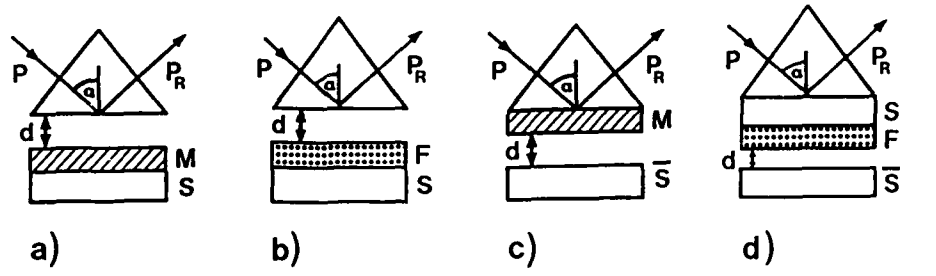

Fig. 1. Schematic of set-up for prism coupler excitation of a,c) surface plasmons, and b,d) guided modes in a planar waveguide. P, incident power; P_R, reflected power; α, angle of incidence in glass prism; M, metal film (e.g., Au or Ag); F, waveguiding film; S, glass substrate (e.g. of refractive index n_s=1.5); $\bar{S}$, glass plate; d, width of air gap.

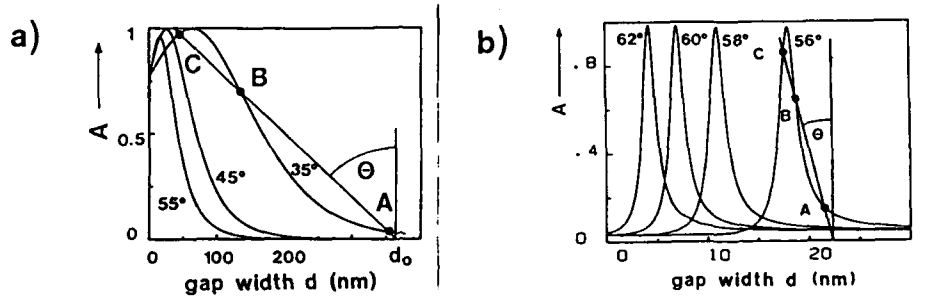

Fig. 2. Calculated absorption A(d) versus gap width d at different angles of incidence α. a) Configuration 1a with 300 nm thick gold film (λ=488 nm) and b) configuration 1c with 50 nm thick silver film (λ=514 nm). Intersections A and C of straight line with A(d) curve yield the stationary bistable states. tanΘ is proportional to the incident power P.

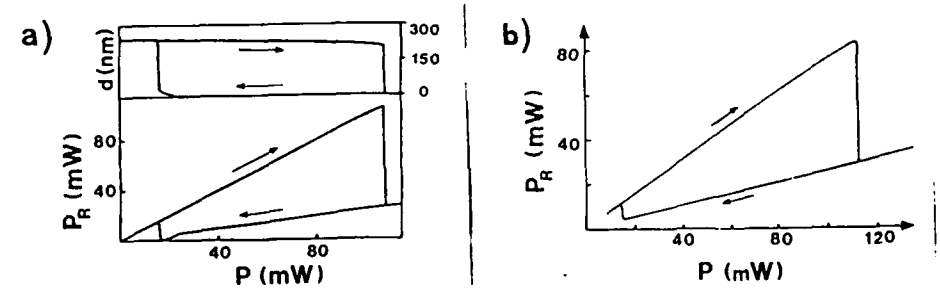

Fig. 3. a) Calculated reflected power P_R=[1-A(d)]P and gap width d and b) observed P_R versus input power P in configuration corresponding to Figs. 1a and 2a. α=42.6°, d_o=240 nm. Calculations with constant gβ/Λ=13 nm/mW. λ=488 nm. Scan time T≈200 s ( ). The prism was a high refractive index (n_p=2.05) glass prism.

BISTABILITY OF COUPLED CAVITIES

M.V.Vasnetsov, A.I.Petropavlovskii

Institute of Physics, Acad. Sci. UkrSSR, Kiev

The study of optical bistability is promising now for the use in optical computing devices. In this communication we are going to analyse the specific case of optical bistability based on the existence of two eigenmodes in coupled oscillators with nearly equal frequencies. We concentrate our attention on a very simple system composed of a three-mirror laser, one of the partial cavities being filled with an active media and the other empty. The optical lengths of the partial cavities are nearly equal (or multiple). Thus we may expect the splitting of the oscillating axial mode (the output is assumed to be single-frequency) to symmetric and asymmetric modes and possible transitions between them (see e.g. ref 1). This situation was firstly to our knowledge analysed in refs 2,3 and here we give more completed solution of the system of equations derived in ref. 3. The initial system of equations describing slow varying amplitudes is expressed as follows:

$$\frac{da_1}{dt} = \frac{\alpha}{2} a_1 - \frac{\beta}{2} a_1^3 - g a_2 \sin\Phi$$

$$\frac{da_2}{dt} = -\eta a_2 + g a_1 \sin\Phi$$

$$\frac{d\Phi}{dt} = -\tilde{\delta} + \gamma a_1^2 + g\left(\frac{a_1}{a_2} - \frac{a_2}{a_1}\right)\cos\Phi,$$

where $a_{1,2}$ are slowly varying amplitudes of fields in the first (active) and the second (empty) resonators respectively, Φ is slowly varying phase difference between oscillations in the partial cavities, δ frequency detuning, g coupling coefficient, α gain in active cavity, β saturation coefficient, γ coefficient of nonlinear phase drift, η - losses in the empty cavity.

The solution of the system gives in the stationary case (with neglecting a nonlinear phase drift) the following relation between stationary phase difference Φ_s and normalized detuning $\tilde{\delta}$ ($\tilde{\delta}=\delta/g$, $\tilde{\eta}=\eta/g$):

$$\tilde{\delta} = (\tilde{\eta}^2 - \sin^2\Phi_s)/\tilde{\eta}\,tg\Phi_s .$$

This relation exhibits a cusp catastrophe in coordinates $\tilde{\delta}$, $\tilde{\eta}$ and Φ_s when $\tilde{\eta} \leq 1$. We analyze the stability of stationary solution and show that the point of transition between two existing modes depends of the gain α. In the point of stationary breakdown a limiting cycle occures in accordance with the Hopf theorem (ref 4).

We expect that a system of coupled microcavities may be useful in neural network construction.

References

1. W.W.Show.- IEEE J. Quantum Electr., QE-22, n8, p.1174 (1986).
2. V.I.Perel', I.V.Rogova.- Opt. Spektr., 25, p.716 (1968).
3. V.I.Perel', I.V.Rogova.- Opt. Spektr., 25, p.943 (1968).
4. B.D.Hassard, N.D.Kazarinoff and Y.-H.Wan. Theory and applications of Hopf bifurcation, -Cambridge University Press, 1981.

OPTICAL BISTABILITY IN THIN-FILM WAVEGUIDES WITH LIQUID CRYSTALLINE NONLINEAR PRISM COUPLER.

Tomasz R. Woliński, Mirosław A. Karpierz, and Andrzej W. Domański

Institute of Physics, Warsaw University of Technology
Koszykowa 75, 00-662 Warsaw, Poland.

Katarzyna Chałasińska-Macukow and Tomasz Szoplik

Institute of Geophysics, University of Warsaw
Pasteura 7, 02-093 Warsaw, Poland.

Potential application in optical computers of devices based on nonlinear optical effects and in particular on optical bistability [1] is becoming more and more attractive. It was shown that the power reguired for optical bistability is minimized by using thin dielectric film waveguides [2]. In such a waveguide it is possible to limit the beam cross-sectional area to, typically, an optical wavelength. Therefore, it seems that optical waveguides offer an optimum interaction geometry for nonlinear all-optical devices [3]. Some experiments were reported, in which existence of nonlinear guided waves [4], limiting action in prism coupler [5], bistability in thin-film waveguides with liquid-crystal cladding [6] etc. were proved.

A basis in nonlinear guided wave devices is an optical waveguide where a film or a bounding media exhibit an intensity-dependent refractive index [7]. Liquid crystals (LCs) are very attractive materials for this purpose since they have one of the largest known intensity-dependent refractive indices arising from laser-induced thermal effects and molecular reorientation due to the strong liquid-crystalline molecular ordering. The optical beam intensity of 100 W/cm^2 which is easy of access from a cw argon laser is often sufficient to induce a significant reorientation of the molecular alignment, leading to an avarage refractive index change as large as 0.01 to 0.1 [8].

Many plane-wave, all-optical phenomena which depend on an intensity-dependent refractive index were demonstrated using LC as a nonlinear medium. Recently, LCs were proved to be useful for studing nonlinear effects in waveguides. The slow response of LCs, except for ferroelectric LCs, is not optimistic from the practical point of view. However, it makes transient studies of the nonlinear effects quite easy and provides some new data to these nonlinear optical phenomena.

In this paper we report observation of the intrinsic optical bistability in a thin-film waveguide with nonlinear prism coupling. The gap between the glass (n_1) input coupler and the glass planar waveguide (n_2=1.53 and n_3=1.50, both $<n_1$) was filled with the nematic liquid crystal PCB (also known as 5CB or K15) with its clearing point above the room temperature (T_c=35°). The experiment involved measurement of the guided wave power transmitted through the waveguide and radiated via the linear prism out-coupler vs the power incident on the nonlinear input coupler. A 1.6 W argon ion laser (λ=488 nm) was used to induce nonlinear change in the refractive index of PCB given by $n^{NL}=n_2 I$, where $n_2 \sim 10^{-3}$ cm²/W [9] and I is the local field intensity. The power coupled to the waveguide without the LC between the input coupler to the waveguide was found to be linear with the incident power. In the presence of the LC in the gap the transmitted intensity is not linear any more with the input intensity and under certain conditions reveals bistability. It was shown theoretically [10], that bistability may occur for angles of incidence that are slightly bigger than the angle for which the maximum coupling takes place in the linear approximation. Magnitude of the difference between both angle values influences the threshold power density for which bistability should occur. The time interval between the measurements was chosen to be long relative to the relaxation time associated with the nonlinearity. The optical bistability was observed for both TE and TM cases.

[1] H.M.Gibbs, "Optical Bistability: Controlling Light with Light", Academic Press, London 1985.
[2] G.I.Stegeman, IEEE J.Quantum Electron.QE-18(10),1610 (1982).
[3] G.I.Stegeman, C.I.Seaton, J.Appl.Phys.58, R57 (1985).
[4] H.Vach, G.I.Stegeman, C.T.Seaton, and I.C.Khoo, Opt. Lett. 9, 238 (1984).
[5] J.D.Valera, C.T.Seaton, G.I.Stegeman, R.L.Shoemaker, Xu Mai, and C.Liao , Appl.Phys.Lett. 45, 1013 (1984).
[6] J.D.Valera, B. Svensson, C.T.Seaton, and G.I.Stegeman, Appl.Phys.Lett. 48,573 (1986).
[7] F.Lederer, U.Langbein, H.-E.Ponath, Appl.Phys.B 31,69 (1983).
[8] I.C.Khoo and Y.R.Shen, Opt.Engin. 24,579 (1985).
[9] S.M.Arakelian and J.S.Chilingarian, "Nonlinear optics of liquid crystals" (in Russian), Nauka, Moscow 1984.
[10] V.J.Montemayor, R.T.Deck, J.Opt.Soc.Am. B 3, 12118 (1986).

Authors Etienne Friedrich / Serge Valette

Company CEA / LETI
85 X
F-38041 Grenoble Cedex

Title **Optical interconnections for WSI**

Abstract Integrated optics may be an alternative to metallic interconnection lines in very large and fast circuits. A silicon based technology is described and expected performances are estimated.

Summary

As optical waveguides are free of capacitive effects, they can transmit signals with very low degradations. Meanwhile, the trend of microelectronic circuits is to increase in size and to work at higher frequencies. Forecasts are that metallic lines will not provide satisfying interconnections in the future.

We are studying if optical interconnections are likely to replace on-chip electronic ones. We investigate therefore the feasability of a monolithically integrated optoelectronic circuit which would consist of conventionnally integrated microelectronic components on the top of which an optical circuit would provide interconnections between remote sites [1], [2].

In our scheme, each connection would require the following devices: a laser diode, a laser driver, a waveguide, an optoelectronic coupler and a photodiode. Optical elements such as beam splitters, mirrors, Y-junctions are also necessary in order to achieve fan-out.

Some of the items remain theoretical in this preliminary work.

The laser driver and the photodiode would be integrated with the electronic circuit, possibly by means of process steps that belong anyway to the microelectronic fabrication technology. These two elements are only considered on a semi-empirical basis in the study we have undertaken.

The laser diode would have to be hybridized. As silicon has a high thermal conductivity, it may work as a good heat sink. We assume that the hybridization is achievable although the reliability of it will have to be investigated later on.

We have focused our efforts on the following subjects.

The waveguide material is silica. The guiding layer is slightly doped which results in a refractive index increase. The deposition of this waveguide structure is a low temperature process which would take place after all the microelectronic fabrication steps.

In order to check the compatibility of the two technologies, we will however make the experiment of depositing the optical structure on a microelectronic circuit and observing the alterations that may be introduced. The microelectronic circuit is an adder which works at frequencies around 350 MHz. Results of this experiment will be available by the time of the conference.

The optoelectronic coupler is a grating that deflects the light selectively towards the substrate, i.e. the photodiode. It is fabricated simultaneously with the other optical devices which are needed for the division of the optical signal (beam-splitter, mirror, Y-junction). The performances of these devices when fabricated in a silica waveguide structure will be discussed.

Beside these experimental results, the emphasis will be put on the way all of the above mentionned items are interrelated.

[1] S. Valette, J.P. Jadot, P. Gidon, S. Renard
New integrated optics structure on silicon substrate: application to optical communication and optical interconnects
SPIE 862, Cannes, Nov. 86

[2] S. Valette, J.P. Jadot, P. Gidon, A. Kevorkian
Integrated optics and microelectronics: towards an integration on a single silicon chip
SPIE 862, Cannes, Nov. 86

GEOMETRIES FOR OPTICAL IMPLEMENTATIONS OF THE PERFECT SHUFFLE

A. A. Sawchuk and I. Glaser

Signal and Image Processing Institute, University of Southern California, MC-0272
Los Angeles, CA 90089-0272, USA

The *perfect shuffle (PS)* is well known as a useful building block for complex computing and communication-switching networks *[1]*. Lightwave technology offers potentially higher temporal bandwidth than electronics and optical signal carrying rays can intersect with minimal interaction and crosstalk. These and other considerations led to increased interest in optical networks both for communication and parallel computing. Various planar geometries for optical *PS* have been presented recently *[2]*. Most of these implementations, however, do not use the three dimensional volume characteristics of free space optics, so the total number of communication channels they could handle is quite limited. One attempt to overcome this problem involves the use of a separable multi-dimensional version of the *PS*. Here the input is a 2-D array; lines, then columns, are shuffled using the 1-D *PS* algorithm. This approach can implement similar tasks as the standard *PS* (with an 1-D input array), yet handle many more inputs *[3,4]*. Another approach is to fold a long 1-D input array into a 2-D one that has the same number of elements. An optical implementation of this folded *PS* was recently demonstrated *[5]*.

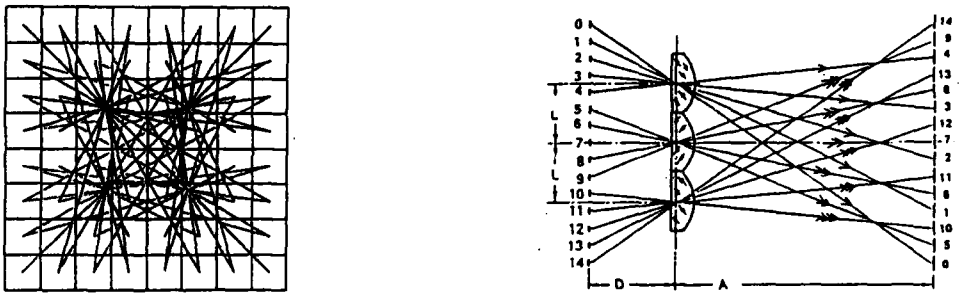

Figure 1: Ray diagrams for some optical implemetations of shuffles. *left:* a front view of an 8×8 2-D perfect shuffle; *right:* side view of a 15 channel 3-shuffle.

We found that both the 2-D input *PS* and the folded 1-D input *PS* can be implemented with a very similar geometry. In this geometry we can use a set of four lenses to produce imaging and shuffling, or we may use a single lens with an OTF synthesis device (such as a hologram) to produce the same result. The left part of Figure 1 shows an example of a 2-D *PS* implemented on an 8×8 array of individual channels. The bold lines show ray paths between elements; note that one quarter of the total rays pass through a single point. Other ray paths are shown with lighter lines; all the rays in the system pass through one of four points. These four points specify the *x-y* locations of the four lenses in a plane-to-plane imaging system used to implement the full 2-D *PS*.

In addition to the standard *PS*, (more precisely called a 2-shuffle), more general networks based on a *p*-shuffle, *[4]* where $p>2$, can be defined. Suppose that a given integer, N, representing the number of

input channels, can be factored into two integers greater than unity such that $N = pq$. If the label x of the N input lines is denoted by integers ranging from 0 to $N-1$, the p-shuffle performs the mapping σ_{pN}

$$\sigma_{pN}(x) = \left(px + \left\lfloor \frac{px}{N} \right\rfloor \right) \bmod N$$

to output lines, where $\lfloor \ldots \rfloor$ denotes the largest integer that is less than or equal to the argument. We note that the inverse p-shuffle is the q-shuffle. These generalized shuffles are useful for certain parallel computing problems *[4]* and can be optically implemented with a class of systems similar to the one depicted in the right part of Figure 1. In that example we see a system for implementing an 1-D 3-shuffle of a 15 element vector, using three lenses.

Optical shuffle stages can be cascaded with photonic switching modules to make a dynamic interconnection network suitable for parallel computing systems. A 3-D example of such a network is the Omega network, which consists of perfect shuffles on a 2-D array interlaced with an array of 4×4 crossbar switching modules. Each 4×4 switching module is a one-to-one crossbar interconnection that connects a 2×2 group of outputs from one stage to a 2×2 group of input lines to the next stage. These modules may be implemented with phododiodes, LEDs and an electronic 4 element crossbar. We shall experimentally demonstrate the optical perfect shuffle and 3-shuffle on 2-D input arrays.

CONCLUSIONS

Perfect shuffles and p-shuffle networks are useful for interconnecting 2-D planes of parallel processing elements in signal or image processing applications; many structured functions such as transforms can be implemented directly. We shall describe some of these applications along with other optical extensions of Ωmega and shuffle exchange networks.

This research is supported by DARPA/ARO Contract No. DAAG29-84-K-0066.

REFERENCES

[1]. H.S. Stone, "Parallel Processing With the Perfect Shuffle," IEEE Trans. Computers C-20, 153-161 (1971).

[2]. A.W. Lohmann, W. Stork and G. Stucke, "Optical Perfect Shuffle," Appl. Opt. 25, 1530-1531, (1986); A.W. Lohmann, "What Classical Optics Can Do for the Digital Computer," Appl. Opt. 25, 1543-1549, (1986); A.W. Lohmann, "Optical Bus Network," Optik 74, 30-35 (1986); K-H Brenner and A. Huang, "Optical implementations of the Perfect Shuffle Interconnection," Appl. Opt. 27, 135-137 (1988).

[3]. A. A. Sawchuk, "3-D Optical Interconnection Networks," *14th Congress of the International Commission for Optics*, Quebec City, August 1987.
Summary in: *Proceedings of the 14th Congress of the ICO, Proc. SPIE* 813, pp. 547-548 (SPIE, Bellingham WA, 1987).

[4]. D.G. Antzoulatos and A.A. Sawchuk, "Mapping to a 3-D Omega Processor Using Kronecker Products," to be published.

[5]. C.W. Stirk, R.A. Athale and M.W. Haney, "The Folded Perfect Shuffle Optical Processor," Appl. Opt. 27, 202-203 (1988).

ARCHITECTURES FOR MASSIVE HOLOGRAPHIC INTERCONNECTION NETWORK

Joseph Shamir, H. John Caulfield
Center for Applied Optics
and
Mir M. Mirsalehi
Department of Electrical & Computer Engineering
University of Alabama in Huntsville
Huntsville, Alabama 35899

Summary

An analysis of previously proposed architectures for optical interconnection networks based on holograms and spatial light modulators (SLM's) has been performed. The results of that analysis (the details will be reported elsewhere) reveal that as the number of interconnections in the network approaches 10^{12}, almost insurmountable technical difficulties are encountered. These include diffraction originated crosstalk, coherent noise, optical aberrations and, probably the most severe of all, the angular and polarization sensitivity of SLM's.

In this presentation we outline the above mentioned practical difficulties and propose new architectures to eliminate many of them. The basic architecture is presented in Fig. 1: A laser diode array, LDA, of N x N elements illuminates an N x N hologram array. The power emitted by the ij-th diode is a_{ij} and it illuminates the ij-th hologram. This hologram transmits light to the various elements, kl, of an N x N detector array, D. If the diffraction efficiency of the hologram towards this kl-th element is T_{ijkl}, then the total power detected by this detector is,

$$b_{kl} = \sum_{ij} a_{ij} T_{ijkl}$$

This system may be viewed either as a matrix-matrix multiplier of a 4-D matrix (or tensor) by a 2-D matrix or as a vector-matrix multiplier with vectors of N x N dimensions. Alternatively, this system can be considered as an interconnection network with N^2 channels and N^4 weighted interconnections that are "hardwired" for a given hologram array.

Many of the practical problems encountered in previous architectures are absent here. Unfortunately, large laser arrays are not yet available but one can still implement an interim version of this architecture by using a single laser that illuminates an SLM, to simulate the diode array.

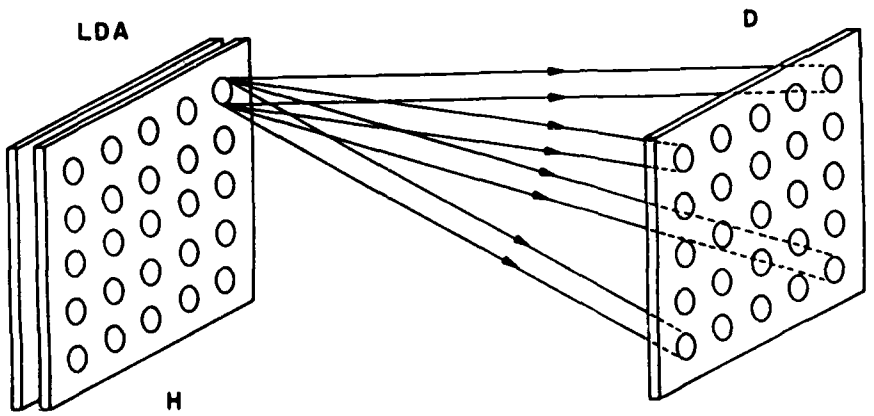

Fig. 1. Laser diode array (LDA) illuminates hologram array (H) with output vector detected at detector array, D.

Pinhole Imaging Holograms For Optical Interconnects

Shenchu Xu, Kaveh Bazargan, Geraldo Mendes and J C Dainty
Optics Section, Blackett Laboratory, Imperial College. London SW7 2BZ

To date, any kind of hologram recorded simultaneously for optical interconnects consists of main gratings and intermodulation gratings. But intermodulation gratings affect the image quality and the efficiency [1,2].

In this paper we use pinhole imaging hologram as a new kind of hologram which can be used for optical interconnects. The object beams pass through the pinhole to construct their image waves on the holographic plate. The image waves interfere with the reference beam. Anywhere the image wave incident to the holographic plate can be considered as a quasi-plane wave, so the phase volume hologram we have made only consists of main gratings. The effects of intermodulation gratings are avoided, because there are no intermodulation gratings.

This hologram brings following potential advantages to optical interconnects:

1. High signal-to-noise ratio,because there is no scattering from any intermodulation grating.
2. High efficiency. Because there are no intermodulation gratings, we can choose the optimum reference-to-object beam ratio to get optimum efficiency of the reconstructed image.
3. The resolution of reconstructed image can be maintained by choosing the suitable pinhole size and the distance between the reconstructed image and the pinhole.
4. Multi-facet hologram can be obtained by using a pinhole array. The arrangement of the images from the objects can be controled by operating the pinhole array. By controlling the number and position of the pinholes the intensity of the reconstructed image can be optimized. When reconstructing, all of the pinholes can be taken away without loss of quality.
5. Using pinhole imaging technique we can get very high image density [3], i.e. we can make interconnect elements smaller than the ordinary one.
6. If we only use a small number of pinholes, we can realize the interconnection by without using all the free space between the hologram and the reconstructed image. Light beams travelling from one place to another only need one or a few pinholes to pass through the other layer. This flexibility may be useful for inserting additional elements e.g. spatial light modulators (SLM).

Relevant experimental results on resolution, signal to noise ratio and eficiency for this hologram will be presented in the paper.

References

1. J. Upatnieks and C. Leonard, JOSA 60, 297 (1970)
2. R. K. Kostuk, J. W. Goodman, L. Hesselink, Appl. Opt. 25 , 4362 (1986)
3. C. P. Grover and R. Tremblay, Appl.Opt. 21, 4500 (1982)

SIGNAL PROCESSING IN CONOSCOPIC HOLOGRAPHY

E.Y. DUFRESNE, J.P. LIKFORMAN, G.Y. SIRAT
Ecole Nationale Supérieure des Télécommunications, Paris (France)
D. CHARLOT, Conoscopics.
D. PSALTIS, California Institute of Technology, Pasadena, CA (USA).

Development of conoscopic holographic cameras and associated processing facilities for 3-D vision applications is described.

OPTICAL COMPUTING 88 - TOULON

"Moments computing using a coherent optical/digital processor"

Christophe GORECKI

Laboratoire d'Optique P.M.Duffieux (associé au CNRS n°214)

Université de Franche-Comté

Route de Gray

25030 BESANCON - FRANCE

Abstract: *Heterodyne interferometry* provides a fast and accurate means of computing surface features by using irradiance moments.

An optical/digital processor is described to analyze reflective surfaces. The low-order irradiance moments are shown to be useful for the fast inspection of objects such as mechanical parts. The system consists of a Mach-Zehnder interferometer including a piezoelectric transducer, a Fourier transforming lens, a CCD detector arrays, and a microcomputer. This system measures the power spectrum of the interference pattern, and computes successives derivates of the Fourier transform, at the Fourier plane origin. To calculate the real and imaginary parts of the intensity distribution at the Fourier plane a PZT transducer is stepped four times, each step corresponding to 45° in phase difference between the object and the reference beams. At each step, the Fourier transform of the interferogram is recorded by a 512x512 CCD camera and stored in a microcomputer. These data are used to

compute the real and imaginary parts of the object Fourier spectrum, then the successive derivatives, and finally, the object moments. The moments measurement accuracy is investigated. As an example the method has been applied to the measurement of topographic characteristics of flat surfaces.

Generalized Falling-Raster/Folded-Spectrum Relationship

David N. Sitter and William T. Rhodes
School of Electrical Engineering
Georgia Institute of Technology
Atlanta, Georgia 30332-0250

The well-known falling-raster/folded-spectrum relationship [1,2] allows the full two-dimensional (2-D) parallel processing capabilities of a coherent optical spectrum analyzer to be applied to the spectrum analysis of time waveforms of extremely large ($\sim 10^6$) time-bandwidth product. The basic relationship has been exploited with considerable success in space-integrating, time-integrating, and hybrid space- and time-integrating optical processors. We show here that the conventional falling-raster/folded-spectrum relationship is a special case of a more general mapping of a 1-D signal and its spectrum into two dimensions. This generalized relationship can also be exploited for optical implementation.

The conventional falling raster recording format is shown in Fig. 1. The numbers indicate the order in which the lines are recorded. The fall angle θ is given by $\theta = \tan^{-1}(H/NW)$, where N is the number of raster lines and W and H are the raster width and height, identified in the figure.

The generalized falling raster is obtained by allowing the fall angle to assume values given by

$$\theta = \tan^{-1}\left(\frac{MH}{NW}\right), \tag{1}$$

where M and N are relatively prime integers. A total of M+N-1 raster lines is recorded in a raster of width W and height H. As illustrated in the example of Fig. 2, the raster record is laid down modulo-W in the horizontal direction and modulo-H in the vertical direction. Thus, if the raster line disappears at the right margin it reappears at the left; if it disappears at the bottom it reappears at the top. The conventional falling raster corresponds to the case where M=1.

The generalized raster record of a 1-D finite-duration signal f(x) can be modeled analytically by

$$f_{rast}(x,y) = \left\{\left[R_\theta\{f(x)\delta(y)\} ** \frac{1}{WH}\mathrm{comb}\left(\frac{x}{W},\frac{y}{H}\right)\right] \mathrm{rect}\left(\frac{x}{W},\frac{y}{H}\right)\right\} ** s(x,y), \tag{2}$$

where $R_\theta\{\ \}$ is an operator that rotates its argument clockwise through the angle θ, comb(x,y) is the Dirac comb function, rect(x,y) is the unit 2-D rectangle function, and ** denotes 2-D convolution. The entirety of the signal f(x) is assumed to be contained in the raster record, requiring that f(x) have support not exceeding

$$L = \left[(MH)^2 + (NW)^2\right]^{1/2}. \tag{3}$$

Fourier transforming Eq. (2) gives the spectrum of the raster record:

$$F_{rast}(x,y) = \left\{\left[R_\theta\{F(u)1(v)\}WH\mathrm{comb}(Wu,Hv)\right] ** \mathrm{sinc}(Wu,Hv)\right\}S(u,v), \tag{4}$$

where 1(v)=1. The spectral distribution F(u)1(v) is rotated through the fall angle θ, and the rotated distribution is sampled at points separated by 1/W in the u-direction and 1/H

in the v-direction. The samples are blurred by the sinc function, and the resulting distribution is then weighted by S(u,v), the transform of the recording spot spread function. Using Eqs. (1) and (3) it can be shown that the *(m,n)th* sample, measured at coordinates (m/W,n/H), has strength proportional to F[(mN-nM)/L]. Since L is the signal duration, these samples satisfy the Nyquist criterion and are sufficient to fully characterize the spectrum of f(x). Blurring by the sinc function smears spectral data between samples, but not at the samples. Thus, if spectral measurements are taken at the sample locations, accurate results can be obtained. The conventional falling raster presents a special case, for then low crosstalk spectral measurements can be made accurately along *lines* (the so-called fine-frequency lines).

References

1. C. E. Thomas, "Optical Spectrum Analysis of Large Space-Bandwidth Signals," Appl. Opt. 5 (1966) 1782-1790.

2. William T. Rhodes, "The Falling Raster in Optical Signal Processing," in *Transformations in Optical Signal Processing*, W. T. Rhodes, J. R. Fienup, and B. E. A. Saleh, eds. (Proc. SPIE, vol. 373, Bellingham, Washington, 1981), pp. 11-19.

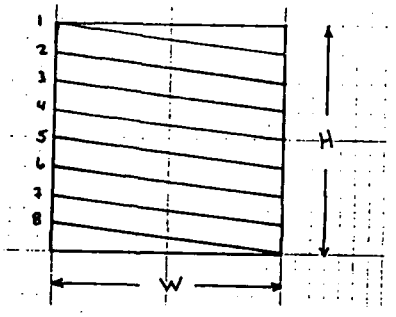

Fig. 1. Conventional falling raster recording with sequentially numbered lines.

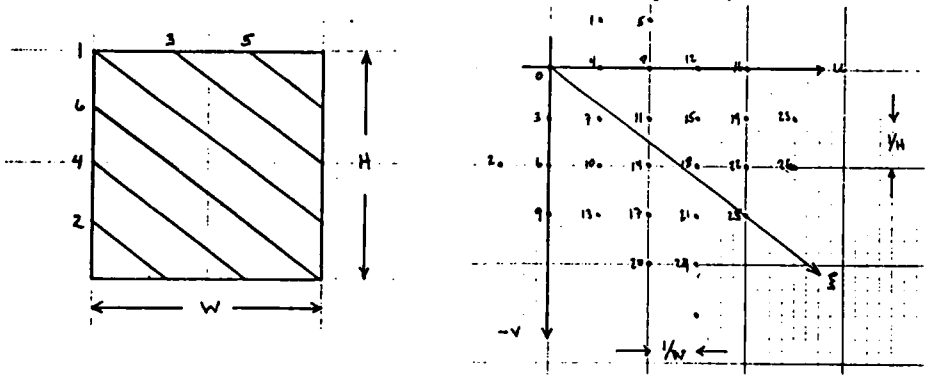

Fig. 2. Generalized falling raster and folded spectrum for N=4 and M=3: (a) shows raster with recording lines numbered in sequence, (b) shows associated spectral distribution F(ξ) with sequential sample locations corresponding to increasing frequency.

Optical Realization of Parity Function and its Application

Ming Hsien Wu

Hamamatsu Corporation
360 Foothill Road
Bridgewater, New Jersey 08807-0910
U S A

Tel: 201-231-0960

SUMMARY:

A parity function is a special class of the symmetric Boolean functions, which deserves a special attention due to its unique algebraic properties and the resuting interesting and useful applications.

The main purpose of this paper is to present and discuss the basic principle and requirement, and various methods for implementing this function , then present some new optical configurations as examples of applications using the proposed approaches.

The parity function in its simplest form is an Exclusive-OR function or its complementation. However, a mere realization of a single stage/level Exclusive-OR logic does not generally serve a very useful or practical purpose. A realization of an algorithm with multiple parity operations is needed in practical applications. This means that at least restoration or better yet, amplification of logic levels is essential for cascadability and multilevel operations. This also sets constraint to the fan-in and fan-out requirements for a device under consideration in order to optimize design and configuration.

Translating the basic requirements into hardwares necessitates an optical (2-Dimensional) device with proper transfer characteris--tics for nonlinearity, spectral match and optical gain in order to carry out the optical implementation. It should be noted that the algorithm is based on the single-rail input logic scheme.

Although the parity function is not lineary seperable, it can be synthesized with linearly seperable functions through dualization and inversion of a function or functions in question.

Thus an optical device with additional capability of dualizing a linearly seperable function can be utilized for simplification of architectures.

(Optical Realization of Pairity Function and its Application)

M. H. Wu

Based on above analyses and detailed discussions in this paper several architectures for the basic optical parallel full adder and subtractor,a combined processor, and the parity generator and checker are presented and discussed, as examples of applications.

Finally, its implications to other applications such as to pattern identification and error detection and correction coding are commented.

LAU EFFECT AND BINARY LOGIC

P. Andrés, J. Ojeda-Castañeda*, and J.C. Barreiro
Departamento de Optica. Universidad de Valencia. 46100 Burjasot. Spain.
**INAOE. Apartado Postal 51. 72000 Puebla, Pue. Mexico.*

Summary

Logic operations are the basis for digital optical computing. In this communication the spatial filtering properties of the Lau experiment at Fresnel distances are used to perform binary logic operations by incoherent optical spatial filtering. In this way, a lensless version of a binary logic processor working under incoherent illumination is presented.

The Lau effect is a well-known interference phenomenon after reintroduction by Lohmann. In the present version of the Lau experiment, monochromatic light from an extended incoherent light source passes through two parallel periodic structures spaced by a distance z. We can observe fringe patterns of high contrast in specific planes behind this double grating configuration, if a consonance condition between the distance z and the spatial periods of both 1-D gratings is fulfilled. In fact, the first grating acts as a spatially incoherent, codified source whereas the second one is the object grating.

A theta-modulated image is prepared independently for each input object, in order to perform binary logic operations. In this nonlinear preprocessing operation, each binary level of both input functions is encoded by a single grating structure that can be a simple square-wave grating. The encoding gratings have the same spatial frequency. They also have different orientations in that both gratings connected with the same logical value are mutually perpendicular, and the binary levels of each object are encoded by two gratings rotated by an angle α from each other.

For logical processing, we substitute the object grating in the Lau experiment by the multiplication of both theta-modulated images. When the angle α is suitably chosen, the selection of any particular logic operation is achieved by a specific codified source. For that purpose, we employ as incoherent source either a single 1-D grating with different orientations or the product of two of them, which is illuminated incoherently. In this

way, any of the 16 binary logic operations can be obtained. In the output plane, i.e. in any Lau pattern plane at finite distance, the logical values 0 and 1 are encoded as a uniform background and clear Lau fringes, respectively.

The present binary logic processor is quite compact and performs in parallel any binary logic operation with a high signal to noise ratio (incoherent illumination). Moreover, with a similar principle we can use pure phase gratings in the theta modulation encoding process. In this manner we implement a logic processor with high light throughput too.

One of the authors (J.C. B.) was supported in this work by the Conselleria de Cultura, Educación y Ciencia de la Generalidad Valenciana, Spain.

Design of Dammann Gratings for Optical Symbolic Substitution

Joseph N. Mait
University of Virginia
Department of Electrical Engineering
Thornton Hall
Charlottesville, Virginia 22901
USA

Symbolic substitution is a method for manipulating binary data that depends on both the value of the data and its spatial location to realize logical operations [1,2]. A substitution system requires only a pattern recognizer, a nonlinear device, and a pattern scriber. The operation of both the recognition and scribing subsystems is based on the replication of an input object to produce several output images; the replicated images are then overlayed.

For optical implementation of symbolic substitution the recognizer and scriber systems can be constructed using classical and holographic optical elements; single-channel and dual-channel systems have been proposed [3]. In a single-channel system holographic elements are used either to replicate an input object or combine several shifted images. The holgraphic elements in a dual-channel system perform both replication and translation.

For single-channel systems, it is possible to design binary-phase gratings [4], referred to herein as Dammann gratings, to be used as both splitters and combiners [5,6]. Dammann's method assumes a symmetric display of the replicated images and determines the locations of phase changes based on the number of desired replicas. A modification to Dammann's method of design allows for an asymmetric display [3]. The method requires a dual-channel system, i.e., an interferometer, but the asymmetry provides simultaneous replication and translation.

An interferometric system has been constructed and binary-amplitude gratings designed and fabricated according to the modified method of Dammann. Preliminary results indicate moderate performance of the system.

References

1. K.-H. Brenner, A. Huang, and N. Streibl, Appl. Opt. 25, 3053 (1986).
2. K.-H. Brenner, Appl. Opt. 25, 3061 (1986).
3. J. N. Mait and K.-H. Brenner, Appl. Opt. 27, XXXX (1988).
4. H. Dammann and E. Klotz, Opt. Acta 24, 404 (1977).
5. J. Jahns, M. E. Prise, M. M. Downs, S. J. Walker, and N. Streibl, J. Opt. Soc. Am. A 4(13), P69 (1987).
6. W. B. Veldkamp, J. R. Leger, and G. J. Swanson, Opt. Lett. 11, 303 (1986).

SYMBOLIC SUBSTITUTION USING SHADOW--CASTING

Wei Xue, Li-Xue Chen, Qiang-Sheng Hu and Chun-Fei Li

(Department of Applied Physics, Harbin Institute of Technology,

Harbin, the People's Republic of China)

A new implementation of digital optical computing called symbolic substitution has been introduced by Huang and developed further by Brenner et al. [1] [2] We have discussed the generic procedure of symbolic substitution. [3] Now the systems which complete symbolic substitution consisting of many prisms, mirrors and lenses are more complex, so it is necessary to seek simpler systems.

Shadow--casting which was first proposed by Tanida and Ichioka[4] is a method of implementing optical parallel pattern logic and optical computing. So we propose that symbolic substitution be completed by shadow--casting.

According to the conclusion in [3], the symbolic substitution of pattern (see Fig.1.) consisting of four cells requires four translational overlapping images of input image. These can be done by the lensless shadow--casting system. Because the shadow--casting system can not be cascaded, it is necessary to add a sequential logic gates array and a record set. Sequential logic gate has double function, memory and logical operation. A record set is used in order to record the results after recognition. The recognition and substitution phase are illustrated in Fig.2. In substitution phase, the input, middle screen, mask, and logic array are removed. The result recorded after recognition is taken as an input, making use of the shadow--casting system once more, we obtain the substitution result on the output screen.

A LED(*light-emitting* diode) array consisting of four LED's is used as a light source. Divergent light beams radiating from the LED's illuminate the input plane and project multiple shadowgrams (multi-images) of input onto the middle screen. Choosing the spacing between the LED's and distances from the source plane to the input plane and from input plane to the middle screen properly, we can make shadowgrams of input projected by the individual LED's be superposed on the middle screen, shifting one another by an amount of one cell size along the vertical and horizontal directions, the numbers and location of the multiple images is controlled by the combination of the spatial position of the LED's switched to the on state, so the on-off state of the LED's depends on the structure of recognition and substitution patterns. Each cell in patterns only have two state, white(transparent) or black(opaque). We take the white cell as logic one and the black cell as logic zero. we define that the superposition operation of cells is logical AND in recognition and logical OR in substitution.

We have made a experiment to confirm the system above. A binary image in Fig.3. is used as the input, we want to recognize the pattern in Fig.1(a) from the input and substitute the pattern in Fig.1(b) for the pattern in Fig.1(a). Fig.4. shows the experimental result.

REFERENCES

[1] A.Huang, "Parallel Algorithms for Optical Digital Computers", in Technical Digest, IEEE Tenth International Optical Computing Conference, (1983), pp13—17.

[2] K.Brenner, A.Huang, and N.Streil, "Digital Optical Computing with Symbolic Substitution", Appl.Opt. 25. 18,(1986).

[3] W.Xue, L.Chen, C.Li, and J.Hong, "The Common Procedure of symbolic substitution", Technical Digest, International Topic Meeting on Optical Bistability, Instability and Optical computing, Beijing, China, August 24-29, 1987.

[4] J.Tanida and Y.Ichioka, "Optical Logical Array Processor Using Shadowgrams", J.Opt.Soc.Am.73.6. (1983).

Fig.1. Patterns consisting of four cells; (a) recognition pattern, (b) substitution pattern.

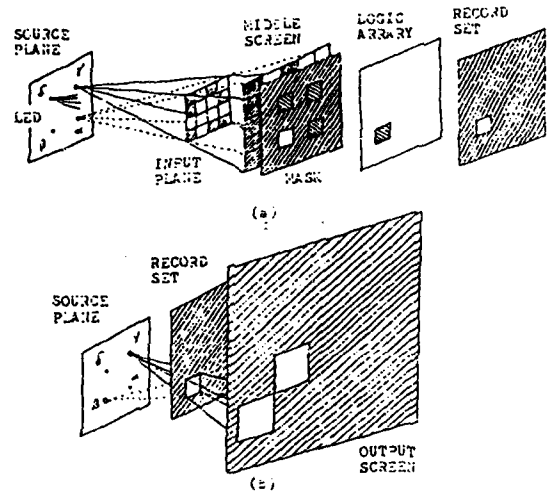

Fig.2. Schematic diagrams of implementing symbolic substitution using shadow-casting; (a) recognition phase, (b) substitution phase.

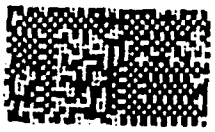

Fig.3. Input image

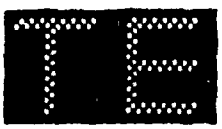

Fig.4. Experimental result

Thursday september, 1, 14.45

SESSION 9 (Chairman P. CHAVEL)

OPTICAL NEURONAL PROCESSORS
PROCESSEURS OPTIQUES NEURONAUX

D2 - K. KYUMA and T. NAKAYAMA : Optical neural networks, system and device technologies.

D3 - K.M. JOHNSON, L. COTTER, L. ZHANG and J. BIGNER : A compact optoelectronic connectionist machine.

D4 - G.Y. SIRAT, R.C. CHEVALLIER and A.D. MARUANI : Frequency multiplexed raster and neural networks.

D5 - M. ISHIKAWA, N. MUKOHZAKA, H. TOYODA and Y. SUZUKI : Experimental studies on adaptive optical associative memory.

D6 - E. BARNARD and D. CASASENT : New optical neural system architectures and applications.

Optical Neural Networks
—System and Device Technologies—

Kazuo Kyuma and Takashi Nakayama

Central Research Laboratory,
Mitsubishi Electric Corporation,
8-1-1 Tsukaguchi-Honmachi,Amagasaki-city,
Hyogo,661,Japan

Abstract

Optical computing technologies based on the neural networks are reviewed. Several optical devices required for implementing these systems are also discussed.

"A Compact Optoelectronic Connectionist Machine"

Kristina M. Johnson, Lise Cotter,
Ling Zhang, and Jack Bigner
Center for Optoelectronic Computing Systems
University of Colorado
Boulder, Colorado 80309-0425

Abstract

In this paper we describe the design and construction of a compact multi-layer optoelectronic architecture which uses the backpropagation of error learning rule. The phase I machine is a sandwich consisting of alternate layers of two-dimensional ferroelectric liquid crystal (FLC) and nematic liquid crystal television (LCTV) spatial light modulators. The FLC's comprise the input, hidden, and output layers; while two nematic LCTV's represent the weight matrix layers. This machine has 32 processing units, each unit is .800 mm x 25 mm. The connection matrix cells are .8 x .8 mm in size. The processing units are connected optically, and the backpropagation learning rule is implemented electronically.

A phase II machine will be described which performs weight adaptation optically. Signal-to-noise considerations limit the size of connectionist networks using spatial light modulators for storing discrete weights.

We also present computer simulations of system performance with real device characteristics, showing the origin of these limitations.

FREQUENCY MULTIPLEXED RASTER AND NEURAL NETWORKS

Gabriel Y. SIRAT ,Raymond C. CHEVALLIER and Alain D. MARUANI
Ecole Nationale Supérieure des Télécommunications,Département Images,
Groupe Optique, 46 rue Barrault, 75634 PARIS cedex 13 FRANCE

In the first part of this paper we will present Frequency Multiplexed Raster (FMR) optical implementation of neural networks. A hidden difficulty for hardware (optical and electronic) implementation is the dimension of the synaptic matrix which is twice the dimension of the input and output matrices or vectors. For two-dimensional images, which is we believe one of the greatest potentialities of neural networks, the synaptic matrix is *4D* and cannot be directly implemented in optics.

We propose Frequency Multiplexed Raster (FMR) as a method to fold this matrix in a two-dimensional format. We will show that the FMR scheme induce invariances in the neural network system.

In the second part of this paper we will describe the system built in our laboratory showing the feasability of FMR optical neural networks. The system is built from an optical input module, a fixed synaptic matrix coded on a transparency, a CCD camera and a micro-computer which perform the thresholding and feedback operations. In a later stage the fixed matrix will be replaced by a programmable matrix. we will show experimental results and will discuss foreseable capacity of this technology and possible applications of this system.

Experimental studies on adaptive optical associative memory

M. Ishikawa, N. Mukohzaka*, H. Toyoda*, and Y. Suzuki*

Industrial Products Research Institute
1-1-4, Higashi, Tsukuba, 305 Japan

*Hamamatsu Photonics K.K.
1126-1, Ichino-cho, Hamamatsu, 435 Japan

Introduction

Recently, there are growing interests in studying various models of neural network for optical computing. These models are capable of performing massively parallel computing such as image processsing, simulations of partial differential equations and combinational network problems. In particular, the architectures based on the models of associative memory for optical computing are potentially realizable in practice. Therefore, many architectures based on the optical associative memory have been proposed. However, there are very few experimental data for the proposed architectures. Especially in the area concerning the performance of learning, a proper experimental study is needed.

In this papar, a new architecture of neural network for optical computing is proposed. It can be used for implementing a simple system of associative memory based on one of the modified theories of the associative memory. It is shown that the memorized patterns can be recalled perfectly by an experimental system using two Microchannel Spatial Light Modulators[1] (MSLMs). The system and its basic experimental results of the recalling and learning operation are also described and discussed. Especially, various experimental results of the learning operation are newly shown.

Theory

The architecture proposed in this paper is called OPTICAL ASSOCIATRON. The main purpose of the OPTICAL ASSOCIATRON is to realize analog and adaptive processing for optical associative memory. In principle, it uses autoassociative operation similar to Nakano's Associatron[2] and the orthogonal recollection methods proposed by Kohonen[3] for a straightfoward implementation of simple associative memory. These methods have been properly modified in order to represent the pattern information suitable for the optical system and compatible with the method for orthogonal learning. As a result, optical operations in the OPTICAL ASSOCIATRON can be expanded to a class of operation readily realizable by optical devices.

Experimental system

An experimental electrical and optical hybrid system using two MSLMs, an electronic processing unit and a computer is shown in Fig. 1. This system demonstrates for 4x4 elements of input/output patterns and 16x16 elements of memory matrix. MSLM 1 memorizes a memory matrix.

MSLM 2 performs a real-time readout executing Hadamard product with MSLM 1. The computer calculates the terms of learning operation from a temporary recalled pattern and a learning input pattern then displays the results on LED array 1 for the modification of memory matrix. The computer also controls the recalling and learning operations of the system. It is shown that the features of analog processing and feedback processing for optimal and adaptive learning are inherently important for the optical processing.

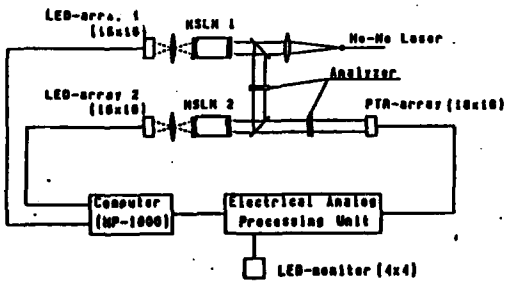

Fig. 1 Schematic diagram of experimental OPTICAL ASSOCIATRON

Experimental results

From the experimental system, the basic experimental results of the recalling and learning process have been already obtained[4]. The various experiments of the learning operation are realized by this system. The perfect recollections are obtained by using the analog processing capability of the MSLM and the recursive feedback method for the leraning process. By cordinating all these functions, the system can operate adaptively even under the necessity of compensation for noise including the shading, and for the orthogonalization for the mutually interfered patterns. These features including the system perfomance related to a learning methods and a learning parameters are experimentally evaluated by the system as illustrated in Fig. 2 as an example.

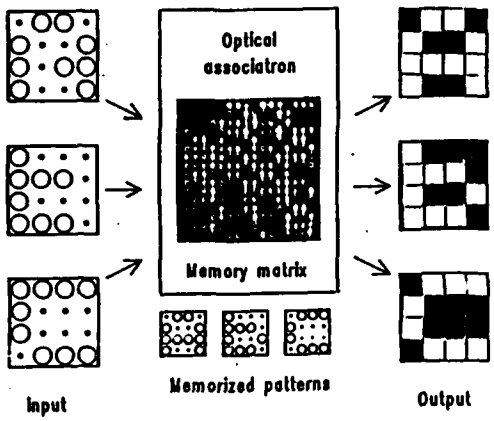

Fig. 2 An example of the orthogonal learning by the adaptive method for a nonorthogonal input patterns such as the characters "A", "b", and "C".

Conclusion

In this paper, a modified theory of OPTICAL ASSOCIATRON and an architecture for an experimental system are presented. The various results of the learning operation of the experimental system are described and discussed. The results indicate that an adaptive learning method plays an important role for optical analog processing including a neural network system.

References

1. Tsutomu Hara, Yoshiharu Ooi, Takahito Kato, and Yoshiji Suzuki, Proc. SPIE, 613, 153 (1986)
2. K. Nakano, IEEE Trans. Syst. Man. Cybern. SMC-2, 380 (1972)
3. T. Kohonen, Self-Organization and Associative Memory (Springer-Verlag, New York, 1984)
4. M. Ishikawa, N. Mukohzaka, H. Toyoda, and Y. Suzuki, Appl. Opt.: to be published

TOULON OPTICAL COMPUTING CONFERENCE, AUGUST 1988

New Optical Neural System Architectures and Applications

Etienne Barnard and David Casasent

Carnegie Mellon University
Center for Excellence in Optical Data Processing
Department of Electrical and Computer Engineering
Pittsburgh, PA 15213 USA

Abstract

Optical neural networks for multi-target tracking, inference processors, imaging spectrometer data and matrix inversion are described, and initial results are presented.

Summary

Optical neural processors have been described that realize various neural models. We consider four specific applications of optical neural processors that address different optimization problems. The first problem considered is multi-target tracking. The resultant energy function is minimized when the distance measurements are grouped into acceptable tracks. This has a cubic energy term and thus a simple matrix-vector processor alone does not suffice. A new optical processor results (this is described and its implementation with bistable devices and ferroelectric liquid crystals is discussed). The second problem considered is an optical neural network to realize an inference processor. The case study chosen is the guidance and control of a mobile robot. For this application, a matrix-vector processor with a fixed matrix mask (set of interconnections) suffices. The parallelism provided by the neural net makes it much faster than conventional sequential expert systems. The third case study is the analysis of imaging spectrometer data to determine the basic elements (minerals) comprising the compounds present in each spatially resolved region of an input image from the measured spectra . A different neural network results for this case and initial data results are provided on the ability of this

network to provide analysis of mineral compound mixtures in each region of the input scene. Finally, we study matrix inversion with neural nets. It is shown that the appropriate energy function leads to an efficient optical architecture, using a multi-channel acousto-optic device. This solution avoids some of the problems of other optical matrix processors, especially cumulative error build-up.

Thursday september, 1, 17.00

SESSION 10 (Chairman A.W. LOHMANN)

PARALLEL PROCESSORS
PROCESSEURS PARALLELES

E2 - M.J. MURDOCCA and A. HUANG : Symbolic substitution methods for optical computing.

E5 - K.H BRENNER and G. STUCKE : Architectures for digital optical image processing using morphological filters.

E6 - P. GARDA, K. MADANI, F. DEVOS, P. CHAVEL, P. LALANNE and J. TABOURY : A massively parallel image processor for stochastic relaxation using optical random number generation.

E7 - B. SUGLA : Computing on a digital optical computer using regular interconnections.

E8 - J.C. BRADLEY, E.C. MALARKEY, P.R. BEAUDET and G.E. MARX : A residue number system optical adaptive processor.

Symbolic Substitution Methods for Optical Computing

M. J. Murdocca and A. Huang
AT&T Bell Laboratories 4G–538
Crawfords Corner Road
Holmdel, New Jersey 07733

Abstract

Symbolic substitution is a method of computing based on parallel binary pattern replacement, and can be implemented with *simple optical components* and *free–space interconnects*.

1 Discussion

Symbolic substitution [1] is a method of computing based on pattern replacement. A two–dimensional pattern is searched for in parallel in an array and is replaced with another pattern. Parallel pattern transformation rules can be applied sequentially or in parallel to realize complex functions. When the substitution space is modified to be log_2N–connected for N binary spots and fixed masks are allowed to initialize the system, then optical digital circuits based on symbolic substitution can be made nearly as efficient in terms of gate count and circuit depth as any other interconnection method would allow. We describe an optical setup that requires no more than a fanin and fanout of two from optically nonlinear logic devices and uses free space as the interconnection medium.

An example of symbolic substitution is shown in Figure 1. The pattern being searched for is called the *left hand side* (LHS) of the transformation rule and the pattern that replaces the LHS is called the *right hand side* (RHS) of the transformation rule. In Figure 1 the LHS of the rule is satisfied at two locations, so the RHS is written at those locations. Any bits that do not contribute to a LHS pattern disappear after the rule is applied. Transformation rules can be customized to perform specific functions such as addition [1], Turing machines [2] and packet switching which is described here.

A simple optical setup that makes use of array–scale split/shift/combine operations is shown in Figure 2a. The operations at each stage can be described by two symbolic substitution rules as shown in Figure 3. A rule can be prevented from firing at a selected location by setting appropriate sites on the masks to be opaque. If a prism grating and a mirror is added to each stage to implement one stage of a crossover network [3] (Figure 2b) then a great amount of connection complexity can be achieved at the expense of a small amount of hardware. Properties of log_2N networks can then be used in the design of optical digital circuits [4].

An example of a circuit designed with this approach is shown in Figure 4. In the left side of this diagram, a two channel sorting node is designed in eight connection levels with 128 switching components (the top row is not included in the count). Dimmed connections are masked out. The electronic equivalent using VLSI is shown in Figure 5. The VLSI implementation uses 106 switching components in six connection levels. Registering is performed after three levels so that data can be pipelined, which increases throughput by a factor of two. For the free–space approach optical pathlengths can be made equal within a tolerance of a few femtoseconds so that data can be pipelined at the gate level, increasing throughput by a factor of three over the VLSI design. We conclude that symbolic substitution implemented with free–space optics is a preferred method for designing optical digital circuits.

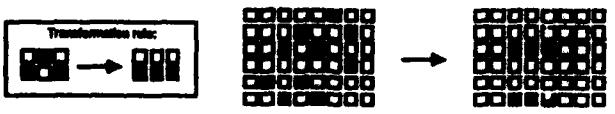

Figure 1: Symbolic substitution. The transformation rule is applied to the grid on the left side of the arrow to produce the grid on the right side of the arrow.

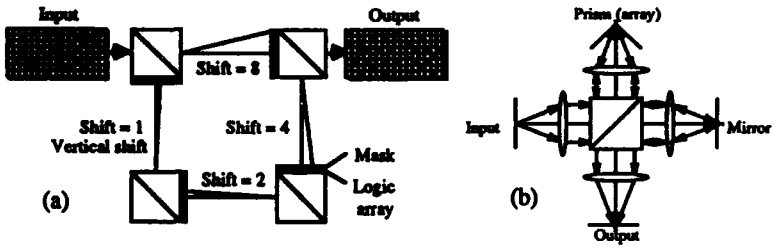

Figure 2: Split/shift/combine setup (a) and optical implementation of one stage of a crossover network (b) (Jürgen Jahns).

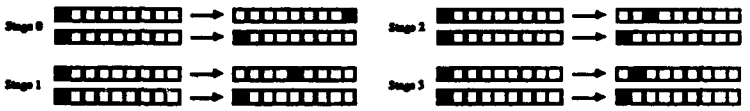

Figure 3: Symbolic substitution rules for split/shift/combine setup.

[1] Huang, A., "Parallel Algorithms for Optical Digital Computers," *IEEE 1983 10th International Optical Computing Conference*, 13, (1983).

[2] Brenner, K.-H., A. Huang and N. Streibl, "Digital optical computing with symbolic substitution," *Appl. Opt.*, **25**, 3054, (1986).

[3] Jahns, J. and M. J. Murdocca, "Crossover networks and their optical implementation," Submitted to *Appl. Opt.*.

[4] Murdocca, M. J., A. Huang, J. Jahns, and N. Streibl, "Optical design of programmable arrays," *Appl. Opt.*, **27**, (May 1, 1988).

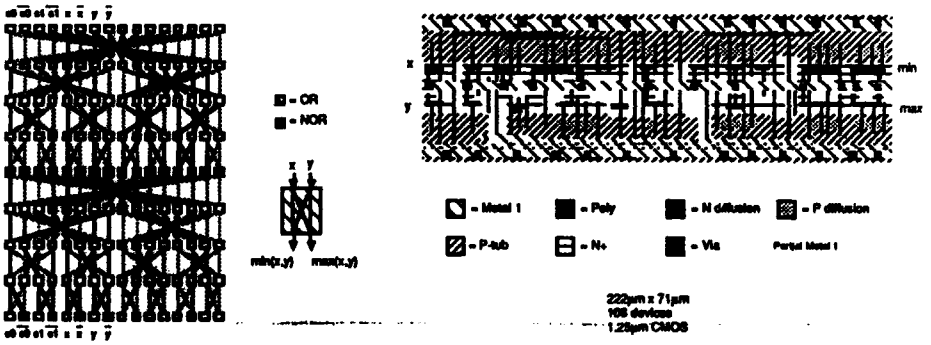

Figure 4: Left: crossover implementation of a sorting node. Right: electronic VLSI implementation of a sorting node (Jay O'Neill.)

ARCHITECTURES FOR DIGITAL OPTICAL IMAGE PROCESSING USING MORPHOLIGICAL FILTERS

K.-H. Brenner, G. Stucke
Physikalisches Institut der Universität Erlangen-Nürnberg
Erwin-Rommel-Str. 1
D-8520 Erlangen

MATHEMATICAL MORPHOLOGY

Digital processing of binary images using the concepts of 'mathematical morphology' is a well known set-theoretic method for image analysis [1]. Morphological filters are defined for digitized binary images (sets) in the discrete plane Z^2. For two sets A and B, the main set processing operations (SP-filters) are:

set symmetric of A	$A^s = \{-a: a \in A\}$
set complement of A	$A^c = \{a \in Z^2: a \notin A\}$
set translation of A by p	$A_p = \{p+a: a \in A\}$
set difference of B from A	$A - B = \{a: a \in A, a \notin B\}$
Minkowski set addition of A and B	$A \oplus B = \{a+b: a \in A, b \in B\}$

The Minkowski addition is very similar to a convolution. Based on these operations one can define other filter operations like set dilation, erosion, closing, opening, etc. In additon to binary images also gray-tone images (functions) can be processed with binary morphological filters after decomposing the image into a family of binary images, called cross sections. A finite set of amplitudes serves as threshold levels for these cross sections. After applying the desired SP-filters to all binary images, the processed gray-tone image can be obtained from the cross sections. The mathematical justification for this decomposition is the fact, that function-set-operations commute with thresholding.

DIGITAL OPTICAL ARCHITECTURES

The commutation property and the space invariant nature of the problem lend itself to an optical implementation. Because morphological operations can be decomposed into two tasks - a nonlinear point to point operation and a linear space invariant operation - especially digital optical processors are attractive. The architectures we have investigated are based on symbolic substitution and on Dual Input Array Logic (DIAL).

SYMBOLIC SUBSTITUTION: This spatial logic [2] is well suited for implementations of SP-filters. The Minkowski set addition, for example, can be described as a substitution of isolated pixels by the pattern of the structuring element.

DUAL INPUT ARRAY LOGIC: An optical processor based on DIAL is described in [3]. It consists of a parallel logic module with two inputs and one output, and a programmable interconnection module. The processor provides the instructions AND, NOT and SHIFT on data arrays. Therefore the basic SP-operations could be performed directly.

EFFICIENCY

Since the Minkowski addition plays the central role in SP-filters, the efficiency of a certain computer architecture for morphological image processing can be estimated by the time required for this operation. Let t_s be the time for shifting a data plane, t_{OR} the time for logical ORing two data planes, and $|B|$ the cardinality of the structuring element. Then

$$T_{MA} = |B| \cdot (t_s + t_{OR})$$

is the time for a complete Minkowski addition using DIAL. The size of the array does not influence the processing time because of spatial parallelism of the architecture. With symbolic substitution the cardinality of the structuring element has no effect on the processing time, however at the expense of fan-out. With a pipeline architecture t_s and t_{OR} can be reduced to the switching time of nonlinear optical devices.

References:

[1] J. Serra, "Image Analysis and Mathematical Morphology", Wiley, New York (1975).

[2] K.-H. Brenner, A. Huang, N. Streibl, "Digital optical computing with Symbolic Substitution", Appl.Opt. **25** (1986) 3054.

[3] G. Stucke, "Parallel architecture for a digital optical computer", submitted to Appl.Opt.

A massively parallel image processor for stochastic relaxation using optical random number generation[1].

P.Garda, K.Madani, F.Devos
I.E.F., C.N.R.S. L.A. 22, Batt. 220, Université de Paris Sud, 91405 ORSAY CEDEX

P.Chavel, P.Lalanne, J.Taboury
I.O.T.A., C.N.R.S. L.A. 14, B.P. 43, 91406 ORSAY CEDEX

ABSTRACT

The architecture of an electronic mesh array for image processing by simulated annealing is described. Intended for VLSI monolithic implementation, it features mixed analog/digital devices and optical random number generator.

Introduction.

Simulated annealing has been more and more popular since its introduction [1] for several optimization problems classes. A large number of applications to image processing, called stochastic relaxation, have been reported after [2], for which some parallel simulations have been described, but real time executions are still out of reach [3]. In this paper, we describe electronic parallel architectures which perform very fast stochastic relaxation thanks to optical random number generators.

Stochastic relaxation for low level image processing.

The use of stochastic relaxation for low level image processing is sketched hereafter ; more detailed descriptions are given by [2] and [4]. The low level task we want to perform is defined as an optimization problem to which simulated annealing can be applied. For that purpose we model pictures as the states of some two-dimensional physical system : we choose some finite square lattice S, and we suppose that the state of each site s in S belongs to some finite set Q. According to the low level task to be performed, these states can be considered as intensity values, as labels or both. Then we choose some energy E (L) on the (intensity, label) space such that the low level task can be defined as follows : given some observed picture O, compute some label picture L which minimizes E (L). This energy is hand tuned to hardwire some a priori knowledge on the relationships between observations and labels (such as noise, linearities, ...).

The optimization process itself is derived from simulated annealing and several dynamics have been proposed : Metropolis, Heat Bath and Glauber. In the Metropolis dynamics ([1], [4]), a site s is randomly chosen (with a uniform distribution over the lattice S), and its state q is changed according to the following rule : choose at random a new state q' (with a uniform distribution over the set Q), compute the energy variation $\Delta E = E(L_{q'}) - E(L_q)$ it produces, and give the site s the state q' either if ΔE is negative or if some coin tossing with probability $\exp(-\Delta E)$ gives a positive result. Alternatively in the Heat Bath dynamics [2], one gives the site s the state q' if some coin tossing with probability $1/(1 + \exp(-\Delta E))$ gives a positive result, whatever the sign of ΔE. The Glauber dynamics of [2] is not developped here. In all cases, the computation burden is rather heavy and a large number of iterations is required, depending on the chosen annealing schedule. We give some examples in the applications section.

The processor architecture.

We describe the design of some massively parallel electronic architectures well suited to low level image processing through stochastic relaxation. Moreover they rely on

[1]Abstract submitted to I.C.O. Topical Meeting on Optical Computing, Aug. 29 - Sept.2rd, 1988, Toulon

full custom very large scale integration, and are intended to fit in as few chips as possible, ideally in a single chip.

We have suggested in [6] an optical random number generator which delivers random numbers to a monolithic processor array at a very high throughput. An optical system is built in front of the processor array, and projects a speckle image on a photodiode array ; this speckle picture is sampled by the processors to get a random sample array in parallel. Moreover the specifications of the system have been studied to avoid spatial or temporal correlations. [7] This optical random number generator combines chip surface economy and very high throughput.

We have designed a monolithic processor array to profit of these optically generated random number arrays. Two slightly different schemes are possible, according to the chosen dynamics : one for Metropolis, the other for Heat Bath. We give here their common features. This parallel machine is built out of a large number of very small Processor Elements (PE). It is of SIMD type, i.e. all PEs execute the same instruction at each instant, and all the PE work in a bit serial way. These PE are connected in a mesh thanks to a quadridirectional shift register, providing neighborhood access for any local computation. In order to result in a sensible PE size, an attractive restriction, as far as hardware complexity is concerned, is to restrict ourselves to the relaxation of binary label pictures. Thus the memory requirements are clearly reduced. Moreover Heat Bath and Glauber dynamics define the same algorithm in this case, and the computation requirements of each iteration are reduced to energy variation evaluation, exponentiation and random number generation. These are performed thanks to an hybrid arithmetic unit, partly built out of analog devices. This mixed analog and digital implementation results in a fairly compact computation unit : a strictly digital implementation would increase the PE complexity by an order of magnitude at least, whereas the success of a strictly analog one would be questionable. Each PE finally has a photodiode in order to acquire some grey-level picture or to sample some random laser speckle patterns.

The overall PE fits in less than 100 transistors in a standard CMOS process. (figure 1) Its surface in a 2 μ 2 metals CMOS process is about 50000 μ^2, allowing a 32 x 32 processor array to fit in a 1 cm^2 chip. Its design has been functionnally and electrically simulated. A first prototype has been laid out and it has been submitted to a foundery in February 1988.

An application example.

Applications of binary pictures stochastic relaxation include digital halftoning and boundary sites relaxation. The latter is the stochastic equivalent of probabilistic relaxation, and yields higher quality boundary pictures from edge element pictures [8]. We develop here the former example of picture halftoning [4]. This process involves the encoding of the grey level information in the density of the white pixels of a binary picture, and can be considered as an approximation of an acquired grey-level picture A by a convolution by some fixed kernel K of its binary representation B. Furthermore one can measure the quality of this approximation through some distance between A and K * B, such as the quadratic distance $E(B) = ||A - K * B||^2$, hence suiting it for stochastic relaxation. Simulation results are given in figure 2.

Conclusion.

The described architectures take advantage of mixed analog implementations. They give successful examples of close cooperations between optical and electronic means to solve some computation limited problem.

References.

[1] Kirkpatrick S., Gelatt S.D., Vecchi M.P.
Optimization by simulated annealing
Science, 8, 67, 1983

[2] Geman S., Geman D.
Stochastic relaxation, Gibbs distribution and the Bayesian restoration of images
IEEE Trans. PAMI, Vol. 3, 1984, pp. 721-741
[3] Murray D.W., Kashko A., Buxton H.
A parallel approach to the picture restoration algorithm of Geman and Geman
Image Vision Computing, Vol. 4, N° 6, August 1986, pp. 133-142
[4] Carnevalli P., Coletti L., Patarnello S.
Image processing by simulated annealing
IBM J. of res. & Devlpt., Vol. 29, N° 6, Nov. 1985, pp. 569-579
[5] Garda P., Devos F. Zavidovique B.
Cellular hardware for a NCP based vision
3rd IEEE Workshop on CAPAIDM, November 17-20, 1985, Miami
[6] Devos F., Garda P., Chavel P.
Optical generation of random number arrays for on-chip massively parallel Monte Carlo cellular processors
Optics Letters, Vol. 12, N° 3, March 1987, pp. 152- 154
[7] Chavel P., Taboury J., Devos F., Garda P., Madani K.
Utilisation du speckle comme générateur rapide de tableaux aléatoires binaires : optimisation des paramètres
Annales des Télécommunications, March 1988

Figure 1 : Lena halftoned through stochastic relaxation. (3x3 neighborhood)

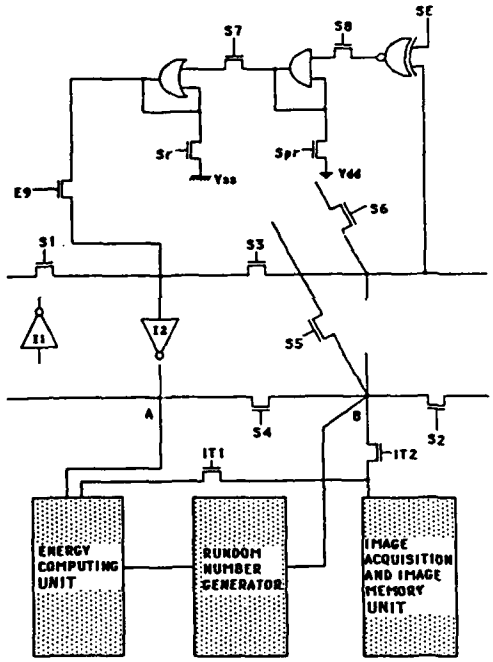

Figure 2 : Processing Element structure.

Computing on a Digital Optical Computer Using Regular Interconnections

Binay Sugla
AT&T Bell Laboratories
Holmdel, New Jersey 07733

Introduction

It is increasingly recognized that parallel processing is one of the most promising avenues to exploit the potential of the emerging optical technology. In the past several architectures based on symbolic substitution have been proposed for building a digital optical computer [1]. Using the idea of symbolic substitution, architectures using two dimensional arrays of logical bits communicating via regular interconnection methods have also been proposed. Since many of these architectures are truly novel the formidable task of establishing their computational feasibility vis-a-vis electronics remains to be demonstrated. Indeed some progress has been taken in that direction. Murdocca and Streibl [2] gave a design technique to implement a *serial* adder based on programmable logic arrays using only regular interconnects. Murdocca and Sugla [3] considered arbitrary (parallel /serial) boolean circuits and presented methods by which they could be implemented with little or no loss in depth. More recently, Murdocca and Sugla [4] designed a *random-access* memory using free space and regular interconnections only. These techniques do prove that *low* level operations can be performed in a reasonable manner on these machines. It is clear however, that in order to achieve realistic computations, architectures that assist in combining functions and their results in meaningful ways have to be devised.

This paper resolves the above mentioned computational issue by providing architectures and solutions which perform more complex computations. Specifically techniques and modifications to the regular interconnection architecture, that make the computing of an arbitrary sequence of operations feasible, are presented.

Mapping The Computation on to the modified Architecture

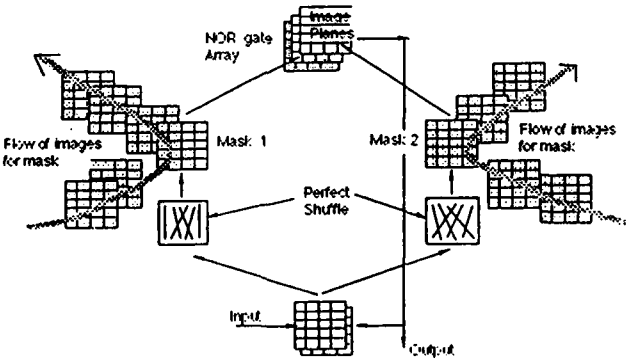

Figure 1. A modified digital optical computer based on the symbolic substitution. The input image is split into two, perfect shuffled, passed through the two masks and shone on the *NOR* gate array. A sequence of masks is accomplished by imaging a sequence of mask images onto the mask plane.

Consider the architecture shown in figure 1. It consists of modules of two dimensional array which are interconnected by a fixed interconnection network such as *perfect shuffle*. All gates require a fan-in and fan-out of at most two and in the following discussion all gates considered will have a fan-in and fan-out of at most two. Consistent with the notation of earlier research the boundary bits $e_{0,y}, e_{N+1,y}, e_{x,0}, e_{x,N+1}$ are assumed to be zero. Any bits imaged outside the array do not participate in the computation. An operation is enabled or disabled by putting the appropriate mask bits transparent or opaque. The logic array shown in the figure consists of *NOR* gates. The single *NOR* array may be replaced by arrays of *AND* and *OR*. Using this configuration it can be shown that a circuit consisting of *NOR* gates or *AND*,*OR* gates with inversion, with successive levels connected by perfect shuffle in space and time on to this architecture [2,3,4].

Let us consider the following example of a computation typical of a problem like matrix multiplication. Given a set of data values we are required to perform the a priori known sequence of operations $+,*,+,/,..,+$. Each of these isolated operations can be realized on this machine. Trying to compute an arbitrary sequence of operations however, poses several difficulties. One simple way to accomplish this is to dedicate a portion of the two dimensional array to each of the operation desired . Such a scheme however is not practical because of the large number of possible operations and/or sequences and the large number of gates that are required. An architecture and a mapping scheme which solves this problem efficiently is shown in figure 1.

The basic architecture requires that a pipeline of masks for the intervening mask be implemented. A sequence of masks can be accomplished by imaging a sequence of two-dimensional arrays on to the mask thus controlling the behavior of the masks. Corresponding to the sequence of operations the sequence of masks flows in a direction orthogonal to the direction of travel of the plane of data. This control pipeline then induces the mask to have desired behavior corresponding to the desired computation at the appropriate times.

The desired mask sequence is determined at "compile time" - before the computation begins. First a description of the masks implementing a standard function (e.g. addition) and description of the data placements of input and output are obtained using [3,4]. Two extra functions performing movement and duplication of data are then used to place the inputs for the next function correctly. The mask sequence of standard functions taken together with the mask sequence of these two functions turns out to be sufficient to realize any sequence of operations. For example, consider the computation $(a+b)*(a+b)$. In this architecture the computation proceeds as follows. First, the mask corresponding to addition is determined. Then the mask corresponding to duplication of data is calculated, followed by the mask for proper positioning of data for the next mask. Then the mask for multiplication is determined. Note that the mask sequence of standard functions need not be modified to accommodate the stringent requirements of data placement a sequence might impose. As the data circulates through the masks and perfect shuffle the control arrays for the masks are imaged on to the masks at the appropriate times. This then results in the computation of the desired value. A detailed example illustrating the technique will be presented in the full version of this paper.

Conclusion

This abstract presents a solution to the problem of computing an arbitrary sequence of operations on a digital optical computer based on symbolic substitution and regular interconnects making minimum demands on the optical technology. It may therefore be concluded that the architectures based on symbolic substitution are suitable for computing the class of problems whose sequence of operations is known at "compile time".

Acknowledgement This author appreciates the influence of Miles Murdocca and Alan Huang on this work.

REFERENCES

[1] K.H. Brenner, A. Huang, and N. Streibl, "Digital optical computing with symbolic substitution," *Applied Optics*, vol. 25, pp. 3054-3060 (1986).
[2] M. J. Murdocca, A. Huang, J. Jahns and N. Streibl, "Optical design of programmable logic arrays," *Applied Optics*, May 1988, to appear.
[3] M. J. Murdocca and B. Sugla, "Regular Interconnection Method and Memory Model for Free-Space Digital Optical Computing," unpublished manuscript.
[4] M. J. Murdocca and B. Sugla, "Design for an Optical Random Access Memory," submitted for publication to *Applied Optics*.

A RESIDUE NUMBER SYSTEM OPTICAL ADAPTIVE PROCESSOR

J.C. Bradley, E.C. Malarkey, P.R. Beaudet and G.E. Marx

Westinghouse Electric Corporation

Box 1521, Baltimore, MD 21203 (USA)

This is a summary of work that led to the design of an adaptive processor that uses residue arithmetic and digital optics to achieve adaptive beam nulling in less than two microseconds and is capable of handling up to four jamming signals.

The ratio of the signal to the jamming-plus-noise power is maximized by a vector of adaptive weights that is the solution of a linear algebraic system of equations expressed as the covariance matrix which operates on the unknown weight vector to produce the steering vector. The covariance matrix is the product of the Hermitian conjugate of the sample data matrix with this data matrix. The steering vector (a known quantity) is replaced by the product of the system determinant and itself to insure that integer weights are calculated; this is a requirement when using a residue number system (RNS). The final set of weights is obtained from this solution by multiplication of the integer weight vector by the inverse of the system determinant, and this step is executed outside the RNS. The order of the system is N=4.

We briefly describe the parallel-pipelined architecture necessary to achieve this goal in the steps enumerated below and conclude with discussions of timing, hardware requirements and the position encoded factored look-up tables (LUTs).

(1) The optical processor accepts 8-bit complex data in I and Q Gaussian (i.e., complex) data pairs on parallel input channels. The data flow into digital electronic RAM buffer chips where they are translated using position encoded LUTs from 8-bit binary numbers into factored residue values for each of four moduli.

(2) Gaussian integer residue data are fed in pairs into quadratic RNS (QRNS) encoders which perform calculations in half the number of operations required in complex arithmetic.

(3) Data are fed into a covariance matrix builder which performs vector inner products necessary to construct the full covariance matrix.

(4) Matrix elements are decoded back into Gaussian residues, scaled down to values commensurate with computational accuracy and base extended to a larger set of moduli that are necessary to meet the RNS dynamic range requirement. This extended base uses 8 Archimedean prime moduli for N=4. The process of base extension occurs in the mixed radix conversion (MRC) subprocessor which contains a multiplier-accumulator (M-A) for each modulus.

(5) Base extended results are re-encoded into a QRNS and fed to a Gauss Elimination subprocessor which triangularizes the covariance matrix (augmented with the steering vector). This subprocessor requires one M-A for each modulus

(6) The final integer weights are computed using backward substitution of the triangularized augmented matrix, and these results are decoded into Gaussian integers and finally into real and imaginary elements using MRC.

(7) The results, which contain more than 40 bits of binary accuracy at this juncture, are truncated to a more manageable 8- to 16- bit word length by means of an easily performed MRC truncation and then fed to a set of RAM output registers.

The total time elapsed from input of the first snapshot of a data batch to reporting the elements of the solution vector, called latency, is determined by the number M of time slices and the number N of degrees of freedom. For N=4 and M=8 a total of 354 clock cycles are required for the entire computation. For a clock rate of 200 MHz the latency is then 1.77 μsec.

Eight prime moduli sufficient for use in the base extended format described above are 13, 29, 37, 41, 61, 73, 89 and 181. The processor using these moduli requires a total of 20 M-A tables together with 4 additional add tables.

RNS computations would be seriously limited if factorization of the LUTs was not employed. LUTs were described in detail in a recent article of ours ("Residue Arithmetic Techniques for Optical Processing of Adaptive Phased Array Radars," Appl. Opt. 21, 3097, 1986). A modulo p add or multiply LUT requires 2p detectors (Ds) and p^2 laser diodes (LDs). The "factorization" we refer to uses the factorization of the multiplicative group of modulo p multiplies to reduce the size of tables required. For example, 122 Ds and 3721 LDs are required in the construction of a modulo 61 multiply table, and, in the factored form, this table is replaced by a 3x3, a 4x4 and a 5x5 table and requires $2\cdot(3+4+5) = 24$ Ds and $3^2+4^2+5^2 = 50$ LDs for non-zero multiplies and an additional component of each type for operations involving zero.

A modulo 61 M-A that makes full use of table factorization has been built and operated at 200 MHz. Experimental results obtained with this device will be discussed at the meeting.

In conclusion it is worth noting that the basic mathematics involved in this optical computer embodies an RNS Gauss Eliminator that can be used for solving general algebraic systems of equations.

Friday september, 2, 8.30

SESSION 11 (Chairman B.H. SOFFER)

PARALLEL PROCESSORS
PROCESSEURS PARALLELES

K3 - Y. ICHIOKA : Optical parallel array logic system.

K4 - T. KUROKAWA AND S. FUKUSHIMA : Real-time image processing based on optical array logic.

K10 - J. TABOURY, C. CHAUVE and P. CHAVEL : An optical approach to lattice gas automata.

K11 - K.S. HUANG, A.A. SAWCHUK, B.K. JENKINS, P. CHAVEL, J.H. WANG, A.G. WEBER, C.H. WANG and I. GLASER : Implementation of a prototype Digital Optical Cellular Image Processor (DOCIP).

K12 - M.M. ESHAGHIAN, V.K. PRASANNA-KUMAR and H.I. JEON : Massively parallel architectures with optical interconnection networks.

OPTICAL PARALLEL ARRAY LOGIC SYSTEM

Yoshiki Ichioka

Department of Applied Physics, Faculty of Engineering,
Osaka University, Suita, Osaka Japan

The Optical Parallel Array Logic System (OPALS) is a parallel optical digital computing systems using the concept of optical array logic. Its salient features are the capability of implementing fully 2-D parallel logic operation, and parallel neighborhood operation, programmability, the capability of iterative processing, and separability into modules.

In this paper, we describe optical array logic and realizable versions [1-4] of OPALS's. Then we demonstrate capability and programmability of the OPALS through experimental results of parallel 2-D digital processing.

Optical Array Logic

Optical array logic is a technique to implement any parallel neighborhood operation using techniques of image coding, 2-D correlation, sampling, and logical sum. Optical array logic can achieve parallel neighborhood logical operation, or cellular logic for 2-D binary images.

Figure 1 shows the processing procedures of optical array logic. Its processing principle is the same as that of array logic in electronics except for the parallelism. Two binary input images consisting of N X N pixels are spatially coded and converted into a coded image. N^2 logical operations are concurrently executed for a coded image. An operation for the specific pixel is expressed by the logical sum of several product terms and by a product term operation and OR operation. A product term operation is carried out by 2-D correlation of a coded image and an operation kernel followed by a coding process. The decoding process cosists of spatial sampling and thresholding. The parallel OR operation for the decoded signals provides the result of the given operation. In optical array logic, the type of an operation is established by the combination of operation kernels selected.

Construction of OPALS

Optical array logic is a technique implementing parallel processing of two input and one output 2-D signals. Feeding the output signal back to the input part as one of the input signals in the following

processing of output signals, and feedbacking of an intermediate processed result are performed by electronic techniques.

In the pure optical version of OPALS, a dynamic coding method using spatial light modulators and a dynamic optical correlation technique using a multi-focus imaging system are utilized. The 2-D S-R type flip-flop and D type flip-flop to be developed in future are required to execute the sequence of product term operations or to carry out iterative processing.

The modularized OPALS can be constructed from several functional modules : mixing/distributing, encoding, correlation, and decoding modules. The encoding module is opt-electronic devices integrating PDs and LEDs for pixel-divided processing, which can be fabricated by LSI technology. 2-D array of pixel processing elements is easily composed by increasing the number of the element module. The correlation module performs the real-time 2-D correlation for optical array logic.

The birefringent OPALS is a kind of pure optical version of OPALS using the principle of the birefringent encoding. The birefringent encoding is a parallel and space-variant image coding method, referring to the principle of a digital light deflector [5] and polarization logic [6]. Advantages of birefringent encoding are simplicity, stability, parallel nature, and light power efficiency.

We have already constructed experimental systems of the electro-optical version of OPALS and the birefringent OPALS.

Parallel Processing Executed by the OPALS

In order to demonstrate the capability and programmability of the OPALS as a parallel digital computing system, some simulation experiments have been attempted. We first proved that the OPALS has the fundamental functions as a digital computer through the experiment realizing the Turing machine. Then we have written the program for executing parallel numerical calculations (parallel addition or parallel binary multiplication) on the OPALS. We also attempted to make parallel digital image processing on the OPALS.

Figure 3 represents the experimental result for searching for the right path in a maze. The processing for one iteration can be achieved by five steps of product term operations and a OR operation. After 13 iterations, the desired result is obtained.

On the OPALS, operations for parallel processing are programmed in optical array logic and the program can be optically carried out. This programmability offers flexibility for optical parallel processing.

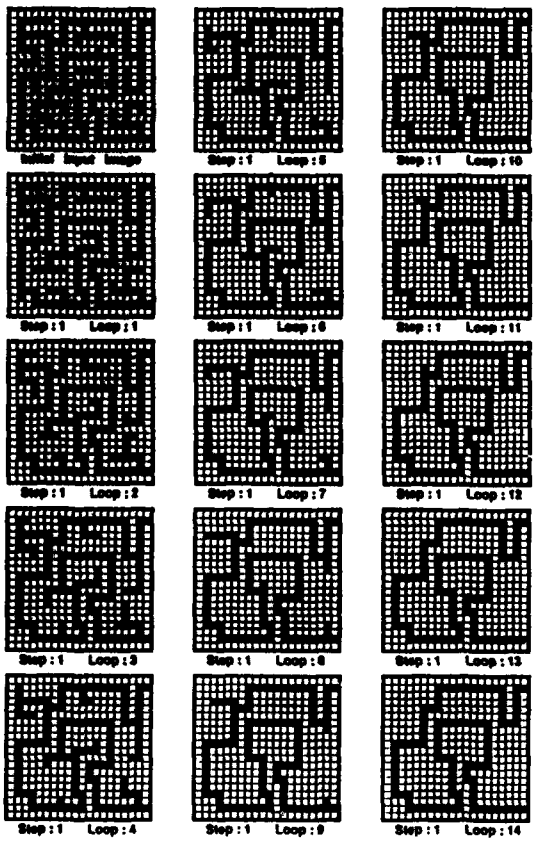

Fig.3 Simulation result searching for the right path in a maze.

References

1. J.Tanida and Y.Ichioka, Appl.Opt. 25, 1565 (1986).
2. J.Tanida and Y.Ichioka, Appl.Opt. 25, 3751 (1986).
3. J.Tanida and Y.Ichioka, Appl.Opt. 26, 3954 (1987).
4. J.Tanida and Y.Ichioka, "Birefringent optical logic processor," in Technical Digest, XVI International Conference on Quantum Electronics, Tokyo (1988).
5. W.Kulcke, et al. "Convergent beam digital light deflector," in Optical and Electro-optical Information Processing (Ed.J.T.Tippett, et al, M.I.T. press, Cambridge, (1965).
6. A.W.Lohmann and J.Weigelt, Appl.Opt. 26, 131 (1987).

REAL-TIME IMAGE PROCESSING BASED ON OPTICAL ARRAY LOGIC

Takashi KUROKAWA and Seiji FUKUSHIMA
NTT Opto-electronics Laboratories
3-1, Morinosato wakamiya, Atsugi-shi, Kanagawa, 243-01 Japan

1. Introduction

Recently, considerable interest has focussed on optical computing because of its inherent massive parallelism. A number of optical pattern logic operations, such as optical array logic[1] and symbolic substitution,[2] have been proposed for performing digital computations and image processing. Note that neither of these systems can be operated or programmed in real-time. The main problems in developing a flexible real-time processor are how to encode input data in real-time and how to control the optical gates dynamically.[3]

In this paper, we propose a method of real-time encoding and programming based on optical array logic using an electro-optic effect and stripe-structured analyzers. Input images are encoded as symbolic light patterns in pixels and switched with an optical gate matrix, according to instruction signals. In addition, a real-time programmable image processor that uses liquid crystal (LC) panels is demonstrated.

2. Principles of Real-time Encoding and Programmable Operation

A schematic diagram of the proposed processing principle is shown in Fig. 1. Two binary input data, A and B, are encoded to the coded logic pattern in which a quarter of the cell is transparent, corresponding to the combinations of input data values. Some of these coded logic patterns are selected through a optical gate matrix according to the given instruction signal.

Polarisation rotation in a twist nematic LC and stripe-structured analyzer are used to encode the input data. When the bias voltage is not supplied to the LC1 layer in the signal ' 0 ' input pixel, the polarization of the transmitted light through the layer is rotated by 90°, and vice versa. Analyzer A1 has a horizontal stripe structure and its polarizations of every other line are orthogonal. Thus, the transmitted light from polarizer P to A1 via LC1 is modulated to the horizontal stripe, as shown in Fig. 2. In the case of LC2 and A2, the transmitted light is modulated vertically. As a result, one of the four subcells becomes transparent according to the input combination of the two binary data. External image data are input to the LC layer electrically, but also optically using liquid crystal light valves. Furthermore, other electro-optic materials with even faster response times can be used instead of LC layers. The optical gates of the last LC panel, LC3, can select the encoded patterns according to the instruction signals applied to the panel. The transmitted light dynamically processed in parallel indicates the output logic operation.

3. Real-time Image Processing

The image processor was constructed by using LC panels, as shown in Fig. 3. Binary images read by CCD cameras were transferred into LC1 and LC2. Optical gate panel LC3 was controlled by instruction signals from a pattern generator. All LC panels and analyzers were stacked together. Encoding and programming was then performed optically in parallel. The only role of electronics is to input NTSC image signals into the LCs. The image processing results are shown in Fig. 4. (a) is a coincidence operation between the two input images, and (b) is a contour extraction, in which the same image was input into LC1 and LC2, but was shifted by one pixel horizontally and vertically by aligning two CCD camera positions. The contour of the original 'triangle pattern' was obtained through an exclusive-OR operation. This compact image processor can optically perform various kinds of image processing at video rates.

4. Conclusion

A real-time encoding and programming method based on array logic have been proposed by using a polarisation rotation in an electro-optic effect and stripe-structured analyzers. We have demonstrated a programmable image processor which performs several operations at video rates. This system could be readily extended to execute much faster processing by using optical access spatial light modulators.

References

1 . Y. Ichioka and J. Tanida: Proc. IEEE 72, 787 (1984).
2 . K. H. Brenner, A. Huang and N. Streibl: Appl. Opt. 25, 3054 (1986)
3 . S. Fukushima and T. Kurokawa: Opt. Lett. 12, 965 (1987).

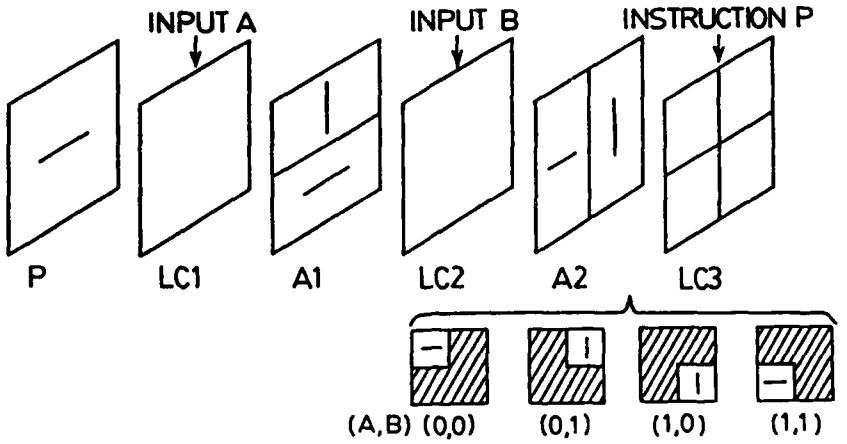

Fig. 1 Schematic diagram of optical processing in a pixel.

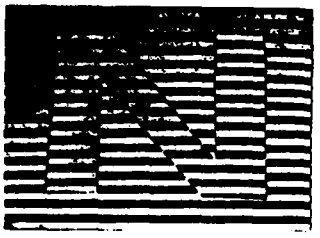

Fig. 2 Horizontally coded pattern for an input image.

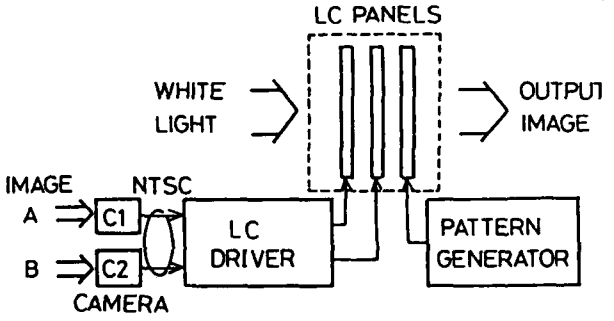

Fig. 3 Configuration of programmable image processor.

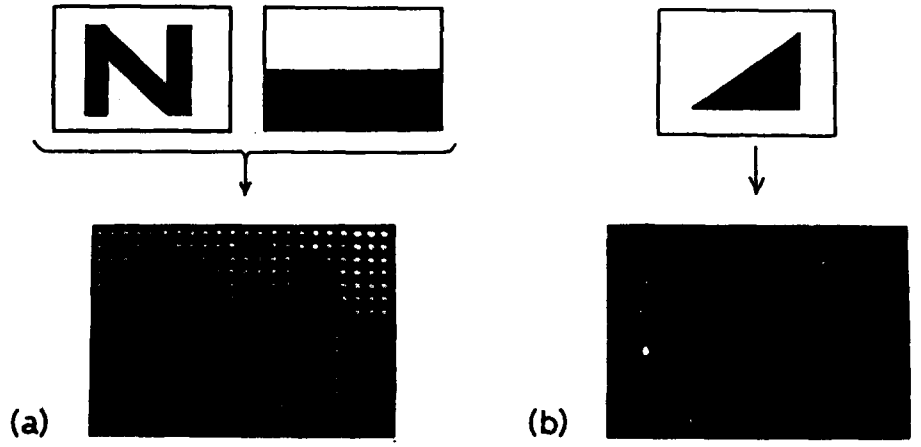

Fig. 4 Image processing results. (a) coincidence operation. (b) contour extraction.

AN OPTICAL APPROACH TO LATTICE GAS AUTOMATA

Jean Taboury, Catherine Chauve and Pierre Chavel.
Institut d'Optique (laboratoire associé au C.N.R.S.)
Université de Paris-Sud, B.P.43, 91406 ORSAY cedex, France.

Introduction.

Optical computing using non-linear devices interconnected through free space is an attractive alternative to electronics. Common approaches are derived from imaging and shadow casting (1). Both techniques give rise to systems dedicated to mainly digital processors such as symbolic substitution automata (2) and boolean automata (1,3).

Hereby we propose an implementation of a symbolic substitution automaton in an optical shadow casting approach. Using an hexagonal lattice gas automaton as illustration, we show that space parallelism and adequate timing sequences could be combined with bistable and other non-linear devices into a powerful optical machine.

Lattice gas cellular automata.

It has been shown that discrete boolean elements arranged in a triangular 2D lattice simulate succesfully the Navier-Stokes equations (4). Optical symbolic substitution are suitable for the deterministic collision rules used in such algorithms.

Each site of a triangular 2D lattice consists of an hexagonal pattern whose binary state encodes the presence of incident particules before collision occurs. A fixed particule may be present at the center of the hexagon (fig. 1). Finally, compliance with conservation rules leads to introduce an eighth pixel with a random binary state.

A maximum of 2^8=256 different binary patterns may be simultaneously present within the 2D lattice for a given iteration. In fact, not as many are useful. A time sequential analysis of all meaningful patterns must be tested in parallel over the lattice and then substituted in parallel according to a lookup table. After that each result is stored in a memory data plane before the next iteration. The optical memory plane could be a bistable device.

Optical implementation.

The principle of each binary pattern analysis can be summarized as a symbolic substitution (fig. 2).

1) A set of 8 LEDs (7+1) suitably arranged in a triangular lattice, encodes all the requested collision patterns P and illuminates simultaneously all hexagonal sites of the input lattice. The seven

beams passing through the pixels encoding a local collision situation separately test the presence or the absence of a particule with a proper velocity vector. If pattern P matches the local situation, no light illuminates a mask M located behind the hexagonal site in a place where the 7 beams geometrically overlap. The mask consists of a triangular 2D lattice of pinholes. Using polarization to encode data it is possible to recognize a given match pattern in one step (5).

2) An appropriate spatial light modulator implementing the NOR boolean fonction placed in the mask plane allows to produce bright spots at the sites where P has been recognized.

3) A second set of 7 LEDs encoding the substitution pattern P' according to the lookup table illuminates sites of the nonlinear device output plane so that the spatial light modulator reflects (or transmits) the 7 beams only if P has been recognized. Each beam illuminates only one pixel of the neighboring hexagonal sites of the triangular 2D output plane in which a data memory plane has been placed. It is important to note that the substitution must, on the one hand preserve the number of incident particules and, on the other hand implement the translation occuring between two iterations.

Photographic experimental results will be presented illustrating the three setps above. With adequate SLMs, this experiment shows the potential for a meaningful and powerful specialized optical processor.

We acknowledge stimulating discussion with F. Devos and P. Garda.

References.

1) Y. Ichioka and J. Tanida.
Proc. of the IEEE 72, 787-801, (1984).
2) K.H. Brenner.
Appl. Opt. 25(18), 3061-3064, (1984).
3) A.W. Lohmann and J. Weigelt.
Appl. Opt. 25(18), 3047-3053, (1986).
4) U. Frisch, B. Hasslacher and Y. Pommeau.
Phys. Rev. Let. 56,1505-1508, (1986).
5) J. Taboury, J.M. Wang, P. Chavel, F. Devos and P. Garda.
Appl. Opt. 1st may 1988.

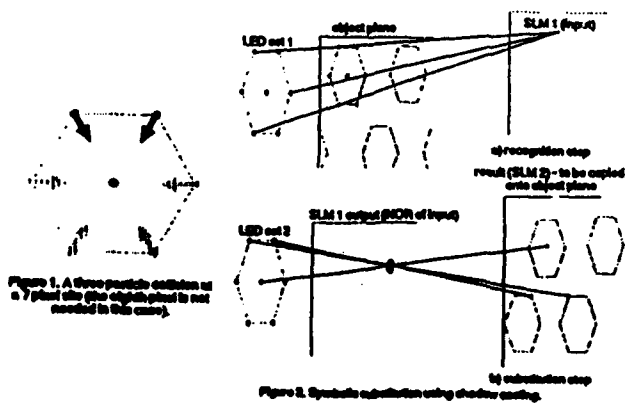

Implementation of A Prototype Digital Optical Cellular Image Processor (DOCIP)

K. S. Huang, A. A. Sawchuk, B. K. Jenkins, P. Chavel*, J. M. Wang*, A. G. Weber, C. H. Wang, I. Glaser

Signal and Image Processing Institute, Department of Electrical Engineering,
University of Southern California, Los Angeles, CA 90089-0272, USA

*Institut d'Optique, Laboratoire Associé au CNRS,
Université de Paris Sud, BP43, 91406 Orsay cedex, FRANCE

Summary

Digital optical cellular image processor (DOCIP) architectures, DOCIP-array and DOCIP-hypercube, can perform the tasks of parallel binary image processing and parallel binary arithmetic [1]. The use of optical interconnections permits a cellular hypercube topology to be implemented without paying a large penalty in chip area (the cellular hypercube interconnections are space-invariant which implies relatively low hologram complexity); it also enables images to be input to and output from the machine in parallel. Table 1 gives a comparison of three different interconnection networks: cellular array (DOCIP-array interconnection network), conventional hypercube, and cellular hypercube (DOCIP-hypercube interconnection network). In this paper we experimentally demonstrate the concept of the DOCIP architecture by implementing one processing element of a prototype optical computer including a 49-gate processor, an instruction decoder, and electronic input/output interfaces.

A multiple-exposure multi-facet interconnection hologram provides the fixed interconnections between the outputs and the inputs of an array of 7×7 optical gates. The input data and the instructions are supplied from an LED array. The outputs of optical gates are detected by a video camera and compared with the results of a software simulation. A diagram of the main components of this experimental system is shown in Fig. 1.

A space-variant interconnection system [2] for within-processor interconnection is used in this experimental demonstration. A computer controlled system is used to make an array of 49 interconnection subholograms. An optical point source S, whose position is controlled by the mirror M2 with two rotational stages (Fig. 1), is used to provide an object beam for determining an interconnection of a subhologram in the multi-facet hologram. A mask with a circular aperture, controlled by two translational stages, is used to determine the sizes and positions of subholograms in a holographic plate. The interconnection hologram for this 49-gate optical processing element comprises 49 subholograms, which are laid out in a 7×7 array. Each subhologram covers a circular area with a diameter of 1.5 mm. The spacing between the centers of two subholograms is 3.0 mm. Note that the path of the object beam and the mask for subholograms are only used for making the interconnection hologram; they are blocked or moved when we reconstruct the hologram to implement the interconnections of the optical gates. We use a volume phase hologram with a dichromated gelatin medium for obtaining high diffraction efficiencies.

The array of 7×7 optical gates is implemented by a Hughes liquid-crystal light valve (LCLV) with liquid-crystal molecules in a 45° twisted nematic configuration [2]. The LCLV is read out between crossed polarisers and is biased to implement a NOR operation. The gate size in this experiment has a diameter of 0.3 mm and the spacing between the centers of two gates is 0.6 mm.

The circuit diagram of the processing element, as shown in Fig. 2, consists of 49 NOR gates with maximum fan-in of 3 and fan-out of 4. The processing element includes a 3-bit destination selector, a 3-bit master-slave flip-flop memory, a 6-bit memory selector with a union module, and a 5-bit neighborhood selector (for DOCIP-array4 [1]) with a dilation module. This experimental DOCIP system has one instruction, supplied from an LED array and decoded by the optical hardware. This instruction has the format: $(c, d_1, d_2, d_3, s_1, s_2, ..., s_6, n_1, n_2, ..., n_5)$ where c selects the image from the input or from the feedback; d_1, d_2, and d_3 select the destination memory for storing the image; $s_1, s_2, ..., s_6$ select the output from the memory elements; and $n_1, n_2, ..., n_5$ control the neighborhood mask, i.e. supply the reference image. We will experimentally demonstrate the DOCIP architecture concept with this system.

References

[1] K. S. Huang, B. K. Jenkins, A. A. Sawchuk, "Binary Image Algebra and Optical Cellular Logic Processor Design," submitted to *Computer Vision, Graphics, and Image Processing*; K. S. Huang, B. K. Jenkins, A. A. Sawchuk, "An Image Algebra Representation of Parallel Optical Binary Arithmetic", submitted to *Applied Optics*.

[2] A. A. Sawchuk and T. C. Strand, "Digital Optical Computing," *Proc. IEEE*, Vol.72, pp. 758-779,1984; B. K. Jenkins, et al, "Sequential Optical Logic Implementation," *Applied Optics*, Vol. 23, No. 19, pp. 3455-3464, 1984; B. K. Jenkins, et al, "Architectural Implications of A Digital Optical Processor," *Applied Optics*, Vol. 23, No. 19, pp. 3465-3474, 1984.

Acknowledgements

The authors thank W. Kressen, K. Prager and T. Mayeda for their contributions to this work. This research was supported by the Air Force Office of Scientific Research under grant AFOSR-84-0181 and by an IBM graduate fellowship.

Interconnections	Cellular Array	Conventional Hypercube	Cellular Hypercube
Connectivity (Interconnections per PE)	O(1)	O(logN)	O(logN)
2-D Spatial Invariance	Yes	No	Yes
Inter-PE Communication Time Complexity	O(N)	O(logN)	O(logN)
VLSI Chip Area	$O(N^2)$	$O(N^2)$	$O(N^2)$
Hologram Space-bandwidth Product	$O(N^2)$	$O(N^2 \log N)$	$O(N^2)$

Table 1. A comparison between three different interconnection networks of NxN processeng elements (PEs): cellular array, conventional hypercube and cellular hypercube. When laid out on a VLSI chip, both the conventional hypercube and cellular hypercube pay a large penalty in chip area while the cellular hypercube has a relatively low hologram complexity.

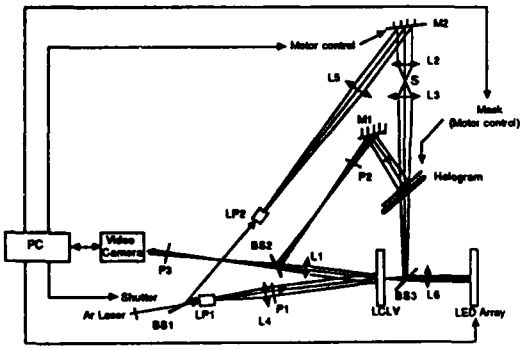

Figure 1. Experimental DOCIP system. Lens L1 images from the LCLV gate output plane to the hologram plane. Beam Splitter BS3 combines the external input signals from LED array and the feedback signals from interconnection hologram. LP1 and LP2 are lens-pinhole assemblies. P1 and P2 are crossed polarizers. The hologram comprises an array of subholograms. Mirror M2 controls the position of point source S during hologram exposure. After the hologram is made, the mask and all components in the path from BS1 to the hologram are not needed.

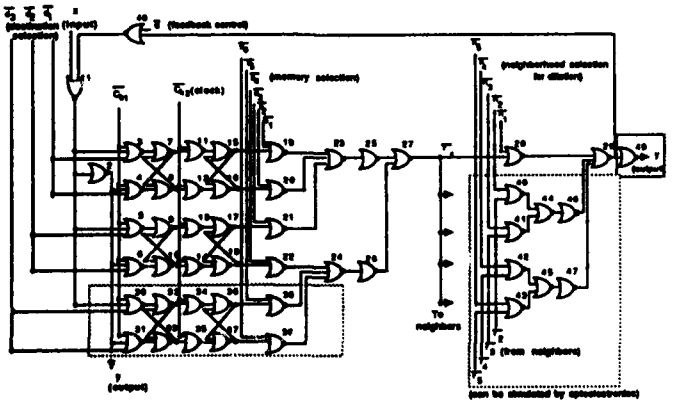

Figure 2. The circuit diagram of a 49-gate processing element of the DOCIP-array4.

Massively Parallel Architectures with Optical Interconnection Networks *

Mehrnoosh Mary Eshaghian and V. K. Prasanna-Kumar
University of Southern California
Ho-in Jeon
University of Alabama in Huntsville

Abstract

We derive the computational limits of optical technology using a proposed model, and present parallel architectures for implementing it. We show the superiority of the unit delay optical interconnection network of these designs by presenting efficient algorithms for many problems in image processing and AI.

1. Introduction

Recently, there have been many parallel algorithms designed based on a theoretical shared memory model, the Parallel Random Access Machine (PRAM), in which a unit delay interconnection network is assumed. Using electronic technology, simulation of such an interconnection network will lead to an $O(\log N)$ time loss. In this paper, we will focus on this issue and propose possible realizations of such a unit-time interconnection network using optical technology. We start by developing an abstract optical model of computation and in section 3, we propose three possible implementations of this model. In the last section, we present efficient parallel algorithms for several problems in image processing and AI using these architectures.

2. An Optical Model of Computation

In this section, we introduce an abstract optical model of computation to explore speed size relationship in using free space optical beams, as opposed to wires, as means of interprocessor communication. This model closely captures currently implementable optical network of processors. So the derived lower bounds on its computational efficiency gives us a tool to analyze the optimality of various physical implementations of the proposed model in solving problems.

Definition: An optical model of computation represents a network of N processors each associated with a deflecting unit capable of establishing direct optical connection to any other processor.

In the full version of the paper, we derive bounds on the computational efficiency in using such an optical model. While due to limitations on the number of layers of a VLSI chip, implementing a three-dimensional VLSI model of computation is not possible in current technology, we have shown that such bounds can be obtained using an optical model of computation which is implementable.

3. Parallel Architectures

In this section, we present a class of optical interconnection networks to realize the optical model of computation presented in the previous section. Each of the proposed designs uses a different optical device technology for redirection of the optical beams to establish a new topology at any clock cycle.

3.1 Optical Mesh In this design, there are N processors on the processing layer of area N. Similarly, the deflecting layer has area N and holds N mirrors. These layers are aligned so that each of

* This research was supported in part by the National Science Foundation under grant IRI-8710836 and a grant from TRW.

the mirrors is located directly below its associated processor. A connection phase consists of two cycles. In the first cycle, the processor sends the destination address of the processor it wants to connect to, to the mirror associated with it using its laser directed up ward. After receiving the address, the arithmetic unit of the mirror computes a rotation degree to create a position such that both the origin and destination processors have equal angle with the line perpendicular to the surface of the mirror in the plane formed by the mirror, the source processor and the destination processor. Once the angle is computed , the mirror is rotated to the desired destination. At this time, in the second cycle, connection is established between the source and the destination processor. However, note that since the connection is done through a mechanical movement of the mirror, with the current technology this leads to an order of millisecond reconfiguration time.

3.2 Optical Linear Array In this organization, N processors are arranged to form a one-dimensional processing layer and the corresponding acoustic optics devices are similarly located on a one-dimensional deflecting layer. Similar to the design using the mirrors, every connection phase is made up of two cycles. In the first cycle, the processor sends the destination address of the processor to which it wants to connect to, to its associated acoustic optic cell using its laser beam. The acoustic optic cell's arithmetic unit, after receiving that address, computes the angle and phase of the wave to be generated inside the crystal to redirect the beam to the destination processor. As the wave moves upwards through the acoustic optic device, the beam gets redirected and the desired connection is established. In this architecture the reconfiguration speed is dominated by the speed of sound wave which is in the order of microseconds.

3.3 Electro Optical Crossbar This design uses a hybrid reconfiguration technique for interconnecting processors. There are N processors each located in a distinct row and column of the $N \times N$ processing layer and for each processor there is a hologram unit having N cells, such that the ith cell has grating angle corresponding to the processor located at the grid point (i,i). To establish or reconfigure to a new connection pattern, each processor broadcasts the address of the desired destination processor to all N cells of its hologram unit via its associated electrical bus. A cell is activated if the broadcast address matches the ID of its only accessible processor. Therefore, since the grating angles are predefined, the reconfiguration time of this design is bounded by the electrical to opitcal signal conversion time, which is in the order of nano-seconds using Gallium Arsenide technology.

4. Implementing Parallel Algorithms

An important property of the proposed networks is that any processor can communicate with any other in one unit of time. This leads to significant improvement in time complexity of parallel algorithms for many problems with irregular communication needs such as those arising in implementing AI problem solving techniques. As an example, we present an efficient implementation of production systems. We also illustrate the suitability of optical mesh for image processing by showing fast optimal parallel algorithms for many tasks in low to medium level vision such as, labeling figures, finding the convex hulls, determining distances, etc.

5. Conclusion

We have established a theoretical foundation for optical parallel processing by developing an optical model of computation, parallel architectures implementing this model, and efficient parallel algorithms. Our results substantiate the preference of optical medium over electronic medium as a means of interprocessor communication.

Friday september, 2, 10.45

SESSION 12 (Chairman B. WHERRETT)

PARALLEL PROCESSORS
PROCESSEURS PARALLELES

R4 - P.S. GUILFOYLE : General purpose optical digital computer.

OPTICAL PROCESSING CONCEPTS
CONCEPTS DE TRAITEMENT OPTIQUE

C5 - B.K. JENKINS and C.L. GILES : Superposition in optical computing.

C6 - S.D. SMITH, A.C. WALKER, M.R. TAGHIZADEH, I.R. REDMOND and B. ROBERTSON : The optical wiring of photonic digital processing arrays for optical computing.

General Purpose Optical Digital Computer

P.S. Guilfoyle
OptiComp Corporation
PO Box 10779
310 Dorla Court, Suite 210
Zephyr Cove, Lake Tahoe, NV 89448

Abstract

Previous optical computing schemes offered analog or quasi-digital accuracies with a single fixed primitive. This paper describes how programmable, arbitrary bit length all digital Central Processing Unit (CPU) computations are now possible. In addition, the current state-of-the-art in optical computer subsystem devices such as acousto-optic modulators, detector and source arrays, posture this architecture as a revolutionary technology in and of itself, as it may be applied to an implementation plethora.

Technical Summary

Our research has produced a new class of optical computing architecture — a general purpose digital optical computer of *arbitrary* bit length. Shannon's theorem on general purpose digital computation states that all digital logic functions can be represented by two sets of equations. The first set takes the input data vector represented by bits x_1 through x_n and combines the bits in such a way to produce k output combinatorial functionals f_1 through f_k. Note that f_1 through f_k represent the logical/Boolean "multiplication" or "AND"ing of any combination of x_1 through x_n. These inputs, x_1 through x_n, are represented in "dual rail" format, i.e. both x_i and its complement (shown with a bar over them) are available. We shall refer to this first step as the combinational "AND"ing of the arbitrary input data vectors.

The second step in Shannon's generalized formulation is to take these arbitrary combinational functionals and produce arbitrary combinational summations. Inputs to the second step are the outputs from the first step above, i.e., the combinational "AND" products f_1 through f_k. These are then "OR"ed or Boolean summed as shown in arbitrary dual rail form. The equivalent function of $\overline{f_a}$ can be realized at worst as a sum of only f_m (high true) functionals.

To facilitate the selection of the appropriate terms in both sets of equations, control selection logic must be used on the dual rail input data before either of Shannon's equations can be realized. Consider the optical matrix/vector computing architecture shown in figure 1 titled Fixed Program Flash N bit CPU. This architecture utilizes the three dimensional capability of optical computing. The input source data vector is input in dual rail format to the input source array. This vertical input vector parallel illuminates a control operator plane which consists on α, N bit control sequences. In parallel all combinatorial functionals, f_1 through f_α (α could equal k if desired) are available simultaneously at the output detector array. Consequently the system is computing microcoded combinatorial functionals in parallel.

This architecture can be represented as a Boolean logic matrix/vector multiplication which produces all of the combinatorial output functionals f_1 through f_k. The only difference between this matrix vector formulation and one use commonly in mathematics is that the inner product summation terms are actually threshold detections, Booleansummations, or "OR"ings. The only precision that is needed is binary, i.e. 1 or 0. The maximum inner product answer is 1. However the effect is to have multiple parallel

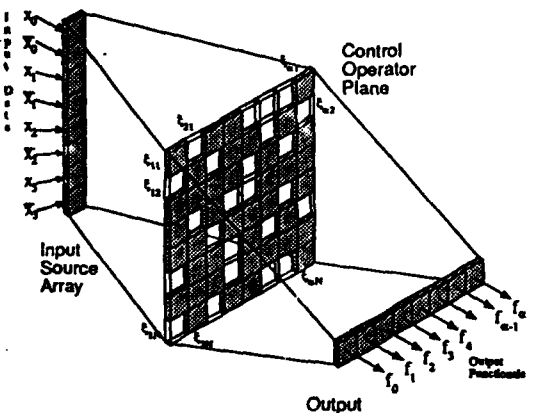

Figure 1: Fixed Program Flash N bit CPU.

$$\begin{bmatrix} \xi_{11} & \xi_{12} & \cdots & \xi_{1N} \\ \xi_{21} & \xi_{22} & \cdots & \xi_{2N} \\ \vdots & \vdots & & \vdots \\ \xi_{n-1,1} & \xi_{n-1,2} & \cdots & \xi_{n-1,N} \\ \xi_{n1} & \xi_{n2} & \cdots & \xi_{nN} \end{bmatrix} \begin{bmatrix} x_0 \\ \overline{x_0} \\ \vdots \\ x_{\frac{N}{2}} \\ \overline{x_{\frac{N}{2}}} \end{bmatrix} = \begin{bmatrix} f_0 \\ \overline{f_1} \\ \vdots \\ f_{n-1} \\ \overline{f_n} \end{bmatrix} = \begin{bmatrix} x_0\xi_{11} + \overline{x_0}\xi_{12} + x_1\xi_{13} + \overline{x_1}\xi_{14} + \cdots + x_{\frac{N}{2}}\xi_{1,N-1} + \overline{x_{\frac{N}{2}}}\xi_{1,N} \\ x_0\xi_{21} + \overline{x_0}\xi_{22} + x_1\xi_{23} + \overline{x_1}\xi_{24} + \cdots + x_{\frac{N}{2}}\xi_{2,N-1} + \overline{x_{\frac{N}{2}}}\xi_{2,N} \\ \vdots \\ x_0\xi_{n-1,1} + \overline{x_0}\xi_{n-1,2} + x_1\xi_{n-1,3} + \overline{x_1}\xi_{n-1,4} + \cdots + x_{\frac{N}{2}}\xi_{n-1,N-1} + \overline{x_{\frac{N}{2}}}\xi_{n-1,N} \\ x_0\xi_{n1} + \overline{x_0}\xi_{n2} + x_1\xi_{n3} + \overline{x_1}\xi_{n4} + \cdots + x_{\frac{N}{2}}\xi_{n,N-1} + \overline{x_{\frac{N}{2}}}\xi_{nN} \end{bmatrix}$$

Control matrix — Data vector — Output functional vector

input "AND" gates.

The control logic matrix shown in the above equation operating on the input data vector x_1 through x_n produces a ***complete set of combinatorial functionals***. The output is the first set of answers required by Shannon's theorem. These combinatorial output functionals can be "OR"ed to produce Shannon's second set of equations by (1) passing the functionals back through the optical system, (2) supplying the correct microcode for the second set of equations, and (3) ignoring DeMorgan's law, i.e. do not take the inverted output. This now represents what is commonly referred to as an *instruction*. It is thus possible by downloading the correct microcode stored in a memory subsystem, to program the machine to perform instructions. Different microcoded sequences will act on the data in different fashions thereby providing the user access to a ***microcode instruction set***. If this instruction set comprises a complete set of operations, a compiler code generator can be written for any desired higher level languages. *A fully general purpose optical computer can thus be realized.*

Hardware Implementation

This general purpose design methodology can be expanded and implemented in hardware. An architecture is shown which is an expansion of the above concept to a full parallel optical implementation using currently available of-the-shelf devices. The optical CPU consists of 3 planes of I/O. Rather than the first plane being a point source array as described above, it is replaced by a multi-channel acousto-optic spatial light modulator. Plane 2, formerly a fixed control operator plane, is replaced as well with a multi-channel spatial light modulator to allow matrices of instructions to be downloaded randomly under software control. Both input planes can be ultimately replaced with more sophisticated spatial light modulators if and when they are ever available. The output plane consists of a linear avalanche photodiode array driving an off chip electronic unidirectional shift register.

The two multi-channel acousto-optic devices act as counter propagating bit windows in a "convolver" mode. Consider for the moment the input data. Data is input word parallel. Successive data words from memory are down loaded time sequentially. First word is fed to the first multi-channel acousto-optic device. The number of bits fed to the cell is twice the word length to enable all bits and their complements to be input, i.e. dual rail operation. Therefore if a 16 bit CPU is desired, then a 32 channel acousto-optic cell is required for a single clock data cycle.

Two 32 channel acousto-optic devices be used in a parallel telecentric imaging configuration focused on an avalanche photodiode array of length 128. Using a 10 ns clock this will provide 100 million combinatorial equations per second. Partitioning the array into segments of length 16 will increase this throughput rate to 800 million combinatorial equations per second.

For additional information, the reader sould review reference [1]. which is the fourth of a series of papers describing combinatorial logic based optical computing methods. For furthur background information the reader is encouraged to review in addition references 2-4 cited below. Reference 5 describes the author's original transition architecture from analog to digital optical computing.

REFERENCES

[1.] P.S. Guilfoyle, "Programmable Optical Digital Computing," Proc. of the 21st Annual Asilomar Conference on Signals, Systems and Computers, Nov. 3, 1987.

[2.] P.S. Guilfoyle, W.J. Wiley, " Globally Folding Combinatorial Logic Cells in Digital Optical Systolic Computing Arrays," Proceedings of the 1987 2nd Topical Meeting on Optical Computing, Lake Tahoe, NV., March 1987.

[3.] P.S. Guilfoyle, W.J. Wiley, "Digital Optical Linear 3 x 3 Bit Combinatorial Systolic Multiplication Array," PROCEEDINGS OF THE SPIE, Real Time Signal Processing IX, Vol. 698-30, August, 1986.

[4.] P.S. Guilfoyle, W.J. Wiley,"Combinatorial Logic Based Optical Computing," PROCEEDINGS OF THE SPIE, Vol. 639-17, April,1986.

[5.] P.S. Guilfoyle, "Systolic Acousto-Optic Binary Convolver," OPTICAL ENGINEERING, vol. 23, Number 1, pg. 20-25, Jan./ Feb., 1984.

Superposition in Optical Computing

B. Keith Jenkins
Signal and Image Processing Institute
University of Southern California, Los Angeles, California 90089-0272

and

C. Lee Giles
Air Force Office of Scientific Research/NE, Bolling AFB, D.C. 20332-6448

SUMMARY

Fundamental differences in the properties of electrons and photons provide for expected differences in computational systems based on these elements. Some, such as the relative ease with which optics can implement regular, massively parallel interconnections are well known. In this paper we examine how the property of superposition of optical signals in a linear medium can be exploited in building an optical or hybrid optical/electronic computer. This property enables many optical signals to pass through the same point in space at the same time without causing mutual interference or crosstalk. Since electrons do not have this property, this may shed more light on the role that optics could play in computing. We will separately consider the use of this property in interconnections, memory, and gates.

Interconnections. A technique for implementing hybrid space-variant/space-invariant optical interconnections from one 2-D array to another (or within the same array) has been described [1]. It utilizes two holograms in succession, where the first hologram serves as an array of facets that each address facets in the second hologram. The superposition property allows many optical beams to pass through a facet in the second hologram, permitting many input nodes to effectively share the same routing "wire" to output nodes. This decreases the complexity (space-bandwidth product) of both holograms.

Using this as a model for interconnections in parallel computing, a comparison can be made between the complexity of these optical interconnections with those of electronic VLSI for various interconnection networks [2]. It is found that in general the optical interconnections have an equal or lower space complexity than electronic interconnections, with the difference becoming more pronounced as the connectivity increases. Also, a slight variation in a given network can further reduce the space complexity in the optics case. An example is a hypercube ($O(n^2)$ in VLSI, $O(n \log n)$ in optics) [2] vs. a 2-D cellular hypercube (twice as many connections, at least $O(n^2)$ in VLSI, yet $O(n)$ in optics).

Shared memory. The same superposition principle can be applied to memory cells, where many optical beams can read the same memory location simultaneously. This concept is useful in building a parallel shared memory machine.

For this concept, we consider abstract models of parallel computation based on shared memories [3]. The reason for this approach is to abstract out inherent limitations of electronic technology (such as limited interconnection capability); in designing an architecture one would adapt the abstract model to the limitations of optical systems. In Fig. 1 we see a typical shared memory model where individual processing elements (PE's) have variable simultaneous access to an individual memory cell.

In general, these shared memory are not physically realizable because of actual fan-in limitations. As an electronic example, the ultracomputer [4] is an architectural manifestation of a shared memory model, and uses a hardwired Omega network between the PE's and memories; it simulates the shared memory model with a time penalty of $O(\log^2 n)$.

Optical systems could in principle be used to implement this parallel memory read capability. As a simple example, a single 1-bit memory cell can be represented by one pixel of a 1-D or 2-D array; the bit could be represented by the state (opaque or transparent) of the memory cell. Many optical beams can simultaneously read the contents of this memory cell without contention, by the superposition property. A system based on this concept includes an array of memory cells,

an interconnection network, and an array of PE's. The interconnection network is needed between the PE's and the memory, and must allow any PE to communicate with any memory cell, preferably in one step, and with no contention. A regular crossbar is not sufficient for this because fan-in to a given memory cell must be allowed. Optical systems can potentially implement crossbars that also allow this fan-in (e.g., some of the systems described in [5]).

Gates. Since the superposition property of optics only applies in linear media, it cannot in general be used for gates, which are (by definition) nonlinear. However, for important special cases superposition can allow many optical gates to be replaced with one optical switch.

Consider an aperture whose state (opaque or transparent) is controlled by an optical beam, with again many optical beams being able to read its state simultaneously. Here the aperture is being used as a switch or relay, and the control beam opens or closes the switch. If b represents the control beam and a_i the signal beams, this in effect computes $b \cdot a_i$ or $\overline{b} \cdot a_i$, depending on which state of b closes the switch, where $\cdot$ denotes the AND operation (Fig. 2).

Using this concept, a set of gates with a common input in an SIMD machine can be replaced with one optical switch or "superimposed gate". It also obviates the need for broadcasting the instructions to all PE's; instead, a fan-in of all signals to a common control switch is performed.

These superimposed gates are not true 3-terminal devices, since the a_i inputs are not regenerated. As a result, a design constraint must be adhered to: these a_i signals should not go through too many superimposed gates in succession without being regenerated by a conventional gate. Note, however the following features. The total switching energy required for a given processing operation is reduced, because N gates are replaced with one superimposed gate. This is important because it is likely that the total switching energy will ultimately be the limiting factor on the switching speed and number of gates in an optical computer. Also, it permits an increase in computing speed since some of the gates are effectively passive, and reduces requirements on the device used to implement the optical gates.

In summary, architectures for optical computing must incorporate the capabilities of optics as opposed to electronics. A familiar but important inherent difference lies in the superposition property of optical beams, which can be expoited in opitcal interconnections, gates, and memory.

REFERENCES

[1] B.K. Jenkins, et al., *Applied Optics*, Vol. 23, No. 19, pp. 3465-3474, 1984.

[2] C.L. Giles and B.K. Jenkins, *Proc. Twentieth Annual Asilomar Conference on Signals, Systems, and Computers*, Pacific Grove, Calif., IEEE Cat. No. 87CH2461-2, 513-517 (1986).

[3] B.K. Jenkins and C.L. Giles, *Proc. SPIE*, 625 22-29 (1986)

[4] J.T. Schwartz, *A.C.M. Trans on Prog. Lang. and Sys.* 2, No. 4, 484-521 (1980).

[5] A.A. Sawchuk, B.K. Jenkins, C.S. Raghavendra, and A. Varma, *Computer* 20, No. 6, 50-60 (1987).

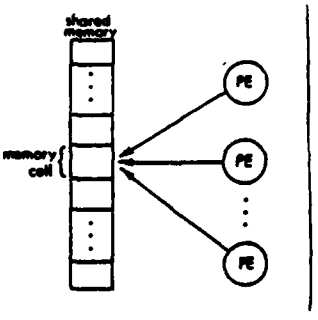

Fig. 1. Conceptual diagram of shared memory models.

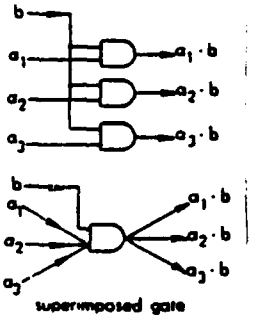

Fig. 2. One optical relay or superimposed gate versus individual gates with a common input.

THE OPTICAL WIRING OF PHOTONIC DIGITAL PROCESSING ARRAYS FOR OPTICAL COMPUTING

S.D. Smith, A.C. Walker, M.R. Taghizadeh,

I.R. Redmond and B. Robertson

Department of Physics, Heriot-Watt University,

Riccarton, Edinburgh EH14 4AS, UK

and

G. Lebreton

GESSY, Université de Toulon

639 Bd. des Armaris

83100 Toulon, France

Summary

Key building blocks of future optical computers are likely to be massively parallel array processors capable of all binary digital functions as well as read/write memory capability. Parallelism of at least 10^4, combined with processing times of 1 μs or less, represents a convenient target for demonstration within the next few years.

Several possible sources of the required optical nonlinearity exist and may be ultimately successful. These include: direct optical nonlinearity of electronic origin, opto-thermal nonlinearity and a variety of forms of hybrid nonlinearity in which electrical assistance is used to increase the effective magnitude of the nonlinearity and hence reduce operating powers. In any event, operating powers of sub-milliwatt level seem essential to operate sufficient parallel elements. On the basis of present experimental

results the size scaling of the elements becomes important and implies that elements of dimension of a few microns will be necessary. In all cases this requirement sets the problem of providing between 10^4 and 10^7 illumination paths most probably derived from a single laser source. The micro optics also demands spot diameters of a few microns and a high level of uniformity of intensity over the area of the array.

In this paper we describe the characteristics of a particular class of logic switching element - optothermally activated nonlinear interference filter arrays - both theoretically and experimentally. It is predicted that powers as low as 100 μW will be possible on micron size pixels of such an array. Experiments so far reaching one milliwatt or less per pixel will be presented.

The development of laser beamlet array generators from highly efficient dichromated gelatin volume hologram lenslet arrays is described. Results including the generation of < 4 μm beam diameter at the focus and array sizes as large as 1024 elements will be presented. The copying of computer generated halide holograms with efficiencies of approx. 4% on to DCG, yielding 99% efficiency and uniformity within 2%, is described together with the special optical testing methods which have been utilised.

The implications of this work are that efficient conversion of a 10 W laser beam (derivable from a single argon ion laser or diode laser array) to at least 10^4 beamlets can be achieved and that logic elements that can be driven by this array can be fabricated. Implications of data rates greater than 10^{10} bits per second thus exist.

Friday september, 2, 13.30

SESSION POSTERS P3

ACTIVE COMPONENTS
COMPOSANTS ACTIFS

Ps 01 - J. BOTINEAU, C. LEYCURAS and C. MONTES : A several MHz optical clock using stimulated Brillouin scattering and a ring fiber cavity.

Ps 02 - M. CANVA, G. LE SAUX, M. DUMONT, J.C. LOULERGUE, A. BRUN and F. KAJZAR : Ultrafast Kerr effect resonance in 4BCMU polydiacetylene solution.

Ps 03 - G. LE SAUX, J.P. POCHOLLE, J.P. HIRTZ, F. SALIN, D. DELACOURT, A. BRUN and M. PAPUCHON : Picosecond time resolved absorption saturation in Si doped MQWS.

Ps 04 - M. TANAKA, Y. MIYAZAKI, M. MIKAMI, M. KOSAKA and T. TOMODA : Inspection of patterned wafer surface using electrooptic spatial light modulator.

Ps 05 - M. THIENPONT, L. PEIRLINCKX and M. SMEDTS : Finesse switching : an alternative intensity independent commutation mechanism.

OPTICAL PROCESSING CONCEPTS
CONCEPTS DE TRAITEMENT OPTIQUE

Ps 06 - N.N. EVTIKIEV, N.A. ESEPKINA, S.U. BONDARTSEV, A.V. LAVROV and V.V. PEREPELITSA : Time integrating acoustooptic spectrum analyser.

Ps 07 - C. GONZALO, J. BESCOS and L.R. BERRIEL-VALDOS : Recovery of space variant filtered images through the Wigner distribution function by an hybrid optical-digital processor.

Ps 08 - K. ITOH, T. NOMURA and Y. ICHIOKA : Optical-digital hybrid processor for high-speed pattern matching.

Ps 09 - M. PRIBAN and S. SAIC : Multifunctional hybrid optical-digital coprocessor with BGO transparents.

Ps 10 - P. UHRICH, B. MOREAU, B. GOULAR, F. BRETAUDEAU and J. RIEHL : Non coherent optical processor with CCD "add and shift" for synthetic aperture radar data.

Ps 11 - F.T.S. YU, T. LU and P.B. GIANINO : A digital optical processor for optical computing.

OPTICAL NEURONAL PROCESSORS
PROCESSEURS OPTIQUES NEURONAUX

PARALLEL PROCESSORS
PROCESSEURS PARALLELES

A Several MHz Optical Clock Using Stimulated Brillouin Scattering in a Ring Fiber Cavity

by

Jean BOTINEAU, Claude LEYCURAS and Carlos MONTES

Laboratoire de Physique de la Matière Condensée (UA CNRS n° 190)

Parc Valrose - 06034 NICE Cedex - FRANCE

Abstract

An optical clock, temporal characteristics of which is determined by geometrical parameters, works by stationary pulsed emission of a CW-pumped Brillouin fiber ring laser.

Summary

A CW-single frequency wave travelling in a single-mode fiber interacts with acoustical phonons induced by thermal fluctuations, and gives rise to a stimulated backward scattered Stokes optical wave, to the amplification of a particular forward acoustical phonon, and to the depletion of the pump wave : this is the stimulated Brillouin scattering, which is generally considered as an undesirable effect, because it prevents an intense CW-beam to be transmitted through a single-mode fiber. We suggest here to use this effect to design a purely optical clock of some MHz repetition rate, the temporal characteristics of which are only determined by geometrical parameters.

If, in properly normalized units, E_p is the pump wave amplitude, E_S the Stokes wave amplitude and E_a the electric amplitude induced locally by the acoustical phonons, the phenomenon may be well approximated by the 3 equations set :

$$[\partial_t + \partial_z] E_p = - E_S E_a$$

$$[\partial_t - \partial_z] E_S = E_p E_a^*$$

$$[\partial_t + (v/c)\,\partial_z + \mu] E_a = E_p E_S^*$$

where t is a temporal coordinate, z the abscissa along the fiber, v the

sound velocity, c the light velocity in the fiber and μ a phonon damping coefficient. Stationary solutions of this equations set are generally depending on space and time. In particular, if the fiber is mounted inside an oscillator, the Stokes signal corresponding to a CW pumping is a periodical pulses train.

We have designed a ring oscillator such that pump and Stokes waves will be always counterpropagating, allowing the process to be constructive. The oscillator acts then as a Brillouin fiber ring laser, and the repetition rate of Stokes pulses is an integral multiple of the pulse round trip frequency inside the oscillator. In fact, an elementary configuration leads to several problems because the pump laser is not optically isolated and induces a forward scattering, and also because the stimulated phonons cannot be damped between two Stokes pulses. The solution which we have succesfully tested is to couple the pump wave inside the cavity with an acousto-optic modulator drived by the oscillator characteristic frequency. In our experiment, the modulator is drived externally, but it also be drived by the Stokes train itself.

We have used in this experiment a 83 m pure silica core single-mode birefringent fiber pumped by a CW-single frequency ionized Argon laser emitting at 5145 Å. Pump power output threshold is below 200 mW, and the Stokes frequency repetition rate of 2,4 MHz. A numerical simulation including the optical Kerr effect gives a very good accordance with the experiment.

A higher repetition rate would be possible with a shorter fiber, but the price to pay will be then a higher pump level.

ULTRAFAST KERR EFFECT RESONANCE IN 4BCMU POLYDIACETYLENE SOLUTION

M. CANVA, G. LE SAUX, M. DUMONT, J.C. LOULERGUE, A. BRUN, F. KAJZAR*

Institut d'Optique Théorique et Appliquée
Centre Universitaire d'Orsay, U.A. 14
B.P. 43, Bâtiment 503
91406 ORSAY Cédex - France

* I.R.D.I. - CEN-Saclay
Département d'Electronique et d'Instrumentation Nucléaire
Laboratoire d'Etudes Avancées
91191 GIF/YVETTE Cédex - France

We have performed femtosecond time resolved Kerr effect measurements on a yellow solution of 4BCMU polydiacetylene (Butoxy-Carbonyl-Methyl-Urethane R-C≡C-C≡C-R, R = -(CH2)4-O-CO-NH-CO-O-C4H9). The experiment is conducted in the transparent region. Femtosecond pulses, (duration about 100 fs), are produced by a passively mode-locked ring dye laser in which the dispersion is controlled by a sequence of four prisms. The pulses are amplified by a 4 stage amplifier pumped by a Nd:YAG laser working at a 10 Hz repetition rate giving an energy of about 0.5 mJ per pulse (1).

Two different types of experimental arrangements are used. In the first one, the pulse is split into a pump (96 %) and a probe (4 %). The polarization angle between them is set at 45°. The two beams are then focused on the sample, crossing each other at a few degrees, the delay (positive or negative) between the arrival of the pump and the probe is adjustable with a 6 fs accuracy. The probe beam is analyzed through a crossed polarizer (no light is transmitted in absence of a pump pulse) by a spectrograph and an Optical Multichannel Analyzer which averages the pulse spectrum on several shots (Figure 1). In the second arrangement, before splitting, the pulse is focused in a watercell and a white continuum is created. On the pump path, a filter selects a narrow band frequency, about 10 nm is necessary to keep a pulse shorter than 100 fs. On the contrary, the probe beam contains the whole spectrum.

The data obtained with the first experimental setup are reported in Figure 2 that shows the input pulse spectrum (2.a) the spectrum transmitted by the Kerr shutter (2.b) and the shutter transmission as a function of wavelength. We observe an ultrafast electronic response followed by a slower decay. A similar behaviour has been observed in red solutions of the same polymer (2) but in that case the experiment was performed near the absorption band. Moreover our results show a shift in the fast response range indicating a probable two-photon resonant effect at a wavelength smaller that the pump one. The results given by our second type of experiment seems to confirm this interpretation. The present study would locate the two-photon state slightly higher than was found by Chance et al. (3) using the three-wave-mixing measurement technique.

(1) F. Salin, P. Georges, G. Roger, A. Brun
Applied Optics, 26, 4528, (1987).

(2) P.P. Ho, R. Dorsinville, N.L. Yang, G. Odian, G. Eichmann, T. Jimbo, Q.Z. Wang, G.C. Tang, N.D. Chen, W.K. Zou, Y. Li, R.R. Alfano
SPIE 682, 36, (1986).

(3) R.R. Chance, M.L. Shand, E. Hogg, R. Silbey
Phys. Rev. B 22, 3540 (1980).

FIGURES

Fig 1 : Principle of our Kerr effect experiments

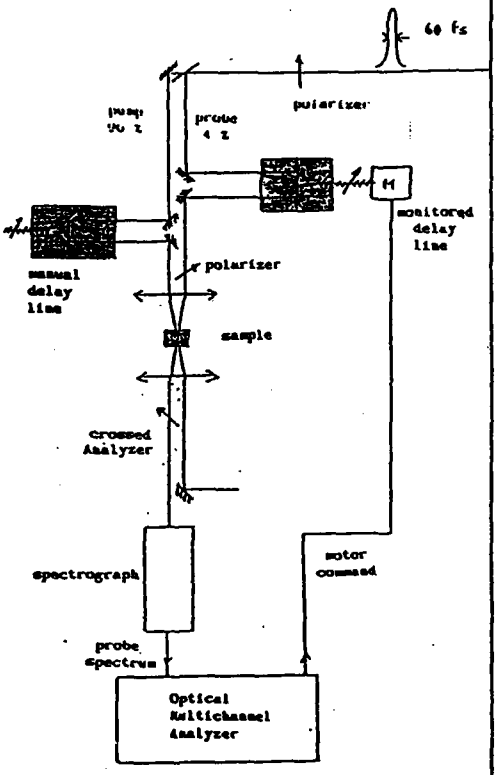

Fig. 2 : Data from the first experiment. The delay between two consecutive curves is 66 fs.

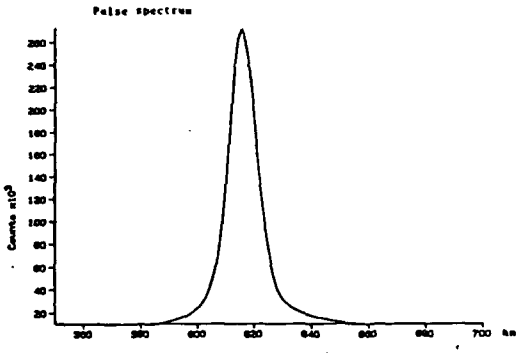

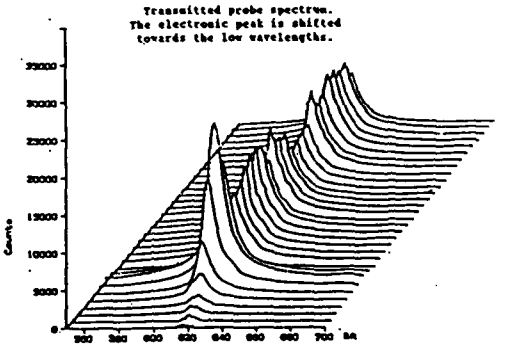

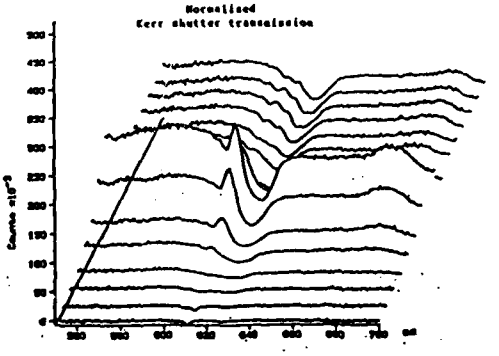

Picosecond time resolved absorption saturation in Si doped MQWS

G. LE SAUX*, J.P. POCHOLLE, J.P. HIRTZ, F. SALIN*, D. DELACOURT, A. BRUN*, M. PAPUCHON

Thomson-CSF - Laboratoire Central de Recherches
Domaine de Corbeville - BP 10 - 91401 Orsay (France)

*I.O.T.A., Centre Universitaire d'Orsay, BP 43, Bâtiment 503, 91406 ORSAY Cédex (FRANCE)

=====

New concepts in infrared photodetection and modulation have been recently developed [1, 2, 3] using intersubband absorption in multiple quantum well structures (MQWS). This paper presents the experimental study of the relaxation of highly excited electrons in MQWS design as IR detector using a femtosecond correlation technique.

The studied structure was grown on a molecular beam epitaxy machine and consisted of 100 periods MQW of 85 A GaAs wells and 300 A $Ga_{0.78}Al_{0.22}$ barriers. We chose this structure, composition and well thickness to produce only two quantum states in the well of the conduction band with an energy spacing close to 95 meV (13 µm). The barriers are doped with Si donors ($n=7.10^{17}cm^{-3}$) to provide free electrons to populate the ground states in the quantum wells [4, 5], and make the sample absorbing near 13 µm.

The room temperature transmission spectrum of the unperturbed sample (Figure 1) clearly shows the excitonic structures and interbands transitions.

In the experiment reported here, we monitor in time the change in excitonic absorption bands induced by the non thermal population distribution. We follow the absorption changes as the carriers thermalize to occupy the near band edge states.

For that we use a femtosecond pump and probe technique. The pump beam has a wavelength of 750 nm (1.65 eV) with a spectral width of 10 nm. The probe beam has a large spectrum distributed over the intersubband transitions window from 790 to 900 nm (1.59 to 1.38 eV). The large spectral probe transmission is then analyzed and recorded by using an optical Multichannel Analyzer placed at the exit of a spectrometer.

The figure 2 shows the differential transmission spectra of the sample for various time delays between the pump and probe pulses. The sampling time is 200 fs and each spectrum corresponds to the accumulation of 100 successive laser shots.

As in the case of undoped samples, we obtain large saturation levels (30 %) using deposited energies about a few pJ. The maximum level is obtained after about 1.4 ps. This time corresponds to the thermalization of the photoexcited electrons. Recent experiments [6] have demonstrated that the time constant for intersubband transitions was about 11 ps and this relaxation time will limit the ultimate response time of such detectors.

[1] B.F. LEVINE, K.K. CHOI, C.G. BETHEA, J. WALKER, R.J. MALIK Paper MCC2, Technical Digest, XV International Quantum Electronics Conference, (IQEC), Baltimore, Maryland, 26 April-1 May, 1987.
[2] L.C. WEST, S.J. EGLASH, Appl. Phys. Lett. 46, 1158, (1985).
[3] B.F. LEVINE, K.K. CHOI, C.G. BETHEA, J. WALKER, R.J. MALIK Appl. Phys. Lett. 50, 1092 (1987).

[4] A. HARMITT, J.S. HARRIS, Appl. Phys. Lett. 50, 685 (1987).

[5] B.F. LEVINE, R.J. MALIK, J. WALKER, K.K. CHOI, C.G. BETHEA, D.A. KLEINMAN, J.M. VANDENBERG Appl. Phys. Lett. 50, 273 (1987).

[6] A. SEILMEIER, H.J. HUBUER, G. ABSTIERTER, G. WEIMANN and W. SCHLAPP, Appl. Phys. Lett. 59, 1345 (1987).

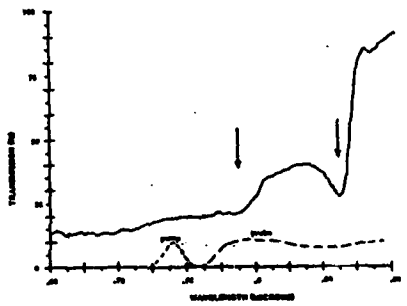

Figure 1 : Absorption spectra of the MQW structure at room temperature. Probe and pump beams wavelength spectra are represented. Arrows indicates the e-hh/lh excitonic bands.

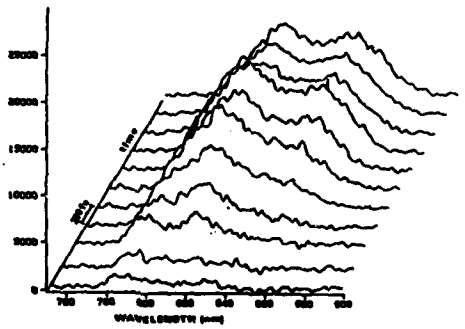

Figure 2 : Differential transmission spectra of sample for various time delay between the probe and pump pulses. The temporal sampling is 200 fs and the sample temperature is T = 300 K.

Inspection of patterned wafer surface using electrooptic spatial light modulator

Hitoshi Tanaka, Youko Miyazaki, Noboru Mikami,
Nobuyuki Kosaka and Toshimasa Tomoda

In production lines of large scale integrated circuits(LSI), automated systems have been demanded for the inspection of patterned wafers to replace the time-consuming and pains taking labor work. The spatial frequency filtering technique has been often applied to the inspection of periodic pattern defects, especially optically transparent objects such as LSI photo-masks to take advantage of its inherent high inspection speed. Although this technique is valid also for inspection of reflective objects such as patterned wafers of LSI, it is usually required to make a precise adjustment of alignment between the filter and the test object so that the Fourier pattern from the reflective surface pattern does not deviate from the pattern of the spatial filter. This alignment requirement could be a big obstacle in practical applications, particularly in mass production lines, and should preferably be avoided. In addition, the filter should be specific for a specific pattern and its preparation which includes a photo development process is a nuisance. In order to avoid these obstacle and nuisance, we decided to use an electrooptic spatial light modulator as the spatial filter. Then, in-situ filter preparation and inspection which immediately follows can be carried out in real-time for each test object. Thus, the problems of alignment and in-advance-filter-preparation are eliminated. We verified experimentally the applicability of an electrooptic spatial light modulator to the real-time inspection of periodic pattern defects.

Fig.1 shows a block-diagram of the inspection system. A $Bi_{12}GeO_{20}$ (BGO) thin crystal was used as a spatial light modulator. The wavelength of laser was 488nm at which BGO shows both the photoconductivity and the linear electrooptic effect. Thus, both the Fourier pattern production in the filter and the defect inspection were conducted with the single laser. The light diffracted by a periodic pattern forms a spotty pattern on the focal plane. Because the light has a strong intensity, its pattern of spots is swiftly recorded on the BGO which is placed at the focal plane. On the other hand, the light from a defect forms a broad pattern on the focal plane, and it takes a long time to be recorded on the BGO because of

its weakness in intensity. Therefore, by selecting the time of exposure, we can record on the BGO only the Fourier pattern due to the periodic pattern of test objects. An analizer placed in front of the camera refrains the light coming from the periodic pattern from reaching the camera. Only the light from defects goes through the analizer and the image of defects without the periodic pattern is formed on the camera. The spatial resolution of the BGO was ~1.5/mm. The objective lens had a focal length of 95mm and a N.A of 0.1. A microscope-objective-scale of 10μm pitch was used as a periodic pattern sample, on which a particle of about 10μm was placed as a defect. Fig.2 shows a decrease in signals of the periodic pattern and the defect with the time after the laser irradiation. It is observed that the signal of the periodic pattern soon disappeared and only the defect signal remained to be detected.

We are now trying to apply this system to the inspection of patterned wafers.

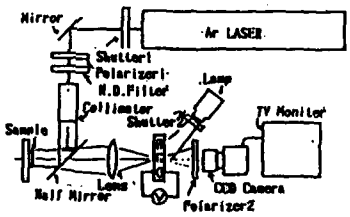

Fig.1 Optical System

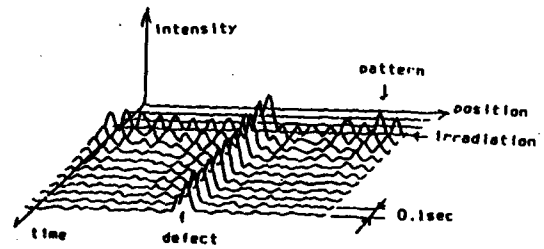

Fig.2 decrease in signals of the pattern and the defect with the time after the laser irradiation

Finesse Switching : an Alternative, Intensity Independent Commutation Mechanism.

H. Thienpont, L. Peirlinckx, M. Smedts
Vrije Universteit Brussel, Departement Toegepaste Natuurkunde, Toegepaste Wetenschappen, Pleinlaan 2, 1050 Brussel, Belgium.

A non-linear Fabry-Perot is commonly switched by varying the amount of incident irradiance or by adding optical/electrical energy to the non-linear medium. An alternative commutation mechanism is proposed, based on a change of either one or both reflection coefficients of the resonatorinterfaces. The changes in finesse, thus obtained, transform the Airy function and affect the feedback mechanism (Fig. 1a). This leads to a commutation of the device for appropriate variations of the reflection coefficients (Fig. 1b). To obtain these variations two techniques are highlighted

a) Changing the state of polarization of the oblique incident light beam. This allows intensity independent commutation (1).
b) Creating a plasma at the second interface of the resonator and altering its density by optical means in order to modulate the plasma reflection (2). Therefore a multi-layerd device should be considered.

Switching energy, commutation speed, cascadability and other features of both techniques are discussed. The a-type finesse switching appears to be faster and less energy consuming than a more common mechanism. But it presents the drawback of not being cascadable. However, it appears to be an excellent tool to scrutinize the dynamic behaviour of the N.L.F.P., regardless the nature of the nonlinearity.

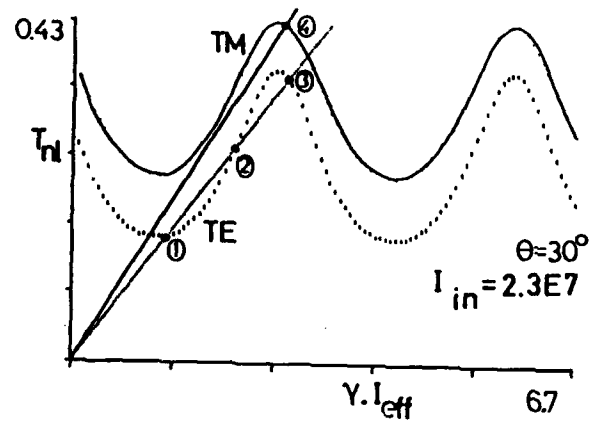

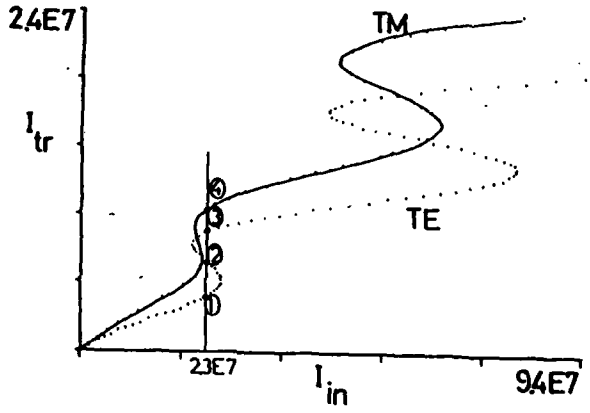

(Fig. 1a, 1b) Starting from level 1 and switching the polarization of the incident beam from TE to TM and back to TE, forces the device to call at levels 4 and 3 respectively

(1) H. Thienpont and I. Veretennicoff, "Changes in the Bistable Behaviour of a Nonlinear Fabry-Perot Etalon for Oblique Incidence", Laser 87, Opto-Elektronik Mikrowellen.

(2) K. Seeger, "Semiconductor Physics", Springer Series in Solid-State Sciences, Vol. 40, p 355.

TIME INTEGRATING ACOUSTOOPTIC SPECTRUM ANALYSER

N.N.Evtihiev, N.A.Esepkina, S.U.Bondartsev, A.V.Lavrov,
V.V.Perepelitsa

Time integrating acoustooptic spectrum analyser in comparison with space domain spectrum analyser provides the possibility of parallel analysis of radiosignals with high frequency resolution. Semiconductor lasers and multielement CCD-photodetector improve their qualitative and practical characteristics. CCD converts the optical spectrum into the electrical signal and also plays a role of a buffer, connecting the optical and digital parts of a hybrid optical processor. Direct injection current modulation of a semiconductor laser provides the input of radiosignals into the processor. The scheme of acoustooptic spectrum analyser is based on a hard interferometer. In order to increase the SNR an additional analogue processing was carried out by CCD. The results of the experimental study of such time integrating acoustooptic spectrum analyser are discussed.

The compact construction of spectrum analyser, examined in our work is presented on fig.1. The collimated beam of a semiconductor laser formed by the two-lens device C illuminates the acoustooptic modulator aperture, excited by a "chirped" (linear frequency modulated) impulse. Waves from two arms of interferometer form the interference pattern in the output plane (CCD-plane). The array of frequences in time domain is formed by the chirped signal in acoustooptic modulator with changing frequences from element to element of CCD. The spectral information of the examined signal is formed as the charge distribution in CCD by the modulation of the semiconductor laser emission with the input signal S(t) after the accumulation time, equal to the duration of the chirped signal. AlGaAs semiconductor impulse laser ($\lambda = 0{,}66\ \mu m$) and TeO_2 acouatooptic modulator with 10 μs time aperture were used in experiments. Frequency resolution over the spectrum at a level of 10 Hz was achieved with the time accumulation of 100 ms in the frequency range up to 1 kHz. High SNR was provided by the additional analogue processing in CCD diminishig the noise figure.

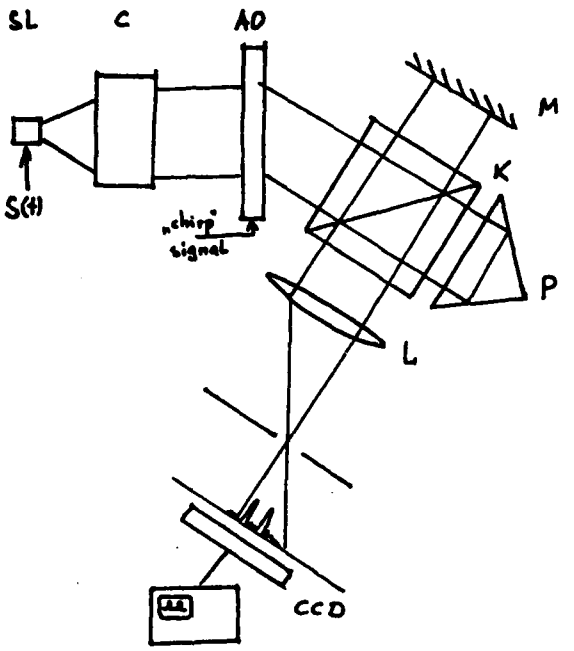

Fig. 1.

RECOVERY OF SPACE VARIANT FILTERED IMAGES THROUGH THE WIGNER DISTRIBUTION FUNCTION BY AN HYBRID OPTICAL-DIGITAL PROCESSOR.

C.Gonzalo, J.Bescós and L.R.Berriel-Valdós*
Instituto de Optica, Serrano 121. 28006-Madrid. Spain.
*INAOE, A.P. 51/216, 7200 Puebla, Pue., México.

SUMMARY.

The Wigner Distribution Function (WDF) has attracted considerable interest in recent years. This is due to the fact that the WDF is an useful tool to hand variant signals, since it is a joint representation in the signal's variable and in its associated frequency. In optics, for example, this simultaneous representation of images in spatial and frequency variables can be used to carry out space variant filterings. The WDF can be generated via digital or optical processing, the first way has the advantage that it is not contaminated with the noise that characterizes to optical processing; however it requires an important amount of computer time, and also it suffers from aliasing effects (1). Because of this, sometimes is more adequate optical processing than the digital one, since the computer time is extraordinarily decreased and aliasing problems are not present .

In this contribution, space variant filtered images are optically obtained through the WDF. This distribution is generated by an optical processor, which produces the Fourier Transform (FT) of the product function $r(x,x_o,y,y_o)=f(x+x_o/2,y+y_o/2)\ f^*(x-x_o,y-y_o/2)$ for each (x_o,y_o) point. The WDF generated in the Fourier plane is modified with filters that can be changed for each shift carried out to generate $r(x,x_o,y,y_o)$, and therefore, each image point can be filtered with a different mask. A second lenses system gives the filtered product function $(r'(x,x_o,y,y_o))$, that is introduced in a digital image processor in order to select in each step the adequate information from $r(x,x_o,y,y_o)$ to recover the image. In accordance with the theory (1) and for images with unidimensional variation along the x_o axis, the local image power is recovered when x_o is equal to zero in $r(x,x_o)$. The image samples are recovered when $x_o=2x$, that requires the application of oversampling, otherwise the even samples are only recovered. The oversampling is not necessary to recover the local image power, which is given by the digital processor when it reads at the central point of the $r(x,x_o)$ for each shift (x_o). The samples recovery requires besides the oversampling a perfect knowledge of the definition domain of $r(x,x_o)$ in order to make accurate readings at $x=x_o/2$.

Figure 1 shows preliminary results obtained via the hybrid processor. A representation (2) of $f(x+x_o/2)\ f^*(x-x_o/2)$, generated optically, is shown in the left part for a composite rectangular grating of three frequencies . In this representacion the horizontal variable is x_o and x the vertical one. The different size of domain for the vertical and horizontal axis is due to oversampling ($x=x_o/2$). The right part shows on the top the original image recovered from its WDF, and on the bottom the space variant filtered image. In the high and medium frequency regions lowpass filtering has been used and highpass filtering in the low frequency region.

References

1._T.A.C.Claasen and W.F.G.Mecklenbräuker. The Wigner distribution -a tool for time-frequency signal analysis-. Part I: continuous time signals. Part II: discrete time-signals. Philips J.Res.35(1980)

2._C.Gonzalo, J.Bescós, L.R.Berriel-Valdós and J.Santamaría. Space Variant Filtering through The Wigner Distribution Function. Applied Optics (Submitted).

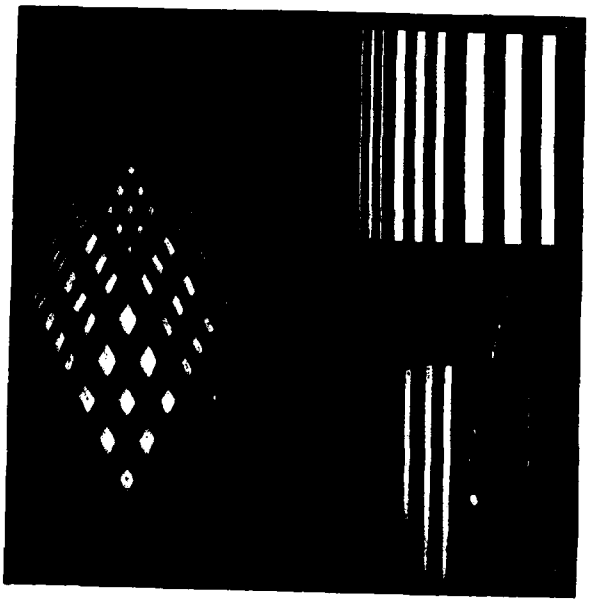

Optical-Digital Hybrid Processor for High-Speed Pattern Matching

K. Itoh, T. Nomura, and Y. Ichioka

Department of Applied Physics, Osaka University

Yamadaoka 2-1, Suita, Osaka, 565, Japan

SUMMARY

The optical and electronic hybrid processing is a natural way to take advantage of the attractive features of the optical information processing and the state-of-the-art digital video techniques. However, several problems still limit it's range of applications. 1) If a coherent optical system is to be employed, requisite spatial light modulators (SLMs) with moderate characteristics are hardly available at reasonable prices. 2) On the other hand, powerful incoherent optical systems often assume extremely bright light sources with variable intensity distributions. 3) The throughputs of hybrid systems are hitherto limited primarily by the speed of electronic processors due to their serial architectures.

We propose in this paper, a hybrid system to alleviate these problems. We adopted a rotational shearing interferometer of a variable-shear type [1] as an optical processor and combined it with a commercially available digital image processor dedicated for real-time operations (Imaging Technology Inc., Series 100). The use of rotational shearing interferometer eliminates the problems of SLM. The rotational shearing interferometer can perform cosine (or sine) transform of an incoherent object such as an image displayed on a CRT. Furthermore, the interferometer can readily be designed to collect so much light flux that we can use the image on the CRT as a sufficiently bright light source. The digital section is equipped with several frames of image memories and can carry out frame-to-frame or input-to-frame subtraction and multiplication at the video rate. Thus, the system throughput is kept quite high. The bias term is subtracted or added in this digital section to conform the inputs and outputs to the nonnegativity constraints. The principle of the

incoherent optical processing is based on the well-known Van Cittert-Zernike theorem. The application of this theory to astronomical imaging has been studied by many workers and application to image processing has recently been suggested by George and Wang [2] and Marathey [3].

We will present the principle and implementations of the high-speed pattern matching along with experimental results. The experimental results will show the distinct potential of the present approach to the high-speed pattern matching. The results include an output of the first correlation experiment. A sharp auto-correlation peak of a special character was obtained among the cross-correlation clouds, although the system is not yet tuned for the fastest processing speed. The whole system is schematize in Fig.1. An image displayed on the CRT is cosine-transformed by the interferometer. The resultant transform pattern is detected by the CCD camera. The image processor and the optical path difference in the interferometer are controlled by the main processor.

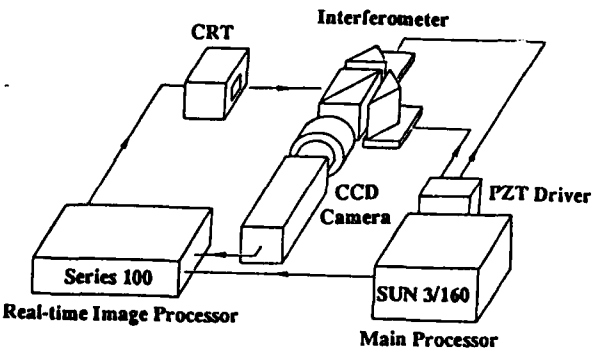

Fig.1. Proposed hybrid system.

REFERENCES

1. L. Mertz, *Transformations in Optics* (Wiley, New York, 1965) pp. 111-112.
2. N. George and S. Wang, "Cosinusoidal transforms in white light," Appl. Opt. 23 , 787-796 (1984).
3. A.S. Marathey, "Noncoherent-object hologram: its reconstruction and optical processing," J. Opt. Soc. Am. A 4 , 1861-1867 (1987).

Summary:

Multifunctional hybrid optical/digital coprocessor with BGO transparents

Miroslav Přibáň, Stanislav Saic

ÚTIA ČSAV Praha, ČSSR

Application of the optical controled transparent PRIZ [1] based on crystal $Bi_{12}Ge\ O_{20}$, emploing transverse Pockel's effect, which is attached to the microcomputer systems makes it possible effective realization of the special multidimensional signal processing system [2],[3].

Special processor consists of two optical controled transparent PRIZ. First one is used for signal input, second one is used for filter realisation. Filter can be generated by computer or by standard Van der Lught method. Optical images for input informations and filters are generated in the terminal units.

Controling of the optical processor, images writing on the transparents and images erasing is implemented on the microcomputer LSI 11/23.

Optical processor provides:

1) Fourier transformation
2) Image derivation
3) Second image derivation
4) Laplacian
5) Solution of the equation $\nabla u = -g(x,y)$
6) Filtration
7) Image correlation
8) Image convolution

Outputs from the optical part are digitized and processed in the microcomputer and either again introduced to the optical part or transmit to the higher computing system.

Hybrid processor can works in the indipendent operation and can be controled from attached terminal.

Literature:

[1] Petrov M.P., Stepanov S.I., Chomenko A.W.:
Fotoczustvitelnyje elektroopticeskije sredy v golografii i opticeskoj obrabotke infomacii, Nauka, Leningrad, 1983

[2] Přibáň M., Saic S.:
Řízené transparenty v optickém zpracování informace, International symposium " Aplikovaná optika ", Praha, 1987

[3] Parygin V.N., Balakshin V.I.:
Opticeskaja obrabotka informacii, Izdatelstvo Moskovskogo universiteta, Moskva, 1987

Abstract:
Using of PRIZ transparent, which are based on BGO crystals make it possible effective realisation of the specialized image processing coprocessor.

NON COHERENT OPTICAL PROCESSOR WITH CCD "ADD AND SHIFT" FOR SYNTHETIC APERTURE RADAR DATA

P.UHRICH, B.MOREAU, D.GOULAR, F.BRETAUDEAU, J.RIEHL.
OFFICE NATIONAL D'ETUDES ET RECHERCHES AEROSPATIALES.
ONERA
B.P. 72 - 92322 CHATILLON CEDEX FRANCE

INTRODUCTION.

The use of a CCD "Add and Shift" correlator to process Synthetic Aperture Radar (SAR) data is a very elegant and useful solution proposed by D.PSALTIS *et al.* ((1) et (2)) some years ago. However the use of the acousto-optical processor is restricted to "chirp" coded SAR. A generalized real-time non-coherent optical processor for SAR data, based on "Add and Shift" correlation process is depicted. Some problems relative to the use of CCD are described. Early experimental results are also analyzed.

OPTICAL PROCESSOR.

A natural way to input SAR data into an optical processor is to display the sequence of return pulses from the ground on a Cathode Ray Tube(CRT). The successive pulses are displayed on a single amplitude-modulated vertical trace on the screen (column). In case of a coded pulse SAR ("chirp" or phase coded for instance), we suppose that the pulses are compressed before being displayed on the CRT. Each point of the column is projected on a line on a matched filter in front of an "Add and shift" CCD by a cylindrical lens. The optical processor is shown on fig.1.

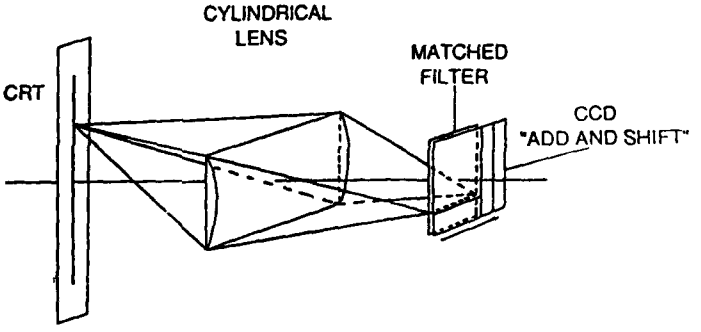

Fig.1. OPTICAL PROCESSOR.

After one pulse is displayed at the input of the optical processor, the whole detection array of the CCD is electronically shifted towards the output register (fig.2). If we suppose that the CCD has N columns on the detection plane, the first resolved column of the filtered image will appear at the output register when the N+1 pulse is displayed on the CRT. At this point of the process, a new resolved column of the filtered image will be available at the output for each new pulse displayed at the input, giving continuously the processed image.

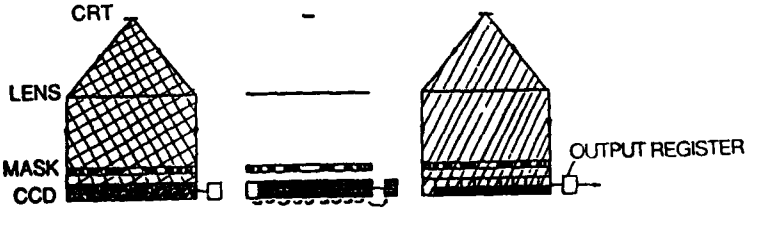

Fig.2. ADD AND SHIFT PROCESS.

Simulation of this processing shows that SAR angular resolution is preserved, provided that enough points are available on the CCD in the shifted direction.

Non-coherent light implies the use of at least two processing channels in order to treat the constant phase of SAR signal.

PROBLEMS ENCOUNTERED.

The CCD shift frequency depends only on the Pulse Repetition Frequency (PRF) of the SAR. The problem is that typical PRFs are very low, usually a few hundred Hz. This is too slow for most of the CCDs, which are rapidly saturated by dark current. There are only two solutions to improve dynamic on the CCD: to find a way to substract electronically this dark current on the detection plane at each step of the process, or to cool the CCD detection plane to temperature such as -70°C or -100°C.

Another problem is that the matched filter has to be bonded directly on the CCD detection plane to avoid overlap of information of one pixel over its neighbours. At the stage of our investigations this was not possible. So it was necessary to make a separate mask and to image it on the CCD the best way we could.

The last major problem is the input of the processor. CRT optical properties are not very well known, and difficult to control. We are still looking for the best solution , including optical and electronical simplifications.

EXPERIMENTAL RESULTS.

We use a THOMSON TH 7882 CCD(384 x 576 pixels), which was not intended to work in an "Add and Shift" mode. We have then made some electronical modifications on the CCD in order to use it first in the normal way to control the optical adjustment of the system, and second in the "Add and Shift" way to perform the correlation. The shift frequency was choosen such that no dark current problem appears during this experiment.

Matched filters were realized on photographic support using a VIZIR type printer (25µm resolution). They are imaged on the CCD with an optimized spherical lens to avoid aberration. The input of the system is a Light Emitting Diode (LED) for the moment: we only tried to prove that "Add and Shift" correlation is possible with the THOMSON CCD.

First experiment: spectral analyzer. We use a $\sin(\alpha\ y\ x)$ filter. When a square wave at a frequency contained by the mask is displayed at the input of the processor, this particular frequency, and all the harmonics written on the mask, are obtained at the output of the CCD.

Second experiment: chirp compression. The SAR signal is typically $\cos(\beta x^2 - \phi)$. When such a signal at input of the processor is filtered by a $\cos(\alpha\ y\ x^2)$ mask, one compression peak is obtained at output of the CCD on the line $\alpha\ y = \beta$.

CONCLUSION.

Simulations of experiments proved that excellent results were obtained, once the optical system was correctly adjusted. To go further we have to solve dynamic problems with CCD, to get matched filters that simplify the adjustment of optical system, and to solve the problem of the input of this optical processor.

REFERENCES.

(1) D.PSALTIS, K.WAGNER Optical Engineering, Vol.21, N°5 (sept-oct. 82).
(2) M.HANEY, K.WAGNER, D.PSALTIS SPIE, Vol.495 (1984).

A DIGITAL OPTICAL PROCESSOR FOR OPTICAL COMPUTING

Francis T.S. Yu and Taiwei Lu
Department of Electrical Engineering
The Pennsylvania State University
University Park, PA 16802
Peter D. Gianino
Rome Air Development Center
Hanscom AFB, MA 01731

The essential merit of an optical signal processor is its parallelism, large capacity, high speed and diversified wavelength. In this paper, we shall exploit the efficient operation of optics and the flexibility of electronics to come up with a hybrid digital optical processor, which is able to perform multiple matrix multiplication and bilinear transformations.

A binary number encoding algorithm is introduced in order to increase the accuracy of the optical processor, as shown in Fig.1 .

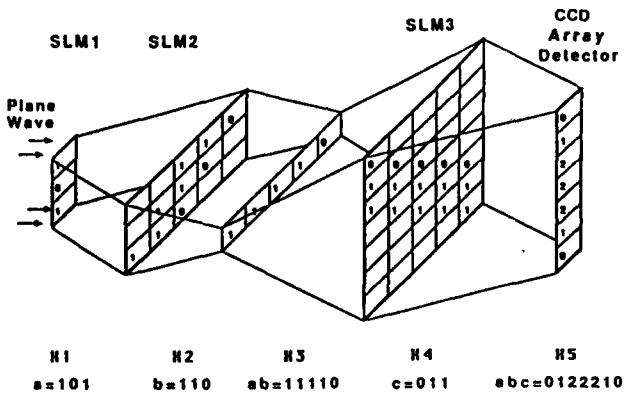

Fig.1 A Binary Number Encoding Algorithm

Three binary numbers a=101, b=110 and c=011 are encoded onto three spatial light modulaters (SLMs) on planes X1, X2 and X4 respectively. The product abc= 0122210 is detected simultaneously on the output plane X5. Based on this technique, two digital optical architectures have been developed. One of the architectures utilizes inner-product method with grating masks to perform multiple matrix multiplication in parallel. In the other architecture, systolic engagement is combined with the inner-product technique to process large matrix. A hybrid digital optical processor has been developed to implement these architectures, as shown in Fig.2. In this system, three Magneto-Optic Spatial Light Modulators (MOSLM's) serve as the inputs and the transformation mask. A CCD array detects the result and feeds back to a high speed memory. A microcomputer is used as a data

controller in the system.

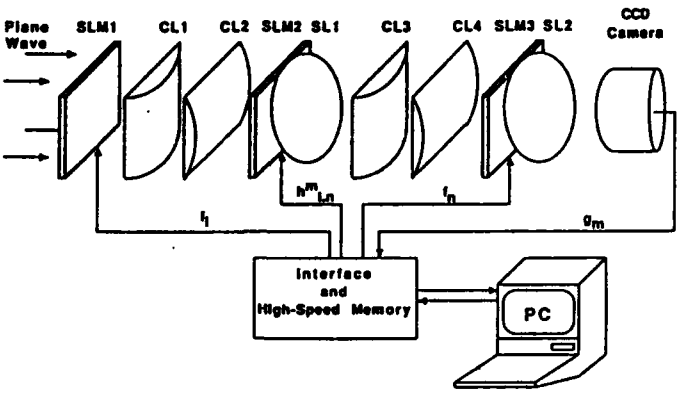

Fig.2 A Digital Optical Processor for Optical Computing

One of the preliminary experimental demonstrations of bilinear transformations is provided, as shown in Fig.3, where f_l and f_n are two input signals, $h^m_{l,n}$ is the transformation function. The output g_m is displayed on a CRT. This hybrid optical processor is able to carry out bilinear transformations with high accuracy and moderate speed.

f_l $h^m_{l,n}$ f_n g_m

Fig.3 An Experimental Demonstration for Bilinear Transformation

We acknowledge the support of the U.S. Air Force Rome Air Development Center, Hanscom Air Force Base, under contract No. F19628-87-C-0086.

References

1. H. Nakano and K. Hotate, "Real-time Processing of the Multiple Matrix Product Using an Incoherent Optical System," Appl. Opt. 24, 4238(1985).
2. F.T.S. Yu, M.F. Cao and J.E. Ludman, "Microcomputer-Based Programmable Optical Signal Processor," Opt. Eng. 25, 846(1986).

ASSOCIATIVE MEMORY NEURAL NETWORKS WITH CONCATENATED VECTORS

by

E. Marom*, B. H. Soffer†, U. Efron† and Y. Owechko†

* Faculty of Engineering, Tel-Aviv University, Tel-Aviv, Israel

† Hughes Research Laboratories, Malibu, CA 90265, USA.

The outer product neural network model of associative memories stores vectors by means of a matrix T where each component T_{ij} sums the interconnection weights between the i^{th} and j^{th} neurons of all stored states. This storage mechanism allows associative recall of initial vectors (states) even if distorted or only partial information is available, provided nonlinear thresholding and feedback are applied in the process. Extensive published simulation results have shown that the storage capacity of such a model is merely a fraction of N (the individual vector length), typically 0.15 N. Most of the models studied that were based on this configuration required that the diagonal T_{ii} shoud vanish.

In this present work we will look into the properties of outer-product matrix memories and will question, the role of the diagonal terms as well as the effects of vector concatenation onto the recall capabilities of such matrices.

The recall process consists of a matrix vector multiplication, whereas the storage matrix is multiplied with the initial state vector, to be followed by a threshold operation which generates a new vector that is used as a new input vector that addresses the same matrix again. The operation ends when a steady state solution is reached.

It has been shown that the mean and variance of this result reproduce vector m_0 with a probability related to the strength of the inner product, between the addressing vector and the corresponding stored one.

This strong dependence of the result on the inner product, or the peak correlation strength, suggests that one should consider coding the vectors, so that the resulting correlation function would provide an improved peak to background ratio. One such coding possibility is to use concatenated vectors, where the concatenation sequence is provided by a Barker code.

A storage matrix T of size (KN x KN) has thus been used, K being the concatenation order. A large number of vectors have been stored and later tried to be recalled with no error (i.e. verification of belonging to the stored set) or with errors. The association process is supposed to correct and restore the correct sequence. The processing involved a vector matrix multiplication, thresholding (set at 0 since vectors in most cases were balanced) and hard clipping (to the 0 and 1 level) followed by a repetition of the above. Only synchronous addressing has been tested (all vector bits adjusted simultaneously at each iteration, if necessary) and the process was repeated for up to 5 times for each new addressing vector. If no correct recall was achieved within the five iterations, the recall was counted as a failure.

Typical recall curves for K=7, when using the original vector with no error (H=0) or with errors (H=1,2...) is shown in Fig. 1. The errors were not concatenated, but rather distributed randomly within the "KN" bits of the addressing vector. A single concatenated error was tested too.

At the same time a large number of false recalls was experienced (Fig. 2). The increasing number of spurious (false) recalls is indicative of the fact that the interconnection matrix contains a "built-in test" for concatenation, and when sufficient vectors are stored, a new un-stored concatenated vector is wrongly "recognized" as belonging to the set. The concatenation, rather than the content is thus tested.

The appearance of large elements along several pseudo-diagonals due to the strong correlations that exist between the concatenated sequences, indicates that similar behaviour would probably be achieved also by removing the restriction of the zero-diagonal in the original Hopfield definition of the interconnection matrix. This is shown in Figures 3 and 4.

The strong diagonal terms enhance the recognition process but make the system less flexible and less adaptable, thus reducing its associative property. The error correction capability is restricted, since the diagonal terms tend to preserve the addressing vector in its given form. The elimination of the restriction on the diagonal seems to improve the storage capacity, increasing it to just about N if

one is ready to accept a spurious error rate of 10-20%. However, when this is coupled to an almost total loss of error correction capability, the attractiveness of non-zero diagonal trace associative matrices is highly reduced.

A comparison of Figures 1-2 and 3-4 shows that although a concatenated sequence has similar curves for correct and spurious states recognition, it has a much better error correction capability. The storage capability is however, only slightly increased. For a 5-fold concatenation (K=5) of 12 bits vectors (N=12), one gets about 15 stored vectors in the presence of a spurious error rate of less than 20%. The total length of a coded sequence is 60, so that the 15 stored vectors provide a storage rate of 0.25. On a 7-fold concatenation system (K=7), one gets about 18 vectors stored for the same spurious error rate which means a stored vector ratio of $18/84 \simeq 0.22$. These ratios are about 60% higher than those expected on statistical mechanics ground but lower than the theoretical limit.

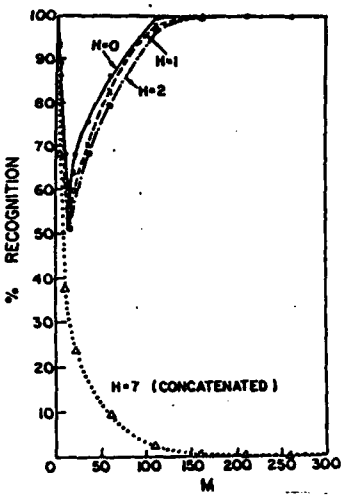

Fig. 1 Probability of recognition of 7-fold concatenated vectors (K=7)

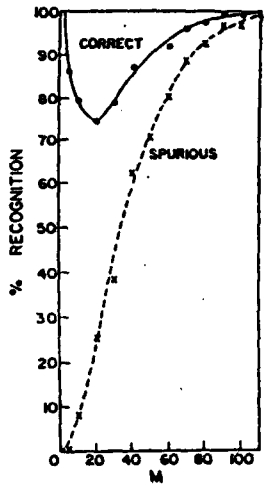

Fig. 2 Stored (solid) and unstored (dotted) probability of recognition for concatenated vectors of order 7.

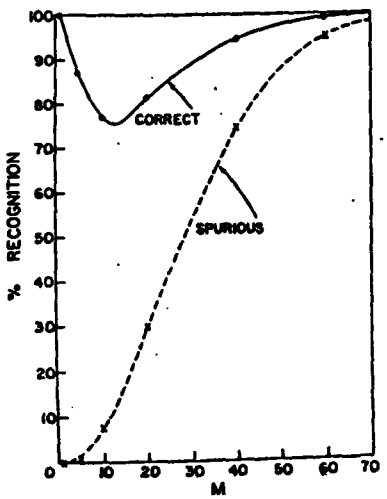

Fig. 3 Probability of recognition for matrices with non-zero diagonal terms.

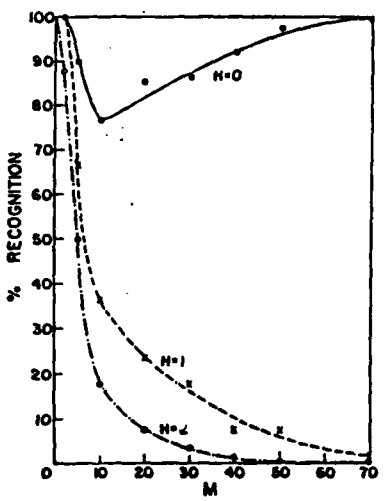

Fig. 4 Error correction capability of associative memory matrices with non-zero diagonal terms.

Real-time Fourier Transformed Holographic Associative Memory with Photorefractive Material

Chang Suk Oh, Han Kyu Park

Abstract

Hologram is formed with angular multiplexed reference beam in $BaTiO_3$. Complete image can be recalled by partial input of original stored image in correlation domain.

Summary

The optical implementation of associative memory using conventional dichromatic gelatine plate hologram and phase conjugate mirror has been investigated recently. But it is impossible to realize the real-time associative memory with these methods because the formation of hologram requires much time and stored data cannot be altered. In these respects, if photorefractive materials, $BaTiO_3$, BSO etc., are used for holographic memory, real-time associative memory can be possible at mW range.

In this letter, volume grating is formed in $BaTiO_3$ crystal (7.8 x 5.5 x 5.1mm) by intensity interference pattern of object beam and reference beam. The experimental set-up is illustrated in Fig. 1. Two original images, PARKHK and OHCHAS, are Fourier transformed by lens L1 in the $BaTiO_3$ crystal with angular multiplexed reference beams R1 and R2 at angle 7 °, 14 °, respectively, where strong beam coupling occurs between object beam and reference beam.

When the hologram is addressed by $\hat{A}_{1o}$, a partial or distorted input of original stored image A_{1o}, the output in the first order of the hologram is given by

$$\dot{A}_{1o} = (\hat{A}_{1o} * A_{1o}) \star A_{1o} + \sum_{i \neq 1} (\hat{A}_{1o} * A_i) \star A_i$$

where $\dot{A}_{1o}$ is reconstructed image at the output plane, * and $\star$ denote correlation and convolution, respectively. The first term is a desired version of the desired object (auto-correlation) while the second term is the cross-correlation noise.

In order to increase auto-correlation peak and reduce the cross-correlation, the zero order term of Fourier transformed object is suppressed and higher order terms of it are enhanced by edge enhancement mechanism. The ratio of object beam Ai to reference beam Ri is 2 : 1. Recording times of objects A1 and A2 are 12.5 sec, respectively, to prevent the erasing effect of previously stored image during the recording of second image.

The first order diffracted beam generated by the correlation between stored image and partial input image is retraced to the $BaTiO_3$ using pin hole array and conventional planar mirror which acts as a reading beam later. Phase conjugated image is inverse transformed by lens L1 and reconstructed output image is detected by CCTV camera through beam splitter BS1. And recalled image is displayed on CRT monitor. The size of original image is 21 x 4 mm (each character, 3 x 4 mm) and 5 mW He-Ne laser at 0.6328 μm is used as a light source.

Complete image is reconstructed by 1/6 partial input of stored image without any additional iteration process as illustrated in Fig. 2. It is proved that shift invariant range is wider than conventional holographic system. Moreover when $BaTiO_3$ crystal is addressed by reference beam R1, PARKHK image is recalled and by reference beam R2 , OHKHAS is recalled, separately.

From these mechanisms, our system is useful for optical implementaion of real-time associative memory and location addressable memory.

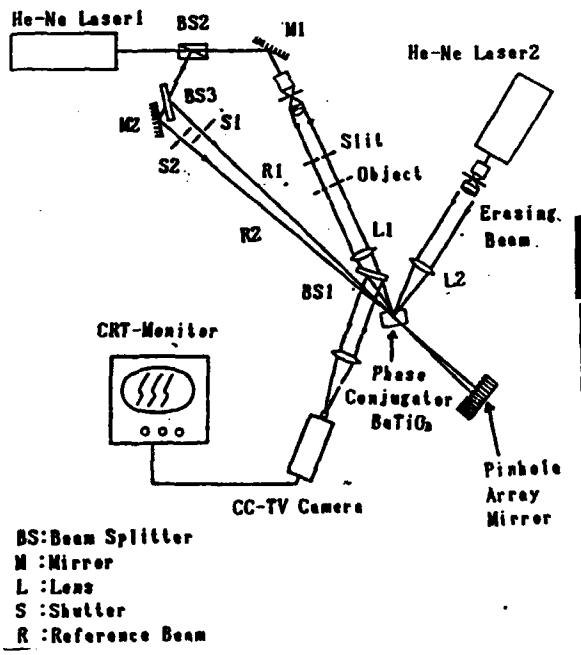

Fig. 1 Experimental set-up

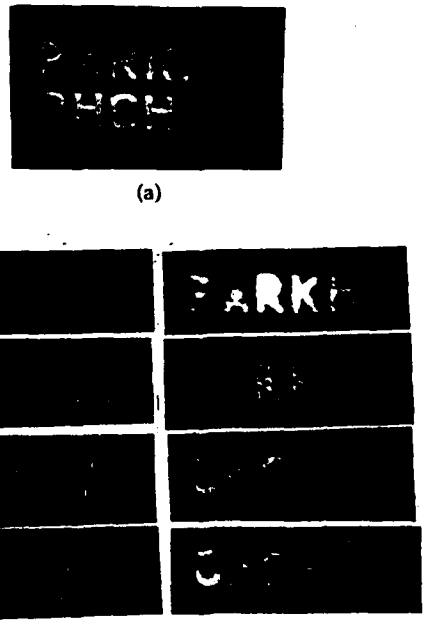

Fig. 2 (a) Stored image in $BaTiO_3$
(b) Partial input image
(c) Reconstructed image

Optical associative memory model with threshold modification using complementary vector

Bian Shaoping, Xu kebin and Hong Jing
Department of Applied Physics, Harbin Institute of Technology,
Heilongjiang, P.R.China

Summary

The inner product (or the correlation) of vectors was used to evaluate the degree of the similarity between two vectors in previous research work about content addressable associative memory[1,2]. But, generally speaking, it is required that all the stored vectors have the same magnitude. This greatly limits the number of stored vectors. The reason which the inner product can not evaluate accurately the similarity between two vectors is that the logic zero element of a vector can not recognize the logic value of the corresponding element of another vector. For example, if we intend to evaluate the similarity between vector

$$A \quad 1\,0\,0\,1\,0\,1\,0\,1$$

and the following three vectors respectively

$$B \quad 1\,0\,1\,1\,0\,1\,1\,1$$
$$C \quad 1\,0\,0\,1\,0\,1\,0\,1$$
$$D \quad 0\,1\,0\,1\,1\,1\,1\,0$$

The three inner products are

$$A*B=4 \qquad A*C=4 \qquad A*D=2 \qquad (1)$$

Obviously it can not be recognized that which of vectors B and C is more similar to vector A by the value of inner product. But if we calculate the inner product between the complementary vector of A

$$\overline{A} \quad 0\,1\,1\,0\,1\,0\,1\,0$$

which is contrast reversed version of A, and vector B, C, D respectively, we get

$$\overline{A}*B=2 \qquad \overline{A}*C=0 \qquad \overline{A}*D=3 \qquad (2)$$

In addition, subtracting the values of the inner product of (2) respectively from the corresponding ones of (1), it yields

$$\begin{aligned} A*B-\overline{A}*B&=2\\ A*C-\overline{A}*C&=4\\ A*D-\overline{A}*D&=-1 \end{aligned} \qquad (3)$$

Apparently the above expression could be a better criterion to evaluate the similarity between two vectors.

So the degree of the similarity between two unipolar binary N-dimensional vectors

$$\begin{aligned} A&=(A_1 \quad A_2 \cdots\cdots A_n)\\ B&=(B_1 \quad B_2 \cdots\cdots B_n) \end{aligned} \qquad (4)$$

is defined as the following expression

$$\begin{aligned} E&=A*B-\overline{A}*B\\ &=\sum_i A_iB_i-\sum_i \overline{A}_iB_i \end{aligned} \qquad (5)$$

the value of the second term of expression (5) represents the number of elements (or part of the Hamming distance between vector A and B) of vector A being zero and the corresponding element of B being one. It represents the difference between vector A and B in contrast to the first term.

The schematic diagram of optical associative memory model with threshold modification using the complementary vector in the correlation domain is shown in Fig.1.

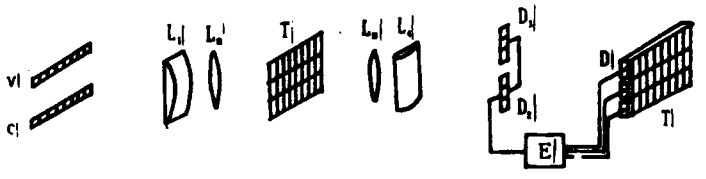

Fig.1 Diagram of the optical associative memory experiment setup

V and C represent the input vector and it's complementary vector respectively at input panel.

$L_1 \sim L_4$ constitute a vector matrix multiplier. T is stored matrix composed of array of stored vectors. D_1, D_2 are detectors oppositely connected to realize the subtraction of the two inner product of expression (5) by incorporating electronic circuit. E represents an electronic amplifier and threshold circuit. D and T constitute output display panel.

Experiment and digital simulation results are indicated in table 1. The stored matrix T is composed of the following three 8 dimensional vectors

V_1 1 0 0 1 1 0 1 0
V_2 1 1 0 1 1 0 1 0
V_3 0 1 1 0 1 0 1 1

Table 1 Experiment and digital simulation results of CAM

Input vector	Output vector	Digital simulation Max $[E_i]$	Output vector
1 0 0 1 1 0 1 0	1	$E_1 = 4$	1
0 1 0 0 1 0 1 1	3	$E_3 = 3$	3
1 1 0 0 1 1 1 0	2	$E_2 = 3$	2
0 1 1 1 1 0 1 0	3	$E_3 = 4$	3
1 1 0 1 0 0 1 1	2	$E_2 = 3$	2
1 0 1 1 0 0 1 0	1	$E_1 = 3$	1
0 1 1 0 1 0 1 0	3	$E_3 = 3$	3
1 0 0 1 0 0 1 0	1	$E_1 = 2$	1

It can be seen that by adequate thresholding the output of the CAM model is identical to the results obtained with digital simulation. An improved optical associative memory which utilizes only one memory matrix to realize search and read out vector is shown in Fig. 2. P may be composed of space light modulator.

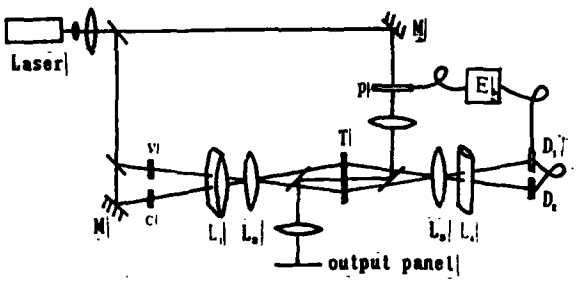

Fig. 2 Diagram of improved optical associative memory

This kind of optical content addresable associative memory (CAM) eleminates the error rate to read out. So the accuracy to read out vector is improved.

Reference

1. R. A. Athale et al., 'Optical implementation of associative memory with controlled nonlearity in the correlation domain' Opt. Lett. 11, 482-4, 1986.

Optical Table Look-up Approach to General Purpose Digital Computing

R. A. Falk, C. D. Capps and T. L. Houk

Boeing Aerospace Company
P.O. Box 3999, M/S 87-50
Seattle, WA USA 98124

Recent work [1-4] on residue arithmetic optical look-up tables using positional (one-of-many) notation has yielded significant experimental and theoretical results. In these devices, the low dispersion and parallel interconnect capability of optics is used to simultaneously address the entire table producing single step addition, subtraction and multiplication. An incoherent look-up table for performing modulo 3 addition is shown in Figure 1. The device shown is an extension of our previously demonstrated fiber optic device[2] into integrated opto-electronic technology. The device uses dual substrates; an optical substrate for routing signals and an opto-electronic substrate for performing the non-linear functions[5]. As shown, scattering patches on the optical substrate are used to route light onto pairs of photoconductive detectors arranged as AND (coincidence) gates. Equivalent gates are wire OR'ed to drive a photo-emitter supplying the input for the next operation. Operation rates of up to 10 Gops are estimated.

The positional notation table look-up architecture can be generalized to perform any multilevel logic function and allow for more than two inputs. The defining equation is given by

$$L(\epsilon_{i,j,\cdots,k}) = L(\alpha_i) \cdot \text{AND} \cdot L(\beta_j) \cdots \cdot \text{AND} \cdot L(\gamma_k)$$

where the L's have logic values of zero (off) or one (on) for the each group of lines (represented by Greek letter) with the subscripts indicating individual lines. Single subscripted functions are inputs and the multiple subscripted function is the output. The logic performed by the table depends on the final grouping of the output lines.

Examples of two-input functions include Boolean logic, modular arithmetic, single throw switches and multiple throw switches. Multiple input tables have been shown useful for conversion between number representations. Recent work[6] on coherent look-up tables has shown how they can be configured into a programmable Boolean gate. We will show how this same functionality can be generalized to any type of look-up table. Additionally, tables can be configured to perform programmable residue arithmetic, latch/register, full adder and other functions.

References

1. C.D. Capps, R.A. Falk, and T.L. Houk, "Optical Arithmetic/Logic Unit Based on Residue Arithmetic and Symbolic Substitution," Appl. Opt. 27, to be published (1 May 1988).

2. R.A. Falk, C.D. Capps, and T.L. Houk, "Optical Arithmetic/Logic Unit Based on Optical Crossbar Architecture," Appl. Opt. 27, to be published (1 May 1988).

3. P.R. Beaudet, A.P. Goutzoulis, E.C. Malarkey, and J.C. Bradley, "Residue Arithmetic Techniques for Optical Processing of Adaptive Phased Array Radars," Appl. Opt. 25, 3097 (1986).

4. S.F. Habiby, and S.A. Collins Jr., "Demonstration of a Digital Optical Matrix-Vector Multiplier Using a Holographic Look-up Table and Residue Arithmetic," Topical Meeting on Optical Computing, Tech. Dig. Series 1987, Vol. II, 66 (OSA, Washington D.C. 1987).

5. R.I. MacDonald, D.K. W. Lam, and B.A. Syrett, "Hybrid Opto-electronic Integrated Circuit," Appl. Opt. 26, 842 (1987).

6. D. Casasent, and E. Botha, "Multi-Functional Optical Logic, Numerical and Pattern Recognition Processor, " AIAA Computers in Aerospace VI Conference, 213 (Wakefield, Mass. 1987).

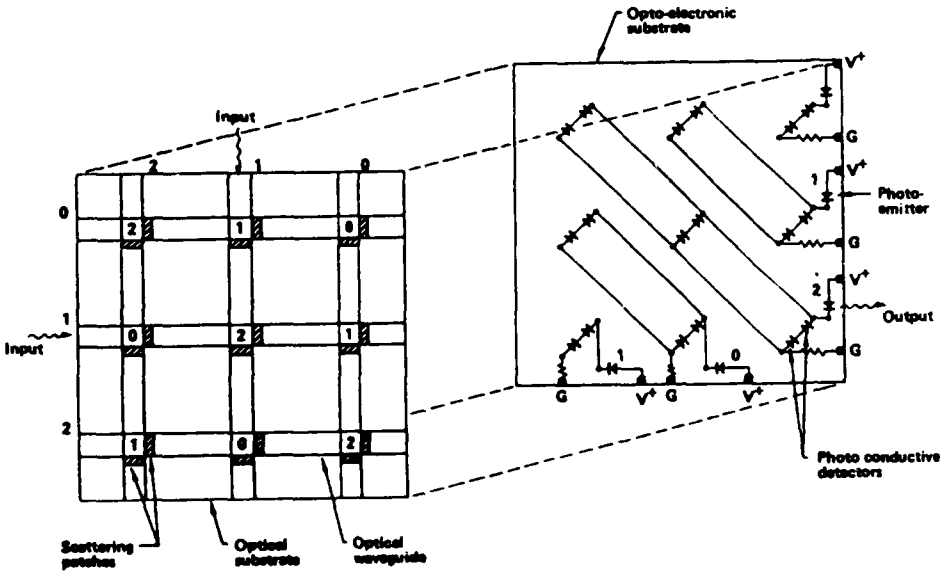

Figure 1 Modulo 3 addition table using dual substrate fabrication.

The Possible Encoding Approaches In Optical Computing

Liang Minhua Wu Shudong Wang Zhijiang

Shanghai Institute of Optics and Fine Mechanics,
Academia Sinica
P.O.Box 8216,Shanghai China

Encoding is a very important step in computing and information processing.We give encoding such a definition that it is a procedure in which operants are represented by some regular organizations of real physical states which can be detected by man.Furthermore,computing and/or information processing can be regarded as a procedure of reorganization of such real physical states.Each real physical state occupies one space-point.If a system has more space-points,it has a big capacity to represent more operants.

To evaluate such capacity of a system,we use parallelity [1],[2] which is the number of the coded operants processed in the system during a time unit.Let N be parallelity of a system,a_i be the number of the operants which have W_i word width,N_{ch} be the number of channels or space-points which can be afforded by the system,then we have two following basic equations:

$$N_{ch} = \sum a_i W_i \qquad (1)$$

$$N = \sum a_i \qquad (2)$$

On the situation of optical computing the information carriers used to encode operants are photons which have such physical characteristics:intencity(amplitude),phase,polarization and frequency.According to photon's features we make such a division in which photons have five encoding dimensions(see table 1).Pick up one element in each dimension and combine them,we will have 72 groups which have a possibility to encode operants.But possibility differs with certainty.If a certain group has a certainty of encoding ,then photons under the circumstances of that group should have a feature of reorganization ,which means that information processing can be realized in that encoding way.How to choose a encoding group is the key to optical computing.

Table 1. Photon's encoding dimension

DIMENSION	ELEMENTS
Intensity(Amplitude) dimension	two:binary and nonbinary
Space dimension	three:1-,2-,3-dimension
Time dimension	two:serial and parallel
Frequency dimension	two:mono- and poly-
Additional dimension	three:none,phase,and polarization

Providing each operant has a same word width,then

$$N_{ch} = \sum a_i W_i = aW \qquad (3)$$

$$N = \sum a_i = a = N_{ch} / W \qquad (4)$$

Let P represent processing accuracy (its unit is bit),A be dynamic range of optical information carrier,then we have:

$$P = W \log A \qquad (5)$$

so

$$N = N_{ch} \log A / P \qquad (6)$$

$$PN = N_{ch} \log A \qquad (7)$$

PN also means a processed bit-number of an algorithm,$N_{ch} \log A$ means a bit-capacity of an optical processing system, then the rule:

$$PN \leq N_{ch} \log A \qquad (8)$$

should be observed.Modulate A,the bit-capacity of a processing system can also be varied,accompanied by a variation of the system's noise-resitivity.

The parallelity of an optical system depends upon the encoding group that the system uses.From the first two basic equations and concise analysis we will naturally arrive to a conclusion:the higher the word width is,i.e. higher processing accuracy,the lower the parallelity of a system is.Encoding groups also have effects on a computing system's quality factor Q [3], i.e.

$$Q = \frac{[\text{FUNCTION}] * [\text{Vcomp}]}{[\text{STRUCTURE}] * [\text{VOLUME}] * [\text{CONSUMED ENERGY}]}$$

In the paper we discuss some typical encoding groups (time expansion encoding and space expansion encoding) and find that optics has an inclination of pipeline processing in which optical parallelism can be realized to the best.

References

[1]. P.H.Enslow,Jr.(ed.) Multiprocessors and parallel processing,Jhon Wiley&Sons,1974

[2]. Liang Minhua et al,Fundamental parallelism in optics, Beijing international topical meeting on Optical Bistability Instability Optical Computing,Beijing China 24-29 August,1987

[3]. Liang Minhua et al,Function analysis a good approach to optical computing system, Beijing international topical meeting on Optical Bistability Instability Optical Computing,Beijing China 24-29 August,1987

Friday september, 2, 14.45

SESSION 13 (Chairman H.H. ARSENAULT)

ACTIVE COMPONENTS
COMPOSANTS ACTIFS

A6 - V.N. MOROZOV : Diode lasers in optical computers.

A8 - A.J. TICKNOR, J.I. TACKARA, M.A. STILLER, G.F. LIPSCOMB and R. LYTEL : Electro-optic polymer waveguide devices.

A9 - B. IMBERT, H. RAJBENBACH, S. MALLICK, J.P. HERRIAU and J.P. HUIGNARD : Wave mixing in photorefractive GaAs and InP semiconductors : amplification, phase conjugaison and oscillations.

A10 - K.K. REBANE, R.K. KAARLI, P.M. SAARI and A.K. REBANE : Time-and-space domain holography and optical information processing based on photoburning of spectral holes.

A11 - J.I. PANKOVE : A light-emitting optical switch.

DIODE LASERS IN OPTICAL COMPUTERS

Valentin N. Morozov

P.N.Lebedev Physical Institute, Academy of Sciences of the USSR,
Moscow, USSR

Introduction.

Optical computing needs sufficiently powerful and bright sources of radiation with highly effective transformation of pumping into the coherent radiation and small size, because their number may be quite appreciable. Diode lasers provide the best choice in terms of the power assumption and size. At the same time, diode lasers have enough coherence for the image reconstruction from holograms and match filtering. Moreover, logic gates may be built around DL, and DL may be integrated on the chip with electronic control circuits, photodiodes etc. Integrated opto-electronic circuits may be designed with various logic and arithmetic operations.

Basic parameters of DL.

Today most popular are GaAlAs/GaAs and GaInAsP/InP DL. The continuous output power varies from several to several hundred milliwatt. The lifetime is more than 100.000 hours and the reliability is steadily improving. MQW DL are developed with small threshold current, high quantum efficiency and weaker temperature dependence of the threshold current. Threshold current of 1-2 mA is achieved. DL emitting perpendicular p-n junction are created.

Generation of short pulses by DL.

Short pulses of light are necessary for optical communication in optical computer and for switching logic gates. Optical commu-

nication requires a bandwidth of several GHz, and logic gates are switched by picosecond or even short pulses. Controlled generation of light pulses with 10-100 ps duration and up to 10 GHz frequency is provided by high-frequency current modulation and psec-long light pulses are generated by means of various mode locking techniques. The summary results of the generation of short pulses by DL are presented.

Writing and reconstruction of holograms by DL.

Historically, the holograms studies were using gas lasers radiating in visual range due to their high coherence and the availability of high resolution photographic material sensitive to the visible-light spectrum. DL devices for optical computing and storage based on holographic technique needs to develop proper photoplate and experimental experience. Results for recording and reconstruction of holograms with DL are reported. Optical computing demands optical memory for fast input of digital picture to processing scheme. The holographic storage gives possibilities for data input rate of 10^{12} bit/sec corresponding to throughput of future optical computing. Basic design of holographic memory with DL is reported.

Integration of holograms with optical waveguide.

The possibilities of integrating of holograms with optical waveguide is of great importance due to the fact that integrated optical modulator, switches and deflectors have high speed and small control voltage. Such an integration improves functional capabilities of optoelectronic integrated circuits. If DL are us

as radiative source small-size multi-functional optical computing circuits become feasible. The results on waveguide hologram recording and reconstruction are reported. High efficiency of 60% is a remarkable feature of waveguiding holograms. The results of match filtering with waveguided holograms are presented.

Optical logic gate on DL.

DL-based optical logic gates were proposed by N.Basov as early as in 1965 and were implemented some years later. The first integrated optical logical scheme on DL will be shown. Development of DL technology and improvement of their parameters took 20 years. It was largely motivated by the need to introduce DL into fiber communication and videodisk system. It seems reasonable to turn again to the DL-based logic gates because they are the best in terms of the requirements to digital logic gates, on the one hand and enable integration with electronic control circuits and photodiodes within the same crystal, on the other. The properties of bistable diode laser will be reported. Version of DL logic gates combined with photodiode is discussed to improve fan-in and fan-out characteristics of optical logic gates.

Integration of DL with electronic circuits.

The strategy of designing components for optical computing must take into account the experience accumulated by electronic technology. The logic components for optical computing should enable integration into a single integrated circuit. The state of art of integrated optoelectronics circuits is discussed briefly. The scheme of optical interconnection in VLCI circuits based on DL waveguides holograms and electronic counterpart will be presented.

Conclusion.

The treatment of possibilities of DL demonstrates that they provide a unique way for optical computing. The development of integrated circuits having optical input and output would be an important step towards high performance optical computers.

Designing of large-scale integrated circuits having optical input and output and connected to the optical schemes would lead to joining the philosophies of electronic and optical computers into a single one featuring the merits of both.

References.

1. N.Basov. Nobel lecture 1964 Uspekhi Fiz.Nauk,v.85,N 4,p.585,196
2. K.Lau, A.Yariv. Ultra-high speed semiconductor lasers, IEEE J. of QE, v.QE-21,N 2, February 1985.
3. P.Vasiliev, V.Morozov, Yu.Popov, A.Sergeev. "Subpicosecond pulse generation by a tandem-type AlGaAs DH laser with colliding pulse mode locking", JEEE J.QE, 1986, vol.22,N 1,p.149-152.
4. V.Morozov, A.Putilin. "Waveguide holograms for match filtering systems", Proc. OFC-JOOC-87, Reno, Nevada, 1987, TUQ-41 p134
5. N.Basov, W.Culver, B.Shan. "Application of lasers to computer", in Laser Handbook, North-Holland, 1972,p.1051-1080.
6. O.Wada, T.Sakuzai, T.Nakagami. "Recent progress in optoelectron integrated circuits", IEEE QE, v.QE-22, N 6, June 1986.
7. H.Elion, V.Morozov. "Optoelectronic switching systems in telecommunication andcomputer", Marcel Dekker, N.Y. 1984.

Electro-optic Polymer Waveguide Devices

A. J. Ticknor, J. I. Thackara, M. A. Stiller, G. F. Lipscomb, R. Lytel

Lockheed Research and Development Division

SUMMARY

Thin polymer films are strong candidate materials for constructing electro-optical (EO) and nonlinear optical (NLO) waveguide devices. These films can be engineered to have good optical qualities, and they can have EO figures-of-merit comparable with lithium niobate. They have low microwave dielectric constants compared to more conventional EO materials, allowing the propagation of microwave signals and optical signals to be better matched, promising much higher bandwidth devices for a given level of development. Standard methods for forming these films are simple spin-coating or dip-coating. There is generally no need for extreme temperatures or pressures or for crystal-growing techniques in the processing of these films. These properties make polymer films attractive materials for optical waveguides. In this presentation we shall describe our work on utilizing the properties of these films in the construction of EO waveguide devices and some results of these efforts.

Glassy (amorphous) polymer films do not posess a second-order polarizability. Hence, after formation by conventional coating methods, these films do not exhibit a linear EO effect. To make the films suitable for EO devices, one must induce a molecular alignment to create a macroscopic second-order polarizability. Singer, Sohn, and Lalama (Appl. Phys. Lett. 49, 248 (1986)) described an electrical poling method to accomplish this. The poling is done by heating the film above its glass-transition temperature, applying a strong electric field to partially align the dipoles of the polymer molecules, and cooling the film with the field applied to "freeze" the alignment into the film. When the field is removed, the alignment remains, and the film can exhibit linear EO effects.

The microscopic linear polarizability of most optically useful polymers is anisotropic. Consequently, the poled films exhibit uniaxial birefringence, with the extraordinary axis oriented along the direction of the poling field and with an extraordinay index of refraction higher than the index in the unpoled film. This effect can be used to create channel waveguides by selectively poling the film only in the regions of the desired channels. These areas can then function as channel waveguides for light polarized parallel to the original poling field. By poling the film in a given pattern,

the EO susceptibility and waveguide pattern are created in a single process. This gives a profoundly simple way to fabricate, and particularly to duplicate, waveguide devices.

We have used this selective-poling technique to construct some common waveguide devices in films made from polymer samples provided by Hoechst-Celanese Research Division (HCRD). These devices include traveling-wave phase modulators, Y-branch interferometers, and multimode directional couplers. We have demonstrated guiding in the channels of these devices and EO operation of their intended functions, including traveling-wave phase modulation at frequencies up to one gigahertz. Using this selective poling technique to define channel waveguides promises an easier route to the production of waveguide devices requiring more sophisticated patterning. The process in general also hints at the possibility of stacking layers of patterned films to produce three-dimensional collections of waveguide devices. With these qualities in mind, we have designed and are fabricating EO multiplexers, demultiplexers, and crossbars that take some advantage of these design freedoms. The optical switches we have designed promise greater crosstalk rejection than is found in the simpler patterns of conventional EO waveguide switches, and the concepts developed in the design of these devices also show ways of switching optical signals between layers. In this presentation we shall review our recent work on poled-polymer channel-waveguide devices, and report performance results and characteristics for these devices.

VAVE MIXING IN PHOTOREFRACTIVE GaAs AND InP SEMICONDUCTORS: AMPLIFICATION, PHASE CONJUGAISON AND OSCILLATIONS

B. Imbert, H. Rajbenbach, S. Mallick,
J. P. Herriau and J. P. Huignard

Thomson-CSF, Laboratoire Central de Recherches,
Domaine de Corbeville, B. P. 10, 91401 Orsay Cedex, France
Telephone: (1) 60.19.76.56

The photorefractive behavior of semiconductor materials is receiving much attention for applications involving high nonlinerarities at vavelengths compatible with solid state lasers. Bulk GaAs and InP semiconductors are currently examined with regards to achieving efficient interactions in vave mixing experiments.[1-4]

In this paper, ve present the characteristics of GaAs:Cr and InP:Fe photorefractive amplifiers vith applications to image amplification, phase conjugation and self-induced oscillations.

The experimental set-up for two beam coupling is shovn in Fig. 1. A lov power cv diode pumped YAG laser (40 mW, λ = 1.06 µm) provides a signal beam I_{s0} and a pump beam I_{p0} vhose frequency is Doppler shifted by reflection on the piezomiror M (moving grating recording mode). The experimental gain coefficient is measured as a function of the most influencing parameters (fringe spacing Λ, input beam ratio β, pump beam intensity I_{p0}, fringe velocity v and externally applied voltage V_0). Gain coefficients as high as 6-7 cm^{-1} are observed for the first time in semiconductor GaAs:Cr for the folloving optimum recording conditions: Λ = 18 µm, $\beta > 10^3$, $I_{p0} \simeq 50$ mV/cm², v = 1 mm/sec and V_0 = 5 kV (interelectrode distance 5.8 mm). Fig. 2 represents the exponential gain coefficient as a funtion of the fringe spacing and shovs the bandpass type characteristic of GaAs amplifiers.

The large values of the gain obtainable in a vide range of recording conditions[4] permit the amplification of near infrared complex vavefronts. A binary photographic transparency vas inserted across the signal beam path; the amplified image is shovn in Fig. 1.

Self-induced optical ring cavities can be implemented vhen providing the GaAs amplifier vith an optical feedback (Fig. 3). The oscillation is self-starting at the optimum matched frequency detuning (= 10 Hz). No input signal is necessary since the optical noise due to the pump beam is sufficient to generate a veak probe beam vhich is then amplified after each round trip in the cavity. When the direction M_1-M_2 is chosen so that the fringe spacing $\Lambda = \lambda/2\sin\theta$ is optimum, then more than 20% of the pump beam is transfered into the ring oscillator in less than 30 msec ($I_{p0} \simeq 50$ mV/cm²).

Phase conjugation is obtained vhen a third beam I_{R0} is added to the configuration of Fig. 1. Beam I_{R0} is contrapropagating to I_{p0} and generates the phase conjugate replica I_C of the sinal I_{s0}. The reflectivity $R = I_C/I_{s0}$ measurements vill be presented. In particular, the conditions for vhich $R > 1$ vill be discussed theoritically and experimentally.

REFERENCES:

(1) A. M. Glass, A. M. Johnson, D. H. Olson, V. Simpson and A. A. Ballman, Appl. Phys. Lett. 44, 948 (1984)
(2) M. B. Klein, Opt. Let. 9, 350 (1984)
(3) G. Albanese, J. Kumar and V. H. Steier, Opt. Lett. 11, 650 (1986)
(4) B. Imbert, H. Rajbenbach, S. Mallick, J. P. Herriau and J. P. Huignard, Opt. Lett. 3 (1988)

ACKNOVLEDGMENTS

The authors vish to thank the DRET (Direction des Recherches et Etudes Techniques) for partial support of this work.

FIGURE CAPTIONS:

Fig. 1 Experimental arrangement of two beam coupling with moving fringes at $\lambda = 1.06\ \mu m$ in photorefractive GaAs:Cr crystals. M, piezomirror; ND, variable neutral density; S, shutter; D, detector; AI, amplified binary image; crystal size 5.8 x 4.7 x 3.6 mm

Fig. 2 Exponential gain coefficient as a function of the grating fringe spacing Λ at optimum fringe velocities, and for different applied voltages V_0. ($\blacksquare, \Delta, \bullet$) experimental points; ——— experimental plot ($I_{R0} = 50\ mW/cm^2$, $v = v_{opt}$; $\beta = 10^3$); ----- theoretical curve for $V_0 = 5$ kV.

Fig. 3 Self-induced optical ring cavity with a photorefractive GaAs:Cr amplifier. The rise time is about 30 msec.

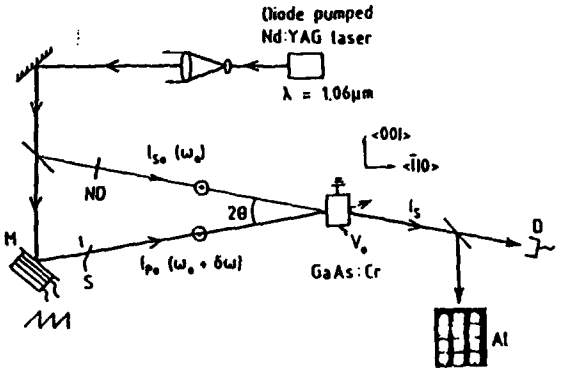

Fig. 1

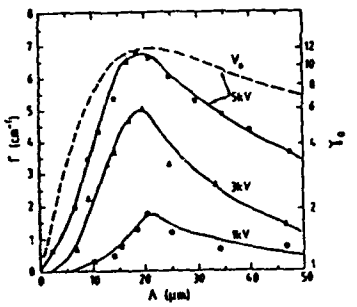

Fig. 2

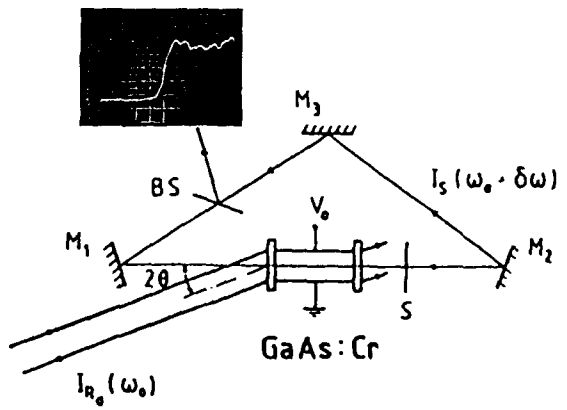

Fig. 3

TIME-AND-SPACE DOMAIN HOLOGRAPHY AND OPTICAL INFORMATION PROCESSING BASED ON PHOTOBURNING OF SPECTRAL HOLES

K.K.Rebane, R.K.Kaarli, P.M.Saari and A.K.Rebane

Institute of Physics, Estonian SSR Academy of Sciences, Tartu 202400, USSR

1. High spectral selectivity peculiar to photochemical hole burning enables the Fourier spectrum of pulsed light fields to be recorded persistently in the medium. On this basis the common holography has been generalized to the time dimension, i.e. to recording and playback of the temporal evolution of object scenes [1-3].

2. Isotropic distribution of photoactive molecular impurity centres in hole burning media enables the polarization of the Fourier components to be recorded. On this basis further generalization results in such a holography which precisely corresponds to the exact meaning of the term - "complete recording", i.e. a holography where restored light fields are completely identical to the stored ones and play back both spatial and temporal dependences of the electric vector of the object field [4].

3. Recording of object signals is based on pulsed photochemical hole burning [3], readout, on the phenomenon called photochemically accumulated photon echo [1]. Temporal duration of the scene is limited by the irreversible phase relaxation time constant T_2 of the resonance transition in impurity molecules which in the case of the media used for experiments is some nanoseconds. Temporal resolution is limited by the reversible dephasing time constant T_2^* (reciprocal width of the inhomogeneous absorption band) and comes to some femtoseconds in the case of the media used.

4. The physical background of the theses listed will be presented in the paper and possible applications of the time-and-space domain holography for optical data-processing will

also be discussed; such as:

- processing of picosecond signals: (a) algebraic summation; (b) spatial-temporal convolution of signals by reading the hologram of one signal by the other signal; (c) filtration of spatial and temporal frequencies by transmitting the signal through the filter-hologram; (d) wavefront conjugation and time reversal of the signal by reading the conjugated wave from the hologram;

- a synthesis of picosecond optical signals through the scattering of pulses on a hologram constructed by means of PHB on exposure to a tunable laser or some other light source with appropriate spatial-spectral parameters;

- recognition of picosecond-domain events - the generalization of the holographic method of image recognition. If a light signal is delivered to the hologram, which coincides with one of the signals recorded on it earlier, and if the outcoming light is focussed, then a δ-shaped pulse appears at a definite point of the focal plane;

- playback of an event by its fragment through the generation of a phantom event and constructing an associative memory;

- parallel information storage (and playback) into the spectral memory.

References

1. A.K.Rebane, R.K.Kaarli, P.M.Saari, Pis'ma JETP, 38, 320, 1983.
2. P.Saari, R.Kaarli, A.Rebane, J.Opt.Soc.Am. B3, 527, 1986.
3. A.K.Rebane, R.K.Kaarli, P.M.Saari, Opt. i Spektr., 55, 405, 1983.
4. P.M.Saari, R.K.Kaarli, R.V.Sarapuu, H.R.Sõnajalg, J.Quant. Electr., Special issue on phase conjugation, 1988, in press.

A Light-Emitting Optical Switch

Jacques I. Pankove
Center for Optoelectronic Computing Systems
University of Colorado, Boulder 80309

Abstract

The device consists of a pnpn structure where the outer two pn junctions are forward-biased heterojunctions, while the inner pn junction is a reverse-biased homojunction. The inner two layers are made of a direct-gap material, while the outer two layers have a larger energy gap. In operation, the reverse-biased central junction breaks down when light is incident on the device. Upon breakdown, the forward-biased heterojunctions inject a high density of electron-hole pairs that recombine radiatively in the narrow-gap, central layers. The structure can be shaped into a colinear surface-emitter, where the triggering light enters one surface while the output emerges from the opposite surface. In an alternate arrangement, the structure forms a Fabry-Perot cavity by cleaving opposite ends, while the triggering light enters through one of the wider gap surfaces. Such a structure forms an injection laser. The triggering light may be of the same or shorter wavelength as the emitted light. A trade-off is available between efficiency and response time.

Friday september, 2, 17.00

SESSION 14 (Chairman S. ISHIHARA)

OPTICAL PROCESSING CONCEPTS
CONCEPTS DE TRAITEMENT OPTIQUE

C_7 - M.W. HANEY and R.A. ATHALE : Optical techniques for increasing the efficiency of tree search algorithms.

OPTICAL NEURONAL PROCESSORS
PROCESSEURS OPTIQUES NEURONAUX

D_7 - H.J. CAULFIELD : How to train a fixed interconnect holograhic neural network.

PARALLEL PROCESSORS
PROCESSEURS PARALLELES

E_{13} - K.S. HUANG, B.K. JENKINS and A.A. SAWCHUK : Optical symbolic substitution and pattern recognition algorithms based on binary image algebra.

E_{14} - D. CASASENT and E. BOTHA : A unified optical symbolic processors.

CONCLUSION OF THE MEETING
CLOTURE DE LA REUNION

A.W. LOHMANN : Conclusions on Optical Computing.

Optical Techniques for Increasing the Efficiency of Tree Search Algorithms

Michael M. Haney and Ravindra A. Athale

BDM Corporation
7915 Jones Branch Drive
McLean, VA, USA, 22102

ABSTRACT

Optical implementations of Boolean matrix operations are proposed to increase the search efficiency in forward checking algorithms for consistent labeling problems.

SUMMARY

Introduction/Background

The tree search or graph matching problem is ubiquitous in Artificial Intelligence. Applications areas include: scheduling, theorem proving, and scene labeling/interpretation for computer vision. In general these problems have exponential time complexity and become intractable rapidly as the number of variables grows. A large body of research has been dedicated to developing "tree-pruning" techniques, which use forward checking to increase the efficiency of the search. These techniques attempt to avert the combinatorial explosion by using the relational constraints of the problem in local graph operations (arc and path consistency checks) to reduce the complexity of the search tree. Under worst case assumptions, forward checking itself requires exponential time; however, for many real world problems, it does increase the efficiency of the search [1].

A tree search can be formulated as a *consistent labeling* (CL) problem [2], in which the goal is to assign a *label*, from a set of L elements, to each *unit*, from a set of U elements. U corresponds to the number of levels in the search tree and L corresponds to the number of branches at each node of the tree. Not all of the L^U possible assignments are permitted by the problem constraints and the goal of a forward checking algorithm is to rule out, in advance, those partial labelings which cannot possibly contribute to a CL, where a CL is defined as a labeling of all U units in which all of the labelings are simultaneously compatible with the problem constraints.

The initial problem constraints are given as tuples of units which mutually constrain each other, along with the sets of allowed labels for each tuple. Here we restrict our attention to *binary constraints*. Many interesting problems in the application areas mentioned above can be cast as CL problems with binary constraints [3]. For such problems the constraint data can be represented as LxL Boolean matrices, $R_{i,j}$, one for each pair of units (i,j) that constrain each other [2]. The L rows correspond to the labels of unit i and the L columns correspond to the labels of unit j. The presence of a 1 in a matrix indicates that the labeling of that pair corresponding to that row and column is allowed by the problem's initial binary constraint. Note that if two units are not given to constrain each other directly, then the initial constraint matrix corresponding to that pair would consists of all 1's and contains no useful information about how that pair of units might ultimately constrain each other through induced constraints.

In this paper we investigate the potential for improving the efficiency of the search by applying highly parallel optical Boolean matrix operations to the set of constraint matrices. The purpose of these operations is two-fold. First, we want to remove, from the initial set of binary constraints, as many as possible of those that do not contribute to any consistent labeling. This improves the efficiency of the search by reducing the size of the domain of allowed pair labelings that must be checked during the search procedure. The second purpose in manipulating the constraint matrices is to make explicit those unary constraints that are implied by the initial set of binary constraints. These induced unary constraints can then be applied directly in the search process to prune the search tree.

Optical Matrix Manipulations for Pruning the Search Tree

It has been suggested that the Boolean matrix operations of intersection and composition (Boolean matrix multiplication) can be used in forward checking [2]. In this paper we propose that these operations can be combined with two others: unary constraint detection and unary constraint propagation, to compute arc and

path consistent networks which will increase the efficiency of the search. Furthermore, for increased speed, all of these operations can be implemented optically, using established low accuracy analog linear algebraic techniques, followed by simple electronic nonlinearities.

The use of intersection and composition in a forward checking operations is as follows. Given a constraint matrix relating units i and j, $R_{i,j}$, and other constraint matrices $R_{i,k}$ and $R_{k,j}$, we can create a new constraint matrix:

$$R'_{i,j} = R_{i,j} \$ R_{i,k} \& R_{k,j}, \qquad (1)$$

where "$" indicates the intersection operation, which is an element by element AND, and "&" indicates a composition operation, which is a Boolean matrix multiplication. Composition takes precedence over intersection. The induced relation R' replaces R and is a stronger constraint between units i and j because it now takes into account the influence of an intermediate unit (k) along the path and not just the single arc between the units. Even stronger constraints can be derived by intersecting $R'_{i,j}$ with other induced constraint matrices derived from the composition of matrices along other paths between i and j. In practice, this operation would be performed on all constraining pairs of units to some level of path length.

The operation of unary constraint detection is accomplished by examining each of the current set of binary constraint matrices for the presence of a row or column containing only 0's. This situation indicates that the unit associated with that matrix can never be assigned the label corresponding to that row or column. This can be detected by performing an OR operation across all rows, and then all columns, for each of the constraint matrices. If an all zero row or column is found, then the resulting induced unary constraint can be propagated to all other contraint matrices that share the same unit by zeroing out the associated row or column associated with that label and unit. This may lead to the discovery of new induced unary constraints which can be detected and propagated until a fixed point is reached.

Note that Equation (1) can also be used to generate new binary constraint matrices which relate pairs of units not originally given to constrain each other. These new matrices are included in the process because they may produce new unary contraints which can be propagated into the original set of constraint matrices, as well as be used to directly prune the search tree.

The operation of intersection can be implemented optically via image multiplication by representing the constraint matrices as binary images, while composition can be implemented by analog optical matrix multiplication, followed by thresholding to restore the levels to 1 or 0. Unary constraint detection is achieved by focusing the light passed through the matrices along each dimension separately and detecting the presence of light with a 1-D threshold detector array. This achieves the required OR operation across all rows or columns simultaneously. To propagate the induced unary constraint the resulting thresholded 1-D data, R(i), is transformed into a light signal, spread out into a 2-D array, and multiplied by all other matrices, $R_{i,*}$, which share the unit that has the unary constraint. For constraint matrices which involve the unit i as the column index, the transpose, $R^T_{*,i}$ is used.

Conclusion

Low accuracy, optical matrix processors with nonlinearities (optical or electronic) have been proposed by Guilfoyle for Optical Numerical Computations, by Psaltis and Farhat for Optical Neural Nets and by Caulfield for Logical Inferencing. In this summary we outlined novel applications of these architectures to a generic and important problem in symbolic computing, namely tree search. Two new optical Boolean matrix operations were also defined that are critically important to problems at hand.

References

[1] Haralick, R. M. and Shapiro, L. G., IEEE Trans. PAMI, Vol. PAMI-2. No. 3, May 1980, pp. 193-203.

[2] Mackworth, A. K., Artificial Intelligence 8 (1977), pp. 99-118.

[3] Haralick, R. M. and Shapiro, L. G., IEEE Trans. PAMI, Vol. PAMI-1. No. 2, April 1979, pp. 173-183.

HOW TO TRAIN A FIXED INTERCONNECT HOLOGRAPHIC NEURAL NETWORK

H. John Caulfield
Center for Applied Optics
The University of Alabama in Huntsville
Huntsville, AL 35899

Page oriented holographic memories offer the potentiality of truly massive interconnections. In particular, it should not be difficult to make somewhere between 10^6 and 10^{12} interconnections in parallel. This gives optics a capability that electronics can never match. On the other hand, this interconnection pattern is fixed. For many purposes, this is quite satisfactory. Learning can be done off line and incorporated into holograms. The fixed learning holograms can carry out all of the operations for which they were trained and, of course, innovate when confronted with new situations not totally different from those used in its training. These neural networks can have many uses, but the most obvious of them is controlling any sort of plant or operation.

There are a variety of applications, however, in which we do not wish to encode off line learning into the hologram. We mentioned two of these here. First, we might wish to make the neural network adaptive. That is, we might wish to let it retain the ability to learn. Alternatively, we might wish to avoid the necessity of making a new hologram for each new set of learned behaviors. Perhaps we could make one hologram that connects everything to everything and then find some other way to have that system learn specialized tasks. Of course, if there is a general solution to either of these needs, it will apply to both. We offer below such a general solution.

Before proceeding, we do need to remark that optics allows us to adjust the "threshold" of each neuron in parallel simply by shining the proper pattern of light on the nonlinear optical elements. While this is

not a good way of doing adaptive learning, it is a good way of directing attention. By proper patterning, we can favor some operations over others. This is somewhat akin to postulated methods whereby biological neural networks change function when bathed in the appropriate chemical, e.g. adrenalin.

We must first consider a two layer neural network. By spacing one spatial light modulator in contact with the first layer and a second one in contact with a second layer, we can easily show that we can program a vector outer product or rank one matrix into the interconnections between those layers. The reason we use a spatial light modulator is that a 2-D array of neurons is required to utilize the tremendous interconnect capability of optics.

Using our favorite learning algorithm (whatever that may be), we can derive a matrix which does the best job of converting the input into the desired output. By doing a Singular Value Decomposition (SVD) on that matrix, we can produce the best rank one representer of that matrix and encoded on the spatial light modulators.

Let us now add a new layer. The interconnects from the input to the second layer will be fixed as those values that the SVD of the derived matrix produced. Now, we input information into the usual place and vary only the interconnections between the second and third layer. Using our favorite learning method, we can arrive at an optimum matrix for converting the input to the system into the best possible output from the third layer. We then SVD that matrix and insert it into the system on the spatial light modulators.

It is clear that this process can be continued until we achieve satisfactory performance. Experienced users of SVD know that the singular values fall off very rapidly. This is true for the linear addition implied in SVD. With the nonlinear steps involved here, it seems likely that we need

far fewer than the in layers it would take to insert as many modulation values as we have interconnects. One expects to need only a few layers to accomplish most purposes. Experimental tests of this approach are shown.

Of course, if we have a sufficient number of neurons and interconnections, we can implement the first several or many terms of the SVD in parallel spatially. We simply divide the input and output arrays into regions which individually implement the outer products contributing to a matrix we have designed. Finally, of course, the first method described (pipelining) and the second method (parallel) are mutually compatible. We might, for example, implement the first four terms in the SVD in parallel in each layer and then pipeline layers of these.

Clearly, massive fixed interconnect holograms can be used to make massively interconnected neural networks that are adapted if we introduce modulation with spatial light modulators.

Optical Symbolic Substitution and Pattern Recognition Algorithms Based on Binary Image Algebra

K. S. Huang, B. K. Jenkins, A. A. Sawchuk
Signal and Image Processing Institute, Department of Electrical Engineering,
University of Southern California, Los Angeles, CA 90089-0272, USA

Summary

Binary image algebra (BIA), a unified systematic complete theory of parallel binary image processing [1], also provides a unified spatial logic of digital optical computing for describing symbolic substitution, cellular logic and Boolean logic in parallel [2]. Symbolic substitution has been used to implement logic, arithmetic, communication and simulating a Turing machine [3]; but its implementation of some operations (e.g. parallel binary arithmetic) is relatively complicated to other BIA implementations [2]. In this paper we further suggest some BIA algebraic techniques and pattern recognition algorithms, including a shift, scale and rotation invariant algorithm, to improve the speed, flexibility and complexity of symbolic substitution.

A symbolic substitution rule involves two steps: 1) recognizing the locations of a certain spatial search-pattern within the 2-D input data, and 2) substituting a new replacement-pattern wherever the search-pattern is recognized. As illustrated in Fig. 1, BIA can be used to realize a symbolic substitution rule defined by:

$$(X \circledast R) \oplus Q = ((X \ominus R_1) \cap (\overline{X} \ominus R_2)) \oplus Q = \overline{(\overline{X} \oplus \hat{R}_1) \cup (X \oplus \hat{R}_2)} \oplus Q \tag{1}$$

where X is the 2-D input data, $R = (R_1, R_2)$ is the reference image pair corresponding to the search-pattern (R_1 and R_2 define the foreground and the background of the search-pattern respectively), $\hat{R}$ defines a reflected reference image given by $\hat{R} = \{(-x, -y) \mid (x, y) \in R\}$, Q is the reference image corresponding to the replacement-pattern, "$\circledast$" denotes the hit or miss transform which is the pattern recognizer, "$\ominus$" denotes the erosion operation, and "$\oplus$" denotes the dilation operation which is the pattern replacement operator. To work with more than one rule (say p substitution rules) for practical applications, a symbolic substitution system (Fig. 2) produces several copies of the input X, provides p different recognizer-substituter units, and then combines the outputs of various units to form a new output. Thus, a symbolic substitution system is implemented by

$$\bigcup_{i=1}^{p} (X \circledast R^{(i)}) \oplus Q^{(i)} \tag{2}$$

where $R^{(i)}$ and $Q^{(i)}$, $i = 1, 2, ..., p$, are the reference image pairs and replacement patterns in the i^{th} symbolic substitution rule. This, then, is the BIA formula for general symbolic substitution.

However, in many cases the above form is inefficient and can be reduced to a relatively simpler form or implemented in a more efficient way by using some BIA algebraic techniques. Here are some examples: 1) the full recognition can be implemented by only the background or foreground recognition under certain conditions; 2) if $Q^{(i)} = \phi$, the i^{th} symbolic substitution rule in Eq. (2) is not needed (e.g. the four rules of binary subtraction in simple intensity coding of arithmetic data can be reduced to only two rules [2]); and 3) if $Q^{(i)} = Q$ for all $1 \le i \le p$ (this happens in those cases that a class of search-patterns is defined by a set of reference image pairs $R^{(i)}$, $i = 1, 2, ..., p$), we should combine the results of the hit or miss transforms first and then replace them by the same replacement-pattern Q instead of implementing p substitution units for realizing the same substitution step, i.e.

$$(\bigcup_{i=1}^{p} X \circledast R^{(i)}) \oplus Q. \tag{3}$$

The practical difficulty with the implementation in Eqs. (2) and (3) is that the hit or miss transform is only efficient for the shift invariant recognition and would require a large number of intricate reference image pairs to perform the recognition step in the presence of changes in scale, rotation or both. Thus, it might be too costly to implement scale and rotation invariant recognition of intricate patterns for symbolic substitution based on the above formula. For example, if we want to substitute all "square patterns" in an input image by the same character "S", it would be very inefficient to use the above symbolic substitution implementation techniques.

To solve this kind of scale and rotation invariant problem, here we recognize all the desired patterns by reversing the growing procedure of a family of patterns. This family defines all patterns in the presence of changes in scale, rotation or both, and transforms all the desired patterns into their original seeds, which are isolated single image points. We have developed a description of this procedure in terms of BIA. For brevity, here we describe only the case of shift and scale invariant recognition. Suppose we want to recognize all square patterns with different scales and locations in the input image X (e.g. Fig. 3(a)) and to produce the output image Y (e.g. Fig. 3(b)). The procedure is: 1) determine a growing sequence of the desired patterns T_i (e.g. Fig. 3(c)), where $0 \le i \le m$ and the largest size of the desired patterns is $m \times m$; 2) find a small set of *good* reference image pairs $\{R(\theta)\}$ (e.g. Fig. 3(d) has only 5 small reference image pairs for recognizing all square objects with different scales) satisfying some criteria, where each reference image pair in $\{R(\theta)\}$ corresponds to a possible neighborhood of a given *foreground* image point in a pattern T_i, $1 \le i \le m$, whose previous state in the pattern T_{i-1} is a *background* point; 3) transform the desired patterns T_i, $i = 1, 2, ..., m$, in the 2-D input image $X = X(t_0)$ into their original seeds (i.e. T_0 which contains one and only one foreground image point) by the recursive relation $X(t_{k+1}) = X(t_k) / \bigcup_{\theta \in \Theta} X(t_k) \circledast R(\theta)$, where $0 \le k \le m$; and 4) pick up the original seeds by $Y = X(t_m) \circledast Q$, where Q (Fig. 3(e))

is a reference image pair with one and only one foreground image point at the center and Y is the final recognition output. By selecting *good* reference image pairs associated the growing sequences of rotation patterns, we can extend shift and scale invariance to include rotation invariance in a similar way. This algorithm can efficiently reduce the computation complexity for a certain class of pattern recognition and symbolic substitution problems; their computation times depend only on the diameter of the largest desired pattern, but not on the number of patterns nor the size of the whole image.

A digital optical cellular image processor (DOCIP) [1] [2] implements all the above algorithms of symbolic substitution and pattern recognition in a flexible and efficient way compared to a symbolic substitution processor (Fig. 2) with p fixed recognizer-substituter units. The DOCIP programming for these algorithms will be illustrated.

References

[1] K. S. Huang, B. K. Jenkins, A. A. Sawchuk, "Binary Image Algebra and Optical Cellular Logic Processor Design," submitted to *Computer Vision, Graphics, and Image Processing.*

[2] K. S. Huang, B. K. Jenkins, A. A. Sawchuk, "An Image Algebra Representation of Parallel Optical Binary Arithmetic", submitted to *Applied Optics.*

[3] K.-H. Brenner, A. Huang, and N. Streibl, "Digital Optical Computing with Symbolic Substitution," *Applied Optics*, Vol. 25, pp. 3054-3060, 1986.

Acknowledgements

This research was supported by the Air Force Office of Scientific Research under grant AFOSR-84-0181, by the Office of Naval Research under contract N00014-86-K-0602, and by an IBM graduate fellowship.

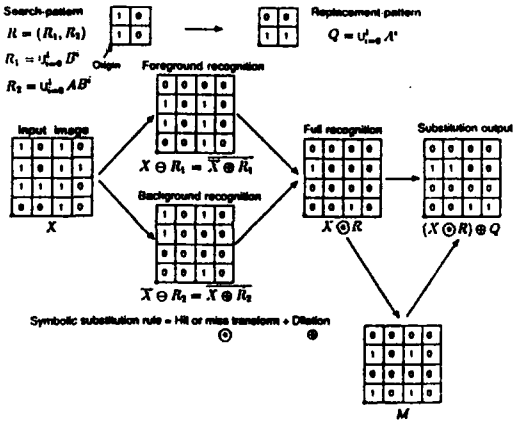

Figure 1. BIA representation of symbolic substitution. The optional mask M is for controlling the block search region.

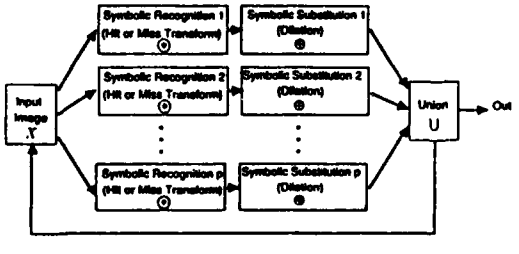

Figure 2. A symbolic substitution system with p symbolic substitution rules.

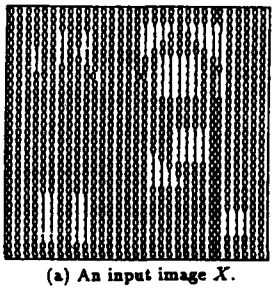

(a) An input image X.

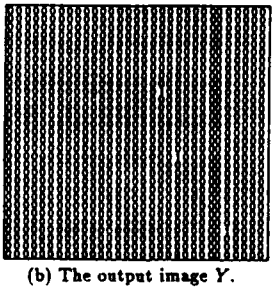

(b) The output image Y.

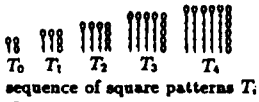

(c) The growing sequence of square patterns T_i, $o \le i \le 4$.

(d) A set of *good* reference image pairs $\{R(\theta)\}$ for square patterns with different scales.

1: foreground points with value 1
b: background points with value 0

(e) The reference image pair Q.

Figure 3. A shift and scale invariant pattern recognition of square patterns.

Toulon Optical Computing Conference, August 1988

A UNIFIED OPTICAL SYMBOLIC PROCESSOR

David Casasent and Elizabeth Botha
Carnegie Mellon University
Center for Excellence in Optical Data Processing
Department of Electrical and Computer Engineering
Pittsburgh, Pa 15213 , USA

Abstract

An optical symbolic processor that performs logic, numeric, morphological and propositional calculus operations is described and initial laboratory results are presented.

Summary

An optical correlator can be used to achieve the symbol recognition and symbolic substitution steps in a symbolic processor. A cascaded optical correlator architecture that can achieve this is reviewed. The basic system uses one fixed set of filters (one for each input symbol digit pair) and a second set of multiple filters or adaptive filters (these determine the substitution rule used). A multiple-instruction multiple-data version of this basic architecture is described. By changing the second set of filters (or by accessing different sets of frequency-*multiplexed filters*) one can control the function or operation that the processor performs. Specifically, by accessing different sets of filters, the same architecture can be shown to perform all logic and numeric functions. The specific substitution rules required are listed and a new optical architecture to achieve the required multiple filter bank access is described. A more near-term architecture system using multiple laser diodes and a multichannel AO cell is also described.

We show that the same basic system can implement the fundamental morphological operations of erosion and dilation and the closure and opening functions and thus how it can achieve morphological image processing. We then show that the same basic architecture can achieve propositional calculus functions (i.e. if-then decisions) and operate as an inference machine.

Initial optical laboratory demonstrations of the basic logic, morphological and propositional calculus operations of the system will be included.

ABSTRACT:

Conclusions on Optical Computing

Adolf W. Lohmann
University of Erlangen, FRG

Everybody agrees: parallelism is the major asset of optics for data processing. Opinions differ on questions like analog or binary, neural processing or number crunching, what is the best nonlinear material, where are the ultimate limitations.

AUTHOR INDEX